Phytoplankton dynamics in the North Sea: influence of fronts and tidal stirring on phytoplankton production

Dissertation

with the aim of achieving a doctoral degree

at the Faculty of Mathematics, Informatics and Natural Sciences

Department of Earth Sciences

at Universität Hamburg

Submitted by Changjin Zhao

From Chongqing, China

Hamburg, 2019

Accepted as Dissertation at the Department of Earth Sciences

Day of oral defense:	03.07.2019
Reviewers:	Dr. Thomas Pohlmann
	Prof. Dr. Corinna Schrum
Chair of the Subject Doctoral Committee:	Prof. Dr. Dirk Gajewski
Dean of Faculty of MIN:	Prof. Dr. Heinrich Graener

Summary

Characterized by high productivity and intense physical forcing, many coastal and shelf seas are typical areas where biological activities are underpinned or dominantly controlled by the physical environment. Particularly for the North Sea, the hydrodynamic processes potentially regulate the vertical distribution of phytoplankton biomass and growth resources, such as nutrients and light. Consequently, the spatial-temporal variability in biological fields will be partly shaped by the hydrodynamical field. This study provides a profound investigation regarding the impact of physical processes on primary production in the North Sea, with special emphasis on spatial-temporal variability.

Observation and simulation were combined to give new insights to physical controls on biological characteristics and primary production. This dissertation consisted of 3 manuscripts to address following questions: 1) using novel observational datasets to identify general patterns of vertical Chlorophyll distribution in the German Bight, 2) utilizing 3D physical-biogeochemical simulation to evaluate the role of one of the dominant drivers, tidal forcing, on shaping the primary production's pattern on a basin scale, 3) quantify the variability of the frontal system and investigate the responsible mechanisms for increased productivity in frontal areas. In **manuscript 1**, heterogeneity of the chlorophyll (CHL) vertical distribution was first quantified systematically in the German Bight. Subsurface CHL maxima (SCM) appeared in case of strongly stratified conditions. Tidal forcing was confirmed as the dominating driver for resuspension and regulation of the mixing-stratification status. To further generalize the findings in **manuscript 1** and to evaluate the spatially different impacts of tidal forcing in regulating primary production basin widely, numerical simulations of the North Sea ecosystem using varying tidal forcings were performed in **manuscript 2**. The results from these numerical simulations highlighted that tides promote primary production most significantly in frontal areas of the southern North Sea, particularly during the stratified season, thus contributing to the high annually averaged productivity. To further investigate the mechanism supporting high productivity and to quantify the variability of related frontal structures, **manuscript 3** provided mapping of frontal occurrence and systematic differentiation in mechanisms responsible for high productivity in the North Sea. The temporal variability of frontal systems and relevant biological responses were further expanded to multiple decades in **manuscript 3**.

The heterogeneity of CHL vertical distribution in the German Bight was rarely addressed attention in the past because of the strong vertical mixing. Making use of sampled vertical transects with high resolution on a seasonal base, **manuscript 1 "Characterizing the vertical distribution of chlorophyll a in the German**

Bight" quantified the heterogeneity of CHL vertical distribution and associate different patterns of CHL vertical profiles with physical and biological features. Subsurface maximum CHL layer only occurred under strong stratified condition. High CHL below the pycnocline (HCL) was frequently observed, especially during the decay phase of the spring bloom, which was supposed associated with resuspension. Physical control on the CHL's vertical distribution was highlighted, since the center of subsurface maximum CHL was vertically well correlated with pycnocline instead of euphotic layer depth. Stability of stratification was well in line with Simpson Hunter parameter number and resuspension signal was well correlated to tidal cycle, which indicated that tidal forcing played major role in regulating mixing-stratification status and drive resuspension of CHL. The result in this study pointed to the importance pf pelagic-benthic coupling in this system and questioned the representativeness of surface sampling of biota in the German Bight.

In **manuscript 2 "Tidal impacts on primary production"**, we explored the response of net primary production to the tidal forcing in the North Sea. Using the 3D hydrodynamic-biochemical coupled model ECOSMO, three scenarios were simulated and NPP (net primary production)'s response to tide was evaluated by the difference between the 3 scenarios on different spatial-temporal scales: 1) scenario with M_2 and S_2 tidal constituents, 2) scenario with only M_2 tidal constituent, 3) a reference scenario without tidal elevation. Basin widely, the overall North Sea NPP increased only by 3% in response to tidal forcing, but local responses were much higher, with local changes of primary production in response to tides reaching 60%, which indicated that tides can be deemed as important for spatial primary production pattern. These results highlighted the importance of tides in controlling the hydrodynamic environment and regulate spatial and temporal diversity of NPP's response. In the near shore areas where the water column stayed well-mixed throughout the year, tidal mixing deteriorated the light condition for phytoplankton growth and subsequently hindered NPP. In frontal and stratified shallow areas, NPP was promoted by tides during the stratified season. Tidal mixing infused nutrients into the euphotic layer and sustained high levels of summer NPP. In the northern North Sea, NPP's response to tidal forcing was small compared to the other regions. The impact of the spring-neap tidal cycle and changes in spring bloom phenology have also been analyzed. We concluded that the impact of tides on NPP varies spatially, depending on the counteracting processes resuspension, responsible for enhanced shading and consequently reduced NPP, and mixing induced nutrient replenishment, which promotes NPP.

To further investigate mechanisms responsible for promoted NPP in frontal areas, simulations of ECOSMO and remote sensing data are combined to reveal frontal dynamics and relevant impacts on ecosystem in **manuscript 3 "Frontal dynamics and impacts on primary production in the North Sea"**. Remote

sensing data of sea surface temperature and chlorophyll-a were utilized to evaluate the models capability to resolve frontal dynamics and characteristics of biological fields in frontal areas. Using frontal detection algorithm, geographical maps of local occurrence of fronts were derived statistically. Relative locations of high productivity to physical fields were also mapped out geographically. The results showed that fronts are comparably stable in the western part of North Sea. However, in the eastern part of North Sea, frontal systems were characterized by temporal variability and were shifting during the summer season. In the northwestern part of the North Sea, especially at the Scottish coastal front, higher NPP was dominantly confined to the mixed side of the front, with a probability of more than 90%. At these stable fronts, such as the front around Dogger Bank, high productivity was mainly fueled by diffusive nutrients fluxes. On the other hand, in the southeastern North Sea, the pattern that higher NPP located at the mixed side of front remained dominant but with lower probability (<50%). In unstable frontal systems, higher NPP was often triggered by shifting of fronts. It is either because of pumping up nutrients in previously stratified areas to release nutrient limitation or keep biomass within upper layers in previously mixed areas when stratification or reduced vertical turbulence occurs, which expose the biomass to more favorable light conditions. Inter-annual variations in frontal NPP showed similar fluctuations and a decreasing trends since 2000, which can be corroborated with estimates derived from observations.

To obtain a better understanding of physical-biogeochemical interactions and related processes relevant for the North Sea ecosystem, a thorough representation of frontal characteristics is necessary in ecosystem models, since tides and tidal fronts play a pivotal role in shaping the spatial variability of ecosystems in the North Sea. Multidisciplinary observations are prerequisite to obtain new insights to this system, particularly for areas with significant temporal variabilities.

Zusammenfassung

In den hoch produktiven und von starken physikalischen Kräften geprägten Shelf- und Küstenregionen werden biologische Aktivitäten hauptsächlich von der Umgebung bestimmt und kontrolliert. Speziell in der Nordsee regulieren die hydrodynamischen Prozesse ebenso die vertikale Verteilung der Phytoplanktonbiomasse wie auch anderer Wachstumsfaktoren wie Nahrung oder Licht. Folglich wird die raum-zeitliche Variabilität der biologischen Umgebung teilweise von den hydrodynamischen Gegebenheiten vorgegeben. In dieser Arbeit wird eine tiefgreifende Untersuchung des Einflusses von physikalischen Prozessen auf die Primärproduktion in der Nordsee mit dem Schwerpunkt auf raum-zeitlicher Variabilität vorgestellt.

Dabei werden Messungen und Simulation kombiniert, um neue Einblicke in physikalische Mechanismen, biologische Charakteristika und Primärproduktion zu erhalten. Diese Dissertation besteht aus drei Masnuskripten, die einen tieferen Einblick in die folgenden Fragestellungen geben soll: 1) Verwendung neuer Forschungsdaten zur Identifizierung der wesentlichen Muster der vertikalen Chlorophyllverteilung in der Deutschen Bucht. 2) Beurteilung des Einflusses einer der treibenden Kräfte, nämlich der Gezeitenkräfte, auf das Ausbilden von Mustern in der Primärproduktion, gestützt auf 3D physikalisch-biogeochemische Simulationen. 3) Quantifizierung der Variabilität von Gewässer-Fronten (Zone im Gewässer mit starker Änderung der Wassereigenschaften wie z.B. Salinität, Temperatur...) und Untersuchung der für eine Erhöhung der Produktivität in Frontgebieten verantwortlichen Mechanismen. Im **Manuskript 1** wird zunächst die Heterogenität der vertikalen Chlorophyll (CHL) -Verteilung in der Deutschen Bucht systematisch quantifiziert.
Oberflächennahe CHL-Maxima traten im Falle starker Stratifizierung auf. Um die Ergebnisse aus **Manuskript 1** weiter zu verallgemeinern und die räumlich verschiedenen Einflüsse der Gezeitenkräfte auf die Regulierung der Primärproduktion einzuschätzen, wurden im **Manuskript 2** numerische Simulationen des Ökosystems der Nordsee vorgenommen unter Anwendung variierender Gezeiten. Die numerischen Simulationen zeigen, dass die Primärproduktion am deutlichsten in Frontalgebieten der südlichen Nordsee und speziell während der Jahreszeit hoher Stratifizierung gefördert wird, und dadurch wesentlich zu der hohen jährlichen Durchschnittsproduktivität beiträgt. Um die Mechanismen, die eine hohe Produktivität fördern und die damit in Verbindung stehende Variabilität von Gewässer-Front-Strukturen genauer zu verstehen, wird in **Manuskript 3** das Auftreten von Front-Strukturen und systematische Differenziation der für hohe Produktivität verantwortlichen Prozesse in der Nordsee abgebildet. Die zeitliche Variabilität von Gewässer-Fronten und relevante biologische Reaktionen werden im **Manuskript 3** für mehrere Jahrzehnte in die Zukunft berechnet und untersucht. Aufgrund der starken Durchmischung (strong mixing) hat in der Vergangenheit die Untersuchung der

Heterogenität der vertikalen CHL-Verteilung in der Deutschen Bucht nur wenig Aufmerksamkeit erhalten. Durch Aufteilung in vertikale Transsekte mit hoher saisonaler Auflösung wurde im **Manuskript 1 "Characterizing the vertical distribution of chlorophyll a in the German Bight"** die Heterogenität der vertikalen CHL-Verteilung und die damit assoziierten verschiedenen Muster der vertikalen CHL-Profile mit biologischen und physikalischen Eigenschaften quantifiziert. Oberflächennahe CHL-Maxima traten nur unter startk stratifizierten Bedingungen auf. Hohe CHL-Werte unterhalb der Pyknokline (HCL) wurden häufig beobachtet, insbesondere während der Abklingphase des spring bloom und konnten mit Resuspension assoziiert werden. Das Zentrum des oberflächennahen CHL-Maximums stimmt vertikal gut mit der Pyrokline überein, nicht aber mit der Euphotischen Zone, wodurch eine physikalische Kontrolle der vertikalen CHL-Verteilung gezeigt werden konnte. Die Stabilität der Stratifikation stimmt gut mit dem Simpson Hunter Parameter überein und das Resuspensionssignal korreliert mit den tidalen Zyklen, was darauf hinweist, dass die Gezeitenkräfte eine wesentliche Rolle in der Regulierung der Durchmischung und Stratifizierung (mixing-stratification-status) spielen und damit die Resuspension des CHL vorantreiben. Die Ergebnisse dieser Studie zeigten die Wichtigkeit der pelagisch-benthischen Kopplung und stellen die Repräsentativität von Stichprobenuntersuchungen von Biota in der Deutschen Bucht in Frage.

Im **Manuskript 2 "Tidal impacts on primary production"** wurde die Resonanz der Primärproduktion auf die Gezeitenkräfte in der Nordsee untersucht. Mithilfe des 3D hydrodynamisch-biochemisch gekoppelten Modells ECOSMO wurden drei verschiedene Szenarien bezüglich unterschiedlicher Raum-zeitlicher-Skalen simuliert und durch deren Vergleich die Antwort der NPP (net primary production) auf die Gezeiten evaluiert:1) Szenarien M_2 und S_2 Gezeiten Konstituenten, 2) Szenarien mit ausschließlich M_2 Konstituenten, 3) Ein Referenzszenario ohne Gezeiten.Küstenweit erhöht sich die NPP in der gesamten Nordsee um nur 3% als Antwort auf Gezeitenkräfte, lokal konnten diese Reaktionen jedoch deutlich größer sein mit Änderungen der Primärproduktion um bis zu 60%, weshalb Gezeiten als wichtiger Faktor für räumliche Verteilung der Primärproduktion erachtet werden können. Durch diese Ergebnisse wird die Bedeutung von Gezeiten für die Kontrolle des hydrodynamischen Umfelds und als Regulierung der räumlichen und zeitlichen Vielfalt der NPP-Antwort besonders hervorgehoben. In den küstennahen Gebieten, in denen die Wassersäule über das Jahr hinweg gut durchmischt ist, verschlechtert die von Gezeiten getriebene Durchmischung die Lichtverhältnisse für das Phytoplanktonwachstum und verringert somit die NPP. In Gewässer-Front- und in stratifizierten flachen Gebieten wurde die NPP durch Gezeiten, während der Jahreszeit verstärkter Stratifikation, erhöht. Von Gezeiten getriebene Durchmischung hat Nährstoffe in die Euphotische Schicht transportiert und konnte dadurch einen hohen NPP Werte im Sommer aufrechterhalten. In der Nordsee war der Einfluss von Gezeiten auf die NPP gering verglichen mit anderen Regionen. Auch der Einfluss von Spring-

Nipptiden Gezeitenzyklen und Änderungen in der spring bloom Phänologie wurde analysiert. Es kann zusammengefasst werden, dass der Einfluss der Gezeiten auf NPP räumlich variiert abhängig von den entgegenarbeitenden Prozessen der Resuspension, die durch shading auf der einen Seite dieNPP reduziert, und auf der anderen Seite durch Nahrungsnachschub, der durch die Durchmischung hervorgerufen wird, die NPP erhöht.

Um die für die Erhöhung des NPP verantwortlichen Mechanismen noch genauer zu untersuchen, wurden im **Manuskript 3 "Frontal dynamics and impacts on primary production in the North Sea"** ECOSMO-Simulationen und Fernerkundungsdaten kombiniert, um relevante Auswirkungen auf Ökosysteme und Gewässer-Front dynamik zu entschlüsseln. Fernerkundungsdaten der Meeresoberfläche, Temperatur und Chlorophyll-a wurden hierbei verwendet um die Fähigkeit des Modells zu evaluieren, Gewässer-Front-Dynamiken und charakteristische biologische Eigenschaften in Gewässer-Front-Gebieten aufzulösen. Unter Zuhilfenahme von front-detektierenden Algorithmen wurden geographische Karten von lokalen auftretenden Gewässer-Fronten statistisch abgeleitet. Die Positionen von hoher Produktivität relativ zu den physikalischen Gegebenheiten (wie z.B. Meeresbodentemperatur) wurden ebenso ermittelt. Die Ergebnisse zeigen, dass Gewässer-Fronten in der westlichen Nordsee im Vergleich stabiler sind. Im östlichen Teil der Nordsee jedoch, werden Gewässer-Fronten durch ihre zeitliche Variabilität und eine Verschiebung im Sommer charakterisiert. Im nordwestlichen Teil der Nordsee, insbesondere an der Schottischen Küstenfront, war hohe NPP, mit einer Wahrscheinlichkeit von mehr als 90%, hauptsächlich gebunden an die durchmischte Seite der Front. An den stabilen Gewässer-Fronten wie im Bereich um die Dogger Bank wurde die hohe Produktivität hauptsächlich getrieben durch diffusive Nährstoffströme. Auf der anderen Seite war das Muster, dass höhere NPP nahe der durchmischten Seite der Gewässer-Front lokalisiert sind, zwar nach wie vor dominant, aber hatte eine geringere Wahrscheinlichkeit (<50%). In instabilen Front-Systemen, wurde eine hohe NPP häufig durch ein Verschieben der Gewässer-Fronten ausgelöst. Dies rührt entweder vom Pumpen von Nährstoffen in vorher stratifizierte Gebiete, oder dem Erhalten der Biomasse in den oberen Schichten vorherig durchmischten Gebiete während der Stratifikation, oder von reduzierter vertikaler Turbulenz, die für die Biomasse günstigere Lichtverhältnisse schafft. Die zwischenjahreszeitliche Variation der NPP in Gewässer-Front-Gebieten zeigte ähnliche Fluktuationen und einen abnehmenden Trend seit dem Jahr 2000, was sich durch Abschätzungen aus Beobachtungen bekräftigten ließ.

Um ein besseres Verständnis der für das Ökosystem Nordsee physikalisch-biogeochemischen Interaktionen und damit verknüpfter Prozesse zu erhalten, ist eine sorgfältige Repräsentation der Gewässer-Front-Charakteristik in Ökosystemmodellen notwenig, da Gezeiten und Gezeitenfronten für das Ausbilden der räumlichen Variabilität des Ökosystems in der Nordsee eine

zentrale Rolle spielen. Multidisziplinare Beobachtungen sind hierbei die Voraussetzung, um neue Einblicke in dieses System zu erhalten, besonders in Gebieten mit signifikanter zeitlicher Variabilit

Table of contents

Chapter 1. Introduction

Shelf seas are characterized by high biological activity; scaled by their area, shelf sea primary production is 2-5 times higher than that in the open ocean (Berger et al., 1989; Simpson and Sharples, 2012). The reasons for the high productivity are still not fully understood. Advancing understanding of the physical biogeochemical couplings remain critical, such as detecting driving mechanisms of spatial heterogeneity of shelf sea production (Capet et al., 2013; Fisher et al., 2015; Hartman et al., 2018), better representations of shelf sea in global earth system models (Holt et al., 2009, 2017; Lavoie et al., 2017; Schrum et al., 2016), improved understanding of spatial-temporal variabilities in shelf seas (Cadier et al., 2017; Hicks et al., 2017; Murphy et al., 2007), accessing vulnerabilities of coastal ecosystems to climate change (Cinner et al., 2012; Glibert et al., 2014; Green et al., 2014; Holt et al., 2016) and evaluating direct anthropogenic impacts (Floeter et al., 2017; Halpern et al., 2007; Schrum et al., 2016; Turner et al., 2003)

Phytoplankton's access to light and nutrients is critical for growth and influenced by the vertical position in the water column. However, plankton has only a limited capacity to regulate its position in the water column. Although they might be able to move relative to the water body, hydrodynamic drivers are critical for their access to growth resources. The influence of physical processes on biological processes covers all scales from microns to thousands of kilometers (Mann, 1992). To which extend physical processes can drive phytoplankton's distribution and dispersion depend on relative importance between physical forcing and phytoplankton's behavioral capabilities (McManus and Woodson, 2012). At scales of microns, the viscous boundary layer around phytoplankton cells influence nutrient uptake (Barton et al., 2014). Larger phytoplankton cells, such as diatoms and flagellates, benefit from self-movement to thin the boundary layer around their cells and increase nutrient gradient thus elevating nutrient uptake rates (Nishihara and Ackerman, 2009) . However, at larger scales and more turbulent environments, the importance of hydrodynamic drivers for controlling nutrient access dominate over plankton behavior (Prairie et al., 2012). Apart from diatom's sinking (Iversen et al., 2010) and diel migration of dinoflagellates (Sullivan et al., 2010), plankton has little ability to overcome stratification and to benefit from high nutrient concentrations below depleted surface layers (Laufkötter et al., 2013). The seasonal decrease of the upper mixed layer is the prime cause for the onset if the spring bloom (Sverdrup, 1953). The pycnoline uplifts phytoplankton cells in the well-lighted upper layer (euphotic zone) and triggers fast growing (Nelson and Smith, 1991). In the subsequent stratified season, in addition to keeping phytoplankton in the euphotic zone, the pycnocline also serves as a barrier to hinder vertical nutrient fluxes. Given the higher stability in the pycnoline, the phytoplankton with swimming capability manages to counteract with lower turbulence to either swim up to access higher irradiance or

migrate down to release nutrients depletion, within the pycnocline (Lewis et al., 1984; Ross and Sharples, 2007).

The upper ocean is generally regarded as photosynthetic active zone because it is well-lighted but potentially lack nutrients given long-time stratification and consumption of nutrients by phytoplankton. In temperate marine systems, the water column undergoes seasonal cycles of onset stratification in late spring, persisting stratification in summer and unstratified in winter. The onset and duration of stratification, stability, extend, deepening and shallowing of the pycnocline are controlled by the hydrodynamic environment. Important key hydrodynamic drivers in shelf sea systems are tides, wind and baroclinic forcing such as solar heating, atmospheric cooling, fresh water runoff and evaporation (Simpson and Sharples, 2012). Solar heating and fresh water input provide buoyancy to the surface ocean and stabilizes the water column such that stratification develops. Tides and wind, on the contrary, provide energy to support turbulent mixing which counteracts the stability of the water column and supports vertical mixing. Besides solar heating, in estuarine areas, the river runoff further increase the buoyancy, which triggers earlier spring bloom. The scale of river plume occurs on a broad range of spatial scales (Mestres et al., 2007; O'Donnell et al., 2008), can reach the scale up to hundreds of kilometers.

Another example of physical influence on the scale of hundreds of kilometers is tidal fronts, especially in shelf seas and oceans (Belkin et al., 2009). Frontal systems are known to be biologically highly productive and are characterized by biomass aggregation (Lough and Aretxabaleta, 2014; Pingree et al., 1975). Variations in mixing-stratification conditions driven by tide and breaking internal waves replenish nutrients to fuel 'new' production, especially in summer (Brickman and Loder, 1993).Driven by density gradients, along-front current jets and cross frontal residual currents are suggested to influence nutrients transport and biomass distribution in frontal areas (Chen et al., 1995). Besides the spatial scale, biological-physical interaction is further modulated by temporal variations of the physical characteristics (e.g. tidal cycle, North Atlantic Oscillation NAO) (Castelao et al., 2005; Oziel et al., 2016) and typical time scale of biogeochemical process (e.g. cell division time, CHL adaptation to nutrient status) (Jones and Halpern, 1981; Landeira et al., 2014). Due to temporal and spatial variability characterizing by multiple scales, building quantitative understanding of how frontal dynamics impact ecosystem dynamics is challenging (Le Fèvre, 1987; Franks, 1992).

In this study, hydrodynamic drivers for primary production in shelf seas and their spatial heterogeneity are addressed. The focus will be on the investigation of the role of stratification, mixing and frontal transition zones for phytoplankton position in the water column and consequent primary production dynamics. An example for a typical highly productive shallow shelf sea system is the North Sea

which is part of the Northwest European Shelf (Charnock et al., 1994; Otto et al., 1990).

The objective of this thesis is to obtain a more profound knowledge of the impact of physical processes on primary production in the North Sea, with potential relevance for the general understanding of shelf sea primary production dynamics. The thesis will focus on three aspects, the vertical distribution of chlorophyll (CHL) in relation to the mixing-stratification pattern in the shallow German Bight, the tidal influence on primary production in the North Sea and the relevance of frontal dynamics to North Sea primary production.

As mentioned before, the physical processes in the North Sea play a pivotal role in regulating the temporal and spatial variabilities of ecosystem dynamics on multiple scales. The variation of physical–biogeochemical interactions are hardly captured only by observations due to their limited time and spatial resolution. To obtain new insights into physical–biogeochemical interactions on basin scale and multiple time scales, new observation material and 3D physical- biogeochemical coupled model are combined within this study. In particular, the following phenomena or questions are investigated, each addressed in a separate manuscript:

- The occurrence of vertical heterogeneous CHL profile in the German Bight where we assume the water column stays well mixed throughout the year
- The temporal and spatial impacts of tides on primary production in the North Sea.
- Position and variability of fronts and related local primary production maxima

For each of the research topics, a number of specific questions were addressed:

Part 1

1. To what extent does the vertical CHL distribution show heterogeneity in the inner German Bight?
2. Are there any temporal and spatial patterns in the observed vertical CHL distribution that are related to the hydrodynamic environment or phytoplankton growth dynamics?
3. Besides primary production, what is the major factor influencing the CHL vertical distribution? Are there any systematic differences from phenomena found in open oceans?

Part 2

1. What is the magnitude of the tidal induced changes in primary production in the North Sea?

2. How does the primary production respond to tidal forcing in different biogeochemical-hydrodynamic sub-systems and what is the specific dominating mechanism behind it?
3. What is the impact of spring-neap tidal cycle on primary production?

Part 3

1. What is the seasonality of frontal occurrence, provided by a systematic and quantitative descriptions based on simulation and observations.
2. Is there any systematic difference between beneficial mechanisms for phytoplankton growth at fronts in different sub-regions of the North Sea?
3. Reveal the relationship between Stability & variability of frontal systems and local productivity.

The general aim of this thesis is to identify how hydrodynamic environments, such as the mixing-stratification pattern, fronts, tidal forcing's influence the phytoplankton dynamics in the North Sea. Spatial and temporal variability in phytoplankton's biomass and growth condition appears on multiple scales (river plume, tidal mixing fronts, basin scale) and potential drivers for variabilities (wind, tidal energy distribution, bathymetry) are investigated. In the first paper, by analyzing observed vertical transects in the German Bight, tidal forcing and wind events are revealed as the dominant processes which regulates stratification-mixing pattern and resuspension, thus influencing the CHL vertical distribution. In the second paper the influence of the tidal forcing, as the major hydrodynamic driver, on the ecosystem is further evaluated using numerical simulations covering the major part of the North Sea. By investigating the tidal influence primary production and the vertical biomass distribution, the study of the second paper generalizes the conclusion of the first paper and provides quantitative estimates for tidal induced production. The results of the numerical simulations suggest that tides promote primary production most significantly in frontal areas in the southern North Sea. This leads to the third paper, which provides quantitative description of frontal dynamics in the North Sea and their impacts on primary production with systematic difference, using remote sensing data and model results. To further investigate mechanisms which benefit primary production in frontal systems, related mechanisms such as enhanced vertical pumping of nutrients and convergent circulation are explored using simulation results. The third manuscript provides further in-depth insights based on conclusions of second paper from basin scale to mesoscale.

The whole thesis is composed of this introduction chapter, a following chapter which provides a characterization of the North Sea hydrodynamics and biogeochemistry, the main body and a conclusion chapter. The main body of this thesis consists of three chapters which follows the outline as just described. Two of these chapters (Zhao et al., 2019a, 2019b) are already published for publication

peer review journals. Methods and conclusions are provided as part of the respective papers and manuscripts.

Chapter 2. Characterization of the North Sea dynamics

2.1 Hydrodynamical features in the North Sea

The North Sea is one of the most anthropogenic influenced and highly investigated marine areas in the world (Emeis et al., 2015; O'Driscoll et al., 2013). It a continental shelf sea connected to the northeastern Atlantic Ocean in the north and, through the English Channel, in the south-western, and to the Baltic Sea through the Skagerrak (Fig. 1.1). Due to its wide open connection in the north, the North Sea is characterized by a significant response to oceanic influences, such as astronomical tide, internal waves and lateral exchange of salinity and nutrients (Holt et al. 2015). As a shelf sea the North Sea is additionally influenced from land by e.g. fresh water inflow, terrestrial input of organic matter and nutrient loads (Brockmann et al., 1990a; Skogen et al., 1995). Besides, the circulation and stratification of the North Sea are strongly determined by atmospheric conditions (Backhaus, 1989, Schrum et al., 2003) and show a relationship to large scale atmospheric pattern such as the North Atlantic Oscillation (NAO) (Gröger et al., 2013). Oceanic, atmospheric and continental influences generate a specific regime that requires proper simulation and observational methods to investigate biological and physical characteristics and processes (Hufnagl et al., 2013; Mathis and Pohlmann, 2014)

The North Sea is a typical shallow shelf sea, with water depth generally less than 50m (Fig.1.1). The depth increases gradually toward the north and reaches 200m at the northern shelf edge. An exception is in the Norwegian Trench region where the water depth can reach 700m. The bathymetry influences the propagation and dissipation of astronomical tides, waves and residual currents.

A dominant feature of the North Sea is the propagation of incoming tidal waves entering the basin from the North Atlantic at the open boundary in the north, which is dominated by the semidiurnal tidal constituent. As a results of a Kelvin wave entering a semi-enclosed "rectangular" basin like the North Sea (Taylor, 1922), an amphidromic system with two amphidromic points is generated for the M2 constituent in the northern North Sea (NNS), where one amphidromic point is near Norway and the other one is near the eastern edge of the Dogger Bank (DB). The displacement of the amphidromic points towards the east is the result of friction and corresponding energy loss of the tidal wave on its way through the North Sea. A third amphidromic point emerges at the mouth of the southern channel as a result from the tidal entering the area through the English Channel

(Brown, 1987). With its increasing amplitude along the British Coast, the tidal wave strongly dissipated in the shallower southern coastal waters, generating reflected waves with less amplitudes on the eastern boundary (Sündermann and Pohlmann, 2011). Thus, areas in the north-eastern part displays weak tidal energy, with amplitude less than 0.5m off the Danish and Norwegian coasts (Sager, 1959)

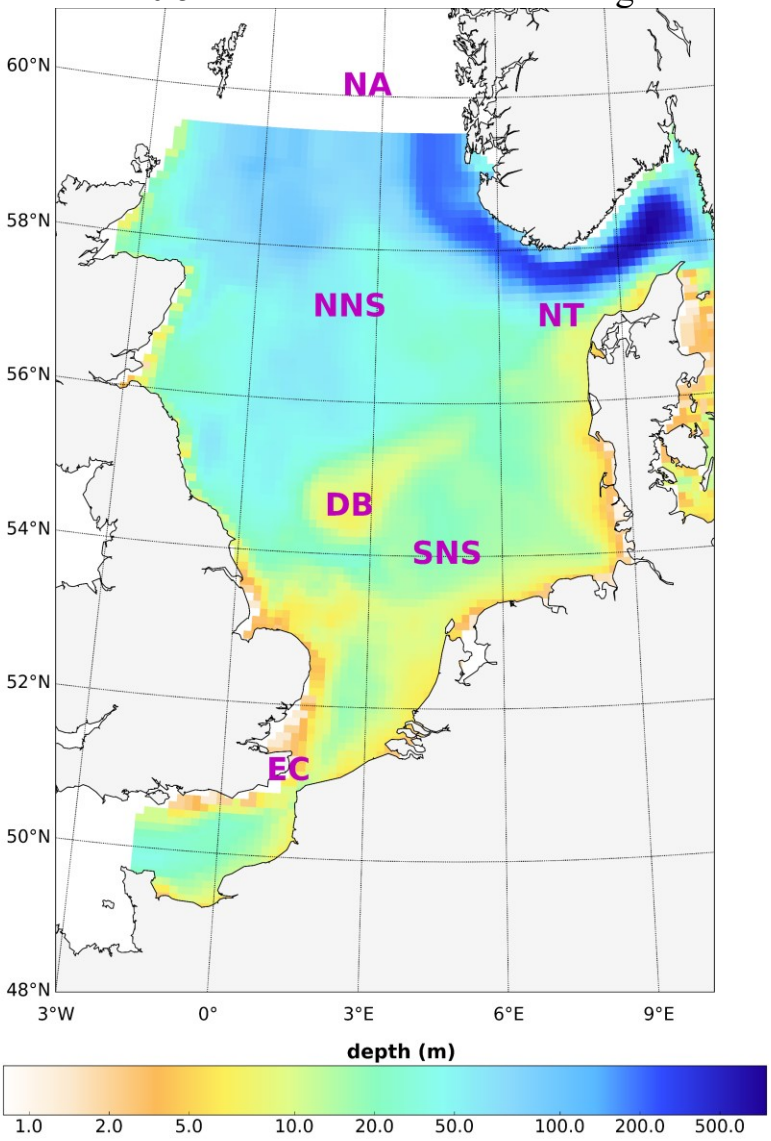

Figure 1.1 Bathymetry of the North Sea. NNS and SNS are short for northern North Sea and southern North Sea. BS is short for the Baltic Sea, DB for Dogger Bank, EC for English Channel, NT for Norwegian Trench. The northern boundary of the North Sea is open to the North Atlantic Ocean (NA).

A regime of seasonal stratification occupies much of the central and northern North Sea. In the central and deeper part of the NNS, the water column remain mixed in winter due to winter convection but become thermally stratified in early summer when surface heating overcomes the mixing induced mainly by wind and

tidal dissipation (Pohlmann, 1996a, 1996b). The Norwegian Trench, in contrast, exhibits a haline-stratification throughout the year due to the outflow of low saline Baltic Sea surface waters (Mork, 1981). Along the western and southern coast of the North Sea, with stronger dissipation of tidal energy and shallower water depth, tidal currents are strong enough to keep the shallower water column vertically mixed throughout the whole year, except for regions of freshwater inflows (ROFIs) where haline-stratification potentially superimposes the strong mixing (Simpson and Rippeth, 1993). Apart from solar heating, the stratification in the south-eastern part is additional influenced by land born freshwater supply and wind forcing (Jacobs, 2004; Ruddick et al., 1995; Schrum, 1997). The concurrence of seasonal stratification in the deeper areas and the tidally mixed areas in the shallow regions create a transition area known as the tidal front. The cross-frontal density gradients together with the Coriolis force cause an along-front jet current. A secondary circulation, which is perpendicular to the front, lead to convergence at the surface of the frontal system. The blending of bottom isotherms induce upwelling of cold bottom water from the mixed side. The frontal system cannot be completely described as a steady-state picture because many time-depend processes influence its position and intensity, such as the tidal cycle and episodic wind events (Krause et al., 1986; Schrum et al., 2003)

Considering the spatial variability of tidal energy, the influential factor of the boundaries and the mixing-stratification pattern, the North Sea can generally be separated into several major subsystems with respect to hydrodynamics. Due to the influence of the continental boundaries, from north to south the North Sea is becomes increasingly influenced by fresh water rather than oceanic waters (ICES, 1983; Siegismund, 2001). Based on stratified time length in annual cycle, the North Sea was divided into subsystems which are permanently stratified, seasonally stratified, permanently mixed, intermittently stratified. Areas with significant inter-annual variability were also identified in the south-eastern part of NS and surrounding areas of the Norwegian Trench (Van Leeuwen et al., 2015). In some nearshore area in the southern North Sea, river plumes result in haline stratification, with significant spatial and temporal variability, whereas in the Norwegian Trench, the haline stratification is stable due to the continuous outflow from Skagerrak (Otto et al., 1990).

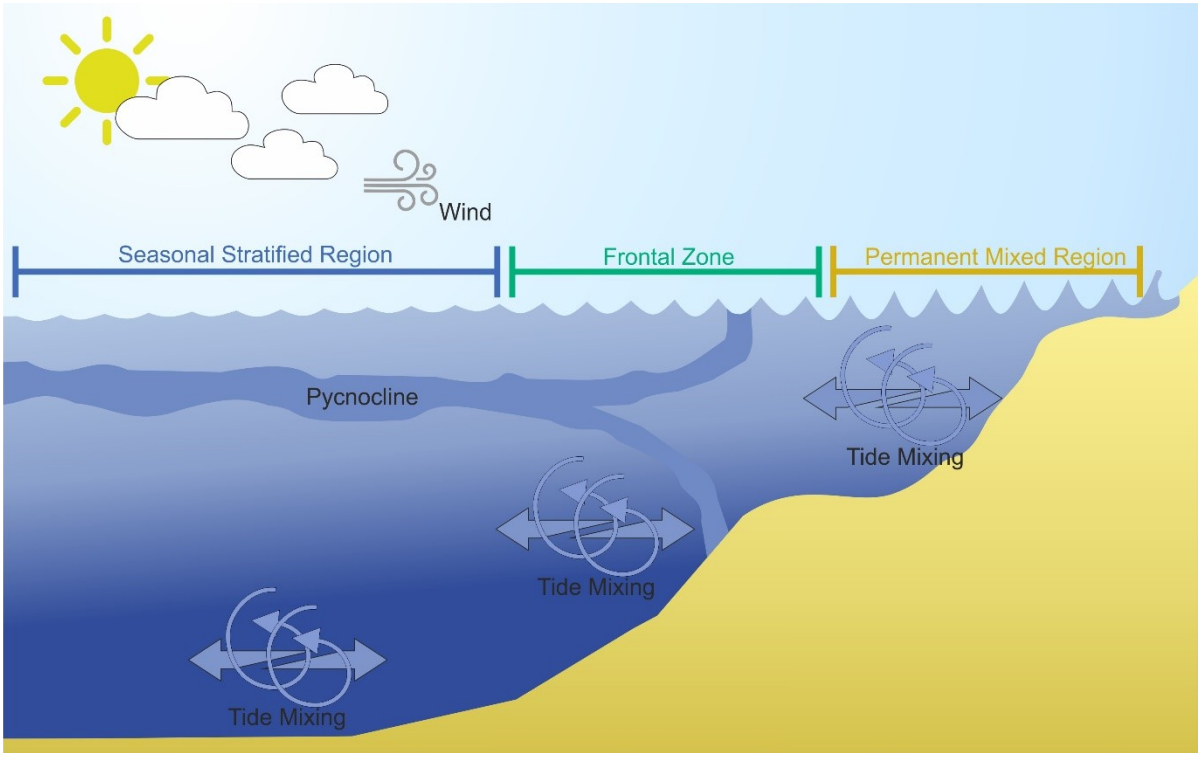

Figure 1.2. Schematic diagram of stratification-mixing status in mixed inshore area, frontal area and seasonal stratified area. Stratification-mixing status are regulated by tidal forcing and bathymetry. From Hendrik Weidemann.

The advective transport of water masses determines the circulation pattern in the North Sea (Pätsch et al., 2017). The basic anti-clockwise circulation pattern has been revealed by observational study (Kautsky, 1987) and numerical simulations (Stanev et al., 2019). Wind, density, bathymetry and oceanic forcing (tidal residuals and large-scale oceanic sea level pressure variation) contribute to the controlling processes of the overall circulation pattern (Holt and Proctor, 2008; Otto et al., 1990). The major exchange of water mass occurs in the northern boundary with the Atlantic Ocean. The amount of water entering the North Sea is in the range of $1.7 \times 10^6\ m^3 s^{-1}$, of which the majority confined to the northern North Sea and joins a northern cyclonic circulation pattern along the 100m isobaths (Svendsen et al., 1991). For the remaining part of the inflow, 5/6 moves further southward and turns eastward at the northern edge of the Dogger Bank thus forming the central circulation cell. Only 1/6 of the remaining inflow water masses from the north reaches the southern Bight and converges with the inflow from the English Channel. The combined water mass flows along the continents and merges with the central circulation cell at the Jutland Coast. The so formed Jutland Current finally enters the Skagerrak. Due to the interaction between the Jutland Current and the low-salinity outflow from the Baltic Sea, a cyclonic circulation forms at the Skagerrak and the outflow subsequently joins the

Norwegian Coastal Current and leaves the North Sea at the eastern part of the northern boundary (Mathis et al., 2015).

2.2 Biogeochemical features in the North Sea

Nutrients entering the North Sea from the Atlantic Ocean, the rivers, the Wadden Sea area and the sediments supporting a high productivity (Vermaat et al., 2008). In addition to the nutrient supply, the primary producers in the North Sea, mainly micro-algae depend on sufficient light conditions to create biomass. The general production pattern in eth North Sea is structured by the availability of sunlight at these latitudes, which regulates the seasonality of phytoplankton dynamics directly and indirectly through physical processes. The typical phytoplankton seasonality involves a spring diatom bloom followed by a flagellate bloom. In the dark winter, nutrient elements are predominantly in dissolved inorganic forms due to the decay of biomass and remineralization processes (Brockmann et al., 1990b). Due to intensified vertical mixing in winter, surface concentration of nutrients is similar to that at the bottom. Given the sufficient nutrient supply, following the increase of irradiance in spring a rapid increase of phytoplankton biomass occurs, given appropriate hydrodynamic environment, such as onset of stratification. The dominating species of spring bloom is diatoms and *Phaeosystis* (Iriarte et al., 1991). High production ceases when nutrients in the upper layer is exhausted, together with increased grazing and sinking (specifically for diatoms), which also removes the biomass from surface. In stratified summer period, production depends mainly on local recycling within the mixed layer depth except for frontal areas where nutrient-rich bottom water is injected upwardly to the euphotic zone and sustains new primary production during the stratified season. Stable stratified areas are characterized by lower biomass and production maxima below the nutrient-depleted surface mixed layer (SML). Particularly areas around the northern edge of the Dogger Bank, subsurface chlorophyll maximum contribute more than half of new production in summer (Fernand et al., 2013). In summer, the dominating species are *Ceratium* and *Dinophysis* (Löder et al., 2012). Given proper mixing and production rates, often an autumn bloom could be triggered by nutrients entrained into the deepening SML. This typical seasonality of nutrients cycling and phytoplankton dynamics appears in most part in the North Sea. In coastal areas where the water column stay well mixed throughout the year, land-borne nutrients supply and mixing processes release the nutrients limitation (Hofmeister et al., 2017). In those areas irradiance is the main limiting factors despite of the shallowness, due to high turbidity and enhanced mixing resulted from tide and wave (Tett and Walne, 1995). In growth season, instead of pulses of production in spring and continuing but lower production in summer, abundance and productivity of phytoplankton in coastal areas show irregular fluctuation, possibly depending on water transparency, advection and predator-prey interactions. The spring bloom may commence early and reaches highest biomass until summer (Tett and Walne, 1995).

The intensity of primary production has been identified by some comprehensive observations, even though the variability between area and seasons cannot be fully covered due to systematic limitation of in situ observations (Capuzzo et al., 2018; van Leeuwen et al., 2013; Tett and Walne, 1995; Weston et al., 2005). In the deeper northern North Sea the primary production has been reported to be around 125 gC m^{-2} y^{-1} (Van Beusekom and Diel-Christiansen, 1994) and at the southern coast the observed NPP is in the range between 199-261 gC m^{-2} y^{-1} (Joint and Pomroy, 1993). The NPP in the British Coast shows lower value, ranges from 75-79 gC m^{-2} y^{-1}(Joint and Pomroy, 1993). In the central part of the North Sea, the primary production ranges around 100-119 gC m^{-2} y^{-1} for the seasonal stratified area (Joint and Pomroy, 1993), while at the Dogger Bank the annual NPP was found to be 119-147 gC m^{-2} y^{-1}(Joint and Pomroy, 1993). For the area west of Jutland the annual NPP was estimated as 261 gC m^{-2} y^{-1}(Tett and Walne, 1995).

2.3 Biogeochemial-physical interaction

Biogeochemistry and ecosystem dynamics in the North Sea is strongly determined by the physical structure of the system (Schrum et al., 2006a, 2006b). As explained above, tides structure the area into a shallow well-mixed and a seasonal stratified region with different bloom dynamics and nutrient cycles (van Leeuwen et al.,, 2015).

The northern and central part of the North Sea is more influenced by heat, nutrient and organism flux from Atlantic Ocean (Siegismund, 2001). Corresponding to the onset of stratification, phytoplankton cells were lifted in the upper layer, exposed to irradiance for longer time. Once production exceeds loss of respiration and mortality, fast growth is triggered (Sverdrup, 1953). When nutrients are consumed, the pycnocline hinders the nutrients replenishment in the upper layer, subsurface maximum Chlorophyll layers are found to be re-occurrence phenomenon in the stable stratified area in the pycnocline (Fernand et al., 2013). Work as a transient layer between well-lighted but nutrients-poor upper mixed layer and nutrient-rich but shaded deeper layer, the pycnocline is the ideal place for phytoplankton to growth in the stratified season (Cullen, 2015).

Enhanced productivity and elevated biomass was shown in frontal zones (Pedersen, 1994). The stratified side of fronts is characterized by vertical stability to retain phytoplankton cells in the euphotic zone and the upward-doming of deep pycnoclines replenish nutrients to sustain primary production.

In the shallower parts of the southern NS water depth limits the depth of mixing. Provided by sufficient nutrients, this area keeps being productive throughout the year. The produced organic matter provides input into seabed and fuel an active benthic cycling there (Dauwe et al., 1998). The organic matter settled on the sea bed often forms a ‘fluff’ layer which is easily resuspended in to the bottom mixed layer (Jago et al., 2002a). The high productivity, enhanced resuspension by tide and waves and input of inorganic suspended matter make this area turbid, which

make primary production is mainly controlled by light limitation in this area (Tett and Walne, 1995).

The establish and decay of stratification influence the vertical mixing condition in the water column thus regulating the vertical distribution of biomass, nutrient and shading materials. Even if in stratified season, the perturbation of pycnocline in multiple time series, potentially driven by tide or wind, results in deepening or shallowing of mixed layer, thus enhancing flux of nutrients, and subsequently influence biogeochemical processes.

Chapter 3 (Manuscript 1).

Characterizing the vertical distribution of chlorophyll a in the German Bight

Changjin Zhao, Joeran Maerz, Richard Hofmeister, Rüdiger Röttgers, Kai Wirtz, Rolf Riethmüller, Corinna Schrum

Published in: Continental Shelf Research, Vol.175, pp.127-146, 2019

Continental Shelf Research 175 (2019) 127–146

Contents lists available at ScienceDirect

Continental Shelf Research

journal homepage: www.elsevier.com/locate/csr

Research papers

Characterizing the vertical distribution of chlorophyll *a* in the German Bight

Changjin Zhao[a,*], Joeran Maerz[a,b], Richard Hofmeister[a], Rüdiger Röttgers[a], Kai Wirtz[a], Rolf Riethmüller[a], Corinna Schrum[a]

[a] Helmholtz-Zentrum Geesthacht, Institute for Coastal Research, Geesthacht, Germany
[b] Max Plank Institute for Meteorology, Hamburg, Germany

ARTICLE INFO

Keywords:
Vertical chlorophyll-a profiles
SCANFISH
Stratification
Turbulent mixing
Subsurface chlorophyll maximum layers
Resuspension
German Bight

ABSTRACT

Coastal and shelf seas display strong variability in the horizontal and vertical distributions of chlorophyll *a* (CHL). Detailed data are required to identify the processes that drive the observed spatio-temporal dynamics. A high-resolution, vertically resolved transect data set for biogeochemical and physical properties was collected in the inner German Bight (GB) from 2009 to 2011 on a seasonal basis. We used fluorescence as an indicator for phytoplankton biomass via the CHL concentrations. We classified profiles into different types by evaluating the heterogeneity of CHL vertical distribution and identifying vertical location (upper mixed layer, subsurface layer, bottom mixed layer of water column) of high CHL concentration in each profile. We analyzed the spatio-temporal occurrences of the different CHL vertical distribution types in the context of the hydrodynamic environment. More than half (68.7%) of all profiles showed vertically homogeneous CHL distributions. A smaller subset (3.2%) of all profiles showed subsurface CHL maximum layers (SCMLs) in the vicinity of the pycnocline, covarying with strongly stratified conditions in deeper water. Profiles with highest concentration of CHL in the upper part of the water column (HCU) were observed in 11.5% of all profiles. Profiles with highest concentrations of CHL in the lower part of the water column (HCL) comprised 16.6% of all profiles. HCL profiles were extensively observed during the decay phase of the spring bloom and were associated with resuspension and erosion from pre-existing SCMLs, which could be driven by tide; photosynthetic activity below the pycnocline could also contribute. Under moderate weather conditions, tidal currents were the main driver of resuspension. This study highlighted the occurrence of SCMLs and HCL patterns in vertical CHL profiles in shallow shelf seas, such as the GB.

1. Introduction

Temporal and spatial variability in vertical chlorophyll a (CHL) distribution has long been recognized in temperate ocean waters (Boss and Behrenfeld, 2010; Herdman, 1923; Russell, 1927). The vertical distribution of CHL is shaped by a combination of biological processes, including the vertical patterns of growth and grazing influenced by the availability of light, nutrients and predators, and physical processes, such as mixing, resuspension and advection of plankton biomass (Riley, 1942). Surface sampling, e.g., via satellite images, limits the accurate description of the whole system (Charnock et al., 1993) and hampers the mechanistic understanding of the relation between environmental conditions and CHL distributions. Since the method of continuous vertical sampling of fluorescence as a proxy for CHL was introduced (Lorenzen, 1966), previously unappreciated features of the vertical distribution of CHL have been revealed. More than 20 years ago, strong heterogeneity in vertical CHL profiles, such as the occurrence of subsurface CHL maximum layers (SCMLs), has been found in the central and northern North Sea (Nielsen et al., 1993; Richardson and Pedersen, 1998). In the northern Dogger Bank area, recurrent and persistent SCMLs were suggested to significantly contribute to primary production (Fernand et al., 2013). The occurrence of SCMLs was attributed to bottom fronts, where injection of nutrients by tidal pumping supports primary production (Richardson et al., 2000; Weston et al., 2005). In stratified areas without frontal systems, hotspots of SCMLs were found to be related to local tidal mixing resulting from specific bottom bathymetry (Scott et al., 2010). We would expect considerable production in shelf seas contributed by SCML. However, limited estimations are able to confirm this based on available data. First, CHL:C (Chlorophyll a to carbon) ratio varies significantly in different time and spatial scales (Jakobsen and Markager, 2016; Wang et al., 2009). Second, phytoplankton tends to fluoresce more in autumn, when productivity is less due to lower light levels. and increasing light limitation (Kalaji et al., 2017). Third, SCML production also dependents on

* Corresponding author.
E-mail address: changjin.zhao@hzg.de (C. Zhao).

https://doi.org/10.1016/j.csr.2019.01.012
Received 28 February 2018; Received in revised form 16 January 2019; Accepted 27 January 2019
Available online 28 January 2019

injection of nutrients, which would be driven by physical process such as tidal stirring (Zhao et al., 2018) and baroclinic circulation (Pedersen, 1994).

In the southeastern North Sea, especially in the German Bight (GB), the vertical distribution of CHL has seldom been addressed since, as water depths are less than 40 m, tidal and wind-driven mixing were thought to homogenize the vertical CHL distribution at most times of the year. However, observations and simulations have shown stratification in the water column of the German Bight, which displayed an evident variability in extent, duration and intensity (Haren and Howarth, 2004; Pohlmann, 1996a, 1996b; Schrum, 1997). Apart from stratification, which potentially favors the development of SCMLs, other characteristic processes of the inner GB, such as the accumulation of settled detritus (Westernhagen et al., 1986) and low turn-over rates of organic matter (Beusekom and Brockmann, 1999), should further modify the vertical distribution of CHL and make it different from that in deeper areas. We herein investigate to which degree vertical heterogeneous CHL profiles develop and attribute their characteristics to coastal hydrodynamics and biogeochemical cycles.

Here we will employ high resolution transect data from the Coastal Observing System for Northern and Arctic Seas (COSYNA) (Baschek et al., 2017). Fluorescence profiles sampled in the COSYNA project throughout spring to autumn were used as proxy for CHL concentrations and we focused on vertical distribution pattern of CHL which are quantified within each profile. We are aware of the uncertainties resulting from varied fluorescence: CHL ratio; however, in general, the quantification of relative distribution of CHL within each profile, would not be influenced by those uncertainties. Afterwards, we characterize the seasonally variable vertical CHL patterns in the GB and examine potential mechanisms responsible for the observed vertical patterns. Our study thus provides a reference for the vertical CHL distribution in the GB. It will support the interpretation of observations and challenge coupled hydrodynamical-biogeochemical models for the GB in the future.

In this study, we attempt to provide answers to the following questions: (1) To what extent does the vertical CHL distribution show heterogeneity in the inner GB? (2) Are there any temporal and spatial patterns in the observed vertical CHL distribution that are related to the hydrodynamic environment or phytoplankton growth dynamics? Therefore, we first classified the vertical CHL profiles depending on whether relatively high concentrations of CHL were present in the upper or lower part of the water column and on the existence of a SCML. Next, we analyzed the spatial-temporal appearances of different vertical CHL profile types in the context of the seasonal dynamics of phytoplankton and stratification. Additionally, we investigated the potential biological and physical mechanisms responsible for the maintenance of observed SCMLs mainly via an empirical analysis. The potential factors responsible for the wide-spreading of higher CHL in the lower mixed layer, such as resuspension and erosion from a pre-existing SCML, were also explored.

2. Observation data and methods

In this section, we first review the general hydrodynamic and biogeochemical conditions in our study area. Secondly, the data set and sampling methods and the pre-processing of the observational data are described. Thirdly, the detection of SCMLs and the classification of different types of vertical CHL distributions are laid out. In the fourth part, the characteristics of the CHL profiles, such as resuspension signals and CHL gradients in the deeper parts of profiles, are specified. To further analyze the occurrence of types of vertical CHL distributions with respect to the environmental setting, the irradiance, wind speed, and simulated hydrodynamic setting are introduced in the fifth part. To assess the tidal currents, which were not measured simultaneously, simulation results from a 3D hydrodynamic model were incorporated into this study after validation. The hydrodynamic processes potentially influencing the vertical CHL distribution pattern, such as tidal phases and stratification intensity were quantified.

2.1. Study site

The GB is a shallow area located in the southeastern part of the North Sea, with average water depth of approximately 25 m. The hydrodynamics are dominated by tides and wind forcing. The tidal amplitudes in the GB range from 1.8 to 3.4 m, with tidal currents of up to 0.6–1.0 m s^{-1} (Dietrich, 1950). In the near coastal areas of the GB, the water column is continuously mixed by tidal and wave forcing, which act against the seasonal thermal and haline stratification which is supported by the surface buoyancy induced by surface heat fluxes, riverine fresh water fluxes and tidal straining (Simpson et al., 1991). Further offshore, the surface heat flux competes with tidal stirring and generates seasonal thermal stratification (Czitrom et al., 1988). However, seasonal stratification can be interrupted by wind-driven mixing, even in summer. The interplay between the surface heat flux, wind/tidal mixing and river run-off regulates the mixing/stratification status in the GB (Dippner, 1993). The initiation and duration of continuous mixing and stratified conditions show high inter-annual variability (Schrum et al., 2003a, 2003b).

The inner GB exhibits high primary production (Joint and Pomroy, 1993). Driven by tidal and wave forces, resuspended materials are more frequently observed and remain in suspension longer in the southern part than in the northern part of the North Sea (Eisma and Kalf, 1987). The interactions between produced particulate organic matter and suspended sediments enhance aggregation and sinking (Maerz et al., 2016). The GB was suggested to be a temporal deposition area for organic matters, due to its high local productivity (Lohse et al., 1995) and its location in the northeastward transport routs of organic matter in the North Sea (Gehlen et al., 1995). Physical factors, such as frontal systems and estuarine circulation (Krause et al., 1986), also support primary production and confine the high turbidity, high nutrient concentrations and high primary production to the coastal area. The resuspension of settled organic matter containing CHL (Duineveld and Boon, 2002) due to shifts in the stratification/mixing status in the frontal zone (thereby modifying the intensity of vertical mixing) would further complicate the distribution pattern of CHL.

2.2. Sampling and pre-processing of data

High-resolution vertical transect data on biogeochemical and physical properties were provided by the observation project 'Coastal Observing System for Northern and Arctic Seas' (COSYNA) (Baschek et al., 2017). This observation project aimed at mapping interactions between physical and biological processes in the GB, where natural variability is influenced by anthropogenic and environmental changes. The vertical transect campaigns were repeated from 2009 to 2011 and covered most of the German Exclusive Economic Zone in the inner GB beyond 10 m water depth throughout spring to autumn. The observational data were sampled on ten cruises between 2009 and 2011 using the undulating towed system ScanFish Mark III™ (SCANFISH) connected to the RV Heincke (https://www.awi.de/en/expedition/ships/heincke.html) as part of the project "Coastal Observing System for Northern and Arctic Seas" (COSYNA: http://www.cosyna.de, Baschek et al., 2017). The research vessel sailed along a designated grid of east-west and north-south transects in the area of 3.5–8.3°E and 53.5–55.8°N that covered the German Exclusive Economic Zone in the GB (Fig. 1) and captured the across-shore gradients both off the East Frisian (north-south direction) and North Frisian (east-west direction) coast. The operation of the ship and the SCANFISH instrument required water depths deeper than 10 m and wind speeds less than 14 m s^{-1}. Sometimes, weather conditions prevented the completion of observations; the coverage of each cruise is listed below (Table 1). Further analysis was confined to profiles with valid profile depth no less than 10 m.

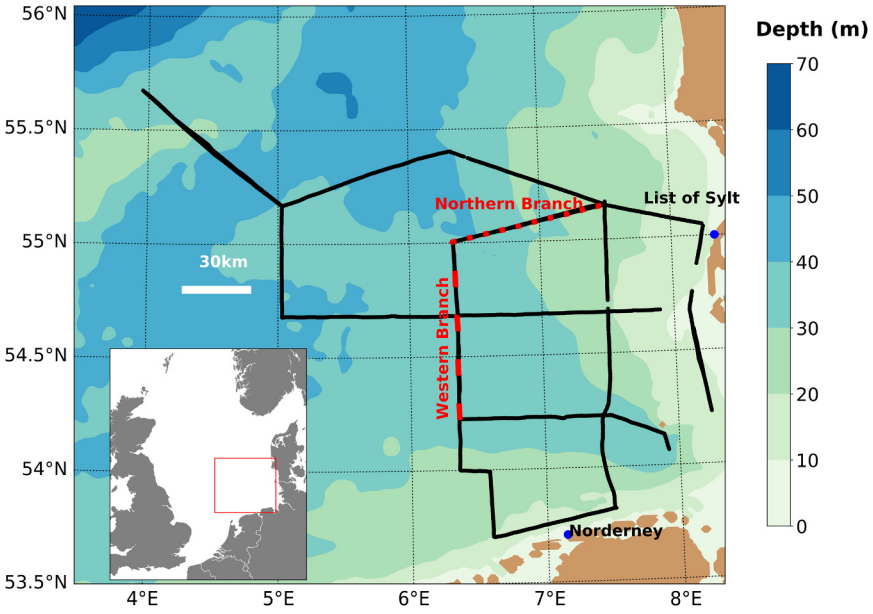

Fig. 1. Bathymetry in the German Bight and SCANFISH sampling transects (black lines). Dashed lines represent the repeatedly measured transects in July 2010 (cf. Section 3.3.3). The inset shows the North Sea and the GB location. The observation sites of surface irradiance, i.e., List on the island of Sylt and the island Norderney, are marked by blue dots.

Table 1
Basic information of the campaigns analyzed in this study.

Cruise number	Time	Wind speed ($m\,s^{-1}$)	Num. profiles(%)	Mileage (km)
303	2009.05.16–2009.05.25	6.6	5989(14.9)	1385
308	2009.07.28–2009.08.06	5.8	5491(13.6)	1281
312	2009.09.14–2009.09.20	8.1	4676(11.6)	920
319	2010.03.05–2010.03.11	8.2	5410(13.4)	1233
325	2010.05.02–2010.05.08	6.6	4566(11.3)	870
331	2010.07.13–2010.07.20	8.1	4870(12.1)	941
336	2010.09.19–2010.09.21	12.2	1164(2.9)	219
353	2011.04.06–2011.04.12	9.2	4850(12.0)	1111
359	2011.06.16–2011.06.19	7.4	1252(3.1)	608
365	2011.09.15–2011.09.19	8.7	2140(5.3)	561
Sum			40,408	9129

The ten cruises covered the growing seasons (spring, summer and autumn) in three consecutive years (Table 1), with similar spatial coverages in the majority of the cruises. Percentage of profiles measured in each campaign among all available profiles were laid out in the brackets behind the profile numbers. Thus, these data are suitable for investigating the seasonality using measured CHL profiles. Tidal phase was not considered in the planning of the cruises. The largely moderate wind conditions during the SCANFISH operation may have created a bias in stratification/mixing status, which is considered in the interpretation of the results.

The SCANFISH undulated 200–250 m behind the vessel and recorded vertical profiles along continuous V-curve paths, while maintaining safety margins of 3–5 m from the surface and the bottom. The vessel sailed at a speed of 6–8 knots. With a vertical speed of the SCANFISH of 0.4 $m\,s^{-1}$ and a sampling frequency of 11 s^{-1}, the vertical spacing between measurements was approximately 0.04 m. The horizontal span of each V curve ranged from 250 to 400 m, varying with the sailing speed of the vessel and the water depth. This sampling strategy provided simultaneous horizontal and vertical observations at a spatial resolution sufficiently high for the purposes of this study.

Among the multiple outputs provided by the sensors mounted on the SCANFISH, our analysis considered water pressure (PA-7, Keller AG, Switzerland), water temperature (PT100, ADM Elektronik, Germany - cruises 303–319; NTC sensor, ISW Wassermesstechnik, Germany - cruises 325–365), conductivity (Conductivity Sensor, ADM Elektronik, Germany), optical turbidity (Seapoint Turbidity Meter 880 nm, Seapoint Sensors Inc., USA), oxygen saturation level (Shallow Water Dissolved Oxygen Micro-Sensor, AMT Analysenmesstechnik GmbH, Germany), chlorophyll a fluorescence (TriOS MicroFlu-chl, TRIOS Inc., Germany). For the chlorophyll a fluorescence instrument, light source ultra-bright blue LED has peak wavelength at 470 nm; detection of peak wavelength is at 685 nm, with 20 nm of full width at half maximum. Optical attenuation coefficient was computed from transmission measurement at 660 nm (C-Star Transmissometer, WETLabs Inc., USA). Salinities and potential water densities (σ_t) were calculated using the international thermodynamic equation of seawater (McDougall et al., 2010; Millero et al., 2008). The sensitivity of the TRIOS fluorescence signal to turbidity was corrected as described in Maerz et al. (2016). TRIOS Inc. delivers the output of the TriOS MicroFlu-chl from raw fluorescence readings that were transferred to physical units calibrated a lab chlorophyll-a standard by a first order polynomial equation. The ratio between fluorescence and chlorophyll pigments is known to vary (Kiefer, 1973) by up to a factor of two or even more (Petersen et al., 2011). In the subsequent data analysis we used fluorescence as a proxy for phytoplankton biomass via the CHL concentrations. For the conversion we assumed a constant ratio between fluorescence and CHL (we call it F: CHL hereafter and use arbitrary unit of CHL as the unit of fluorescence signal). In general, we focus on the relative distribution of CHL in the water column; in another words, we quantified the vertical shape of each CHL-profile in terms of CHL concentration in one segment of water column being “higher than”, “lower than” or “comparable to” to other parts (upper, middle (pycnocline) and lower parts) of the same profile. No comparison was made among different profiles using absolute value. We are aware of the uncertainties resulting from varied fluorescence: CHL ratio and CHL: C ratio (Babin et al., 2008; Claustre et al., 1999). Relevant calibration and estimation of these uncertainties has been conducted to prove that the results would not be influenced by those uncertainties.

183 HPLC measured CHL data were sampled simultaneously during these campaigns. We made use of the available HPLC measured CHL data to estimate the varying range of F: CHL, in each season, each year and between different vertical segments (Appendix A). Influence of quenching on fluorescence profile in the surface water column has also been adjusted (Appendix A). Generally, F: CHL mainly lies in the range between 1 and 2; the seasonal and inter-annual variability also vary no more than a factor of 2. In addition, around 60% of the F: CHL’s variabilities between surface and subsurface segments of water column, are no more than factor of 2. In the following analysis, we took a variation

of factor 2 into account. For the profile classification we also choose this criteria, which exceeds the range of the uncertainty in the F:CHL ratio, to ensure that the difference in fluorescence reflects the difference of CHL, rather than resulting from the varied F: CHL ratio.

The data sets were binned along the observation curve into regular vertical blocks of 10 cm to avoid unevenly sampling. The consecutive data sets were split into up and down profiles. For all parameters except those relevant to oxygen, we used only downward profiles to keep the lag effects of the sensors systematically coherent. A comparison of subsequent downward and upward profiles of oxygen saturation exhibited a substantial lag in the oxygen signal, suggesting a time constant of several seconds in campaigns taken after 2009. This temporal lag corresponds to approximately 5 m in the vertical signals. Rather than detecting the accurate vertical location of the oxygen maximum, we focused on the relative positions of the oxygen maximum and the SCML, under the assumption that the lag effects are stable. Downward profiles covered a horizontal span ranging from 125 to 200 m. We assumed that the lateral change within this horizontal span was negligible and treated the V curves from downward profiles as being perpendicular to the seafloor. As the upper mixed layer generally extended 10 m or more downwards, any disturbances attributable to the ship's hull or quenching effects of CHL in the most uppermost meters should have a negligible impact on the profile classification.

All the binned data sets underwent low-pass Butterworth filtering (Butterworth, 1930) to remove short-term variations. Half of the resolution of the binned vertical step was set to be the higher constraint of the filter to avoid aliasing (Grenander, 1959). This process also damped out most of the artefacts in the computed salinities and water densities at the pycnocline caused by the thermal lag of the conductivity cells.

2.3. Classification of characteristic vertical CHL distribution types

To evaluate and compare the heterogeneity of vertical CHL profiles in a systematic way, we classified the measured CHL profiles into 6 characteristic types depending on whether a SCML was detectable and whether the CHL concentrations differed between the upper part and the lower part of the water column (Fig. 2). Following Dekshenieks et al. (2001), a SCML is defined as a subsurface CHL layer whose amplitude is distinctly higher than adjacent water columns and the thickness is relatively thin compared to whole water column; the characteristics in amplitude and thickness display persistence in reasonable temporal and spatial scales. Considering the transient and turbulent environmental conditions, as well as the notable variability in vertical CHL concentrations in our system, we modified these criteria to capture the layer features and to reflect the general character of SCMLs in our system. To select potential candidates for SCML in the profiles, we applied three steps: First, we identified points where the first-order derivative of the CHL profiles switched from positive to negative (Fig. A.3.b). Second, to identify the edges of a potential SCML, within 5 m of the potential layer peak, the local maxima in the second-order derivative of a CHL profile above and below the peak were assigned as the upper and lower edges of the SCML, respectively (Benoit-Bird et al., 2009) (Fig. A.3.c). Third, to evaluate the significance of the potential SCML, the amplitude of the peak was compared to the background value (Fig. A.3.a). We estimated the local background value by linearly interpolating the upper and lower edges' values to the depth of the peak. A SCML was only recognized if the candidate satisfied the 3 following threshold criteria. Criterion 1: To discard peaks resulting from local fluctuations, the peak amplitude of a potential SCML was required to be 2.5 times larger than the standard deviation of the CHL profiles within a 5 m extent upward and downward from the peak. Criterion 2: The peak value was required to be 2 times higher than the background value (Fig. A.3.a). Criterion 3: To exclude CHL layers with weak gradients, the relative CHL gradient above and below the peak was required to exceed 0.125 m^{-1}. Here, we used the relative gradient instead of the absolute gradient to exclude the effects of spatial variability in CHL amplitudes and to make it possible to process all profiles with the same threshold criteria. The relative gradient was calculated by dividing the CHL gradients between the peak and edges by the peak value.

Under the condition that a SCML was present, we divided the whole water column into 3 sublayers: an upper layer, a middle layer corresponding to the SCML and a lower layer. Otherwise, we divided the water column into sublayers depending on the difference in CHL concentrations between the upper and lower parts of the water column (Fig. A.4). We selected the depth corresponding to the maximum absolute difference between averaged CHL concentration above and below to split the whole water column into upper and lower parts (Fig. A.4.b). The difference in the CHL concentrations among the sublayers was quantified by the ratio between the sublayers (Fig. A.4.a). By applying this method, the spatial variability in CHL was also excluded and we could process all profiles using the same analysis criteria.

After we divided the water column into 3 (SCML present) or 2 (no SCML present) sublayers, we classified the CHL profiles into 6 groups depending on the CHL ratios among the sublayers. A complete flow chart of the profile classification method is presented in Fig. A.5. If the averaged CHL ratio between two sublayers was larger than 2 (Appendix A), the difference between the two sublayers was regarded as significant. The 6 types of vertical CHL profiles (Fig. 2) were then defined as follows. Type 1, SCM: A SCML was present, and the mean CHL concentration of the SCML was notably higher than that of the upper and lower parts of the water column. No significant difference in the mean CHL value between the upper and lower parts of the water column was present (Fig. 2a). Type 2, higher CHL concentrations in the lower layer (HCL): Relatively high CHL concentration was present in the lower part of the water column without the appearance of a SCML (Fig. 2b). Type 3, higher CHL concentrations in the upper layer (HCU): Relatively high CHL concentration was present in the upper part of the water column without the appearance of a SCML (Fig. 3c). Type 4, well-mixed (WM): Neither a SCML nor a significant difference in CHL concentrations between the upper and lower parts of the water column was found. In many profiles with a SCML, the upper or lower parts were not symmetric with respect to the subsurface layer; in other words, the mean CHL value in the SCML was significantly higher than that in one part but not the other. These profiles were classified as two transient types as follows (Fig. 2d). Type 5: The mean CHL value in the SCML was higher than that in the upper part of water column but not that in the lower part (SCM-HCL) (Fig. 2e). Type 6: The mean CHL value in the SCML was higher than that in the lower part of water column but not that in the higher part (SCM-HCU) (Fig. 2f).

To investigate the seasonality of vertical CHL distribution patterns, we binned profiles into 4 segments depending on water depth: 10–15 m, 15–25 m, 25–35 m, 35–45 m. We grouped the 10 campaigns into 4 growing seasons: early spring (319: March 2010; 353: April 2011), late spring (303: May 2009; 325: May 2010), summer (308: July-August 2009; 331: July 2010; 359: June 2011), and autumn (312: September 2009; 336: September 2010; 365: September 2010). The spring season was divided into early and late spring regarding to whether the spring bloom decayed, with reference to the surface CHL concentration estimates from remote sensing data (ESA Ocean Colour Climate Change Initiative (OC-CCI; http://www.esa-oceancolour-cci.org/) (Müller et al., 2015).

We performed several sensitivity analyses on our selection criteria. For the detection of SCMLs, we assessed the sensitivity of the second and third criteria introduced above. Among all profiles with SCML candidates (the first-order derivative of the CHL profile crosses 0 in water columns deeper than 5 m), the proportion of confirmed SCMLs stabilized at approximately 20% when the threshold of peak-background ratio was set between 1.125 and 1.7 and the relative gradient ranged from 0.05 to 0.2 m^{-1}. Fewer SCMLs are recognized with stronger criteria (with higher value), and vice versa. Based on the uncertainty analysis regarding the varied F: CHL, we have to choose the peak-

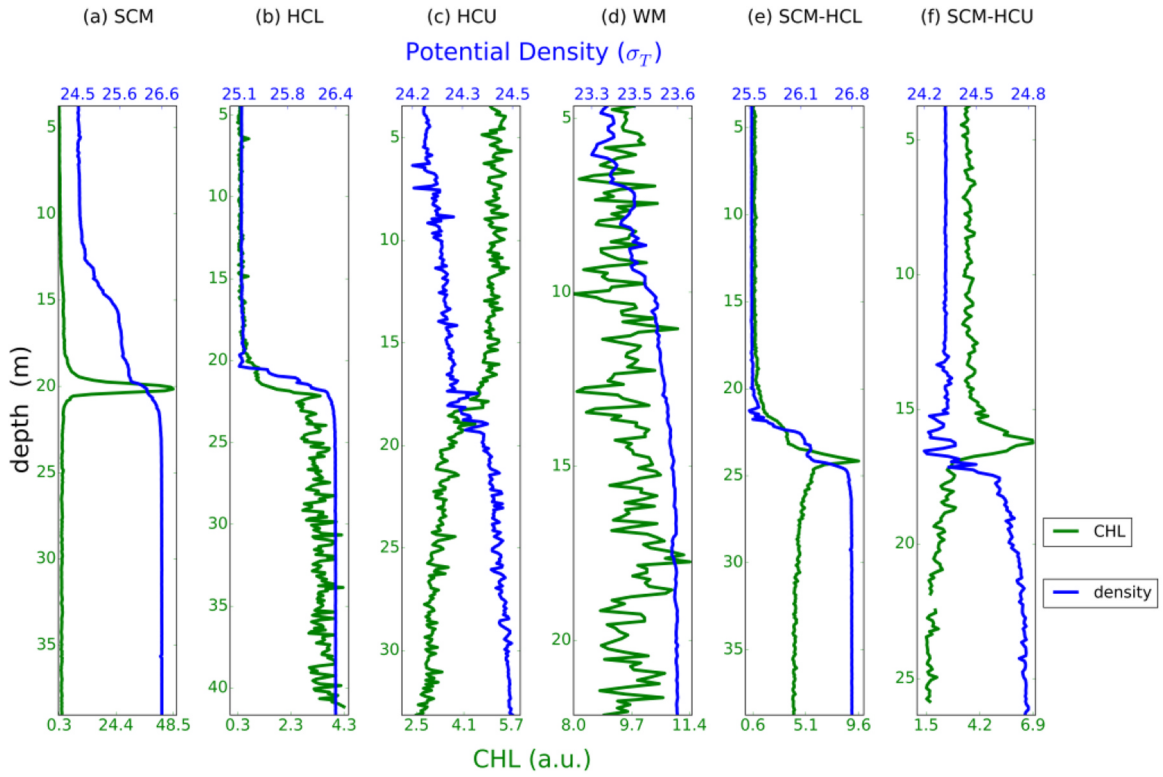

Fig. 2. Example CHL profiles. (a) SCM: Subsurface CHL maximum is detectable. No notable difference of CHL concentration between the upper and lower layer. (b) HCL: CHL concentration in the lower layer of the water column is higher than that in the upper layer. (c) HCU: CHL concentration in the upper layer of the water column is higher than that in the lower layer. (d) WM: Well-mixed CHL profile. (e) SCML-HCL: A subsurface CHL maximum layer is detectable and the averaged CHL concentration in the upper part of the water column is distinguishably lower than that in the lower part. (f) SCML-HCU: A subsurface CHL maximum layer is detectable and the averaged CHL concentration in the upper part of water column is distinguishably higher than that in the lower part.

background ratio as 2 to exclude the condition that the higher CHL indicated by fluorescence signal is due to the increase F: CHL in subsurface layer. When applied this criterion of peak-background ratio, among all potential SCMLs, 10% satisfied the threshold criterion. It indicates that the chosen criteria guaranteed the separation of SCMLs from background noise and, at the same time, ensured that the analysis remained selective.

To select the optimal critical ratio between sublayers, we varied the ratio of averaged CHL concentrations among sublayers from 1.5 to 2.5, with a step of 0.1. More profiles were classified as WM when higher critical ratios were used. Even if SCMLs were present, the profiles were more frequently identified as transient types, i.e., SCM-HCL and SCM-HCU, when higher critical ratios were applied. When we increased the critical ratio values to 1.8, the number of profiles classified into the 4 major types (SCM, HCL, HCU, and WM) was insensitive as it was for smaller critical values. , with the number of profiles changing by no more than 9%. Notably, the appearance of a SCML would not necessarily classify the profile as SCM if the mean CHL value in the SCML was not distinguishable from that of the other sublayers.

2.4. Quantify the resuspension signal in the bottom mixed layer

To investigate the source of high CHL concentrations in the lower mixed layer, we detected CHL peaks near the bottom (CPB) and CHL gradients in the deepest 5 m (CG5) in the CHL profiles to identify resuspension. There were two criteria for the detection of CPB: 1) The peak value in the bottommost 5 m should be at least 1.5 times higher than the average value in the lower layer. The mean value in the lower layer was used as a substitute for defined background values, which we have used for the detection of SCMLs since the layer bound detection possessed high uncertainty near the bottom. 2) The relative gradient had to be larger than 0.0625 m^{-1}. The calculation of the relative gradient was done in a similar way to that of SCMLs. CHL gradients in the deepest 5 m in CHL profiles (CG5) were calculated as follows: the averaged CHL value in the deepest 1.25 m in the profile was subtracted from the averaged CHL value in the deepest 5–7.5 m in the profile and then divided by the depth interval, which is 5 m here. Here, we adopted the average value of depth intervals rather than single points to minimize the bias caused by local spikes and discontinuities in profiles. Since many profiles presented an increasing trend downward instead of a sharp increase at the bottom, we also calculated the mean gradient of CHL in the lower part of the water column (in the SCM-HCL, HCL and SCM profiles), referred to as CGL for short, to represent the general CHL variation trend with depth. If the CHL concentration increased with depth, the gradients (CG5, CGL) mentioned above possess positive values, and if the CHL concentration decreased with depth, the opposite is true.

To further investigate the mechanism driving resuspension, we examined the occurrence of resuspension with respect to tidal phases. We counted the number of profiles belonging to tidal phase segments and the occurrence of resuspension signals (e.g., CPB) in the profiles. By dividing the number of profiles possessing resuspension signals by the number of profiles measured in each tidal-phase segment, we obtained the relative occurrence of resuspension for each tidal phase.

2.5. The physical environment

To analyze the vertical CHL distribution of profiles in the context of the environmental setting, we calculated the irradiance and turbulence as important physical factors for phytoplankton growth and distribution. We calculated euphotic layer depth and assessed stratification using observational data, as measured irradiance and density data were available. As no simultaneous measurements of turbulence were available, the following data from a 3D simulation were used:

dissipation rates ε, velocity shear S^2, kinematic viscosity ν, and current information. To ensure the consistency of our analysis, we also applied squared buoyancy frequency computed from simulated water density profiles to do validation of simulated data sets.

Euphotic layer depth: Euphotic layer depth is an indicator to quantify how deep the irradiance can penetrate and sustains photosynthesis. Here, we calculated the euphotic layer depth to examine whether irradiance is able to influence the SCML depth. We used short-wave radiation records and profiles of attenuation coefficients to calculate the irradiance profiles in the water column according to the Lambert-Beer law (Swinehart, 1962). Daily mean values of two surface short-wave radiation data time series were used to represent the average irradiance conditions for the GB. These two measuring stations for surface short wave radiation are located on Norderney and List on the island of Sylt (Fig. 1) at the southern and eastern border of the GB, respectively (DWD, 2015). The value of 7 W/m^2 was chosen (Brand and Guillard, 1981) as the lowest amount of irradiance necessary for the growth of phytoplankton, and we defined the euphotic layer depth as the depth where absolute irradiance values hit this threshold (Banse, 2004).

To better interpret the vertical distribution of CHL with respect to the hydrodynamic setting, we calculated some proxies to quantify the counteracting processes between mixing and stratification that may help initiate, maintain or undermine the vertically heterogeneous CHL structures. Here, we briefly outline the definitions and calculations of these proxies for the turbulent status, as used in previous analytical work (Steinbuck et al., 2010).

Squared buoyancy frequency: SCMLs and other vertical CHL patterns were often associated to the intensity of stratification. The intensity of stratification can be evaluated by squared Brunt-Väisälä or buoyancy frequency N^2, which is defined as follows:

$$N^2 = -\frac{g}{\rho_0}\frac{d\rho}{dz} \tag{1}$$

where g is the gravitational acceleration, ρ_0 is the averaged potential water density of the whole vertical profile, dz represents the vertical sampling step in binned data sets (10 cm) and ρ is the potential density value at each vertical bin in the profile. To categorize the vertical density profiles with respect to stratification status, we first selected the segments in each profile where N^2 exceeds 0.001 s^{-2} as pycnocline candidates. Among these pycnocline candidates, we merged segments if the distance between them was smaller than 0.5 m and neglected pycnocline candidates that were too thin (i.e., those with thicknesses of less than 1 m). These two steps were designed to exclude the impact of noise. As a final step, the selected and merged segments within the shallowest and deepest 5 m of the measured profiles were also discarded since the undulating motion of the vehicle could generate artificial gradients in the density profiles. Choosing this step-wise criterion allowed the detection of multiple pycnoclines, which have been observed in the GB. We used the observed potential water density to calculate N^2 here. To support the analysis of physical factors of the vertical CHL distribution, similar to the statistical processes applied to determine the seasonality of the vertical CHL distribution pattern, the occurrence of stratification was statistically grouped into segments by depth – 10–15 m, 15–25 m, 25–35 m, and 35–45 m – and into 4 seasons, as mentioned in Section 2.3 (Fig. 3).

Diffusion coefficient: Turbulent mixing can redistribute CHL concentrations between adjacent sublayers and undermine gradients in layers in which CHL potentially accumulates or grows. In our study, the diffusivity was calculated proportionally to the ratio between dissipation rate ε and squared buoyancy frequency (Osborn, 1980):

$$Kz = 0.2\frac{\varepsilon}{N^2} \tag{2}$$

Richardson number: Velocity shear counteracts the stabilizing effect of stratification. This competition is expressed by the gradient Richardson number:

$$Ri = N^2/S^2 \tag{3}$$

The critical gradient Richardsen number is Ri = 0.25. For Ri < 0.25 the flow is likely to remain turbulent (Kundu et al., 2016).

Buoyancy Reynolds number: The interplay between stratification and turbulence is quantified by the buoyancy.

$$Re_b = \varepsilon/(\nu N^2) \tag{4}$$

Reynolds number: When the Re_b is smaller than 15, stratification dominates. In contrast, turbulence is unaffected by stratification when the Re_b is greater than 100. When the Re_b ranges from 15 to 100, stratification is affected by turbulence (Monismith et al., 2018).

Simpson-Hunter parameter: The stability of stratification is quantified by the ratio between the cube of the mean tidal current speed $\bar{u}$ during one tidal cycle and the water depth h (Pingree and Griffiths, 1978; Simpson and Hunter, 1974)

$$SH = log_{10}(\bar{u}^3/h) \tag{5}$$

The Simpson-Hunter parameter indicates the tendency for a formerly stratified water column to become mixed. The larger the value is, the stronger the rates of tidal energy dissipation per unit mass are, and the easier the stratification can be disrupted.

Since only a limited number of the physical factors discussed above were simultaneously measured during the SCANFISH cruises, we obtained values for the turbulence dissipation rate ε, kinematic viscosity ν, squared shear S^2 and mean tidal velocity $\bar{u}$ from a 3D hydrodynamic simulation with the General Estuarine Transport Model (GETM) (Gräwe et al., 2015). By using vertically adaptive coordinates (Hofmeister et al., 2011), the vertical resolution of the computational layers increases at locations where strong stratification occurs, thus ensuring improved resolution of the spatial and temporal variability in stratification. The GETM set-up simulated the southern North Sea and Baltic Sea with a horizontal resolution of 1.8 km and 42 vertical layers. The model simulations covered the time span of all campaigns. We used output from the hindcast run, which was stored in snapshots every 2 h. We interpolated the model results linearly in time and space to obtain the corresponding hydrodynamic conditions for each measured data point.

Before further analysis, we ensured sufficient consistency between the simulated and observed density profiles. First, we binned the simulated data into 10 cm vertical resolution grids and extracted the pycnocline using the same method applied for the observed density profiles. Second, when stratification developed, we calculated the density gradients within the pycnocline to quantify the intensity of the stratification, for which the discrepancy between the observations and simulations should not exceed 0.015 σ_t m^{-1}. Further discussion of the physical conditions of SCMLs was restricted to profiles in which the simulation met the validation criterion.

3. Results and discussion

3.1. General hydrographic conditions during the cruises

In accordance with our criteria, among all analyzed downward profiles 54% were stratified. Stratification mainly emerged in campaigns 303 (May 2009), 331 (July 2010), and 359 (June 2011) when stratification was present in at least 80% of the profiles.

The seasonality of stratification has been revealed by the proportions of stratified profiles (Fig. 3). As noted by previous studies, the onset of thermal stratification occurs in late spring/early summer (Pohlmann, 1996a, 1996b). In the study area, haline stratification could superimpose mixing in regions with freshwater inflows (Simpson et al., 1991). In early spring, the proportion of stratified profiles was not more than 25%. The proportion of stratification peaked in June and began to drop in August. In autumn (September), proportion of stratification decreased down to approximately 50% of the profiles in deeper areas and only approximately 20% of the profiles in shallow areas. Due to the

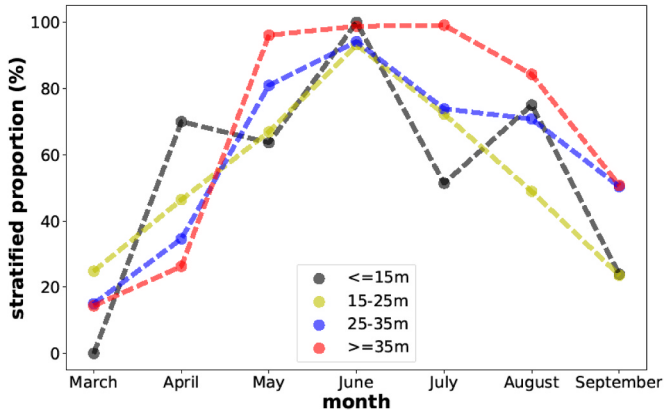

Fig. 3. Seasonality in stratification as revealed by the SCANFISH data. Density profiles are grouped for each month and depth segment; the corresponding stratified percentage is calculated.

rather moderate weather conditions during the sampling periods of the cruises, which is not necessarily representative (Geyer et al., 2015) in terms of the climatological conditions in longer time scales, we expected that the stratified proportions should be higher than the mean climatological conditions.

3.2. Seasonal characteristics of CHL profiles

Approximately 68.7% of all profiles showed a vertically homogeneous CHL distribution. The HCU type were observed in 11.5% of all profiles and the HCL type accounted for approximately 16.6% (Fig. 4). Only a small subset (1.9%) of all profiles were identified as the SCM type. The transient types SCM-HCL and SCM-HCU only represented a tiny proportion in the typology analysis, together accounting for 1.3%. We therefore merged these two transient types with the SCM type (in total accounting for 3.2%) in the following analysis of the seasonality of the vertical CHL profiles. We only separate these two transient types when transformation among different distribution types is discussed (cf. Section 3.4).

The proportions of the WM type corresponded to the seasonal stratification/mixing cycle (Fig. 3). They decreased starting in late spring, reached the lowest level in summer and increased again in autumn. More profiles displaying defined vertically heterogeneous CHL distributions were found in deeper areas. The SCM type only emerged under strong stratification, in summer, its proportion increased with water depth, from 2.0% in the 15–25 m region to 20.0% in regions deeper than 35 m. No SCM type appeared in areas shallower than 15 m. In other seasons, SCM profiles were rarely detected, with proportions no larger than 1.0%. In late spring, the HCL type dominated except for WM type, particularly in areas shallower than 15 m. In autumn, in addition to the increased occurrence of WM, the HCU type dominated in all depth segments except WM type, accounting for 26.7% in areas deeper than 35 m and approximately 2.2–15.2% in shallower areas. The occurrences of the SCM and HCL profiles decreased in autumn.

The high standard deviation in the seasonality of the CHL profile types (Fig. 4) can be attributed to the significant variability in our system and the availability of observed profiles in each season assessed in our study. In deeper regions (≥ 25 m), the appearance of SCM profiles varied among campaigns. In campaigns 331 (July 2010) and 359 (June 2011), the extensive distribution of SCM profiles was closely related to strong stratification; in contrast, in campaign 312 (August 2009), under strong mixing, few SCM profiles were detected, even in deeper areas.

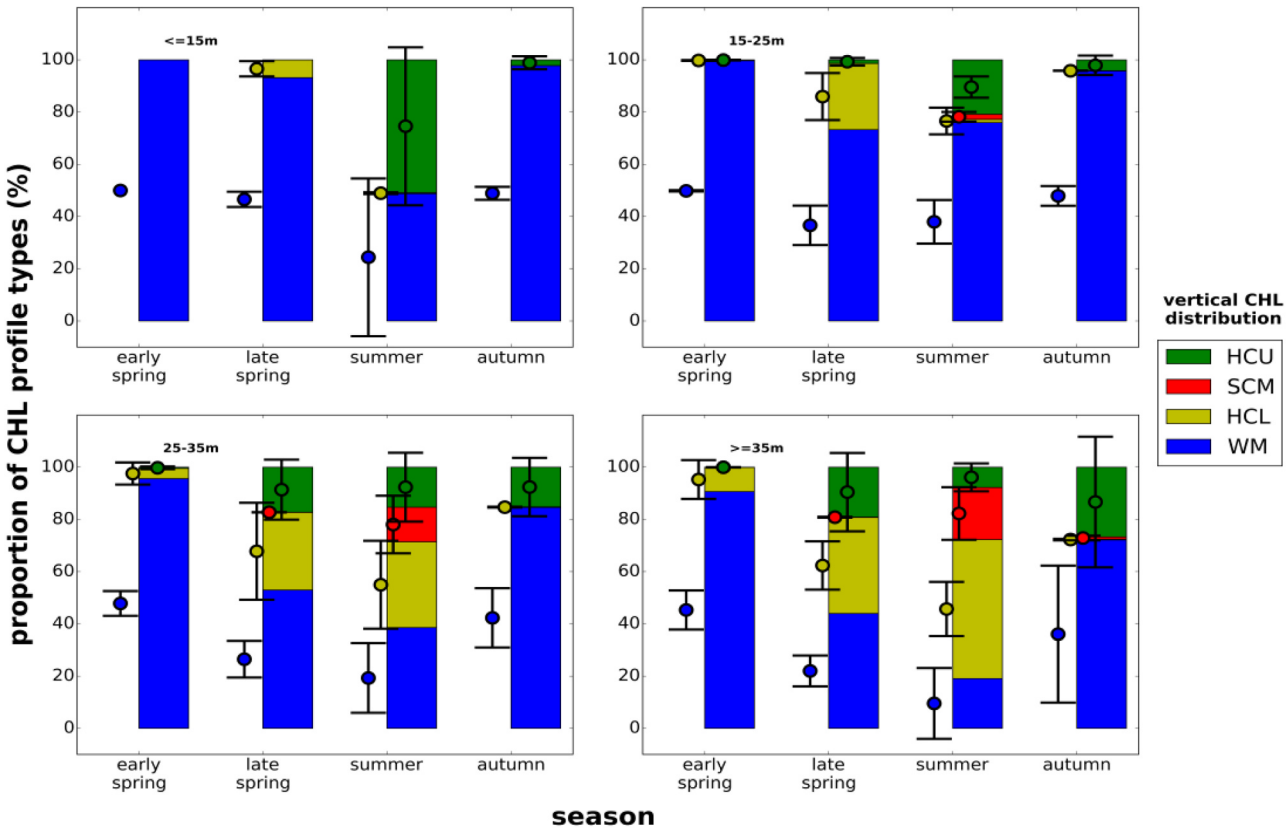

Fig. 4. Occurrences (in percent) of different CHL vertical distribution types in different water depth segments (shallow: 10–15 m, relatively shallow: 15–25 m, relatively deeper: 25–35 m, deep: 35–45 m). WM: well-mixed type. HCU: higher CHL mean concentration in the upper part of the water column than that in the lower part, without a SCML. HCL: higher CHL mean concentration in the lower part of water column than that in the upper part, without a SCML. SCML: subsurface CHL maximum layer. The transient types (SCM-HCU and SCM-HCB) are combined into the SCM type because of the emergence of SCML. Error bars represent standard deviations among cruises.

The SCM type also developed in moderately shallow regions (15–25 m) when strong stratification occurred (campaign 331: July 2010).

The occurrences of the HCU and HCL types also displayed substantial variability, especially in spring. The upper layer of the water column normally favors of phytoplankton growth in spring, due to higher availability of irradiance compared to that of the lower layer. However, higher CHL concentrations in the upper layer were not necessarily detectable in our observations because of the dilution resulting from vertical mixing in the water column. In addition, the proportions of HCU and HCL profiles in the late spring also depended on the variability in the decay phases of spring blooms in specific areas and onset time of stratification, even if we have grouped campaigns into seasonal groups based on the general flourishing patterns from satellite images. The CHL that sank down can remain suspended in the lower part of the water column and barried below the pycnocline.

3.3. Occurrence of subsurface CHL maximum layers (SCMLs)

3.3.1. Physical and biogeochemical characteristics of SCMLs

In a comparison of the stratification patterns among different water depth segments and seasons, the occurrence of SCMLs was basically in line with stratification, and the SCM type was detectable in summer and in deeper water, where stratification was observed in at least 66.8% of the profiles. The most extensive and notable SCMLs were observed in summer during campaigns 331 (July 2010) and 359 (June 2011). In these campaigns, SCMLs were present in 16.0–20.9% of the stratified water columns, with horizontal extents ranging from 50 km to 250 km. More than 90% of the SCMLs exhibited a thickness in the range of 4–6 m. In the SCMLs, the averaged CHL concentrations were primarily 3–9 a.u. and approximately 10% reached 10 a.u. The CHL concentration in the upper mixed layers was lower than that in the SCMLs, and more than 90% of surface layer concentrations were less than 2 a.u. In the calibration process, we found that the variation range of F: CHL is no more than factor 2. Considering the F: CHL's variation in the same profile, 66.7% of F: CHL(subsurface/surface) lies in between 0.5 and 2 (Table A1). If considering this variation, the peak value of fluorescence in Fig. 5a lies no more than 2 (a.u.), the indicated peak value of CHL should be no more than 4 (a.u.). The disparity is not as large as the raw fluorescence data has indicated but we can still expect that the CHL value in the SCML is higher than that in the upper layer. The averaged CHL concentration in the lower mixed layer was distinctly higher than that in the upper mixed layer, which we will address further in Section 3.4.

The characteristics of the physical environment and the CHL concentrations in all profiles with detectable SCMLs are summarized in Fig. 5. SCMLs were only detected within pycnoclines with stable stratification and physical conditions in the pycnoclines were distinct from those in the layers above and below (Fig. 5). The flow within the pycnocline was typically stable (Ri > 1/4, Fig. 5f) and the buoyancy Reynolds numbers were smaller than 15. The vertical diffusivity K_z was primarily in the range 10^{-6} - 10^{-5} m^2s^{-1} within the pycnocline. Shear instability (Ri < 1/4) was present in the lower mixed layer in more than half of the profiles and in the upper mixed layer in 10% of the profiles. Compared to the turbulence in the pycnocline, the turbulence in the upper mixed layers was stronger, but these layers were still dominated by stratification (Re_b < 15). In the lower mixed layers,

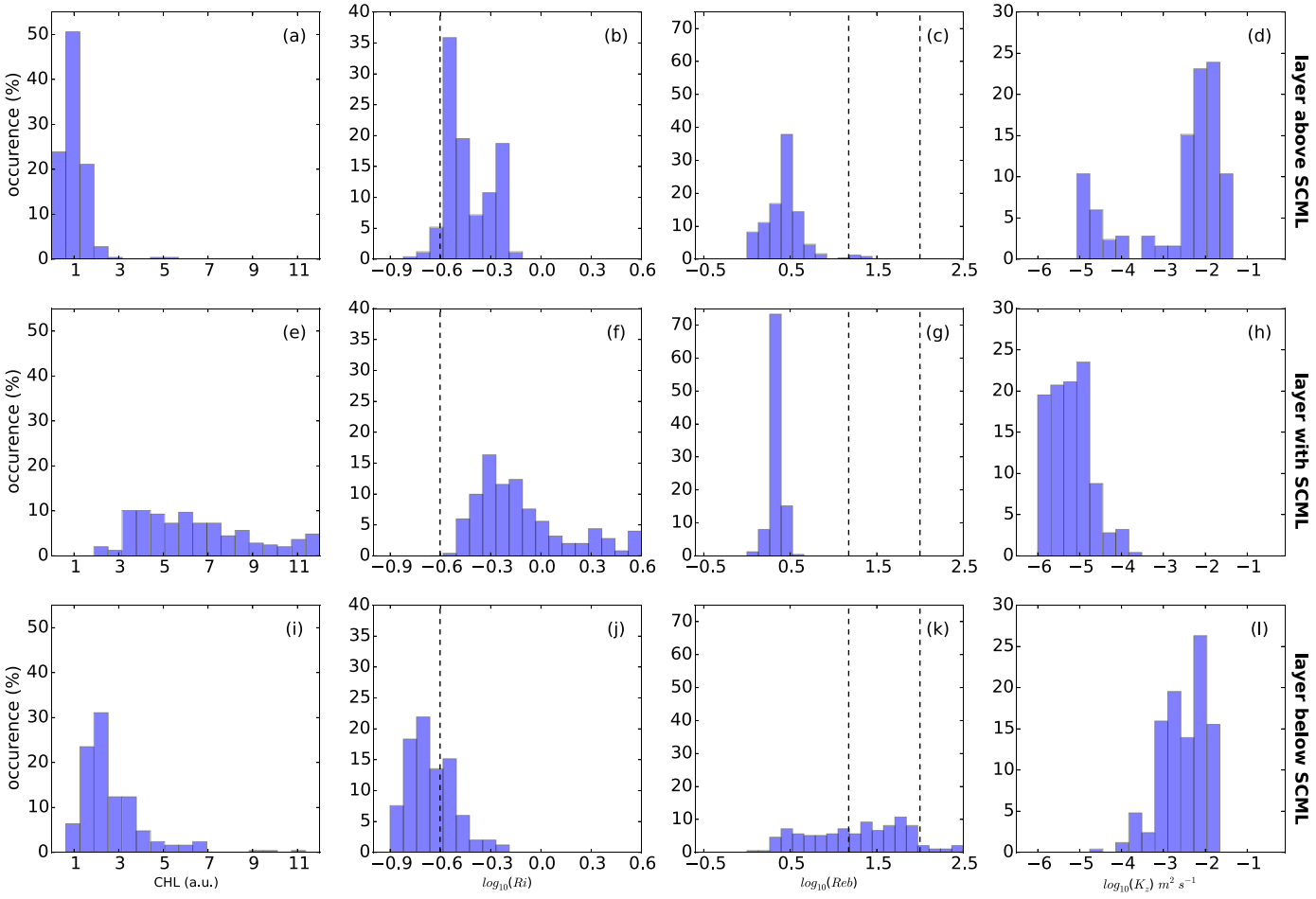

Fig. 5. Histograms of vertically averaged CHL concentration, log_{10}-transformed Richardson number R_i, buoyancy Reynolds number Re_b and vertical diffusivity K_z in 3 sublayers for all profiles with a SCML. The water columns have been segmented into three sublayers: the layer above the SCML (a,b,c,d), the layer containing the SCML (e,f,g,h) and the layer below the SCML (i,j,k,l). Critical values, such R_i = ¼ and Re_b = 15 and 100, have been marked with vertical dashed lines.

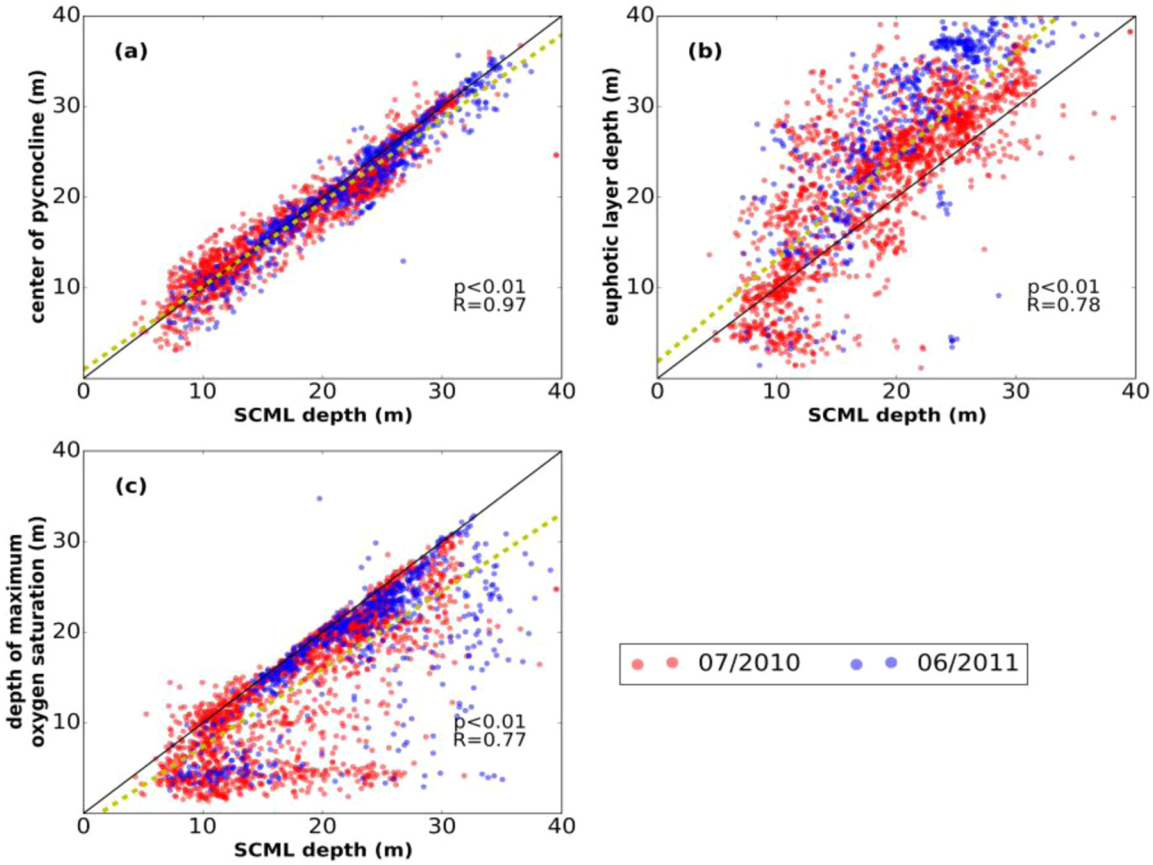

Fig. 6. Pairwise comparison between the depths of the peaks of subsurface CHL maximum layers and the centers of pycnoclines (a), euphotic layer depths (b) and depths of oxygen saturation maxima (c). The regression results are marked by the yellow dashed line, and the 1:1 line is depicted by the black line.

more than half of the records exhibited Re_b values of > 15%, and 10% exhibited Re_b values of > 100; hence, the lower layers were systematically more turbulent than the pycnocline and the upper mixed layer in most profiles, highlighting the dominant role of tidally induced turbulence in the GB. The distribution of vertical diffusivity in the upper and lower mixed layers spanned 6 orders of magnitude, mostly within the range of 10^{-3}–10^{-2} m^2s^{-1}, approximately 3 orders of magnitude higher than that in the pycnocline. The layers corresponding to SCMLs displayed low diffusivity and stable characteristics (Fig. 5). The buoyancy Reynolds number and eddy diffusivity coefficient are not independent of each other; they both rely on the ratio between the dissipation rates and the squared buoyancy frequency. For a given dissipation rate, the higher the buoyancy frequency is, the more stable the interior layer; thus, a SCML is more easily sustained. This was confirmed by the relationship between SCMLs occurrence and the squared buoyancy frequency values for all profiles (Fig. B.1). SCMLs were not observed in weakly stratified water columns until the N^2 reached 0.02 s^{-2}. The occurrence of SCMLs increased with the maximum buoyancy frequency, approaching approximately 90% when the N^2 approached 0.54 s^{-2}.

In addition to the physical conditions, we compared the vertical locations of SCMLs with the pycnocline center and other biochemical parameters to explore the dependence of SCMLs on environmental factors. The CHL peaks in SCMLs were closely co-located with the center of the pycnocline, which we defined as the location of the highest squared buoyancy frequency (Fig. 6a). The locations of CHL peaks in SCMLs were mostly shallower than the euphotic layer depth and were only weakly correlated with the euphotic layer depth (Fig. 6b). Within the euphotic zone, the potential for active photosynthesis is expected, as confirmed by the high correlation between the vertical locations of SCML peaks and highest oxygen saturation values (Fig. 6c). This correlation proved that the SCMLs identified here were photosynthetically active rather than being merely sinking remains. Photosynthesis in SCMLs has also been observed in the Baltic Sea (Bjornsen et al., 1993; Kononen et al., 1998), which were suggested by the consumption of nutrients instead of oxygen, in such an anoxic environment.

3.3.2. Systematic features of SCMLs in the GB

We find that the occurrence of stable SCMLs was related to strong stratification, which reduces turbulent mixing. However, based on previous studies on the preservation of vertical CHL distribution under variable turbulent conditions, several additional mechanisms have been discussed. As suggested by Omand and Mahadevan (2015), the nitracline is co-located with the pycnocline and provides stable conditions with a potentially optimal balance between light and nutrient resources, thereby offering suitable conditions for phytoplankton growth and accumulation (Beckmann and Hense, 2007). In addition, observations have shown that mobile phytoplankton species can swim directionally to nutrient resources diurnally (Cullen and Horrigan, 1981) or position themselves at the nitracline, which can be well below the surface mixed layer depth (Brown et al., 2015). Whether the self-positioning capability of mobile species can result in CHL accumulation depends on how turbulent the physical background setting is compared to the positioning capability of the phytoplankton. Previous studies evaluated the swimming capability of phytoplankton with respect to turbulent mixing via the Péclet number (Simpson and Sharples, 2012):

$$P_e = \frac{L_s^2/K_z}{L_s/\nu_c} \tag{6}$$

where L_s is a representative length scale, such as the thickness of mixed layers or the pycnocline, K_z is the vertical diffusivity, and ν_c is the

vertical swimming speed of phytoplankton.

The Péclet number indicates that turbulent diffusion dominates over motility for $P_e << 1$, while phytoplankton have appreciable control over their position when $P_e >> 1$. If we consider K_z to $10^{-2.5} m^2 \cdot s^{-1}$ for the mixed layer and assume that the length of the mixed layer depth is 15 m for the GB, with typical swimming speeds of phytoplankton ν_c on the order of 10^{-4} m s^{-1} (Cullen and Horrigan, 1981), the Péclet number would correspond to a value of 0.47, which implies that mobile phytoplankton cells would have difficulty positioning themselves in the mixed layer. Once phytoplankton cells are mixed into the vicinity of the pycnocline where K_z is assumed to be $10^{-5} m^2 \cdot s^{-1}$ and the presumably extent is approximately 6 m, the Péclet number would reach 60, indicating that a vertical position in the pycnocline could by maintained by mobile phytoplankton. If we consider that the swimming speed varies among species and when taking typically species in GB in summer, such as species of the genera *Ceratium* and *Dinophysis* (Löder et al., 2012), given the typical swimming speed as 250 $\mu m s^{-1}$ (Levandowsky and Kaneta, 1987) and 104 $\mu m s^{-1}$ (Nielsen and Kiørboe, 2015), the result holds.

In areas with seasonal stable stratification, the CHL concentration has been previously related to physical factors. For example, the CHL concentration decreases with depth (Brown et al., 2015) or increases after nutrients are entrained by wind-driven mixing events (Carranza and Gille, 2014). Based on our data, there were no obvious instantaneous correlations between the vertical CHL distribution and other physical or biological factors, except that the spatial pattern of integrated CHL concentrations in the euphotic zone, i.e. their local maxima, were associated with the occurrence of fronts (not shown here). Time lag correlations could not be studied based on only the snapshots from the SCANFISH data. Our data are not suitable to resolve the revolution process of stratification and the development of SCML, especially in such a shallow and energetic system as the GB, where stratification can be interrupted by strong wind induced mixing, even in summer. In contrast to the southern North Sea, the deeper northern North Sea possesses more stable stratification in summer. The SCMLs in the northern Dogger Bank area have been confirmed to have long durations and to be highly consistent based on observations and simulations (Fernand et al., 2013).

The representativeness of our SCANFISH sampling data for the physical and biological characteristics in the GB merits attention. Considering that the weather condition is representative in the specific years and locations but not necessarily represent the climatological conditions in longer time scales (Geyer et al., 2015), we expected that, the GB should be more turbulent and less stratified than the conditions revealed by our data sets. If continuous data sets covering longer time scales are available, profiles with SCMLs are likely to account for lower proportions.

3.3.3. SCML dynamics during wind mixing

Complementary to the deduction from the statistical analysis, the vertical CHL distribution pattern associated with the hydrodynamic environment has been discussed in a case study. Two transects were sampled twice in July 2010 during campaign 331, i.e., on July 14th and 16th, before and after a significant wind event. The western branch transect extended from 54.2ºN to 55.0ºN in the longitudinal direction, and the northern branch transect extended from 6.3ºE to 7.5ºE in the latitudinal direction (Fig. 1). Since wind mixing events triggered by wind, as pointed out by former studies (Rumyantseva et al., 2015; Williams et al., 2013), are able to re-erode SCM in pycnocline and supply nitrate into pycnocline or even reach the surface water column. We used these sections to explore the conditions under which SCMLs persist or decay during a wind mixing event and how the vertical CHL distribution evolves with changes in the hydrodynamic setting.

According to the re-analysis product from the NCEP Climate Forecast System (Saha et al., 2010), the weather conditions were mild before and during the first sampling event. The wind speed did not exceed 5.38 m s^{-1} during the 24 h before the sampling began (July 13th, 4:00) or during the sampling. In the early morning of July 15th, wind speeds increased and reached 13.77 m s^{-1} at 13:00 on July 15th and dropped to 7.7 m s^{-1} at 16:00 on July 16th. From the early morning of the 15th until noon on the 16th, more than half of the hourly averaged wind speed values were greater than 12 m s^{-1}. The second sampling of the western branch was performed during the diminishing phases of the wind event. For the northern branch, the second sampling was performed after the wind event, when the wind speed was comparable to the earlier calm conditions.

On July 14th before the storm, stable stratification was observed in both transects. A double-pycnocline structure (Fig. 7) was present and contained an intermediary zone with CHL concentrations that were higher than those in the upper mixed layer. A well-structured SCML was present at the base of the lower pycnocline, with average values of 8.1 a.u. in the western branch (Fig. 7a) and 10.0 a.u. in the northern branch (Fig. 7e). In the western branch, below the second pycnocline, the lower mixed layer showed an average CHL concentration of 4.8 a.u., which was around 5 times higher than that in the surface mixed layer (Fig. 7a). Compared to the western branch, there was no evidence for resuspension in the northern branch, and the CHL concentration in the lower mixed layer was comparable to that in the upper mixed layer (Fig. 7e). At the eastern end of the northern transect, the water depth is less than 20 m. Here, CHL concentrations are enhanced in the surface mixed layer, even if a high subsurface CHL concentrations are detectable (Fig. 7e).

Based on a comparison of the observations before and after the storm event, the upper pycnocline vanished as a result of wind-driven mixing, but the lower pycnocline persisted in most areas. In the western branch, the SCML at the base of the lower pycnocline in the first sampling event disappeared (Fig. 7b), except in areas between 54.4°N and 54.5°N where the subsurface CHL layer was more visible than before. Resuspension was prominent in the middle part of the western branch. At the southern end (54.2–54.4°N) of the western branch, the pycnocline broke down, and the CHL subsurface layer decayed (Fig. 7b). In the northern branch, most of the subsurface CHL layer persisted except at the eastern end, where both the pycnocline and the subsurface CHL layer were absent in the second sampling (Fig. 7f).

The persistence or decay of the pycnocline and the corresponding spatial variability was in line with the stability of stratification as quantified by the Simpson-Hunter number (Fig. 7d, h). A higher Simpson-Hunter number indicates stronger tidal mixing, making the stratification more susceptible to mixing. The decay of the pycnocline demonstrated the sensitivity of the stratification to wind events in the shallow southern North Sea, which has been illustrated in previous studies involving simulations (Schrum et al., 2003a, 2003b; Schrum, 1997) and observations (Carpenter et al., 2016; Schultze et al., 2017).

The spatial persistence and decay of the stratification was basically in line with hydrodynamic characteristics, whereas the variation of SCMLs was more complex. Most SCMLs decayed during this wind event. Because of the weakening of the double pycnocline structure after the wind event, the upper boundary of the whole stratified interior (including the whole double pycnocline structure in the first sampling) deepened by approximately 10 m. Furthermore, considering that the SCML was located at the base of the lower pycnocline, we compared the upper and lower boundaries of the lower pycnocline in the first sampling to those in the second sampling. The upper boundary of the lower pycnocline deepened after the wind event in most parts of the two branches (Fig. 7c, g). The variation in the lower boundary of the stratified layer fluctuated around 0, but remained mainly positive, indicating that most of the lower boundary deepened. It is likely that the accumulated CHL was mixed up during the deepening of the pycnocline. Although, it cannot entirely be excluded that biological processes which could contribute to the changes, it is rather unlikely because these are usually not effective enough on such short time scales. The variation in CHL concentration throughout the whole water column and

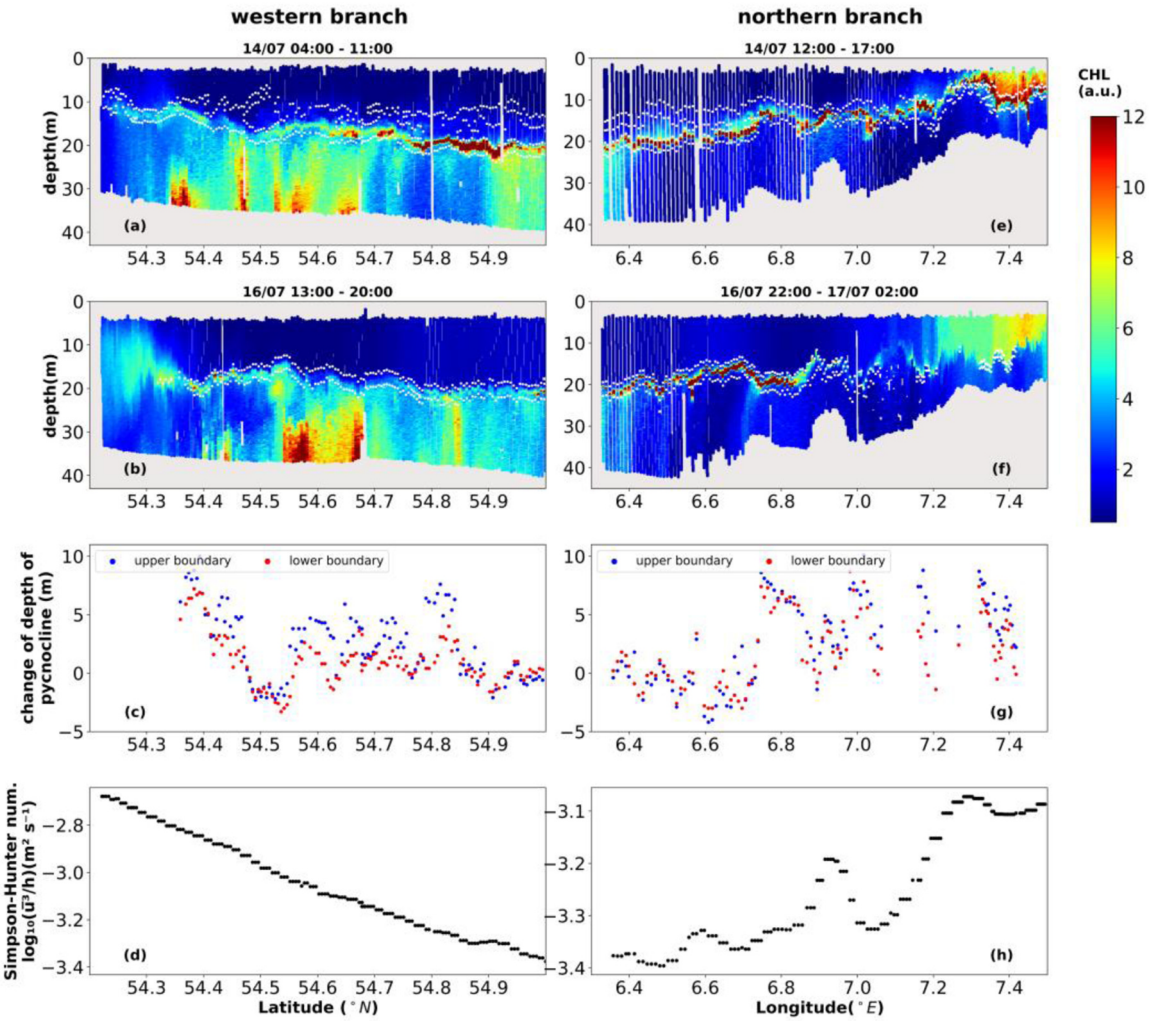

Fig. 7. Scatter plot of CHL (arbitrary units) of two transects measured on 14/07/2010 and repeated on 16/07/2010. The western branch is plotted in the left panels (a,b), and the northern branch is plotted in the right panels (e,f). The detected pycnocline is depicted by white dots for reference. The variations in the depths of the upper and lower boundaries of the pycnocline are depicted in (c) and (g). The distributions of the Simpson-Hunter number are shown in (d) and (h).

in each sublayer divided by the pycnocline was in the range of the natural growth of phytoplankton, but again, natural growth in low light conditions would be an unlikely candidate for the changes. The increase in CHL concentration in the lower mixed layer in the western branch could also come from resuspension (Fig. 7b). The increase in CHL concentration in the upper mixed layer could be either mixed up from a pre-existing SCML or produced following the entrainment of nutrients from lower layers due to the deepening of the pycnocline. The decrease in CHL concentration in the stratified interior could also be induced by enhanced grazing due to suspended zooplankton during wind events, but again this can be considered as rather unlikely due to short timescale and substantial turbulence during the wind event, which would limit capturing success of zooplankton.

3.4. The formation of high CHL concentrations in the lower layers (HCL)

The HCL-type profiles occur frequently, especially in campaigns performed in late spring (Fig. 4). Thus, an exploration of the mechanisms leading to high CHL in the bottom mixed layer is necessary. It is possible that this phenomenon results from different directions of residual currents below and above the pycnocline, which bring phytoplankton from different source regions to the same area (McCandliss et al., 2002). This might be the case especially for floating and non-sinking species, such as *phaeosystis* which also dominates in the German Bight in spring (Iriarte et al., 1991) (together with diatoms). If the local vertical mixing plays a role, there are two related hypotheses: 1) the HCL type profiles involves CHL from layers above either because of sinking or erosion from pre-existing SCMLs or 2) the HCL type involves CHL from below because of re-suspension effects. In this section, we first test these two hypotheses by investigating CHL gradients near the bottom and in the lower layers of water columns. Afterwards, potential hydrodynamic drivers and responsible biochemical factors will be discussed.

Resuspension has been quantified by the presence of a CHL peak in the bottom layer (CPB) and a corresponding CHL gradient in the upper boundary of the CPB. Among the HCL profiles, 30% had detectable CPBs, whereas only 5.7% of SCM profiles and 15% of SCM-HCL profiles had CPBs. The relative upward gradients in the CPBs in HCL profiles were generally larger than those of SCM and SCM-HCL profiles. The higher occurrence of resuspension signals and higher gradients in the upper branch of the CPBs indicate the importance of resuspension in the formation of HCL-type profiles. In addition to the CPB, the CHL gradients in the lower layer (CGL) can be used to approximate the CHL variation with depth across a relatively long vertical segment. In all profiles classified as SCM, CHL continually decreased from the base of the SCML to the bottom. Furthermore, 76% of SCM-HCL profiles also showed higher CHL concentrations at the base of the SCML, indicating that CHL was mixed down or sank from the subsurface layers. However,

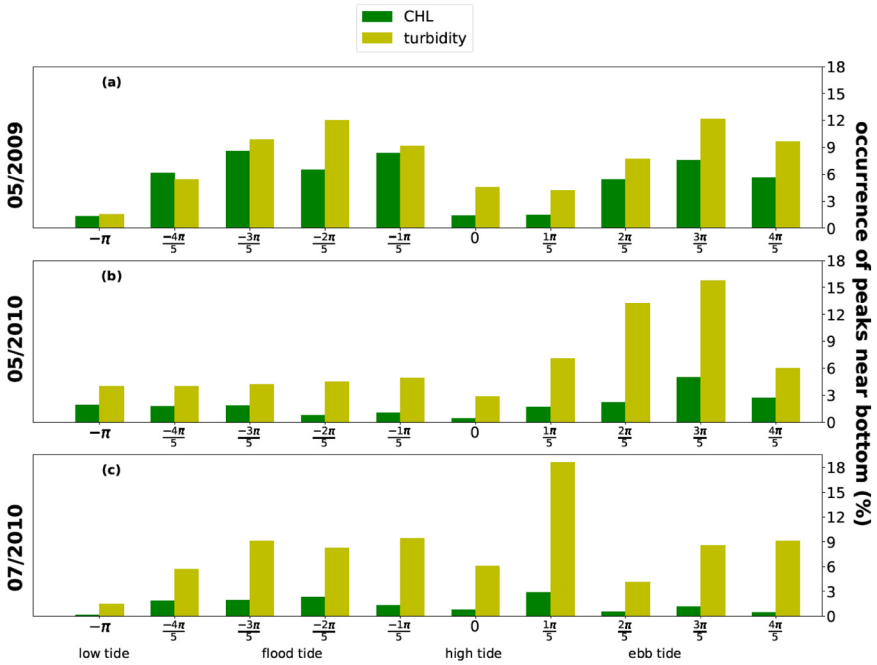

Fig. 8. The occurrence of CHL peaks near the bottom (CPBs) with respect to the tidal cycle. The number of profiles with recognized CPBs was divided by the number of profiles sampled in the corresponding tidal phase interval, yielding the occurrence shown here. Labels on the X-axis represent the tidal cycle: Pi represent low tide; 0 represents high tide; negative values indicate flood tide; positive values indicate ebb tide.

in the remaining 24% of SCM-HCL profiles, the CHL concentration showed that more CHL accumulated towards the bottom. The CHL concentration increased with depth in the lower layers in almost all HCL profiles. By examining the CHL gradients in the bottom mixed layer and the existence of CPBs, we infer that a considerable proportion of the high CHL concentrations come from the bottom in HCL profiles and some SCM-HCL profiles, probably caused by resuspension.

To address the relevance of tides, the dominant hydrodynamic feature in this study area (Otto et al., 1990), to resuspension in the observed profiles, herein we explore the occurrence of resuspension with respect to the tidal cycle, which was retrieved from model simulations. To improve the statistical significance, only campaigns with more than 400 CPBs in total and more than 10 CPBs in each tidal phase segment were included (Fig. 8). We also identified resuspension signals in terms of turbidity as a supplemental forcing indicator, assuming that the resuspension of other materials would not be resource limited, unlike that of CHL.

In the two campaigns performed after the spring bloom, CPBs occurred more frequently during the flood and ebb tidal phases (between $-\frac{3\pi}{5}\sim-\frac{2\pi}{5}$ and $\frac{2\pi}{5}\sim\frac{3\pi}{5}$). Especially in May 2009, the occurrence of CPB during tidal phases $-\frac{4\pi}{5}\sim-\frac{\pi}{5}$ and $\frac{\pi}{5}\sim\frac{4\pi}{5}$ was significantly higher than that near the high tidal phases (phase segments around 0) and low tidal phases (phase segments around π) (Fig. 8a). In May 2010, resuspension was only pronounced during ebb time ($\frac{2\pi}{5}\sim\frac{3\pi}{5}$), as was the resuspension based on turbidity signals (Fig. 8b). In contrast, in the campaign performed during the summer, July 2010, the occurrence of resuspension-related CHL signals exhibited no obvious occurrence pattern with the tidal phase (Fig. 8c). Since the occurrence of resuspension-related turbidity signals displayed a better relationship with the tidal cycle, the decoupling between the resuspension of CHL and turbidity in summer indicated the depletion of CHL containing materials.

Resuspension CPB signals only accounted for approximately 10% of the analyzed downward profiles. Even if the criterion of upward gradient of potential CPB was ignored, i.e. resuspension would be considered if profiles with CHL concentration of the peaks near bottom notably higher than the mean CHL concentration in the lower mixed layer, the occurrence of resuspension would not exceed 27% of all analyzed profiles. One reason could be that resuspended CHL is mixed up by strong turbulence. The widespread high CHL concentrations in the lower mixed layer (in HCL and SCM-HCL profiles), for which most profiles showed a smooth curve rather than a steep gradient in the lower layer, could be resulting from the transformation of profiles with significant resuspension signals in the bottom and by further mixing or advection. The efficiency of vertical dispersion can be estimated by the length scale analysis applied by Denman and Gargett (1983):

$$Z(t)^2 = 2K_z t. \tag{7}$$

Given the eddy diffusivity K_z value of $10^{-2.5}\ m^2 s^{-1}$ in the bottom mixed layer in the GB, it would take 105 min (t) for a cell to be mixed 20 m (Z(t)) vertically away from its original position. Although the vertical diffusivity values are far from vertically homogeneous in the bottom mixed layer, this scale analysis suggests that once CHL-bearing materials on the bottom are resuspended, it would take a short time for them to become mixed throughout the whole lower mixed layer. Bounded by the pycnocline (or an interior layer with low diffusivity), the resuspended CHL would be kept in the lower part of the water column instead of being mixed further upward. Due to the strong tidal mixing in the lower mixed layer, the transient type (SCM-HCL), which only accounts for a small proportion of the measured profiles, should be short-lived. Furthermore, no matter how efficient the bottom tidal currents are in resuspending materials, the resuspension of CHL would be rarely detectable if there is no available resource (Jago and Jones, 1998) at the bottom due to earlier resuspension and/or benthic predation and remineralization.

The seasonal difference in the significance of resuspension signals in CHL profiles could be attributed to seasonal changes of availability of CHL at the bottom. Instead of only using the occurrence of CPBs, which occur in only a small subset of the profiles, we calculated the CHL gradient in the deepest 5 m (CG5) in all the profiles and summarized the increases or decreases in CHL with depth (Fig. 9). The occurrence of positive CG5s, which indicated more CHL available near the bottom than in the adjacent layer above, showed a distinct seasonal pattern. The CG5% increased from approximately 50% in early spring to more than 75% in late spring during the decay of the spring bloom. Thereafter, the percentage decreased throughout summer (30%) to autumn (approximately 20%).

The CG5 seasonality indicated that the resuspension processes of CHL were resource limited in summer and autumn. This pattern was also revealed in the seasonality of vertical CHL distribution patterns (Fig. 4): the proportion of HCL type decreased in summer and especially

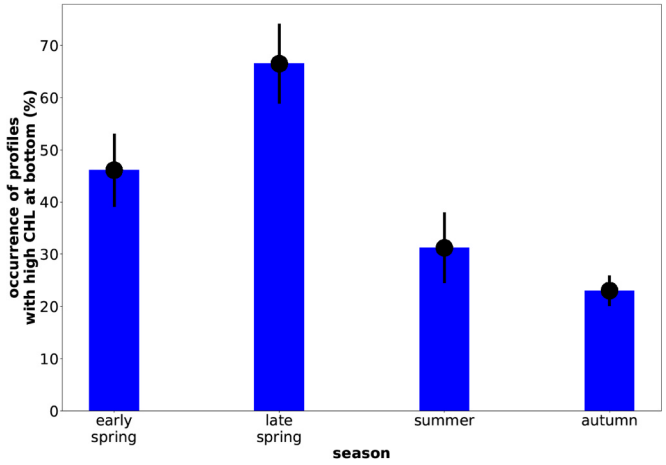

Fig. 9. Percentage of positive CG5 (CHL gradients in the deepest 5 m of profiles) for different seasons. Error bars represent standard deviation among campaigns.

in autumn, when near-bed CHL had been depleted. This seasonal pattern in the availability of resuspension resources at the bottom revealed in our study is similar to previous results for benthic fluff layers. Formed by the sinking of phytoplankton cells, fluff can easily be resuspended and transported (Jago et al., 2002). The amount of fluff resources is greatest after the spring bloom and decreases in other seasons due to resuspension and predation, leading to resource limitation with respect to further resuspension (Jago and Jones, 1998). We have to stay cautious when we derive CHL from fluorescence signal which showed high values near bottom, since fluorescence signals could be influenced by the presence of other organic particles near the bottom, especially in areas with high turbidity, such as the GB. However, the high CHL signals observed near the bottom confirm former measurements of high CHL near bottom at the German Bight and in nearby areas close to the European continent. In these studies, CHL data were derived from water sample directly (Jago and Jones, 1998), from calibrated fluorometer (Millward et al., 1998) or Reineck's box-corer (Dauwe et al., 1998; Jenness and Duineveld, 1985) taken from sea bed. They all confirmed that high CHL concentration can be detected below the pycnocline after the onset of stratification due to phytoplankton sinking or trapped by the pycnoline (Jones et al., 1998). The high concentrations are mostly detectable in late spring because produced organic matters in spring bloom settled down (Boon and Duineveld, 1996; Jago et al., 1993). Compared to other stations (Fourteens, Frisian Front and Skagerrak), the GB showed the strongest predominance of surface deposition and strongest surface accumulation of organic matter at the sea floor, mainly due to longer residence time of water in the GB and the intense local production (Dauwe et al., 1998). Given sufficient settled materials, resuspension driven by tide and waves is detectable (Jago et al., 1993; McCandliss et al., 2002). Due to sinking and aggregation with suspended particulate matter (SPM), the CHL-rich materials in the bottom mixed layer form fluff layers which are also sensitive to resuspension given strong bottom shear stress and sink down in low energy conditions (Jenness and Duineveld, 1985; McCandliss et al., 2002). It is likely that production is able to persist given enough irradiance penetration below the pycnoline (Peeters et al., 1995). However, light limitation plays an important role in controlling primary production in the shallow North Sea, typically in spring and in windy conditions in summer and autumn (Su et al., 2015), since light penetration is very sensitive to resuspension events (Jones et al., 1998).

Separating the resuspension process from sinking based on our data is challenging. It would be problematic to categorize all positive CHL gradients in the bottom mixed layer (increasing CHL concentrations with water depth) as a resuspension signal since many phytoplankton species have a higher densities than water and tend to sink (Smayda, 1971). Especially in the decaying process of the spring bloom, after the nutrients in the surface layer are exhausted, massive amounts of phytoplankton cells sink down. However, the sinking speed of some cells slows once the nutrient status improves and the buoyancy of the cells increases (Steele and Yentsch, 1960). Additionally, some cells may also become neutrally buoyant because of the increasing density with depth.

In addition to CHL accumulating near the bottom, high CHL concentrations in the lower layers may also come from overlying SCMLs, as 76% of SCM-HCLs displayed higher CHL concentrations at the base of the pycnocline than that of segments further below. Considering physical processes, removal of CHL from a pre-existing SCML can result in high CHL concentration at the base of the pycnocline (Sharples et al., 2001). If the elevated CHL levels in the pycnocline are eroded by tidal currents, periodic downward pulses of biomass should be resolved in the time series. This hypothesis has already been corroborated in simulations of frontal systems in which periodic mixing/stratifying processes and the consequent biomass distribution were shown (Schrum et al., 2006; Sharples, 2008). When the turbulent mixing energy in the lower layer reaches the pycnocline, the high gradient of CHL at the base of a SCML can be smoothed or the whole SCM structure can be eroded. A SCM profile can be transformed into an HCL-SCM profile or even an HCL profile when the subsurface layer structure is eroded and disappeared. This assumption was further supported by comparable vertically integrated CHL concentration in the water segment including pycnocline and lower mixed layer in different CHL vertical distribution types (SCM-HCL, HCL, SCM), under conditions that these different CHL vertical distribution type profiles were detected in adjacent areas (Table B1). Notably, tidal mixing processes from the bottom are not always detrimental to the persistence of SCMLs. In addition to mixing organic matter from an SCML down to the bottom of the water column, tidal mixing can also inject nutrients into the pycnocline, triggering the production and maintenance of photosynthetic activity there (Sharples et al., 2007; Zhao et al., 2018). The vertical mixing rates can also influence the persistence of sinking species in the bottom mixed layer by returning phytoplankton cells to depths where irradiance is high enough to sustain photosynthetic activity (Huisman et al., 2002). The light availability is also sensitive to the existence of SCMLs but also to increasing turbidity by mixing.

In the GB system, most SCMLs are shallower than the euphotic layer depth (Fig. 6b), which also indicates that high CHL below the pycnocline has the chance to stay photosynthetic active. This mechanism can further support the formation of HCL and SCM-HCL. This is an interpretation besides the vertical mixing mechanism since phytoplankton biomass or CHL are not conservative. Light penetration below the pycnoline has higher occurrence in summer when the self-shading is not as strong as in spring (Table 2)

Limited by the data availability (no nutrient data and no particulate organic carbon data), we do not have the chance to further investigate biological factors in the vertical CHL distribution. Moreover, the measured CHL concentrations can not be converted directly to biomass and

Table 2
Occurrence of profiles with euphotic layer depth deeper than the lower limit of pycnocline.

Campaign	HCL type profile Eup. deeper than pyc.(%)	SCM-HCL type profile Eup. deeper than pyc.(%)
07/2010	85.4	81.6
06/2011	74.6	85.7
05/2010	48.1	/
05/2009	8.98	/
08/2009	70.9	16.7
09/2009	50.0	/
03/2010	/	/
09/2010	/	/
04/2011	84.0	/
09/2011	/	/

quantitative estimates are hardly possible, since the CHL:C ratio is variable among species and sensitive to the environment and season, particularly in coastal areas (Alvarez-Fernandez and Riegman, 2014). Given adequate nutrients and low irradiance levels, which meet the lower threshold for sustaining photosynthetic activity, phytoplankton cells tend to use nutrients to generate more pigments to harvest more light energy instead of building biomass (Geider et al., 1997; Macintyre et al., 2000). In reality, the measured CHL-rich patches may consist of multiple species with different light and nutrient requirements. More nutrient-efficient competitors should dominate the upper part of the SCML, whereas superior light competitors should mainly inhabit the lower part of the SCML (Huisman et al., 2004). Oscillations in physical mixing, which modify the dispersion rates of phytoplankton and the upward flux of nutrients, could further promote the phytoplankton diversity (Huisman et al., 2006). Implementing a variable allocation of internal resources, simulations suggest that the vertical CHL distribution in the GB critically depends on the cellular storage of nutrients and pigmentary materials (Kerimoglu et al., 2017).

4. Conclusions

By performing an in-depth analysis of vertical CHL profiles in the inner German Bight (GB), we studied the heterogeneity in vertical CHL distribution using measured high-resolution vertical transects. Our analysis provided the first quantitative description on heterogeneity & homogeneity of vertical CHL distribution in the GB and explores potential mechanisms. More than half of profiles show vertical homogeneous distribution of CHL; extrapolating this to the full range of weather conditions, this proportion would further increase considering that the averaged hydrodynamic background is more turbulent than in our observations which mainly encountered calm whether conditions. However, heterogeneous vertical distribution of CHL, especially in stratified season, merits more attention. After the onset of stratification in late spring, higher CHL in the bottom mixed layer than that in the surface layer has been observed. Several mechanisms may lead to this phenomenon, such as diatoms' sinking, water mass advection and phyto-acclimation. Due to the shallowness of the GB, in more than half of the profiles with high CHL concentration below the pycnocline, the euphotic layer depth is deeper than the lower limit of the pycnocline, which indicates that phytoplankton cells in the lower layer have the chance to access enough irradiance to keep photosynthesis active. However, the frequently observed high bottom concentrations can hardly be explained by local growth; resuspension was identified as an important candidate to explain this phenomen.

Our study revealed that the vertical distribution of CHL in a shallow and tidally energetic system can be attribute to both physical processes (i.e. resuspension and turbulent mixing) and biological processes (i.e. growth and sinking of phytoplankton cells). The large fraction of near-bottom high CHL regimes in the stratified season indicates the importance of the benthic-pelagic coupling in tidally energetic shallow areas, such as the German Bight and points to the importance to consider this adequately in theory and modelling studies in tidally influenced shallow seas, which has implications for estimates of carbon flux (Bauer et al., 2013) and nutrients cycling (Beckmann and Hense, 2017). In such a shallow area where small proportion of organic matters will be mineralized in the water column (Lutz et al., 2002; Suess, 1980), the interface of water column and sediments acts as buffer to release nutrients slowly long after the most productive season (Provoost et al., 2013). Particularly in the southern North Sea, the resuspension process (Thompson et al., 2011), the activity of macrobenthos and bacteria (Franco et al., 2010) further complicate the benthic-pelagic coupling (Zhang and Wirtz, 2017). Our study and high resolution observations like those presented here, can help to assess model tools and identify structural limitations. For example, a validation of some new ecosystem models using vertical transects of CHL shows that even ecosystem models specifically developed for shallow seas, which reproduce well SCM type profiles might have difficulties to do so for the HCL type (Baschek et al., 2017; Kerimoglu et al., 2017). This points to the need to improve process descriptions and parametrizations in modelling tools for coastal areas.

Moreover, since seasonality modulates the vertical heterogeneity of CHL distribution, our study suggests refined in-situ monitoring, with more vertical sampling required in deeper areas during the stratified season (Fernand et al., 2013). Besides, our study points also to the need to develop new approaches to conclude on productivity from remote sensing for stratified shallow shelf sea, since subsurface CHL maxima in those regions may provide a reasonable source of error for remote sensing based estimates (Stramska and Stramski, 2005; Yacobi, 2006). We drew conclusions in this study mainly based on statistical analysis. To analyze the vertical distribution of CHL in a simultaneous bio-physical way, coinciding measurements of vertical CHL profile, organic matter and physical settings are necessary (Ediger et al., 2005; Liu et al., 2017; Sharples et al., 2007). For example, adding observations of particulate organic carbon and CHL data sampled by HPLC method in future studies will provide reliable data sets to investigate physiological contributions to the CHL profiles and evaluate the exchange of organic matter between the upper layer and the bottom layer (McTigue et al., 2015; Smith et al., 2012).

Acknowledgments

The first author would like to express her gratitude to the financial support from the China Scholarship Council (CSC. No.: 201406140121). All authors are indebted to the masters and crews of the research vessel RV Heincke and the different chief scientist conducting the cruises. The cruises were conducted under the grant numbers: AWI-HE303-00, AWI-HE308-00, AWI-HE312-00, AWI-HE319-00, AWI-HE325-00, AWI-HE331-00, AWI-HE336-00, AWI-HE353-00, AWI-HE359-00, AWI-HE365-00. All authors thank H. Rink, H. Thomas, M. Heineke, and R. Kopetzky, for operating the SCANFISH, for processing and quality assurance of the observational data and laboratory work. We are grateful to Kerstin Heymann for performing the HPLC analysis. We thank Ryan North, Ingrid M. Angel-Benavides, Lucas Merckelbach, Jeffrey Carpenter and Yangyang Liu for their suggestions regarding data processing. The GETM simulation data were provided by Ulf Gräwe and Onur Kerimoglu. Use of the remote sensing data was suggested by Hajo Krasemann.

Appendix A. Data calibration and adjustment, method uncertainty and classification details

During these campaigns, samples for chlorophyll a measured by HPLC were collected simultaneously along the SCANFISH transects. At most stations, one sample was taken in the surface layer when the water column is mixed or above the pycnoline when it is stratified. When a stratified water column was encountered, sometimes, a deeper sample was additionally taken below the pycnocline. In total, 124 samples from the surface layer are available; and 59 from subsurface layers. We made use of these data to estimate the general ratio between the CHL concentration and fluorescence signal and to prove that the F: CHL ratio obeys a good linear correlation and does not varied significantly among different season and years. For the classification strategy used for identifying CHL vertical distribution types, we chose a criterion which is significant enough to exceed

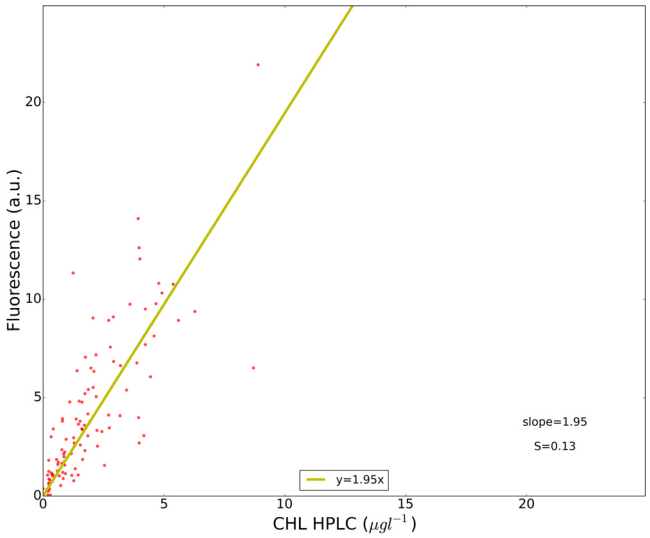

Fig. A1. Relationship between the CHL concentrations estimated from the HPLC measurements and fluorescence value measured by fluorometer.

the range of the uncertainty of F: CHL ratio, therefore the difference of fluorescence over the water column does reflect differences in CHL concentrations, rather than resulting from strongly varying F: CHL ratio. Finally, the classification method was applied for fluorescence profile and HPLC measured CHL data. The similar outcomes from fluorescence profile and HPLC measured CHL data further prove the robustness of the classification method.

The relationship between CHL concentrations and fluorescence was investigated by a simple linear regression analysis. The influence of fluorescence quenching on this relationship was reduced by discarding any data taken around the local noon (9 a.m. to 3 p.m.). For all data points, the obtained regression ratio (F: CHL) is 1.95, with standard error (S) ± 0.13 (with unit of a.u.), from 111 available samples (n) (Fig. A.1). After further distinguishing between below and above pycnocline samples, we found that the F: CHL is 2.15 ± 0.16 in surface samples (n = 76) and 1.73 ± 0.23 in subsurface samples (n = 35) (Table A1). We also checked the F: CHL ratio for its seasonal and inter-annual variability. The F: CHL is 1.95 ± 0.20 in spring (n = 59), 2.28 ± 0.17 in summer (n = 40 and 1.39 ± 0.25 in autumn (n = 12). For different years, the F: CHL is 1.53 ± 0.20 in 2009 (n = 38), 2.10 ± 0.17 in 2010 (n = 49, R = 0.87) and 2.27 ± 0.36 in 2011 (n = 24) (Table A1). Generally, the fluorescence and HPLC measured CHL show a linear relation and the regression is not sensitive to season or inter-annual variability. F: CHL mainly lies in the range between 1.4 and 2.3; the seasonal and inter-annual variability varies but not more than a factor of 2. We take this variation range into consideration when we set the criterion in the classification method (Section 2.3). The influence of varied F: CHL on the classification method was also estimated and given in the following paragraph.

Regarding to the classification of profile types, the issue really matters is the F: CHL's vertical variation within each profile instead of F: CHL's absolute variation among different profiles. To check the relevant influence, we make use of HPLC measured CHL with both surface and subsurface data in the same profile. To quantify the relative variation of F: CHL, we calculated the percentage of profiles with the subsurface vs. surface F: CHL ratio (F: CHL(subsurface/surface)) with value in the range of 0.5–2.0. For dataset excluding noon hours, the percentage is 66.7% (n * = 33) (Fig. A.2). We also checked the seasonal and inter-annual variability (Tabel.A.2). The 0.5 < F: CHL(subsurface/surface) < 2.0% is 61.1% in spring (n * = 18), 71.4% in summer (n = 14). The variation in autumn has not been discussed since there are only 4 profiles available. For the inter-annual variability, the 0.5 < F: CHL(subsurface/surface) < 2.0% is 59.2% in 2009 (n = 13), 66.7% in 2010 (n = 15) and 60% in 2011 (n = 5). As

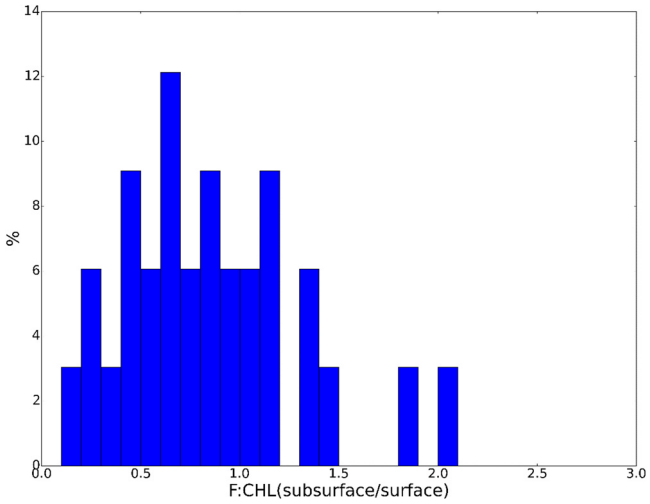

Fig. A.2. Distribution of F:CHL (subsurface/surface) value. Profiles influenced by quenching have been excluded for this analysis.

Table A1
Uncertainty of F: CHL ratio.

Campaign	F: CHL	S	n	0.5 < F: CHL(subsurface/surface) < 2.0 (%)	n*
all samples	1.95(2.0)	0.13(0.13)	111(183)	66.66(56.6)	33(53)
surface	2.15(2.20)	0.16(0.15)	76(124)	/	/
Subsurface	1.73(1.79)	0.23(0.25)	35(59)	/	/
Season	F: CHL	S	n	0.5 < F: CHL(subsurface/surface) < 2.0 (%)	n*
Spring	1.95(2.08)	0.20(0.20)	59(86)	61.1(62.5)	18(24)
Summer	2.28(2.14)	0.17(0.22)	40(71)	71.4(56.0)	14(25)
Autumn	1.39(1.55)	0.25(0.22)	12(26)	100(25.0)	1(4)
Year	F: CHL	S	n	0.5 < F: CHL(subsurface/surface) < 2 (%)	n*
2009	1.53(1.73)	0.20(0.26)	38(67)	69.2(50.0)	13(24)
2010	2.10(2.14)	0.17(0.16)	49(71)	66.7(66.7)	15(21)
2011	2.27(2.31)	0.36(0.25)	24(45)	60.0(50.0)	5(8)

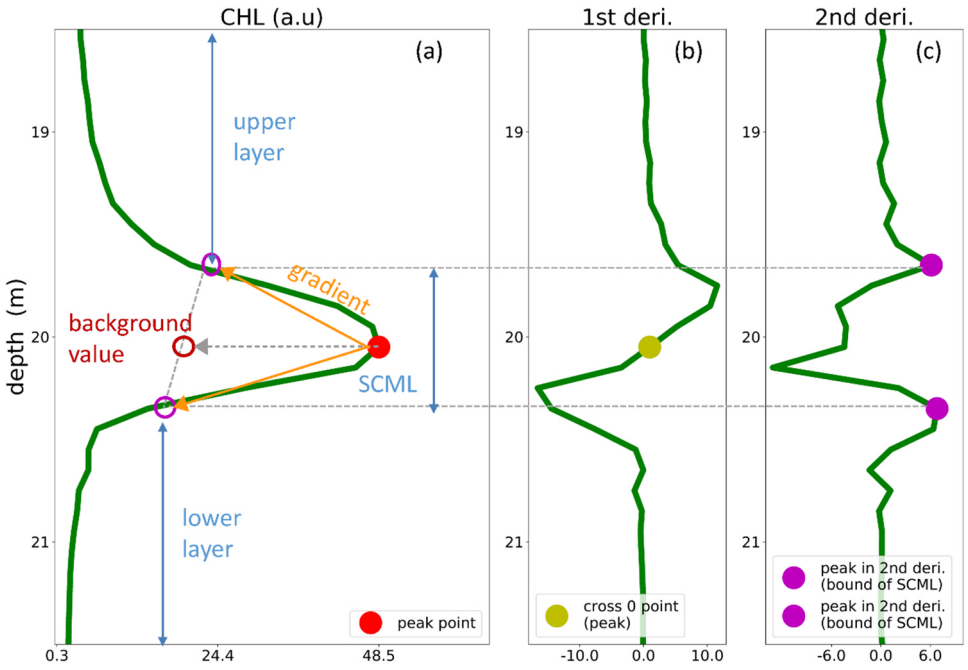

Fig. A3. Schematic diagram for SCML detection in an exemplary CHL profile (a). First (b) and second -order derivative (c) of the measured profiles are used to identify the position of the SCML peak and SCML boundary.

suggested by these cross-validation tests, a factor of 2 in fluorescence between the vertical layers is used as the criterion in the classification of CHL vertical distribution types (Section 2.3). This factor also takes the F: CHL's inter-annual variability and seasonal variability into account.

When we apply the same criterion to classify the fluorescence profile and observed HPLC CHL which possesses both surface and subsurface samples in one station, 75% of joint HPLC CHL samples and fluorescence profiles coming from the same station provide the same profile classification. This is a rather high agreement in classification, taking into account factors adding uncertainty such as comparing profile to single point estimates, the influence of quenching and the variation of CHL fluorescence signals in dependence of species, light availability and other conditions.

Only fluorescence values sampled deeper than 30 m can be assumed to be free of quenching (Guinet et al., 2013), which only holds for the deep ocean but not for shallow coastal waters. We therefore adjusted the surface segment of fluorescence vertical profiles, if the profile was sampled at noon (9 a.m. to 3 p.m.). To identify quenching in noon-profiles, we used exponential regression. If the portion of the profile above the pycnocline (in stratified case) or above the shallowest local maximum fits an exponential regression and the amplitude increases with depth, the influence from quenching is confirmed. In case of a mixed water column, the first local maximum is used to replace all values above (Xing et al., 2012). For the stratified water column, the fluorescence value in the upper limit of the pycnocline was used to replace all values above. In some cases, the quenching effect might pass through the mixed layer into the stratified layer and influence the fluorescence shape within and above the pycnocline, which might be the major source of uncertainty. If the value of surface fluorescence profile approached 0 and showed strong fluctuations which

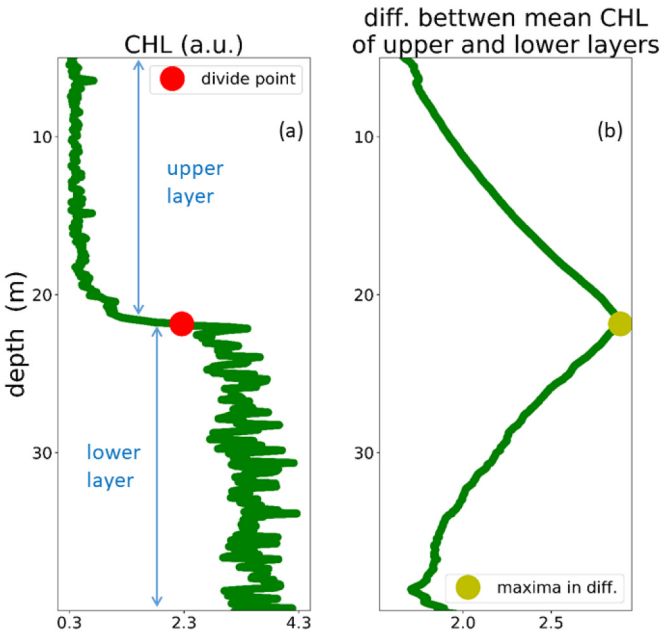

Fig. A4. Schematic diagram for the division of sublayers without a SCML.

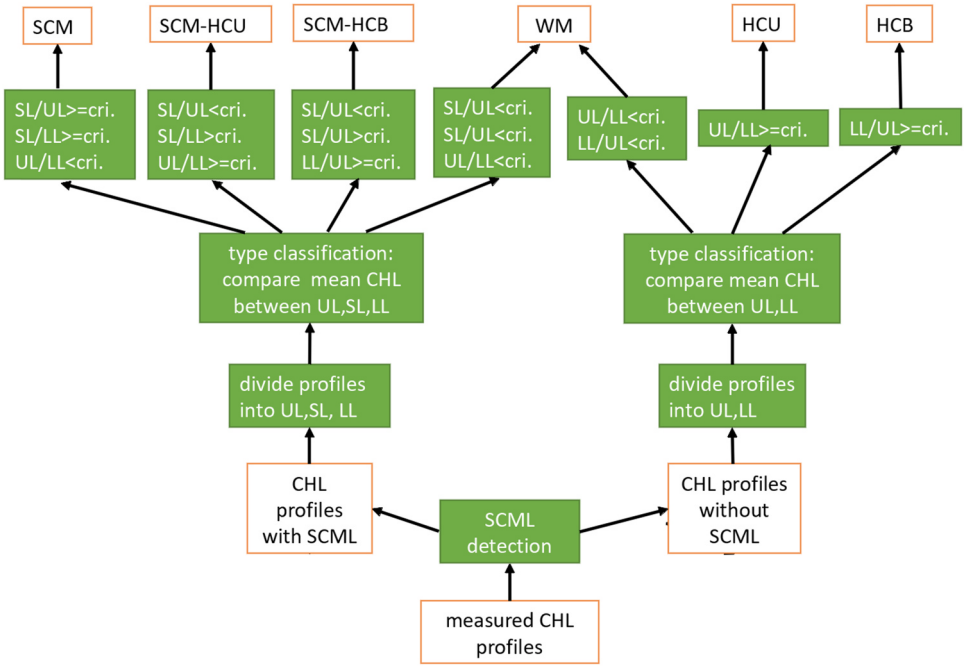

Fig. A5. Flow chart of the classification of CHL profiles.

indicated strong quenching and prohibited exponential fitting, the profile was discarded in following analysis. However, strong quenching rarely happens in the study area.

Appendix B

To test whether vertical mixing could influence vertical distribution of CHL concentration and result in different CHL vertical distribution types (HCL, SCM-HCL, SCM) among adjacent profiles, we compared vertically integrated CHL concentrations in the pycnocline and in lower mixed layers from horizontally adjacent profiles, under the condition that adjacent profiles are classified in different CHL vertical distribution types (HCL, SCM-HCL, SCM) as mentioned above.

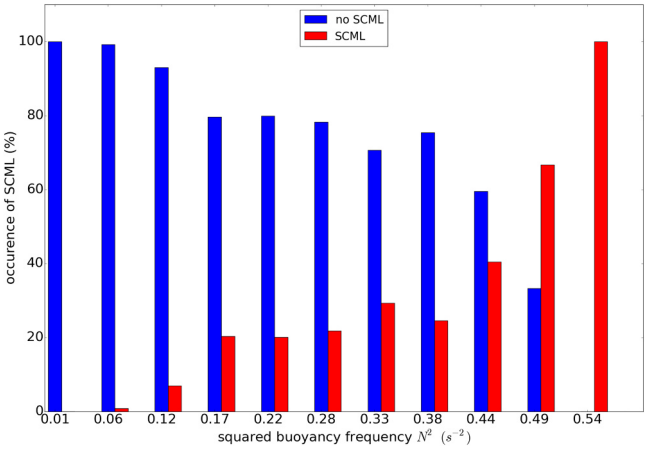

Fig. B.1. The occurrence of subsurface CHL maximum layers in different stratification conditions. The stratification intensity is quantified by the maximum squared buoyancy frequency (N^2) in measured profiles. Note that values of N^2 beyond the listed range are included in the segments of the upper or lower boundaries.

Table B1
relative change of vertical integrated CHL within the pycnocline and bottom mixed layer in different CHL vertical profile types.

Campaign	CHL ratio HCL/SCM (%)	CHL ratio SCM-HCL/SCM (%)	CHL ratio SCM-HCL/HCL (%)
2010,07	70.0	84.3	119.0
2009,08	105.7	115.9	110.0

We pooled profiles classified in type HCL, type SCM-HCL and type SCM within horizontally adjacent 12 profiles (spatial range: 1500–2400 m) and calculated the relative change of integrated CHL concentration in the water column segments including the pycnocline and lower mixed layer. The relative changes of integrated CHL were quantified by the ratio between different CHL vertical distribution types. In Table B1, the relative changes of integrated CHL concentration between HCL type and SCM type profiles are in the first column, between SCM-HCL and SCM type profiles in the second column, between SCM-HCL and HCL type profiles in the third column. Some adjusting profiles in the campaigns July 2010 and August 2009 revealed that relative changes of vertically integrated CHL between different types of CHL profiles vary between 70% and 119%. Vertical integrated CHL concentration (ratios between the pycnocline and lower mixed layer) in different CHL vertical distribution types profiles ending up to similar levels supports the erosion hypothesis that vertical mixing regulates the vertical distribution of phytoplankton. However, this holds for discussion in shorter time scales during which phytoplankton growth and mortality are negligible.

References

Alvarez-Fernandez, S., Riegman, R., 2014. Chlorophyll in North Sea coastal and offshore waters does not reflect long term trends of phytoplankton biomass. J. Sea Res. https://doi.org/10.1016/j.seares.2014.04.005.

Babin, M., Roesler, C.S., Cullen, J.J., 2008. Real-time coastal observing systems for marine ecosystem dynamics and harmful algal blooms: theory, instrumentation and modelling. Oceanogr. Methodol. Ser. https://doi.org/10.1016/j.hal.2010.01.002.2.

Banse, K., 2004. Should we continue to use the 1% light depth convention for estimating the compensation depth of phytoplankton for another 70 years. Limnol. Ocean. Bull. 13, 1–4.

Baschek, B., Schroeder, F., Brix, H., Riethmüller, R., Badewien, T.H., Breitbach, G., Brügge, B., Colijn, F., Doerffer, R., Eschenbach, C., Friedrich, J., Fischer, P., Garthe, S., Horstmann, J., Krasemann, H., Metfies, K., Merckelbach, L., Ohle, N., Petersen, W., Pröfrock, D., Röttgers, R., Schlüter, M., Schulz, J., Schulz-Stellenfleth, J., Stanev, E., Staneva, J., Winter, C., Wirtz, K., Wollschläger, J., Zielinski, O., Ziemer, F., 2017. The coastal observing system for northern and arctic seas (COSYNA). Ocean Sci. https://doi.org/10.5194/os-13-379-2017.

Bauer, J.E., Cai, W.J., Raymond, P.A., Bianchi, T.S., Hopkinson, C.S., Regnier, P.A.G., 2013. The changing carbon cycle of the coastal ocean. Nature. https://doi.org/10.1038/nature12857.

Beckmann, A., Hense, I., 2017. The impact of primary and export production on the formation of the secondary nitrite maximum: a model study. Ecol. Modell. 359, 25–33. https://doi.org/10.1016/J.ECOLMODEL.2017.05.014.

Beckmann, A., Hense, I., 2007. Beneath the surface: characteristics of oceanic ecosystems under weak mixing conditions - a theoretical investigation. Prog. Oceanogr. 75, 771–796. https://doi.org/10.1016/j.pocean.2007.09.002.

Benoit-Bird, K.J., Cowles, T.J., Wingard, C.E., 2009. Edge gradients provide evidence of ecological interactions in planktonic thin layers. Limnol. Oceanogr. 54, 1382–1392. https://doi.org/10.4319/lo.2009.54.4.1382.

Beusekom, J. Van, Brockmann, U., 1999. The importance of sediments in the transformation and turnover of nutrients and organic matter in the Wadden Sea and German Bight. Dtsch. https://doi.org/10.1007/BF02764176.

Bjornsen, P.K., Kaas, H., Kaas, H., Nielsen, T.G., Olesen, M., Richardson, K., 1993. Dynamics of a subsurface phytoplankton maximum in the Skagerrak. Mar. Ecol. Prog. Ser. 95, 279–294. https://doi.org/10.3354/meps095279.

Boon, A.R., Duineveld, G.C.A., 1996. Phytopigments and fatty acids as molecular markers for the. J. Sea Res. 35, 279–291.

Boss, E., Behrenfeld, M., 2010. In situ evaluation of the initiation of the North Atlantic phytoplankton bloom. Geophys. Res. Lett. 37, 1–5. https://doi.org/10.1029/2010GL044174.

Brand, L.E., Guillard, R.R.L., 1981. The effects of continuous light and light intensity on the reproduction rates of twenty-two species of marine phytoplankton. J. Exp. Mar. Biol. Ecol. 50, 119–132. https://doi.org/10.1016/0022-0981(81)90045-9.

Brown, Z.W., Lowry, K.E., Palmer, M.A., van Dijken, G.L., Mills, M.M., Pickart, R.S., Arrigo, K.R., 2015. Characterizing the subsurface chlorophyll a maximum in the Chukchi Sea and Canada Basin. Deep. Res. Part II Top. Stud. Oceanogr. https://doi.org/10.1016/j.dsr2.2015.02.010.

Butterworth, S., 1930. On the theory of filter amplifiers. Exp. Wirel. Wirel. Eng (https://doi.org/citeulike-article-id:5322726).

Carpenter, J., Merckelbach, L., Callies, U., Clark, S., Gaslikova, L., B.B., 2016. A multi-decadal wind-wave hindcast for the North Sea 1949–2014 : coastDat2 11, pp. 1–28. ⟨https://doi.org/10.1594/WDCC/coastDat-2⟩.

Carranza, M.M., Gille, S.T., 2014. Wind forcing, mixed-layer depth and Chl-a response in the Southern Ocean, pp. 22–26.

Charnock, H., Dyer, K.R., Huthnance, J.M., Liss, P.S., Simpson, J.H., Tett, P.B., 1993. Understanding the North Sea system. Philos. Trans. - R. Soc. Lond. A.

Claustre, H., Morel, A., Babin, M., Cailliau, C., Marie, D., Marty, J.-C., Tailliez, D., Vaulot, D., 1999. Variability in particle attenuation and chlorophyll fluorescence in the tropical Pacific: scales, patterns, and biogeochemical implications. J. Geophys. Res. https://doi.org/10.1029/98JC01334.

Cullen, J.J., Horrigan, S.G., 1981. Effects of nitrate on the diurnal vertical migration, carbon to nitrogen ratio, and the photosynthetic capacity of the dinoflagellate Gymnodinium splendens. Mar. Biol. https://doi.org/10.1007/BF00388169.

Czitrom, S.P.R., Budéus, G., Krause, G., 1988. A tidal mixing front in an area influenced by land runoff. Cont. Shelf Res. https://doi.org/10.1016/0278-4343(88)90030-1.

Dauwe, B., Herman, P.M.J., Heip, C.H.R., 1998. Community structure and bioturbation potential of manrofauna at four North Sea station with contrasting food supply. Mar. Ecol. Prog. Ser. 173, 67–83. https://doi.org/10.3354/meps173067.

Dekshenieks, M.M., Donaghay, P.L., Sullivan, J.M., Rines, J.E.B., Osborn, T.R., Twardowski, M.S., 2001. Temporal and spatial occurrence of thin phytoplankton layers in relation to physical processes. Mar. Ecol. Prog. Ser. 223, 61–71. https://doi.org/10.3354/meps223061.

Denman, K.L., Gargett, A.E., 1983. Time and space scales of vertical mixing and advection of phytoplankton in the upper ocean. Limnol. Oceanogr. https://doi.org/10.4319/lo.1983.28.5.0801.

Dietrich, G., 1950. Die natüirlichen Regionen der Nord- und Ostsee auf hydrographischer Grundlage.-Kieler Meeres- forschung. Kiel. Meeres- Forsch. 7, 35–69.

Dippner, J.W., 1993. A frontal-resolving model for the German Bight. Cont. Shelf Res. https://doi.org/10.1016/0278-4343(93)90035-V.

Duineveld, G., Boon, A., 2002. Short-term variations in the fluxes and composition of seston in near-bottom traps in the southern North Sea. Helgol. Mar. Res. 56, 140–148. https://doi.org/10.1007/s10152-001-0091-x.

Ediger, D., Tuğrul, S., Yilmaz, A., 2005. Vertical profiles of particulate organic matter and its relationship with chlorophyll-a in the upper layer of the NE Mediterranean Sea. J. Mar. Syst. https://doi.org/10.1016/j.jmarsys.2004.09.003.

Eisma, D., Kalf, J., 1987. Dispersal, concentration and deposition of suspended matter in the North Sea. J. Geol. Soc. 144, 161–178. https://doi.org/10.1144/gsjgs.144.1.0161.

Fernand, L., Weston, K., Morris, T., Greenwood, N., Brown, J., Jickells, T., 2013. The contribution of the deep chlorophyll maximum to primary production in a seasonally stratified shelf sea, the North Sea. Biogeochemistry 113, 153–166. https://doi.org/10.1007/s10533-013-9831-7.

Franco, M., de, A., Vanaverbeke, J., Van Oevelen, D., Soetaert, K., Costa, M.J., Vincx, M., Moens, T., 2010. Respiration partitioning in contrasting subtidal sediments: seasonality and response to a spring phytoplankton deposition. Mar. Ecol. 31, 276–290. https://doi.org/10.1111/j.1439-0485.2009.00319.x.

Gehlen, M., Malschaert, H., Van Raaphorst, W.R., 1995. Spatial and temporal variability of benthic silica fluxes in the southeastern North Sea. Cont. Shelf Res. 15, 1675–1696. https://doi.org/10.1016/0278-4343(95)00012-P.

Geider, R.J., MacIntyre, H.L., Kana, T.M., 1997. Dynamic model of phytoplankton growth and acclimation: responses of the balanced growth rate and the chlorophyll a: carbon ratio to light, nutrient-limitation and temperature. Mar. Ecol. Prog. Ser. https://doi.org/10.3354/meps148187.

Geyer, B., Weisse, R., Bisling, P., Winterfeldt, J., 2015. Climatology of North Sea wind energy derived from a model hindcast for 1958–2012. J. Wind Eng. Ind. Aerodyn. https://doi.org/10.1016/j.jweia.2015.09.005.

Gräwe, U., Holtermann, P., Klingbeil, K., Burchard, H., 2015. Advantages of vertically adaptive coordinates in numerical models of stratified shelf seas. Ocean Model. https://doi.org/10.1016/j.ocemod.2015.05.008.

Grenander, U., 1959. Probability and Statistics. John Wiley and Sons.

Guinet, C., Xing, X., Walker, E., Monestiez, P., Marchand, S., Picard, B., Jaud, T., Authier, M., Cotté, C., Dragon, A.C., Diamond, E., Antoine, D., Lovell, P., Blain, S., D'Ortenzio, F., Claustre, H., 2013. Calibration procedures and first dataset of Southern Ocean chlorophyll a profiles collected by elephant seals equipped with a newly developed CTD-fluorescence tags. Earth Syst. Sci. Data 5, 15–29. https://doi.org/10.5194/essd-5-15-2013.

Haren H. Van, Howarth M.J., 2004. Enhanced stability during reduction of stratification in the North Sea, 24, pp. 805–819. ⟨https://doi.org/10.1016/j.csr.2004.01.008⟩.

Herdman, W.A.S., 1923. Noounders of Oceanography and their Work; An Introduction to the Science of the Sea. E. Arnold & Co., London. https://doi.org/10.5962/bhl.title.16362.

Hofmeister, R., Beckers, J.M., Burchard, H., 2011. Realistic modelling of the exceptional inflows into the central Baltic Sea in 2003 using terrain-following coordinates. Ocean Model. https://doi.org/10.1016/j.ocemod.2011.04.007.

Huisman, J., Arraya, M., Ebert, U., Sommeijer, B., 2002. How do sinking phytoplankton species manage to persist ? 159.

Huisman, J., Pham Thi, N.N., Karl, D.M., Sommeijer, B., 2006. Reduced mixing generates oscillations and chaos in the oceanic deep chlorophyll maximum. Nature. https://doi.org/10.1038/nature04245.

Huisman, J., Sharples, J., Stroom, J.M., Visser, P.M., Kardinaal, W.E.A., Verspagen, J.M.H., Sommeijer, B., 2004. Changes in turbulent mixing shift competition for light between phytoplankton species. Ecology. https://doi.org/10.1890/03-0763.

Iriarte, A., Daneri, G., Garcia, V.M.T., Purdie, D.A., Crawford, D.W., 1991. Plankton community respiration and its relationship to chlorophyll a concentrationinmarine coastal waters. Oceanol. Acta 14, 379–388.

Jago, C.F., Bale, A.J., Green, M.O., Howarth, M.J., Jones, S.E., McCave, I.N., Millward, G.E., Morris, A.W., Rowden, A.A., Williams, J.J., Hydes, D., Turner, A., Huntley, D., Leussen, W. Van, 1993. Resuspension processes and seston dynamics, southern north sea [and discussion]. Philos. Trans. Phys. Sci. Eng.

Jago, C.F., Jones, S.E., 1998. Observation and modelling of the dynamics of benthic fluff resuspended from a sandy bed in the southern North Sea. Cont. Shelf Res. 18, 1255–1282. https://doi.org/10.1016/S0278-4343(98)00043-0.

Jago, C.F., Jones, S.E., Latter, R.J., Mccandliss, R.R., Hearn, M.R., Howarth, M.J., 2002. Resuspension of benthic fluff by tidal currents in deep stratified waters, northern North Sea, 48, pp. 259–269.

Jakobsen, H.H., Markager, S., 2016. Carbon-to-chlorophyll ratio for phytoplankton in temperate coastal waters: seasonal patterns and relationship to nutrients. Limnol. Oceanogr. https://doi.org/10.1002/lno.10338.

Jenness, M.I., Duineveld, G.C.A., 1985. Effects of tidal currents on chlorophyll a content of sandy sediments in the southern North Sea. Mar. Ecol. Prog. Ser. 21, 283–287. https://doi.org/10.3354/meps021283.

Joint, I., Pomroy, A., 1993. Phytoplankton Biomass and Production in the Southern North-Sea. Mar. Ecol. Ser.

Jones, S.E., Jago, C.F., Bale, a.J., Chapman, D., Howland, R.J.M., Jackson, J., 1998. Aggregation and resuspension of suspended particulate matter at a stratified site in the southern North Sea: physical and biological controls. Cont. Shelf Res. 18, 1283–1309. https://doi.org/10.1016/S0278-4343(98)00044-2.

Kalaji, H.M., Schansker, G., Brestic, M., Bussotti, F., Calatayud, A., Ferroni, L., Goltsev, V., Guidi, L., Jajoo, A., Li, P., Losciale, P., Mishra, V.K., Misra, A.N., Nebauer, S.G., Pancaldi, S., Penella, C., Pollastrini, M., Suresh, K., Tambussi, E., Yanniccari, M., Zivcak, M., Cetner, M.D., Samborska, I.A., Stirbet, A., Olsovska, K., Kunderlikova, K., Shelonzek, H., Rusinowski, S., Bąba, W., 2017. Frequently asked questions about chlorophyll fluorescence, the sequel. Photosynth. Res. https://doi.org/10.1007/s11120-016-0318-y.

Kerimoglu, O., Hofmeister, R., Maerz, J., Riethmüller, R., Wirtz, K.W., 2017. The acclimative biogeochemical model of the southern North Sea. Biogeosciences 14 (19), 4499–4531. https://doi.org/10.5194/bg-14-4499-2017.

Kiefer, D.A., 1973. Chlorophyll a fluorescence in marine centric diatoms: responses of chloroplasts to light and nutrient stress. Mar. Biol. https://doi.org/10.1007/BF00394110.

Kononen, K., Hallfors, S., Kokkonen, M., Kuosa, H., Laanemets, J., Pavelson, J., Autio, R., 1998. Development of a subsurface chlorophyll maximum at the entrance to the Gulf of Finland, Baltic Sea. Limnol. Oceanogr. 43, 1089–1106. https://doi.org/10.4319/lo.1998.43.6.1089.

Krause, G., Budeus, G., Gerdes, D., Schaumann, K., Hesse, K., 1986. Frontal systems in the german bight and their physical and biological effects. Elsevier Oceanogr. Ser. 42, 119–140. https://doi.org/10.1016/S0422-9894(08)71042-0.

Kundu, P.K., Cohen, I.M., Dowling, D.R., 2016. Introduction (Chapter 1) In: Kundu, P.K., Cohen, I.M., Dowling, D.R. (Eds.), Fluid Mechanics, Sixth edition. Academic Press, Boston, pp. 1–48. https://doi.org/10.1016/B978-0-12-405935-1.00001-0. (Chapter 1).

Levandowsky, M., Kaneta, P.J., 1987. Behaviour in dinoflagellates. In: Taylor, F.J.R. (Ed.), The Biology of Dinoflagellates. Blackwell, Oxford, pp. 360–397.

Liu, Q., Kandasamy, S., Lin, B., Wang, H., Chen, C.-T.A., 2017. Biogeochemical characteristics of suspended particulates at deep chlorophyll maximum layers in the East China Sea. Biogeosciences. https://doi.org/10.5194/bg-15-2091-2018.

Löder, M.G.J., Kraberg, A.C., Aberle, N., Peters, S., Wiltshire, K.H., 2012. Dinoflagellates and ciliates at Helgoland Roads, North Sea. Helgol. Mar. Res. 66, 11–23. https://doi.org/10.1007/s10152-010-0242-z.

Lohse, L., Malschaert, J.F.P., Slomp, C.P., Helder, W., van Raaphorst, W., 1995. Sediment-water fluxes of inorganic nitrogen compounds along the transport route of organic matter in the North Sea. Ophelia. https://doi.org/10.1080/00785236.1995.10422043.

Lorenzen, C.J., 1966. A method for the continuous measurement of in vivo chlorophyll concentration. Deep Sea Res. Oceanogr. Abstr. https://doi.org/10.1016/0011-7471(66)91102-8.

Lutz, M., Dunbar, R., Caldeira, K., 2002. Regional variability in the vertical flux of particulate organic carbon in the ocean interior. Glob. Biogeochem. Cycles 16, 11–1-11–18. https://doi.org/10.1029/2000GB001383.

Macintyre, H.L., Kana, T.M., Geider, R.J., 2000. The effect of water motion on short-term rates of photosynthesis by marine phytoplankton. Trends Plant Sci. https://doi.org/10.1016/S1360-1385(99)01504-6.

Maerz, J., Hofmeister, R., Lee, E.M. Van Der, Gräwe, U., Riethmüller, R., Wirtz, W., 2016. Evidence for a maximum of sinking velocities of suspended particulate matter in a coastal transition zone. ⟨https://doi.org/10.5194/bg-2015-667⟩.

McCandliss, R.R., Jones, S.E., Hearn, M., Latter, R., Jago, C.F., 2002. Dynamics of suspended particles in coastal waters (southern North Sea) during a spring bloom. J. Sea Res. 47, 285–302. https://doi.org/10.1016/S1385-1101(02)00123-5.

McDougall, T.J., Feistel, Rainer, Wright, D.G., Pawlowicz, R., Millero, F.J., Jackett, D.R., King, B.A., Marion, G.M., Seitz, S., Spitzer, P., Chen, C.-T.A., 2010. The international thermodynamic equation of seawater - 2010: Calculation and use of thermodynamic properties, Intergovernmental Oceanographic Commission, Manuals and Guides No. 56. ⟨https://doi.org/http://dx.doi.org/10.1109/VETECF.2008.21⟩.

McTigue, N.D., Bucolo, P., Liu, Z., Dunton, K.H., 2015. Pelagic-benthic coupling, food webs, and organic matter degradation in the Chukchi Sea: insights from sedimentary pigments and stable carbon isotopes. Limnol. Oceanogr. https://doi.org/10.1002/lno.10038.

Millero, F.J., Feistel, R., Wright, D.G., McDougall, T.J., 2008. The composition of standard seawater and the definition of the reference-composition salinity scale. Deep. Res. Part I Oceanogr. Res. Pap. https://doi.org/10.1016/j.dsr.2007.10.001.

Millward, G.E., Morris, A.W., Tappin, A.D., 1998. Trace metals at two sites in the southern North Sea: results from a sediment resuspension study. Cont. Shelf Res. 18, 1381–1400. https://doi.org/10.1016/S0278-4343(98)00049-1.

Monismith, S.G., Koseff, J.R., White, B.L., 2018. Mixing efficiency in the presence of stratification: when is it constant? Geophys. Res. Lett. 45, 5627–5634. https://doi.org/10.1029/2018GL077229.

Müller, D., Krasemann, H., Brewin, R.J.W., Brockmann, C., Deschamps, P.Y., Doerffer, R., Fomferra, N., Franz, B.A., Grant, M.G., Groom, S.B., Mélin, F., Platt, T., Regner, P., Sathyendranath, S., Steinmetz, F., Swinton, J., 2015. The Ocean Colour Climate Change Initiative: II. Spatial and temporal homogeneity of satellite data retrieval due to systematic effects in atmospheric correction processors. Remote Sens. Environ. https://doi.org/10.1016/j.rse.2015.01.033.

Nielsen, L.T., Kiørboe, T., 2015. Feeding currents facilitate a mixotrophic way of life. ISME J. 9, 2117–2127. https://doi.org/10.1038/ismej.2015.27.

Nielsen, T.G., Lokkegaard, B., Richardson, K., Pedersen, F.B., Hansen, L., 1993. Structure of plankton communities in the Dogger Bank area (North Sea) during a stratified situation. Mar. Ecol. Prog. Ser. 95, 115–131. https://doi.org/10.3354/meps095115.

Omand, M.M., Mahadevan, A., 2015. The shape of the oceanic nitracline. Biogeosciences 12, 3273–3287. https://doi.org/10.5194/bg-12-3273-2015.

Osborn, T.R., 1980. Estimates of the local rate of vertical diffusion from dissipation

measurements. J. Phys. Oceanogr. https://doi.org/10.1175/1520-0485(1980)010<0083:EOTLRO>2.0.CO;2.
Otto, L., Zimmerman, J.T.F., Furnes, G.K., Mork, M., Saetre, R., Becker, G., 1990. Review of the physical oceanography of the North Sea. Netherlands. J. Sea Res. 26, 161–238. https://doi.org/10.1016/0077-7579(90)90091-T.
Pedersen, F.B., 1994. The oceanographic and biological tidal cycle succession in shallow sea fronts in the north sea and the english channel. Estuar. Coast. Shelf Sci. 38, 249–269. https://doi.org/10.1006/ecss.1994.1017.
Peeters, J.C.H., Los, F.J., Jansen, R., Haas, H.A., Peperzak, L., de Vries, I., 1995. The oxygen dynamics of the oyster ground, north sea. Impact eutrophication Environ. Cond. Ophelia. https://doi.org/10.1080/00785326.1995.10431508.
Petersen, W., Schroeder, F., Bockelmann, F.D., 2011. FerryBox - Application of continuous water quality observations along transects in the North Sea. Ocean Dyn. 61, 1541–1554. https://doi.org/10.1007/s10236-011-0445-0.
Pingree, R.D., Griffiths, D.K., 1978. Tidal fronts on the shelf seas around the British Isles. J. Geophys. Res. 83, 4615. https://doi.org/10.1029/JC083iC09p04615.
Pohlmann, T., 1996a. Calculating the development of the thermal vertical stratification in the North Sea with a three-dimensional baroclinic circulation model. Cont. Shelf Res. https://doi.org/10.1016/0278-4343(95)00018-V.
Pohlmann, T., 1996b. Predicting the thermocline in a circulation model of the North Sea - Part I: model description, calibration and verification. Cont. Shelf Res. 16, 131–146. https://doi.org/10.1016/0278-4343(95)90885-S.
Provoost, P., Braeckman, U., Van Gansbeke, D., Moodley, L., Soetaert, K., Middelburg, J.J., Vanaverbeke, J., 2013. Modelling benthic oxygen consumption and benthic-pelagic coupling at a shallow station in the southern North Sea. Estuar. Coast. Shelf Sci. 120, 1–11. https://doi.org/10.1016/j.ecss.2013.01.008.
Richardson, K., Pedersen, F.B., 1998. Estimation of new production in the North Sea : consequences for temporal and spatial variability of phytoplankton, pp. 574–580.
Richardson, K., Visser, A.W., Bo Pedersen, F., 2000. Subsurface phytoplankton blooms fuel pelagic production in the North Sea. J. Plankton Res 22, 1663–1671. https://doi.org/10.1093/plankt/22.9.1663.
Riley, G.A., 1942. The relationship of vertical turbulence and spring diatom flowerings. J. Mar. Res. 5, 67–87.
Rumyantseva, A., Lucas, N., Rippeth, T., Martin, A., Painter, S.C., Boyd, T.J., Henson, S., 2015. Ocean nutrient pathways associated with the passage of a storm. Glob. Biogeochem. Cycles 29, 1179–1189. https://doi.org/10.1002/2015GB005097.
Russell, F.S., 1927. The vertical distribution of plankton in the sea. Biol. Rev. 213–262. https://doi.org/10.1111/j.1469-185X.1927.tb00878.x.
Saha, S., Moorthi, S., Pan, H.L., Wu, X., Wang, J., Nadiga, S., Tripp, P., Kistler, R., Woollen, J., Behringer, D., Liu, H., Stokes, D., Grumbine, R., Gayno, G., Wang, J., Hou, Y.T., Chuang, H.Y., Juang, H.M.H., Sela, J., Iredell, M., Treadon, R., Kleist, D., Van Delst, P., Keyser, D., Derber, J., Ek, M., Meng, J., Wei, H., Yang, R., Lord, S., Van Den Dool, H., Kumar, A., Wang, W., Long, C., Chelliah, M., Xue, Y., Huang, B., Schemm, J.K., Ebisuzaki, W., Lin, R., Xie, P., Chen, M., Zhou, S., Higgins, W., Zou, C.Z., Liu, Q., Chen, Y., Han, Y., Cucurull, L., Reynolds, R.W., Rutledge, G., Goldberg, M., 2010. The NCEP climate forecast system reanalysis. Bull. Am. Meteorol. Soc. https://doi.org/10.1175/2010BAMS3001.1.
Schrum, C., 1997. Thermohaline stratification and instabilities at tidal mixing fronts: results of an eddy resolving model for the German Bight. Cont. Shelf Res. 17, 689–716. https://doi.org/10.1016/S0278-4343(96)00051-9.
Schrum, C., Hübner, U., Jacob, D., Podzun, R., 2003a. A coupled atmosphere/ice/ocean model for the North Sea and the Baltic Sea. Clim. Dyn. https://doi.org/10.1007/s00382-003-0322-8.
Schrum, C., Siegismund, F., John, M.S., 2003b. Decadal variations in the stratification and circulation patterns of the North Sea. Are the 1990s unusual? ICES Mar. Sci. Symp. 219, 121–131.
Schrum, C., St. John, M., Alekseeva, I., 2006. ECOSMO, a coupled ecosystem model of the North Sea and Baltic Sea: Part II. Spatial-seasonal characteristics in the North Sea as revealed by EOF analysis. J. Mar. Syst. 61, 100–113. https://doi.org/10.1016/j.jmarsys.2006.01.004.
Schultze, L.K.P., Merckelbach, L.M., Carpenter, J.R., 2017. Turbulence and mixing in a shallow shelf sea from underwater gliders. J. Geophys. Res. Ocean. 9092–9109. https://doi.org/10.1002/2017JC012872.
Scott, B.E., Sharples, J., Ross, O.N., Wang, J., Pierce, G.J., Camphuysen, C.J., 2010. Sub-surface hotspots in shallow seas: fine-scale limited locations of top predator foraging habitat indicated By tidal mixing and sub-surface chlorophyll. Mar. Ecol. Prog. Ser. 408, 207–226. https://doi.org/10.3354/meps08552.
Sharples, J., 2008. Potential impacts of the spring-neap tidal cycle on shelf sea primary production. J. Plankton Res. 30, 183–197. https://doi.org/10.1093/plankt/fbm088.
Sharples, J., Moore, M.C., Rippeth, T.P., Holligan, P.M., Hydes, D.J., Fisher, N.R., Simpson, J.H., 2001. Phytoplankton distribution and survival in the thermocline. Limnol. Oceanogr. https://doi.org/10.4319/lo.2001.46.3.0486.
Sharples, J., Tweddle, J.F., Green, J.A.M., Palmer, M.R., Kim, Y., Hickman, A.E., Holligan, P.M., Moore, C.M., Rippeth, T.P., Simpson, J.H., Krivtsov, V., 2007. Spring – neap modulation of internal tide mixing and vertical nitrate fluxes at a shelf edge in summer, 52, pp. 1735–1747.
Simpson, J., J.H.S, 2012. Introduction to the Physical and Biological Oceanography of Shelf Seas. Cambridge University Presshttps://doi.org/10.1017/CBO9781139034098.
Simpson, J.H., Hunter, J.R., 1974. Fronts in the Irish Sea. Nature 250, 404–406. https://doi.org/10.1038/250404a0.
Simpson, J.H., Sharples, J., Rippeth, T.P., 1991. A prescriptive model of stratification induced by freshwater runoff. Estuar. Coast. Shelf Sci. 33, 23–35. https://doi.org/10.1016/0272-7714(91)90068-M.
Smayda, T.J., 1971. Normal and accelerated sinking of phytoplankton in the sea. Mar. Geol. https://doi.org/10.1016/0025-3227(71)90070-3.
Smith, C., DeMaster, D., Thomas, C., Srsen, P., Grange, L., Evrard, V., DeLeo, F., 2012. Pelagic-benthic coupling, food banks, and climate change on the west antarctic peninsula shelf. Oceanography. https://doi.org/10.5670/oceanog.2012.94.
Steele, J.H., Yentsch, C.S., 1960. The vertical distribution of chlorophyll. J. Mar. Biol. Assoc. https://doi.org/10.1017/S0025315400013266.
Steinbuck, J.V., Genin, A., Monismith, S.G., Koseff, J.R., Holzman, R., Labiosa, R.G., 2010. Turbulent mixing in fine-scale phytoplankton layers: observations and inferences of layer dynamics. Cont. Shelf Res. 30, 442–455. https://doi.org/10.1016/j.csr.2009.12.014.
Stramska, M., Stramski, D., 2005. Effects of a nonuniform vertical profile of chlorophyll concentration on remote-sensing reflectance of the ocean. Appl. Opt. https://doi.org/10.1364/AO.44.001735.
Su, J., Tian, T., Krasemann, H., Schartau, M., Wirtz, K., 2015. Response patterns of phytoplankton growth to variations in resuspension in the German Bight revealed by daily MERIS data in 2003 and 2004. Oceanologia. https://doi.org/10.1016/j.oceano.2015.06.001.
Suess, E., 1980. Particulate organic carbon flux in the oceans - surface productivity and oxygen utilization. Nature. https://doi.org/10.1038/288260a0.
Swinehart, D.F., 1962. The Beer-Lambert law. J. Chem. Educ. https://doi.org/10.1021/ed039p333.
Thompson, C.E.L., Couceiro, F., Fones, G.R., Helsby, R., Amos, C.L., Black, K., Parker, E.R., Greenwood, N., Statham, P.J., Kelly-Gerreyn, B.A., 2011. In situ flume measurements of resuspension in the North Sea. Estuar. Coast. Shelf Sci. https://doi.org/10.1016/j.ecss.2011.05.026.
Wang, X.J., Behrenfeld, M., Le Borgne, R., Murtugudde, R., Boss, E., 2009. Regulation of phytoplankton carbon to chlorophyll ratio by light, nutrients and temperature in the equatorial pacific ocean: a basin-scale model. Biogeosciences. https://doi.org/10.5194/bg-6-391-2009.
Westernhagen, H., Hickel, W., Bauerfeind, E., Niermann, U., Kröncke, I., 1986. Sources and effects of oxygen deficiencies in the south-eastern North Sea. Ophelia 26, 457–473. https://doi.org/10.1080/00785326.1986.10422006.
Weston, K., Fernand, L., Mills, D.K., Delahunty, R., Brown, J., 2005. Primary production in the deep chlorophyll maximum of the central North Sea. J. Plankton Res. 27, 909–922. https://doi.org/10.1093/plankt/fbi064.
Williams, C., Sharples, J., Mahaffey, C., Rippeth, T., 2013. Wind-driven nutrient pulses to the subsurface chlorophyll maximum in seasonally stratified shelf seas. Geophys. Res. Lett. 40, 5467–5472. https://doi.org/10.1002/2013GL058171.
Xing, X., Morel, A., Claustre, H., D'Ortenzio, F., Poteau, A., 2012. Combined processing and mutual interpretation of radiometry and fluorometry from autonomous profiling Bio-Argo floats: 2. Colored dissolved organic matter absorption retrieval. J. Geophys. Res. Ocean. 117, 1–14. https://doi.org/10.1029/2011JC007632.
Yacobi, Y.Z., 2006. Temporal and vertical variation of chlorophyll a concentration, phytoplankton photosynthetic activity and light attenuation in Lake Kinneret: possibilities and limitations for simulation by remote sensing. J. Plankton Res. https://doi.org/10.1093/plankt/fbl004.
Zhang, W., Wirtz, K., 2017. Mutual dependence between sedimentary organic carbon and infaunal macrobenthos resolved by mechanistic modeling. J. Geophys. Res. Biogeosci. 122, 2509–2526. https://doi.org/10.1002/2017JG003909.
Zhao, C., Daewel, U., Schrum, C., 2018. Tidal impacts on primary production in the North Sea. Earth Syst. Dyn. Discuss. 1–44. https://doi.org/10.5194/esd-2018-74.

Chapter 4 (Manuscript 2).

Tidal impacts on primary production in the North Sea

Changjin Zhao, Ute Daewel, Corinna Schrum

Published in: Earth System Dynamics, Vol.10, Issue 2, pp.287-317, 2019

Earth Syst. Dynam., 10, 287–317, 2019
https://doi.org/10.5194/esd-10-287-2019

Earth System Dynamics
Open Access
EGU

Tidal impacts on primary production in the North Sea

Changjin Zhao, Ute Daewel, and Corinna Schrum

Helmholtz Centre Geesthacht, Institute of Coastal Research, Max-Planck-Str. 1, 21502 Geesthacht, Germany

Correspondence: Changjin Zhao (changjin.zhao@hzg.de)

Received: 1 October 2018 – Discussion started: 12 October 2018
Revised: 2 April 2019 – Accepted: 3 April 2019 – Published: 26 April 2019

Abstract. This study highlights the importance of tides in controlling the spatial and temporal distributions of phytoplankton and other factors related to growth, such as nutrients and light availability. To quantify the responses of net primary production (NPP) to tidal forcing, we conducted scenario model simulations considering M_2 and S_2 tidal constituents using the physical–biogeochemical coupled model ECOSMO (ECOSystem MOdel). The results were analyzed with respect to a reference simulation without tidal forcing, with particular focus on the spatial scale of the tidally induced changes. Tidal forcing regulates the mixing–stratification processes in shelf seas such as the North Sea and hence also influences ecosystem dynamics. In principle, the results suggest three different response types with respect to primary production: (i) in southern shallow areas with strong tidal energy dissipation, tidal mixing dilutes phytoplankton concentrations in the upper water layers and thereby decreases NPP. Additionally, tides increase turbidity in near-coastal shallow areas, which has the potential to further hamper NPP. (ii) In the frontal region of the southern North Sea, which is a transition zone between stratified and mixed areas, tidal mixing infuses nutrients into the surface mixed layer and resolves summer nutrient depletion, thus sustaining the NPP during the summer season after spring bloom nutrient depletion. (iii) In the northern North Sea, the NPP response to tidal forcing is limited. Additionally, our simulations indicate that spring bloom phenology is impacted by tidal forcing, leading to a later onset of the spring bloom in large parts of the North Sea and to generally higher spring bloom peak phytoplankton biomasses. By testing the related changes in stratification, light conditions and grazing pressure, we found that all three factors potentially contribute to the change in spring bloom phenology with clear local differences. Finally, we also analyzed the impact of the spring–neap tidal cycle on NPP. The annual mean impact of spring–neap tidal forcing on NPP is limited. However, locally, we found substantial differences in NPP either in phase or anti-phase with the spring–neap tidal cycle. These differences could be attributed to locally different dominant factors such as light or nutrient availability during spring tides. In general, we conclude that in shallow shelf seas such as the North Sea, intensified vertical mixing induced by tidal forcing could either promote NPP by counteracting nutrient depletion or hinder NPP by deteriorating the light environment because of the resuspension and mixing of suspended matter into the euphotic zone.

1 Introduction

Coastal and shelf seas, such as the North Sea, generally show primary production up to 3–5 times that of the open ocean (Simpson and Sharples, 2012). Among the potential reasons for this difference are the tides, one of the dominant physical forcing factors in the North Sea, which regulate the mixing–stratification status (Pingree and Griffiths, 1978; Simpson and Souza, 1995), with potential implications for primary production (Daly and Smith, 1993; Otto et al., 1990). The relevance of tides to primary production has been investigated in a number of previous studies, which show substantial co-variability between hydrodynamic tidal characteristics and biogeochemical data (Blauw et al., 2012; Jago et al., 2002; McCandliss et al., 2002; Pietrzak et al., 2011; Richardson et al., 2000). Tides influence biogeochemical cycling in various ways, enhancing the vertical mixing of biomass, suspended matter and nutrients, and causing sediment resuspen-

sion. Vertical mixing injects nutrients (e.g., Hu et al., 2008) into the euphotic zone and thereby sustains primary production. However, vertical mixing also promotes the dilution of phytoplankton biomass (Cloern, 1991), which hinders plankton production. The resuspension and upward vertical mixing of near-bottom sediments (Bowers et al., 1998; Smith and Jones, 2015) deteriorate light conditions (Porter et al., 2010) and result in decreasing productivity. The co-action of these mechanisms results in either favorable or unfavorable impacts on ecosystem productivity depending on local hydrodynamic and biochemical conditions, thus shaping the specific structure and sensitivity of North Sea net primary production (NPP).

In the North Sea, several subsystems emerge with respect to tidal forcing and bathymetry, leading to a high spatial diversity of primary production dynamics (Van Leeuwen et al., 2015) and potentially also NPP sensitivity to tides. In principle, the system can be differentiated into a permanently mixed shallow area in the southern North Sea, a seasonally stratified area in the central and northern North Sea and a transition zone that includes frontal and weakly stratified areas (Schrum et al., 2003). In permanently mixed shallow areas, strong vertical stirring slows the development of the spring bloom and prevents summer nutrient limitation (Wafar et al., 1983). Nutrient availability in shallow coastal areas is additionally enhanced by onshore nutrient and organic matter transport driven by estuarine-type baroclinic circulation (Hofmeister et al., 2017; Rodhe et al., 2004) and land-borne nutrient supplies. Consequently, light limitation is dominant in shallow coastal areas (Tett and Walne, 1995). In contrast, the central and deeper parts of the northern North Sea are seasonally stratified (Pohlmann, 1996), and summer nutrient depletion occurs in the upper mixed layer after the spring bloom (Longhurst, 2006). Because the bottom mixed and surface mixed layers in these regions are largely decoupled, the tidally driven nutrient replenishment from the deeper layers is expected to be rather small. In shallower areas, the bottom mixed layer is able to interfere with the thermocline, and nutrients can be mixed into the euphotic zone (e.g., Rippeth et al., 2009; Richardson et al., 2000; Sharples, 2008; Daewel and Schrum, 2013) and sustain the NPP in the euphotic zone in summer. In these areas, the breaking up of stratification is mainly driven by the spring–neap tidal cycle or wind mixing (Mahadevan et al., 2010; Schrum, 1997). The physical mechanisms of the spring–neap cycle, such as the shifting of fronts (Simpson and Bowers, 1981), periodical erosion of the thermocline and relevant ecological responses (Allen et al., 2004), mainly in regard to replenishment of nutrients (Franks and Chen, 1996) and interruption of biomass building (Balch, 1981; Sharples et al., 2006), have been studied previously. In addition to large-scale stratification patterns that regulate tidal impacts on NPP, local impacts have been observed. The patchiness of chlorophyll (CHL) concentrations at the eastern British coast, for example, was shown to be associated with local vertical mixing generated by tides and bathymetry (Scott et al., 2010). In the Rhine river plume area, suspended particulate matter concentrations are characterized by a periodicity following a fortnight cycle (Pietrzak et al., 2011).

So far, earlier studies have focused largely on the local effects of nutrient injection into the euphotic zone. Understanding key processes and assessing regionally differing responses have been accomplished by cross-frontal field studies and idealized model simulations (e.g., Cloern, 1991; Richardson et al., 2000; Sharples, 2008). Some of these studies have quantitatively evaluated tidal contributions to NPP based on nutrient replenishment from observed data or 1-D simulations using simplified upscaling, neglecting the spatial diversity of the North Sea system. However, it remains an open question how dynamic zooplankton and tide-modulated benthic–pelagic coupling affect the sensitivity of plankton production to tidal forcing. Furthermore, a comprehensive understanding of tidal impacts at a basin scale is still lacking for the North Sea. To answer these questions and investigate highly dynamic tidal impacts on ecosystem productivity in different subsystems in the North Sea, the application of 3-D modeling is indispensable. Here, we will address the above questions using ECOSMO (ECOSystem MOdel) (Daewel and Schrum, 2013; Schrum et al., 2006), a well-validated 3-D-coupled physical–biogeochemical model for scenario simulations to elaborate the relevance of tidal impacts on NPP and underlying processes. The model resolves key physical and biogeochemical processes, such as turbulent mixing, zooplankton growth and predation, and impacts of particulate and dissolved organic matter on light conditions. The model has a bottom component, which is dynamically coupled to the water column through the fluxes of particulate and dissolved matter, allowing for resuspension. We will assess the spatial variability of the responses of NPP to major tidal components, i.e., M_2 and S_2, and disentangle different processes contributing to tidally induced variations in NPP, mainly variations related to stratification–mixing patterns, spring bloom onset time and intensity, and the maintenance of NPP in the subsurface of stratified areas. We will further investigate variations in NPP related to the spring–neap tidal cycle.

2 Methods

2.1 Model description and validation

In this study, we employed the well-validated 3-D-coupled physical–biochemical model ECOSMO (Daewel and Schrum, 2013). The hydrodynamic component of ECOSMO builds on the 3-D baroclinic model HAMSOM (HAMburg Shelf Ocean Model) (Schrum and Backhaus, 1999). The capability to simulate the hydrodynamic status of the North Sea–Baltic Sea system was validated by Janssen et al. (2001) and Schrum et al. (2003). The simulation domain covers the North Sea and Baltic Sea, with open boundaries to the northern Atlantic Ocean in the north and the mouth

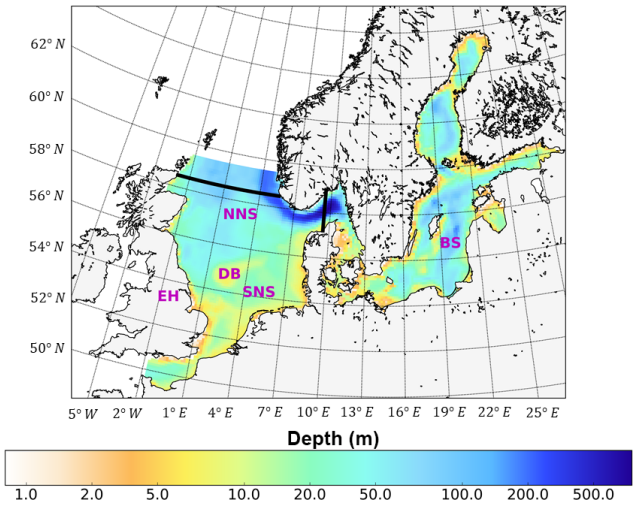

Figure 1. Bathymetry and simulation domain of ECOSMO. Black lines indicate the area of the North Sea used for analysis, from 5° W to 9.5° E in the east–west direction and from 48 to 58.5° N in the south–north direction. SNS and NNS are short for the southern and northern North Sea, respectively. BS is short for the Baltic Sea. DB and EH are short for Dogger Bank and the Estuary of Humber, respectively.

of the English Channel in the south (Fig. 1). The model was formulated on a staggered Arakawa-C grid using spherical coordinates, with a spatial resolution of 6′ in latitude and 10′ in longitude. The model time step was 20 min, which allows for a robust representation of the tidal cycle for physics and biogeochemistry. It was also coupled online using the same time steps as those for hydrodynamics. In this study, we focused on the North Sea region between 48–58.5° N and 5° W–9.5° E because tides are only of minor relevance in the Baltic Sea. To resolve thermal stratification in the upper water column, the vertical resolution was set to 5 m in the upper 40 m of the water column and decreased gradually with depth below 40 m. To reduce numerical diffusion in the implemented upwind advection scheme, a shape-preserving total-variation-diminishing (TVD) scheme (Yee et al., 1985) was adopted, which significantly improved the representation of hydrodynamics and ecosystem processes, especially processes related to fronts. A detailed description of the method and model responses to the changed advection scheme has been provided by Barthel et al. (2012).

The biogeochemical component of ECOSMO was developed to describe the lower trophic level dynamics of the marine ecosystem using a nutrient–phytoplankton–zooplankton–detritus (NPZD) conceptual model framework. The ecosystem model component was first introduced for the North Sea by Schrum et al. (2006) and further developed for a wider range of ecosystems, including relevant characteristics for the Baltic Sea, by Daewel and Schrum (2013). Detailed validations against nutrient observations have shown that the model is capable of simulating lower trophic level ecosystem dynamics in the North Sea, and the temporal variability at interannual to decadal scales simulated by ECOSMO could be corroborated by observations (Daewel and Schrum, 2013). ECOSMO simulates the nutrient cycling of silicate, phosphorus and nitrogen in the water column and in the sediments considering processes such as primary production, grazing and excretion by zooplankton, remineralization and sediment–water coupling. A detailed description of the ecosystem model is given in Daewel and Schrum (2013). In total, 16 state variables were solved, including three functional groups for primary producers (diatoms, flagellates and cyanobacteria). In the second trophic level, two groups of zooplankton were considered and differentiated based on feeding preferences. To additionally account for the shading effects of dissolved organic matter (DOM) and detritus, which were not considered in Daewel and Schrum (2013), the formulation of light attenuation was modified as previously suggested by Nissen (2014). To capture the productive and turbid characteristics, DOM was parameterized by fast remineralization rates and a low sinking velocity, in contrast to the fast sinking velocity and slow remineralization rates of particulate organic matter (detritus). Therefore, the vertical light attenuation consisted of background attenuation (k_{w1}) (induced by the water body and inorganic SPM), phytoplankton self-shading (k_p) and additional shading impacts of DOM (k_{DOM}) and detritus (k_{Det}), as shown in Eq. (1).

$$Kd_1 = k_{w1} + k_p \cdot P + k_{DOM} \cdot \mathrm{DOM} + k_{Det} \cdot \mathrm{Det} \quad (1)$$

While background attenuation k_{w1} ($0.03\,\mathrm{m}^{-1}$; Urtizberea et al., 2013) remained constant in the water column, self-shading depended on both k_p ($0.2\,\mathrm{m}^2\,\mathrm{mmol\,C}^{-1}$) and the phytoplankton concentration (P). As suggested by Stedmon et al. (2000) and Tian et al. (2009), k_{DOM} and detritus k_{Det} were set to $0.29\,\mathrm{m}^2\,\mathrm{gC}^{-1}$ and $0.2\,\mathrm{m}^2\,\mathrm{gC}^{-1}$, respectively. Compared to Daewel and Schrum (2013), these changes enabled the dynamical coupling of turbidity to the seasonal production cycle, as previously discussed by Nissen (2014). A corresponding validation of surface nutrients and comparison of mean primary production (Appendix B) confirms that the performance of ECOSMO in the North Sea region changes only marginally with respect to the original model version. Frontal production and production in deeper stable stratified waters increased slightly, while production near the coast was slightly decreased. The model is thereby capable of resolving tidal influences on primary production via potentially competing processes. Tidal mixing releases nutrient limitation, thus fostering NPP, but tides also cause the resuspension and mixing of suspended matter into the euphotic zone, which reduces light availability in the water column, thus reducing NPP. In addition to relevant bottom-up processes, the model also resolved phytoplankton–zooplankton feedbacks and vertical oxygen and temperature profiles, which alter the remineralization of organic matter and consequently nutrient cycling.

Besides organic matter contribution to light shading, in the coastal area, inorganic SPM also has the potential to filter light and reduce primary production. We do not consider a dynamic coupled SPM modeling approach but consider a simplified consideration of inorganic SPM through implementing the background attenuation. To address the uncertainties related to SPM, we tested the effect of inorganic SPM on our findings with help of an additional numerical simulation, where we implemented a climatological SPM field (daily resolution, with 31 vertical layers in the original dataset) (Große et al., 2016; Heath et al., 2002) and added the SPM's contribution to the light attenuation scheme. Details of the inorganic SPM dataset and implementation are given in Appendix C. The results confirmed the validity of our assumption that the spatial variability of SPM can be neglected for the sensitivity study performed here. Despite the existing effect of inorganic SPM on light conditions and spatial variability of inorganic SPM, there is only minor sensitivity found for the case studies of tidal vs. non-tidal forcing, and Eq. (1) can be considered as a proper parameterization within the context of our study.

The ability to properly resolve intensified frontal production and the consideration of key processes influencing light and nutrient limitation related to tidal forcing make ECOSMO an appropriate tool to assess tidal impacts on NPP in the spatially highly diverse North Sea. As already stated in Daewel and Schrum (2013), ECOSMO estimates of annual NPP in the North Sea (Fig. 2) are at the lower edge of what has been simulated for the area (Holt et al., 2012; van Leeuwen et al., 2013). The relatively low estimates mainly appear in the northern North Sea (NNS), where primary production is estimated to be approximately 125 $gC\,m^{-2}\,year^{-1}$ based on observations (Van Beusekom and Diel-Christiansen, 1994), and on the European continental coast, where NPP observations range between 199 and 261 $gC\,m^{-2}\,year^{-1}$ (Joint and Pomroy, 1993). The simulation fits well with observation-based estimates of NPP on the British coast of approximately 75–79 $gC\,m^{-2}\,year^{-1}$ (Joint and Pomroy, 1992) and primary production estimates of 100 and 119–147 $gC\,m^{-2}\,year^{-1}$ in the central parts of the North Sea and at Dogger Bank, respectively (Joint and Pomroy, 1993).

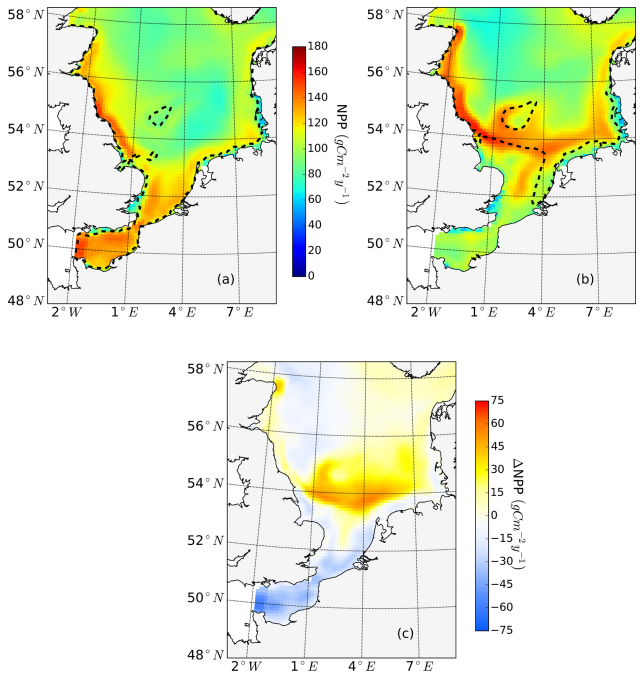

Figure 2. Mean annual net primary production for the analyzed period (1990–2015) of the non-tidal scenario **(a)**, tidal scenario **(b)** and the difference in the mean annual NPP of both scenarios **(c)**. Dashed lines indicate the boundary between stratified (off-shore) and unstratified (near-shore, Dogger Bank) regions. The criterion for stratification is that squared buoyancy frequency N^2 remains higher than 0.013 (s^{-2}) for more than 60 d per year on average.

2.2 Model setup

A detailed description of the model setup was given by Daewel and Schrum (2013); therefore, we will only provide a brief overview of the forcing data used for the model simulation, particularly emphasizing the changes made to the previously described setup. These changes mainly concern the river discharge and nutrient load data sources. The simulation was initialized in 1948 using climatological data from the World Ocean Atlas (WOA) (Conkright et al., 2002) for nutrients and observational climatology for temperature and salinity (Janssen et al., 1999). The full simulation period encompasses 68 years, ending in 2015, and is forced with atmospheric boundary conditions provided by the NCEP/NCAR reanalysis (Kalnay et al., 1996). Additional forcing data include wet deposition for nitrogen, which were prescribed using data from a Community Multiscale Air Quality (CMAQ) model (Matthias et al., 2008), and boundary values for nutrients, temperature and salinity at the open boundaries to the North Atlantic, for which we used the same climatological data as those used for the initial conditions. For salinity, additional annual anomalies were retrieved from observational data available at the ICES (International Council for the Exploration of the Sea) database (http://www.ices.dk, last access: 30 November 2016). An updated set of river runoff and nutrient load data was applied with more complete river forcing data coverage for the North Sea and Baltic Sea. A multitude of data were provided by Sonja van Leeuwen (Royal Netherlands Institute for Sea Research, personal communication, 2016) containing the following datasets: UK data were processed from raw data from the Environment Agency (England and Wales, contains Natural Resources Wales information ©Natural Resources Wales and database rights), the Scottish Environment Protection Agency (Scotland), the Rivers Agency (Northern Ireland) and the National River Flow Archive. French water quality data were provided by

Agence de l'eau Loire-Bretagne, Agence de l'eau Seine-Normandie, OSUR web Loire-Bretagne and SIEAG (Systeme d'information sur l'eau du bassin Adour Garonne), while daily flow data were obtained from Le Banque Hydro (http://www.hydro.eaufrance.fr/, last access: 23 April 2019). German and Dutch riverine data were provided by the University of Hamburg (Pätsch and Lenhart, 2004). Norwegian water quality data were provided by the Norwegian Water Resources and Energy Directorate (NVE), with daily flow data supplied by the Norwegian Institute for Water Research (NIVA). Danish water quality data were provided by the National Environmental Research Institute (NERI). Water quality data for Baltic rivers were provided by the University of Stockholm and the Baltic Nest. Furthermore, nutrient status and freshwater runoff information in the southern and eastern Baltic Sea was supplemented by data from the Balt-HYPE model (Arheimer et al., 2012; Lindström et al., 2010). Nutrient loads from Danish waters were provided by Marie Maar (personal communication, 2016) and were similar to the forcing data used for the HBM-ERGOM simulation (Maar et al., 2016). These data stem from a national monitoring program (Windolf et al., 2011, 2012) and from the hydrological Denmark model, which provides runoff calculations for ungauged areas of Denmark (Henriksen et al., 2003).

We selected a relatively short time period (1990–2015) for our analysis to assure a long enough spin-up time that accounts for the characteristic long timescales of the North Sea–Baltic Sea system (Daewel and Schrum, 2013). The period from 1990 to 2015 will hereafter be called the analyzed period. Tidal cycles with long periods, such as the nodal and elliptical cycles, although considered in the forcing via nodal corrections of partial tide amplitudes and phases (see Sect. 2.3), are not targeted in this study.

2.3 Tidal forcing and scenarios

Sea surface elevation was prescribed at the open boundaries, with a time step of 20 min. Daily mean sea surface elevation data were taken from a diagnostic model simulation for the wider northeast European Shelf (Backhaus and Hainbucher, 1987) and also forced with the NCEP/NCAR reanalysis. In addition, tidal elevations were calculated from tidal constituents provided by the German Federal Maritime and Hydrographic Agency (Federal Maritime and Hydrographic Agency, Deutsches Hydrographisches Institut, 1967). Nodal corrections were implemented in the calculation of tides to represent the long-term variation in lunar nodes. For the standard tidal scenario, partial M_2 tide (principle lunar tide) and S_2 tide (principle solar tide) (Thomson and Emery, 2014) were considered; we hereafter call this scenario the tidal scenario. To evaluate the contribution of the spring–neap tidal cycle, a tidal scenario using only the M_2 partial tide, called the M_2 scenario, was simulated and discussed in comparison to the tidal scenario. To quantify the overall impact of tidal forcing, a scenario without tidal forcing at the open boundary was simulated to yield the non-tidal reference state of the system (non-tidal scenario).

2.4 Postprocessing of model results

The responses of ecosystem productivity to tidal forcing were assessed by comparing the annual mean NPP during the analyzed period between the tidal and non-tidal scenarios (tidal scenario minus non-tidal scenario). Furthermore, we disentangled processes that might contribute to variations in NPP, such as the seasonality of spatial patterns in limitation factors (nutrients vs. light), spring bloom phenology, the impacts of the spring–neap cycle on NPP variability and the contribution of subsurface production to the overall NPP. We quantified these processes using subdomains and further made comparisons between scenarios, emphasizing spatial variability and the seasonal cycle.

2.4.1 Subdomain division and identification of representative grid cells for process based analysis

The pre-division of the area into subdomains is based on a combination of geographic location, bathymetry and the local responses of NPP to tidal forcing (increase, decrease). First, SNS and NNS were divided by the 65 m isobath. In the SNS, areas with positive and negative NPP response to tides were separated (Fig. 2). The negatively responding area in the SNS was further geographically divided into the English Channel (EC, south of 52° N) and an area along the continental coast (neg. SNS). In the NNS, the area of the Norwegian Trench (NT) characterized by a water depth deeper than 200 m was separated. The remaining region of the NNS was further divided based on the response of NPP to tidal forcing. The area along the eastern British coast (BC), which shows elevated NPP in response to tides, was separated from the negative responding area in the middle of NNS (deep NNS) (Fig. 2). In the east of the NNS, a separate area with mild increase of NPP was identified (low-sen. NNS). Based on this pre-division of subdomains, we identified the most representative grid cell within each subdomain using correlation analysis (Eliasen et al., 2017) (Fig. A1 in Appendix A). To identify the most representative grid cell location in each subdomain, we first produced a time series of the NPP differences between the non-tidal scenario and tidal scenario for each grid cell. Subsequently, we estimated, for each of the grid cells, the correlation to the time series of the other grid cells within the same pre-divided subdomain. The grid cell with the highest correlation coefficient to all other grid cells in each subdomain was selected as the most representative point for further analysis.

2.4.2 Quantification of key processes controlling the spring bloom

The peak amplitude and the onset time of the spring bloom for the different scenarios were compared. The onset of the spring bloom is defined here as the day when the daily vertically integrated NPP reaches its maximum prior to the spring maximum in diatom biomass (Fig. A2) (Sharples et al., 2006). Diatom time series were preprocessed by a 15 d running mean to remove short-term maxima induced by the spring–neap tidal cycle (Sharples et al., 2006). To further disentangle mechanisms resulting in spring bloom phenology differences among the scenarios, we quantified potentially related biological and physical factors relevant for spring bloom dynamics, such as the zooplankton biomass prior to the onset of the spring bloom, light conditions and development of stratification, for each grid cell.

In particular, (i) the vertically averaged zooplankton biomass in the winter season (January and February) was considered a proxy for potential grazing pressure at the beginning of the growth season. (ii) The integrated value of the light-limiting term in the upper 50 m of the water column was used to estimate the light conditions for phytoplankton growth. To quantify the time when the light was sufficient for phytoplankton growth in each year, we estimated the date when the integrated light-limiting term exceeded 0.85 for 3 consecutive days. (iii) The stratification was recognized as the critical temperature difference (ΔT) between surface layers and layers below exceeding 0.5°. Similar methods have been used in many other studies (Gong et al., 2014; Karl and Lukas, 1996; Richardson et al., 2002). For the identification of the onset time of stratification, ΔT exceeding 0.5 °C for 3 consecutive days is required. The time window (3 d) (Sharples et al., 2006) was chosen to filter out short-lived stratification variations and the day–night heating/cooling cycle. The mixed layer depth is defined as the thickness of the surface mixed layer, ranging from surface to pycnocline. (iv) The averaged mixed layer depth in May was used as a measure for stratification depth.

The onset of the spring bloom, the first day of the year with stratification and the first day of the year with sufficient light conditions were identified for each grid point for every simulated year; subsequently, the percentage of years in which those time identifiers were advanced or delayed in the tidal scenario compared to that in the non-tidal scenario as a response to tidal forcing was estimated for every grid cell. The tidal induced increase/decrease of winter zooplankton biomass and of peak spring bloom amplitude were also estimated for each grid cell and each year. Using those indexes, we obtained the spatial pattern for the percentage of years with (1) higher spring bloom amplitude, (2) later onset of the spring bloom, (3) later onset of stratification, (4) deeper mixed layer depth, (5) later occurrence of sufficient light conditions for building phytoplankton biomass and (6) higher concentration of winter zooplankton biomass in response to tidal forcing (tidal scenario vs. non-tidal scenario).

Furthermore, we studied the changes in the spring bloom phenology in response to the spring–neap tidal cycle (i.e., whether spring or neap tide promote/hinder NPP). Considering that several spring–neap cycles may take place during the spring bloom development, we studied the NPP difference during of spring bloom development between the tidal scenario and M_2 scenario in relation to the spring–neap tidal phase. The period of spring bloom development was defined as the time period with an increase in NPP from 12.5 % to 87.5 % of the maximum NPP. During this time period, we identified the occurrences (within a time window of one fortnight cycle) of positive/negative maxima of the NPP difference and temporally related the day of maximum difference to the adjacent day of the spring tide. This enabled us to evaluate the impact of spring–neap tidal cycles on spring bloom phenology.

2.4.3 Quantification of limiting pattern of phytoplankton growth: light vs. nutrients

In ECOSMO, NPP is estimated as the sum of net primary production for all phytoplankton functional groups (Eq. 2, denoted by j). For each functional group, the NPP is calculated by multiplying the maximum growth rate specified for the functional group (σ_j) by the minimum value (φ_j) of all limiting terms (θ) (Liebig's law, de Baar, 1994) and the prevailing amount of phytoplankton biomass (standing stock, C_j) (Eq. 2). The limiting term (θ) for each growth resource is derived from the Monod equation (Monod, 1942), using the concentration of each growth resource (β) (Si: silicate-only for diatom growth, N: nitrogen, P: phosphorus, L: light) and the specific half-saturation constant (h) (Eq. 3). Further details of the nutrient-limiting terms are given in Daewel and Schrum (2013). We hereafter call the minimum value of all limiting terms φ (Eq. 4) the limiting value. The limiting value quantifies the availability of growth resources with a range of 0–1. The closer the value is to 1, the more sufficient the resource is. Additionally, we identified the most limiting factors for each phytoplankton type (φ_j) (N, P and L for flagellates; Si, N, P and L for diatoms).

$$\mathrm{NPP} = \sum_{j=1}^{3} \sigma_j \varphi_j C_j \tag{2}$$

$$\theta = \beta/(\beta + h) \tag{3}$$

$$\varphi = \min\left(\theta_{\mathrm{light}}, \theta_{\mathrm{N}}, \theta_{\mathrm{P}}, \theta_{\mathrm{Si}}\right) \tag{4}$$

We analyzed the limiting value to represent the environmental conditions of phytoplankton growth and the spatial and temporal dynamics of the most limiting factor.

2.4.4 Vertical distribution of phytoplankton: detection of subsurface maximum layer

The mixing intensity in the water column controls the distribution of phytoplankton and nutrients. As suggested by previous studies, phytoplankton may develop high subsurface concentrations in layers of low turbulence such as the pycnocline; production continues locally in low-turbulent zones as long as the growth requirements of nutrients and light are balanced (Cullen, 2015). In the stratified season, we differentiated the NPP generated in the surface layer (above 15 m) from that in the subsurface layers, as a subsurface biomass maximum (SBM) emerged. The SBM was defined by its width, which was small compared to the water depth, and was persistent in both time and space (Dekshenieks et al., 2001). In this study, we regarded layers deeper than 15 m as the subsurface. As an SBM necessarily includes local peaks, we first selected the depth at which the first-order derivative of biomass changed from positive to negative in the vertical biomass profile as a potential location for an SBM peak. To further identify the boundaries of the potential SBM, different strategies were applied depending on the number of vertical layers on either side of the potential SBM peak. If there were more than five vertical layers on either side of the potential SBM peak, the vertical layer with the local maximum in the second-order derivative on each side of the potential SBM peak was recognized as the boundary of the SBM layer (Benoit-Bird et al., 2009). Otherwise, the adjacent layers were assumed to confine the potential SBM. The SBM peak could be no shallower than 20 m. We estimated the local background biomass value by linearly interpolating the biomass values of the upper and lower edges to the depth where the peak in biomass emerged. If the peak maximum biomass exceeded a value 1.5 times higher than the estimated background biomass in the respective water column, the local vertical plankton biomass maximum was considered an SBM. Similar methods which have been applied to analyze phytoplankton (chlorophyll a) vertical profiles in the German Bight and more details were laid out in Zhao et al. (2019).

2.4.5 Identification of representative grid cells for spring–neap cycle impacts

In addition to tidal forcing, atmospheric forcing and bathymetry modulate stratification (e.g., Van Leeuwen et al., 2015) and production pattern (Daewel and Schrum, 2017). Consequently, tidal impacts on stratification and primary production are subject to spatial–temporal variability. Furthermore, non-linear interactions among tidal constituents are pronounced in shallower waters, as suggested by Backhaus (1985) in inshore areas for the German Bight and Danish coast. Although we preliminarily estimated the influence of the spring–neap tidal cycle via the difference in NPP between the tidal scenario and the M_2 scenario, related responses would not necessarily be visible in a fortnightly cycle. To better associate the variation in NPP with the spring–neap tidal cycle, we identified specific grid cells where both currents and biochemical factors displayed a distinguishable spring–neap cycle. Those locations were identified by using the estimated squared coherence between the power spectra (SCPS) of currents and NPP (Stoica et al., 2005; Welch, 1967). By adopting the SCPS method, we were able to select representative grid cells where both NPP and velocity showed obvious spring–neap cycles.

3 Results and discussion

3.1 Spatial changes in mean production

The average annual NPP and the difference in NPP between the tidal and non-tidal scenarios are shown in Fig. 2. The area-averaged NPP increases slightly from 100.7 to 103.2 $\mathrm{gC\,m^{-2}\,year^{-1}}$ when tidal forcing is applied (Table 1); however, high spatial diversity in the sensitivity to tidal forcing is shown. Generally, estimated tidal impacts on NPP are highest in the stratified shallow North Sea, with a maximum response of up to 60 $\mathrm{gC\,m^{-2}\,year^{-1}}$ (Fig. 2c). In the non-tidal scenario, high productivity is restricted to the near-shore shallow regions along the British coast and the European continental coast (Fig. 2a), which are the main regions where the euphotic zone reaches the bottom and nutrient remineralization fosters production throughout the year. The primary production at the coast is additionally supported by estuarine-type baroclinic circulation in summer, which transports detritus and nutrient-rich bottom water towards the coast (Ebenhöh et al., 2004; Geyer and MacCready, 2014; Hofmeister et al., 2017). Tides cause a significant reduction in stratification in the shallow near-coastal areas of the North Sea and in the EC at Dogger Bank and south of Dogger Bank and foster the development of tidal mixing fronts. Consequently, the production pattern changes notably when tidal forcing is considered. The primary production maximum is shifted further offshore towards the frontal region (Fig. 2b). Large areas of the SNS, including Dogger Bank, eastern BC and the Danish coast in the east, together with the NT, exhibit an increase in NPP when tidal forcing is prescribed. The shallow near-coastal areas in the south and the deeper areas in the NNS show a negative response of NPP to tidal forcing. A stronger negative response is observed in the highly dynamic EC (Fig. 2c). The NPP of Dogger Bank and the tidal mixing front area south and southeast of Dogger Bank responds the strongest to tidal forcing, with a mean change in NPP of up to 60 $\mathrm{gC\,m^{-2}\,year^{-1}}$, nearly doubling local production. The amplitudes of the decreases in NPP in the negatively responding area are smaller than those of the increases in NPP, with amplitudes no more than 40 $\mathrm{gC\,m^{-2}\,year^{-1}}$ (Fig. 2c); the largest amplitudes are in the EC. The intensity of this difference might be slightly sensitive to the consideration of inorganic SPM (see Appendix C).

Table 1. Average annual NPP and relative difference between the tidal and non-tidal scenarios in each subdomain and in the entire North Sea.

Subdomain	Non-tidal scen. NPP ($gC\,m^2\,year^{-1}$)	Tidal scen. NPP ($gC\,m^2\,year^{-1}$)	Rel. diff (%)
EC	125.2	97.2	−29 %
neg. SNS	114.5	101.6	−13 %
pos. SNS	93.3	118.8	21 %
BC	121.0	135.3	11 %
deep NNS	93.8	82.6	−14 %
NT	97.7	106.4	9 %
non-sen. NNS	92.3	94.5	2 %
Total	100.7	103.2	3 %

The tidally induced change in NPP is associated with variations in the spatial distribution of the main limiting resources (limiting pattern) (Fig. 3). Generally, in the tidal scenario, the area experiencing nutrient limitation decreases due to the enhanced mixing of inorganic nutrients into the euphotic zone, especially in the shallow North Sea where the bottom and surface mixed layer interact with each other. Simultaneously, light limitation increases. The predominantly light-limited regions, which are restricted to the shallow coastal regions in the non-tidal scenario (Fig. 3a), expand offshore in the tidal scenario (Fig. 3b). Tidally induced resuspension and mixing of particulates and DOM into the euphotic zone result in dominant light limitation in almost the entire shallow North Sea (below 50 m depth) (Fig. 3b). In contrast, in the surface layers of the stratified area, summer nutrient limitation is predominant, and the limiting value remains below 0.3 in both scenarios. The change from nutrient to light limitation in the SNS changes the limiting value to > 0.4 in the tidal scenario, allowing better resource exploitation in these areas and sustaining NPP during summer.

The subdomain-division method described in Sect. 2.4.1 identifies seven different subdomains (Fig. 4) that show characteristic responses to tidal forcing. Based on the division and the point-wise correlation of NPP variations in each subdomain (Fig. A1), representative grid cells were selected to study the mechanisms underlying the spatial variability of tidal responses in detail. Areas with correlation coefficients higher than 0.3 occupied at least 53 % of each subdomain, comprising 77 % of the entire study area. This indicates that the division effectively explains the spatial diversity of the system with respect to the tidally induced changes in NPP and the predominantly inherent similarity within each subdomain. The seven identified subdomains are listed below (Fig. 4):

1. *The English Channel (EC; dark blue)*. This area is characterized by an early onset of the spring bloom, strong mixing due to tidal stirring and shallow bathymetry. The EC is the most productive area in the non-tidal scenario (Fig. 2a), with a mean NPP above $120\,gC\,m^{-2}\,year^{-1}$.

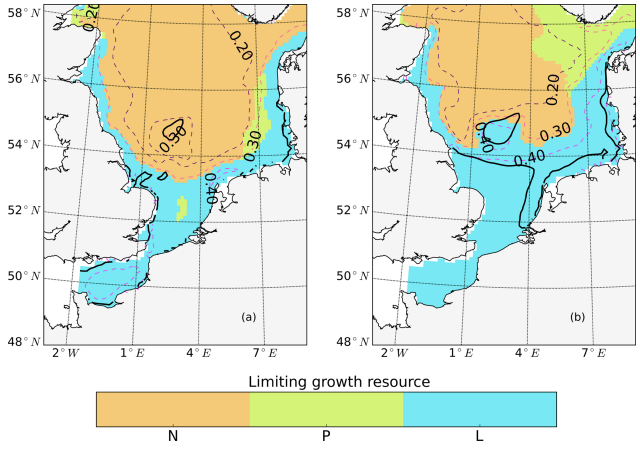

Figure 3. Mean values of the most limiting resources (N: nitrogen, P: phosphorus, L: light) in the surface layer for July (averaged for the analyzed period; 1990–2015) for the non-tidal scenario **(a)** and tidal scenario **(b)**. The limiting value (derived from Liebig's law) is indicated by dashed contour lines. Stratified and unstratified areas are separated by black lines (for definition, see Fig. 2).

2. *Negatively responding southern North Sea (neg. SNS; blue)*. The neg. SNS is separated from the EC by 52° N and from the positively responding area in the southern North Sea. The neg. SNS characterizes the permanently mixed area in the shallow water near the coast.

3. *Positively responding southern North Sea (pos. SNS; light blue)*. This area includes the frontal regions that were identified as the areas with the highest responses in NPP (Fig. 2).

4. *Eastern British coast (BC; green)*. This area is a highly productive, positively responding inshore region of the eastern British coast.

5. *Deeper northern North Sea (deep NNS; yellow)*. The deep NNS region coincides with areas of seasonal stratification and the lowest annual NPP in the tidal scenario

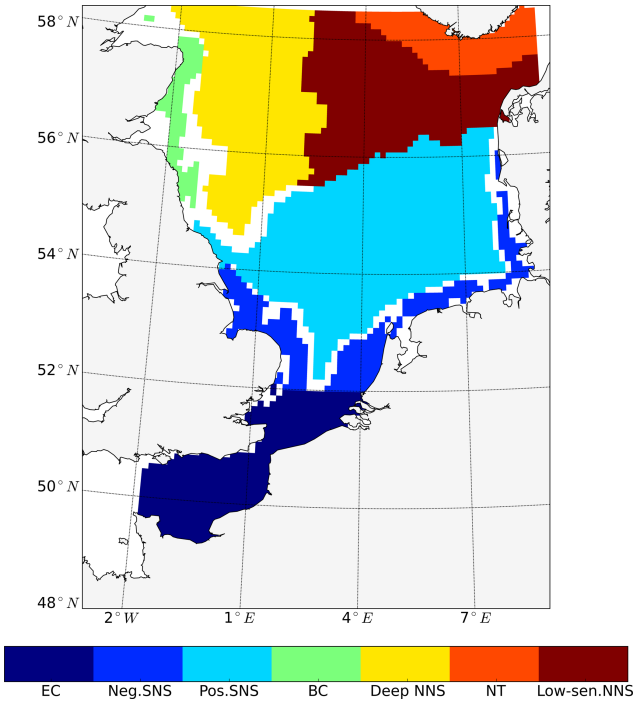

Figure 4. Process-oriented subdomain division of the North Sea based on tidally induced changes in net primary production and bathymetric characteristics (EC: English Channel; neg. SNS: negatively responding southern North Sea; pos. SNS: positively responding southern North Sea; BC: eastern British coast; deep NNS: deeper northern North Sea; NT: Norwegian Trench; low-sen. NNS: low-sensitivity northern North Sea). Areas with an absolute variation in NPP less than 5 gC m^{-2} $year^{-1}$ are excluded, except for the low-sen. NNS areas.

(Fig. 2). In this area, a slight decrease in NPP is estimated when tidal forcing is considered.

6. *The Norwegian Trench (NT; orange).* This represents the area off the Norwegian coast which is strongly impacted by the low saline outflow from the Baltic Sea. The NT shows a slight increase in NPP due to tidal forcing (Fig. 2).

7. *Low-sensitivity area in the northern North Sea (low-sen. NNS).* The magnitude of the response of NPP to tidal forcing here is below 5 gC m^{-2} $year^{-1}$. This subdomain is influenced by two amphidromic points in the eastern North Sea, with tidal amplitudes of the M_2 partial tide generally below 0.5 m.

Some narrow transient zones between the positively responding areas and negatively responding areas are shown in white in Fig. 4. These transient zones with an absolute variation in NPP less than 5 gC m^{-2} $year^{-1}$ are excluded from the following analyses. Changes in NPP in response to tidal forcing for each subdomain are listed in Table 1.

The subdomain division corresponds well with the regional characteristics of M_2 tidal energy dissipation rates, as suggested by the simulation study of Davies et al. (1985). The EC subdomain includes the areas with the highest tidal energy dissipation rates, which exceed 1000 J cm^{-2} s^{-1} (Davies et al., 1985). In most of the neg. SNS and some parts of the EC, the tidal energy dissipation rates are in the range of 100–1000 J cm^{-2} s^{-1}. In the pos. SNS, the BC and part of the deep NS, tidal energy dissipation rates range from 10 to 100 J cm^{-2} s^{-1}. The low-sen. NNS and NT are located in the area with tidal energy dissipation rates below 10 J cm^{-2} s^{-1}. The strong tidal energy in the SNS destabilizes stratification, as also revealed by the subdivision based on stratification patterns presented by Van Leeuwen et al. (2015). Our neg. SNS and EC subdomains coincide with permanently mixed regions defined in the above study; in addition, the defined BC correlates with mixed or temporally stratified belts along the eastern British coast, as suggested by Van Leeuwen et al. (2015). The subdomains identified in the NNS coincide with seasonally stratified areas in the aforementioned study. However, the majority of pos. SNS, which shows the strongest response to tidal forcing, could not be identified with the method of Van Leeuwen et al. (2015) due to the variable stratification in these frontal areas induced by the spring–neap cycle, wind forcing, river runoff and air temperature (Dippner, 1993; Schrum et al., 2003; Sharples and Simpson, 1993). The subdomains also agree well with subdomains previously identified by Otto et al. (1983). Compared to the ICES subdivisions, which were determined considering biochemical and hydrographical characteristics (Otto et al., 1983), the four northern subdomains in our study coincide with regions where the gross water mass influx is mainly influenced by Atlantic water inflow. In contrast, for the three subdomains in the south, the influence of wind is more important for water mass exchange (Siegismund, 2001).

3.2 Characteristic seasonal changes

Out of the seven subdomains (Fig. 4), we selected three representative subdomains for further analysis of the changes in seasonality of NPP and the respective associated mechanisms. The neg. SNS represents the area along European continental coast where strong tidal forcing leads to permanent mixing and the NPP decreases as a consequence of tidal forcing. The pos. SNS embodies the transient zone between the mixed and stratified water column and is characterized by the most significant positive response of NPP to tidal forcing. The deep NNS is characterized by stable seasonal stratification. Here, the bottom mixed layer and surface mixed layer are well separated; thus, tides have a limited impact on the euphotic zone. The averaged time series (1990–2015) for each subdomain and the time series of the vertical profiles of each most representative grid cell (see Sect. 2.4.1) are given in Figs. 5 and 6, respectively.

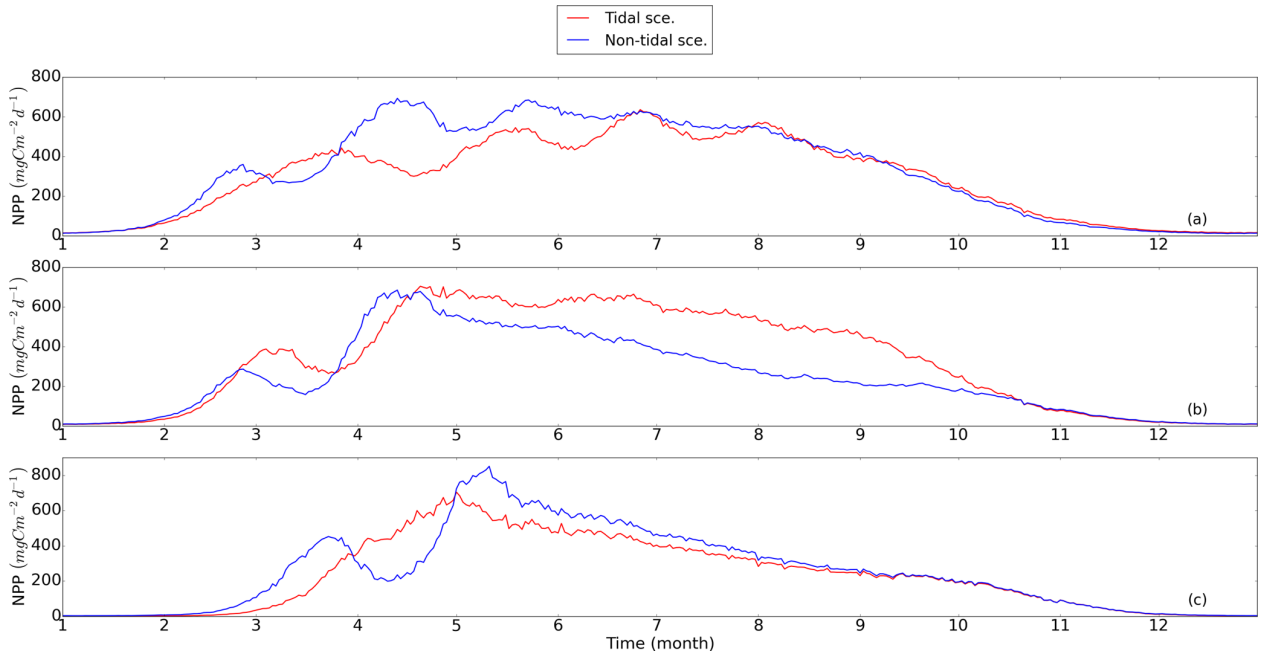

Figure 5. Time series of averaged NPP (blue: non-tidal scenario, red: tidal scenario) in subdomains; **(a)** neg. SNS: negatively responding southern North Sea, **(b)** pos. SNS: positively responding southern North Sea and **(c)** deep NNS: deeper northern North Sea. The NPP is averaged for the analyzed period (1990–2015).

In the neg. SNS (Fig. 5a), the spring bloom is delayed and strong fluctuations appear during the productive season in both scenarios (Figs. 5a and 6a, b, c, d). The pulses in NPP are probably due to predator–prey interactions and possibly modulated by advection. These pulses in NPP have previously been described by Tett and Walne (1995). The length of these fluctuations is slightly longer in the tidal scenario than in the non-tidal scenario, and changes in bloom initiation and the length of the quasi-periodic fluctuations generate positive–negative fluctuations in the NPP difference between both scenarios. We found no nutrient limitation in the water column in either scenario (Fig. 6a, b) and no significant changes in the limiting values (Eq. 4) (note: the minimum limiting value stems from light limitation), except for the slightly higher values in deep water column under the tidal scenario (Fig. 6c, d). This exception is likely caused by the downward mixing of shade-producing organic materials (e.g., phytoplankton, DOM and detritus), which leads to improved light conditions in the upper layer and better penetration. However, this result does not explain the negative NPP response in the area. Lower NPP in the tidal scenario than in the non-tidal scenario, especially in spring and early summer, results in an overall negative response in NPP. A likely reason for the reduction in NPP in the neg. SNS subdomain could be the tidally induced dilution of phytoplankton biomass in the euphotic zone in the shallow areas. The increased mixing in the tidal scenario dilutes the phytoplankton concentration in the upper, highly productive water layer (see vertical profiles of biomass in Fig. A4a, b) and consequently reduces the time during which phytoplankton cells are exposed to high surface irradiance. Considering the small difference in the growth resources between the two scenarios (Fig. 6c, d), we mainly attribute the variation in NPP to the vertical distribution of standing stocks.

The most dominant change in seasonality as a consequence of tidal forcing in the seasonally stratified subdomains (pos. SNS and deep NNS) is the delay of the spring bloom in the tidal scenario (Fig. 5b, c). However, in the pos. SNS, this delay is only a few days long; in the deep NNS, this delay encompasses 1 month. Accompanying the delay, the amplitude of the spring bloom in the tidal scenario, especially in the pos. SNS, exceeds that of the non-tidal scenario. The spring bloom in the NS typically consists of diatoms, while after silicate depletion, flagellates dominate the summer production (McQuatters-Gollop et al., 2007; Schrum et al., 2006). Comparing the seasonality of NPP variation (Fig. 5b, c) with the annual averaged NPP deviation between scenarios (Fig. 2c), we found that the variation in NPP in summer is basically in phase with the direction of the NPP's response to tidal forcing for both the deep NNS and pos. SNS. Especially in the pos. SNS (Fig. 5b), summer blooms are higher in the tidal scenario than in the non-tidal scenario, with a maximum difference in July and August, fostered by weaker stratification and regular nutrient injections into the surface mixed layer due to tidally induced turbulence (Fig. 6f, h). Surface summer production is sustained throughout the summer at values of approximately 50 $mgC\,m^{-3}\,d^{-1}$ and more in the upper 15 m (Fig. 6f), and light remains the

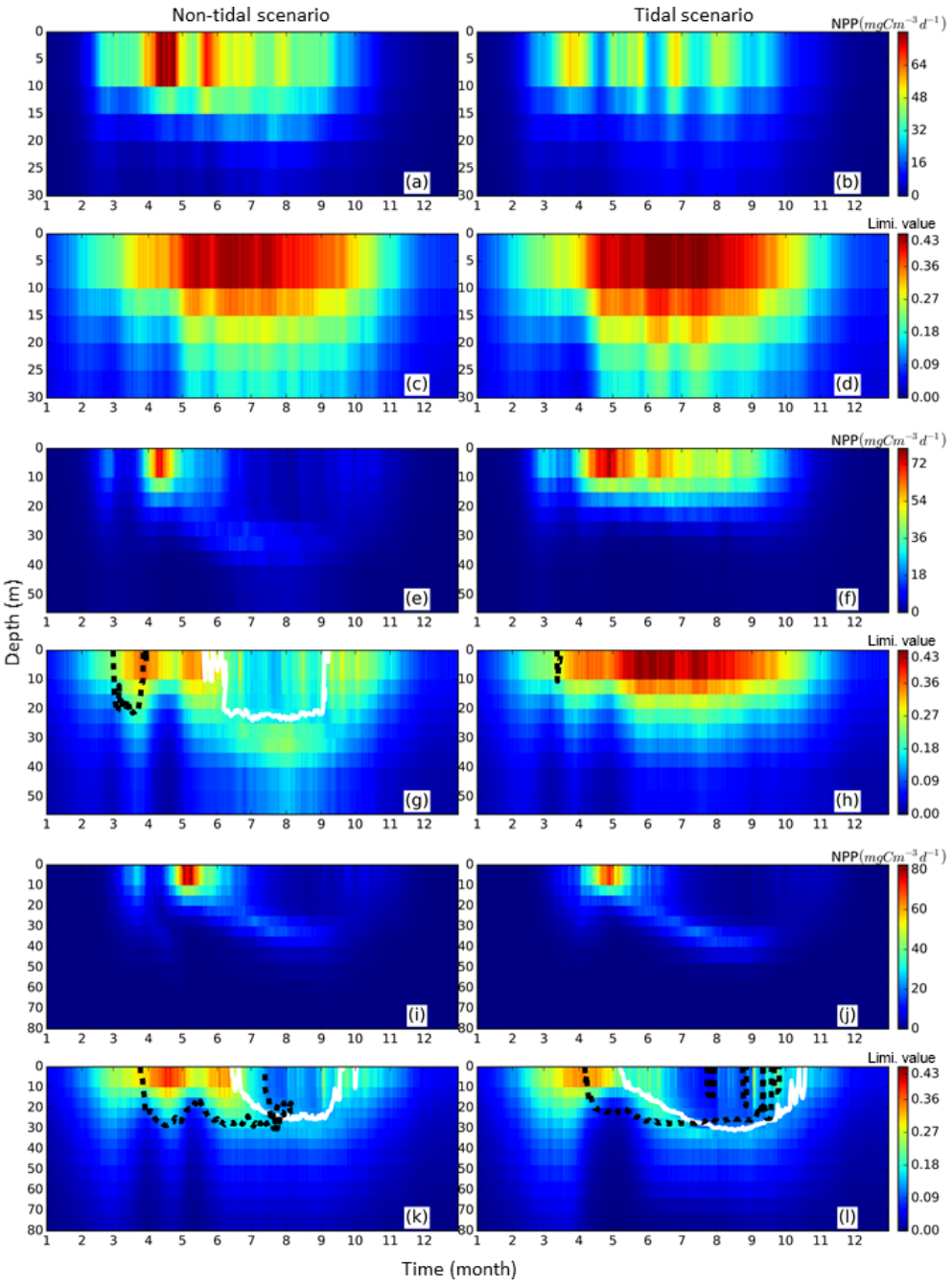

Figure 6. Time series of averaged (1990–2015) NPP vertical profiles (upper panels for each representative grid cell) and the limiting value (lower panels for each representative grid cell) for the tidal (right) and non-tidal (left) scenarios. NPP and limiting values are presented as the mean of each representative point for three subdomains, i.e., neg. SNS, the negatively responding southern North Sea **(a–d)**, pos. SNS, the positively responding southern North Sea **(e–h)** and deep NNS, the deeper northern North Sea **(i–l)**. Additionally, the depth above which a specific nutrient (silicate: solid black line, nitrogen: dashed white line) is limiting to NPP is given.

dominant limiting factor in the surface layer, except for a temporal silicate limitation after the spring bloom (Fig. 6h). In contrast, without tidal stirring, surface waters become nutrient depleted soon after the spring bloom in May. After silicate limitation, nitrogen limitation persists (Fig. 6g) in the surface waters throughout the seasonal stratification, which results in the characteristic subsurface production in summer (Fig. 6e). Due to the weaker stratification and enhanced turbidity caused by tides, no SBM production occurs in this simulation. The nutrient supply advantage in the tidal sce-

nario persists until the beginning of October (Fig. 6f), when the water column in the non-tidal scenario is also mixed by atmospheric conditions, causing an increase in production at the surface. For the pos. SNS, the modulation of nutrient availability is the most important factor responsible for changes in NPP. The high biomass stays in the pycnocline during summer due to the weak mixing in the non-tidal scenario. In contrast, due to the weak stratification and strong mixing, generated high biomass is continuously mixed in the euphotic zone in the tidal scenario (Fig. A4c, d).

In the deep NNS, the influence of tides on NPP is relatively weak and mainly visible in summer (Fig. 5c). The deep NNS (Fig. 6i–l) is typically characterized by stable seasonal stratification and summer subsurface primary production in both the tidal and non-tidal scenarios. The delay of the spring bloom in the tidal scenario causes a quicker succession and consequently overlapping diatom and flagellate blooms (Figs. 6l, 5c). The productive period, which lasts nearly 3 months and includes two pulses of NPP in the non-tidal scenario (Fig. 6i), is shortened to 6 weeks in the tidal scenario (Fig. 6j). The NPP contributed from subsurface production is higher in the tidal scenario than that in the non-tidal scenario (Fig. 6i, j). Because of stratification and nutrient depletion, high biomass is confined to a region within the pycnocline in both scenarios. The SBM in the tidal scenario deepens because of mixed layer deepening due to tides (Fig. A4e, f).

In the other identified subdomains (results not shown), the changes in primary production basically follow the pattern explained above. In the EC subdomain, the tidal impact on production is comparable to that in the neg. SNS, whereas in the BC subdomain, nutrients are rarely the most limiting factors due to weak stratification, and the response can be compared to that in the pos. SNS. In the low-sen. NNS, where tidal dissipation is weak, the vertical distribution pattern of NPP in both scenarios is almost identical.

Our results indicate that, in principle, tidal stirring causes two major changes in the NPP pattern: (i) a change in the spring bloom phenology of some areas and (ii) an altered ratio between surface and subsurface production. Both features merit further discussion, which is given in the following paragraphs.

3.2.1 Changes in spring bloom phenology

As one of the most important biological events in the NPP annual cycle (Bagniewski et al., 2011; Sabine et al., 2004), the spring bloom requires specific attention. As shown by the time series analysis for some subdomains (Fig. 5) and the time series of profiles at the representative points (Fig. 6), the postponement of the spring bloom is a prevalent phenomenon when tidal forcing is applied. The changes in spring bloom phenology and the processes responsible for these changes, such as the delay in the onset of stratification, variations in light conditions, the mixed layer depth and winter zooplankton concentrations (Fig. 7), were analyzed using the method outlined in Sect. 2.4.2.

In line with the distribution of tidal energy dissipation given by Davies et al. (1985), the spring bloom delay is robust in the SNS and along the British coast (Fig. 7a), while in the northeastern part of the North Sea, the spring bloom is delayed in no more than 50 % of all years. An increase in the peak spring bloom biomass (Fig. 7b) is mainly in areas with a positive response of NPP to tidal forcing (Fig. 2c). However, in some isolated locations in the negatively responding areas, such as the neg. SNS and EC, the spring bloom amplitudes are still higher in the tidal scenario than those in the non-tidal scenario in more than 50 % of the years. One potential reason for the spring bloom delay is a change in light conditions, especially in very shallow coastal, non-stratified areas where tidal stirring enhances resuspension in the water column (Fig. 7c). The onset of light conditions sufficient for phytoplankton growth in the well-mixed water column is delayed in the coastal areas of the southern and eastern boundary and in the shallower parts of Dogger Bank. However, the distribution of this impact does not explain the major patterns of changes in the spring bloom phenology. Tides also increase mixing and hence potentially prevent stratification in shallow water columns or delay the onset of stratification, as discussed previously by a number of authors (Bowden and Hamilton, 1975; Loder and Greenberg, 1986). Because tidally induced energy dissipation is cubically proportional to the strength of tidal currents (Simpson and Hunter, 1974), we can expect the strongest variation in stratification in regions with the strongest tidal currents, as observed along the British coast, in the EC and in the German Bight (Davies et al., 1985). This expectation is supported by earlier observations suggesting that the onset of the spring bloom is triggered by improved light conditions because of solar radiation and stratification (van der Woerd et al., 2011). The onset of stratification (Fig. 7e) in the tidal scenario is mainly delayed on the Scottish coast and the frontal areas of the SNS. Furthermore, the response of stratification to tidal forcing is more stable in the southwestern part (the Estuary of Humber, Dogger Bank) than in the southeastern part of the SNS (Fig. 7e). Apart from solar heating, the stratification in the southeastern part of SNS is additionally influenced by freshwater supplies from land and wind forcing (Jacobs, 2004; Ruddick et al., 1995; Schrum, 1997). Consequently, the variation in the onset of stratification is less clear in the southeastern part than in other parts of the SNS. In the NNS, the tidal wave propagation deepens the mixed layer depth (Fig. 7d), which similarly results in a later onset of the spring bloom, despite only weak changes in the onset of stratification. As a consequence of the thicker layer in which phytoplankton are mixed, the phytoplankton are less exposed to the favorable surface light conditions and will thus take longer to build up the spring bloom biomass.

Although the North Sea is in principle a bottom-up-controlled ecosystem, zooplankton predation is occasionally

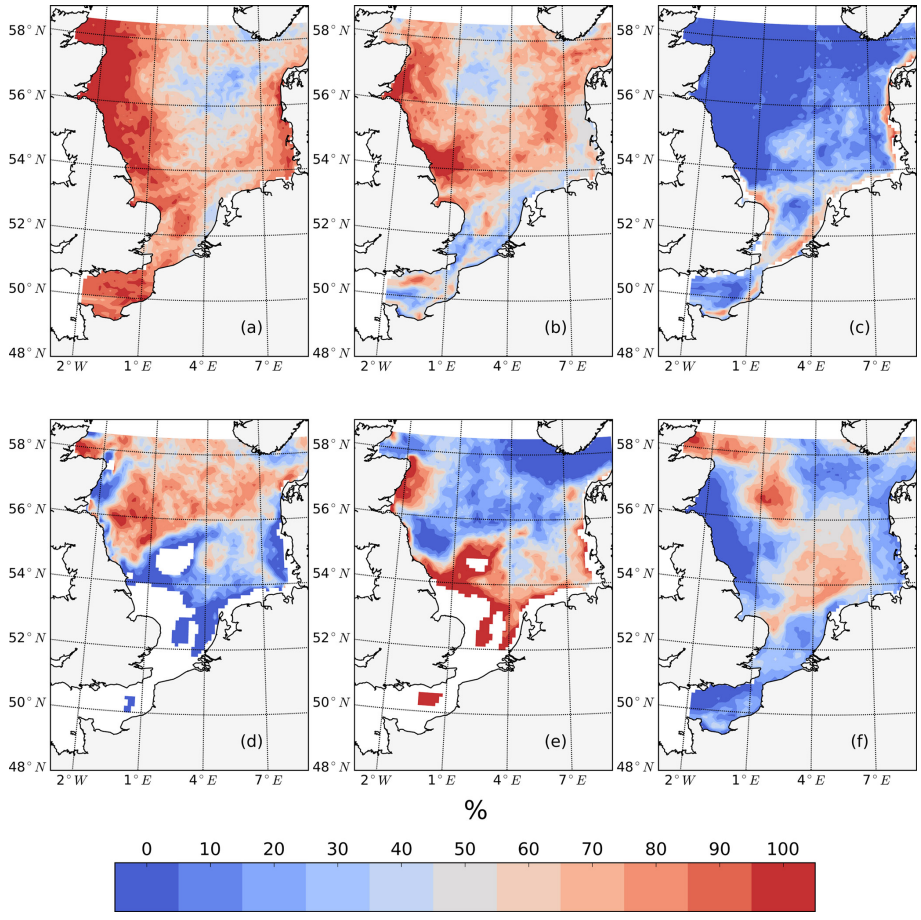

Figure 7. The percentage of years (1990–2015) in which specific processes potentially related to spring bloom phenology changed after considering tides. Changes include a later onset time of the spring bloom **(a)**, higher peak spring bloom biomass amplitudes **(b)**, a delay in the onset of light conditions in the water column sufficient for phytoplankton growth, as indicated by an integrated light-limiting term in the upper 50 m, exceeds 0.85 **(c)**, the deepening of the mixed layer depth in May **(d)**, a later onset time of stratification, which occurs when the maximum vertical temperature difference in the water column exceeds 0.5 °C for 3 consecutive days **(e)** and a higher concentration of overwintering zooplankton biomass **(f)**.

an important process controlling NPP (Daewel et al., 2014). In early spring, even under favorable growth conditions, the spring bloom will only initiate until production exceeds the loss due to grazing (George et al., 2015; Martin, 1965). This grazing pressure is basically correlated with the overwintering zooplankton stock. Based on our results, increases in the winter zooplankton biomass and delays in the spring bloom coincide only in the frontal region of the SNS and central NNS. Therefore, we conclude that the delay in spring bloom by tides is mostly due to bottom-up control.

The spatial pattern given in Fig. 7 shows that the delayed onset of the spring bloom in the tidal scenario may mainly be attributed to deteriorated light conditions in the shallow well-mixed area (Fig. 7c) and changes in the stratification of seasonally stratified areas, such as delays in the development of stratification (Fig. 7e) or the deepening of the upper mixed layer (Fig. 7d). Although the predator biomasses are higher prior to spring bloom in some areas, enhanced grazing pressure at the beginning of the bloom period does not seem to be the main mechanism delaying the onset of the spring bloom (Fig. 7f), although we assume this pressure plays an additional role in the central NNS and frontal regions.

3.2.2 Changes in subsurface production in stratified season

To further quantify the magnitude of the changes in surface and subsurface production during the stratified season, we separated NPP vertically into upper-layer production (above 15 m) and production in the SBM layer and compared the results between scenarios (Fig. 8), using the mean annual value for the analyzed period (1990–2015). At the stratified side of the frontal zones (pos. SNS), the surface production response of NPP is positive almost everywhere, with a maximum reaching $+50\,\mathrm{gC\,m^{-2}\,year^{-1}}$ (Fig. 8b) at south of Dogger Bank. In contrast, the changes in response to tidal

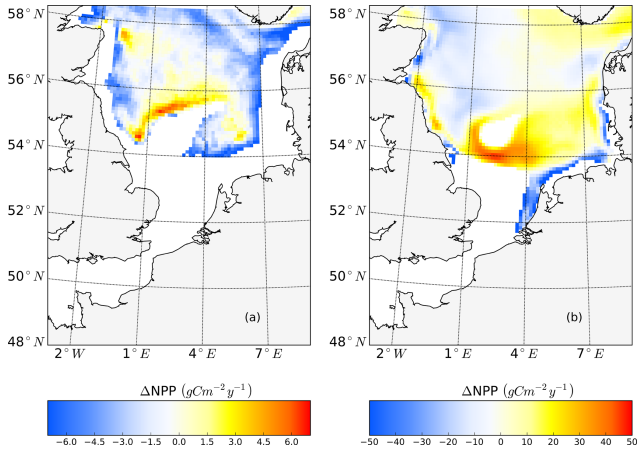

Figure 8. Mean difference in the NPP between the tidal and non-tidal scenarios generated within the SBM layer **(a)** and in the surface layer (above 15 m) **(b)**. The results are averaged for the stratified season. Areas with SBM mean occurrences of less than 10 d per year are excluded in panel **(a)**. Areas with stratification (squared buoyancy frequency $N^2 >= 0.013$ (s^{-2}) averaged less than 60 d per year are excluded in panel **(b)**.

forcing within the SBM show both negative and positive responses around Dogger Bank (Fig. 8a). A positive response to tidal forcing, which is generally 1 order of magnitude smaller than the increased amplitude of NPP in the surface layer, occurs only at the northern edge around Dogger Bank and the deeper part of the German Bight. A similar pattern with a strong positive response to tidal forcing at the surface and a negative response in the SBM appears in the BC area. In line with former studies in the North Sea, the NPP in the upper layer dominates the whole production budget (van Leeuwen et al., 2013). Although the expansion and duration times of the SBM decrease due to tidal forcing, e.g., in the inshore areas along the BC and at the Danish coast (Fig. A3c, d), tidal forcing promotes NPP within the SBM in some areas, especially at the northern edge of Dogger Bank. Observational studies suggested that the productive areas at the edge of Dogger Bank are fueled by baroclinic circulation related to the front and the spring–neap adjustment (Pedersen, 1994). When considering an SBM duration of 110 d (Fig. A3c) at the northern edge of Dogger Bank, the average daily NPP (deduced from the annual NPP; Fig. A3a) is approximately 239 mgC m^{-2} d^{-1}, which corroborates the observation-based estimate of NPP (295 mgC m^{-2} d^{-1}) calculated from measured oxygen surplus concentration data (Richardson et al., 2000).

In the NNS, the variation caused by tidal forcing in NPP is below 15 gC m^{-2} $year^{-1}$ (Fig. 2c). In some parts of the deep NNS, the tidal forcing causes higher production in the SBM and lower production at the surface (Figs. 6i, j; 8a). Due to the decoupling between the surface and bottom mixed layers, the pycnocline acts as a barrier that keeps the stirred-up nutrients below the pycnocline and sustains NPP in the SBM (Fig. 6i, k). Because the amplitude of NPP variations in the upper layers is 10 times higher than that in the SBM (Fig. 8), the overall response to tidal forcing is negative (Fig. 2c) in the deep NNS.

3.3 Impacts of the spring–neap cycle

The spring–neap tidal cycle introduces a fortnightly periodic change in tidal mixing, which has a significant influence along the British coast and in the English Channel (Fig. 9). The differences in current speed between the tidal and M_2 tidal scenarios vary over the spring–neap tidal cycle. The maximum spring–neap range of these differences is up to 0.3–0.6 m s^{-1} (Fig. 9), indicating that a non-negligible change in turbulent kinetic energy is introduced to the water column via the spring–neap cycle. Here, we will provide model estimates on the spatial variability in the resulting response of the NPP to the spring–neap cycle and explore the potential mechanisms of these responses.

Annual NPP changes induced by the spring–neap cycle reach maximum values of up to 5 gC m^{-2} $year^{-1}$ (Fig. 9). Although this amount is relatively small compared to the overall system productivity, the changes due to spring–neap dynamics could be very relevant locally and in specific time periods. An average positive response of NPP emerges in the southeastern part of the North Sea, in the English Channel and along the British coast (Fig. 9). The highest mean changes in NPP are found in the western part of Dogger Bank, in the English Channel and off the Scottish coast. In contrast, a negative response in annual production emerges off the Northumbrian coast and in the Southern Bight off the European continent (Fig. 9). The response of NPP to spring–neap tidal forcing is weak in early spring and winter (data not shown). Under mixed conditions or during periods of the establishment and decay of stratification, spring–neap tidal mixing can be overridden periodically by other mixing events (e.g., driven by wind); hence, pronounced irregularities in NPP responses to spring–neap tidal forcing are detected. A significant response of NPP to spring–neap tidal forcing is found for summer periods under stable stratification. To illustrate the basic mechanisms responsible for the response of NPP due to spring–neap tidal cycle, we present time series of the biomass, nitrate, NPP and turbidity (Eq. 1) profiles for two characteristic grid cells (selection described; see Sect. 2.4.5) that respond differently to spring–neap tidal forcing. The near-shore grid cell off the Estuary of Humber (EH, Fig. 9) shows a negative response, and a grid cell located at the frontal zone at the western edge of Dogger Bank (WDB, Fig. 9) responds positively to spring–neap tidal forcing. The model results are presented for a couple of selected successive spring–neap tidal cycles simulated for the year 2001 (Fig. 10).

The EH site, which is located further inshore compared to the WDB, is characterized by high turbidity. The increased

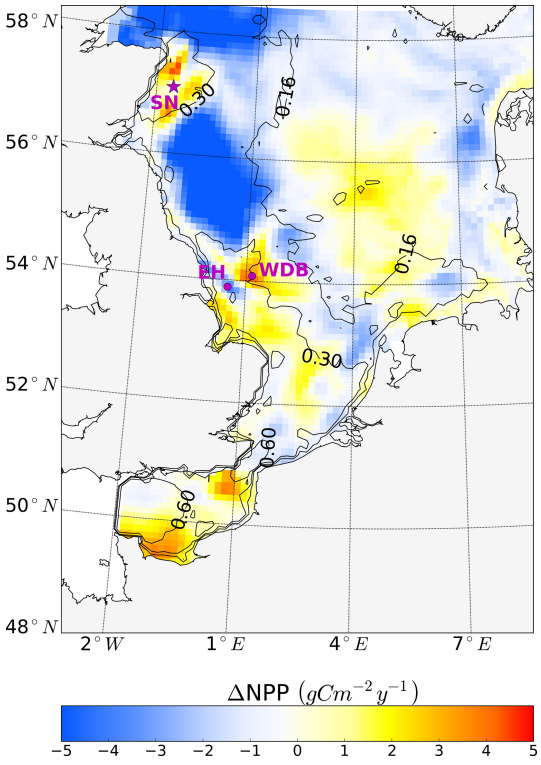

Figure 9. Simulated annual mean NPP difference between the tidal ($M_2 + S_2$) and M_2 scenarios, averaged for 1990–2015. Positive values depict higher NPP values in the tidal scenario (M_2+S_2) than in the M_2 scenario. Contour lines indicate the estimated mean spring–neap cycle range of the tidal current speed difference between the tidal ($M_2 + S_2$) and M_2 scenarios. The two magenta dots indicate the locations of two characteristic grid cells. One grid cell is close to the Estuary of Humber (EH), and the other grid cell is located more offshore at the western edge of Dogger Bank (WDB) (see Fig. 10). The magenta star shows the location of the grid cell (SN site) used for the analysis of the advancement and delay of the spring bloom due to spring–neap tidal forcing (see Fig. 11).

nitrogen in the upper layers is in phase with elevated turbidity but in anti-phase with biomass and NPP. This phenomenon indicates that during spring tide, the process of phytoplankton biomass dilution (Fig. 10c) and shading due to the upward mixing of organic material (Fig. 10b) slows NPP in the upper mixed layer, resulting in a negative NPP response during spring phases (Fig. 10d). The elevated NPP reaches a maximum at the end of the neap phase (Fig. 10d), possibly because of the reduced vertical mixing. The decreasing turbidity in the neap phases, despite increases in phytoplankton biomass, reveals that suspended and resuspended organic material have a reduced impact on the surface light conditions during neap phases compared to the spring phases (Fig. 10b). In neap tidal phase, given less vertical mixing, phytoplankton cells remain in the lighted surface layer for longer time and access better light conditions; hence, the available nutrients can be utilized for phytoplankton growth (Fig. 10c).

In contrast, the WDB site is typically characterized by seasonal stratification and summer nutrient (i.e., nitrate) depletion in the surface layer. However, as the WDB site is located in the frontal zone, relevant factors in this zone do not necessarily show the spring–neap fluctuation as clearly as those at the EH site. During spring tide, enhanced vertical mixing dilutes the phytoplankton biomass in the upper layer and redistributes biomass more evenly in the whole water column, resulting in less phytoplankton biomass in the upper layer (blue) and more biomass in the lower layer (red) compared to that in the M_2 scenario (Fig. 10g). Spring tidal forcing results in the replenishment of nutrients in the euphotic zone and a pulse of increased NPP follows spring tide mixing (Fig. 10e, h). The downward mixing of biomass into lower layers has no substantial negative effect on NPP during spring tide (Fig. 10g). As a consequence of nutrient replenishment in the surface layer during former spring tides, given less vertical mixing during neap tide, biomass increases in the upper layers (Fig. 10g). Resuspension effects resulting in increased turbidity at lower layers are visible from neap to spring but do not significantly change turbidity in the surface layers (Fig. 10f). Surface turbidity changes are consequences of increased NPP (Fig. 10f).

Observation-based estimates of spring–neap impacts on NPP given by Richardson et al. (2000) found that increased nitrate fluxes by tidal pumping contributed to NPP with 4–6 $gC\,m^{-2}$ for one spring–neap cycle at the northern edge of Dogger Bank, mainly due to increased production in the subsurface layer. By upscaling these results to the entire stratified season, considering six to eight spring–neap cycles, Richardson et al. (2000) proposed that the additional NPP contribution by the spring–neap cycle was in the range of 24–48 $gC\,m^{-2}$ for the whole stratified season. We resampled the simulated NPP along the same transect as sampled by Richardson et al. (2000) and for the same time period (29 July–4 August 1997). We extended the time period to 26 July–8 August 1997 to cover a full spring–neap cycle and found our simulated response of NPP to tidal forcing (the tidal scenario – non-tidal scenario) is 3.03 $gC\,m^{-2}$ for one spring–neap cycle (Fig. A5a). These values are slightly below the lower edge of Richardson's estimates (4–6 $gC\,m^{-2}$). However, simulated frontal locations are not always conformed to the observed fronts due to unresolved subscale processes, which remain unconsidered in a 10 km × 10 km model resolution and coarse atmospheric forcing (NCEP/NCAR reanalysis). When we resampled the NPP along the fronts in our simulation, which is at a distance of a few grid points further south from the fronts in Richardson et al. (2000) (Fig. A5a), we found that the simulated change in NPP (5.99 $gC\,m^{-2}$ for one spring–neap cycle) reaches the upper level of estimates based on observations (Fig. A5a, Table A1). When we compare the NPP response throughout the whole stratified season (simulated as

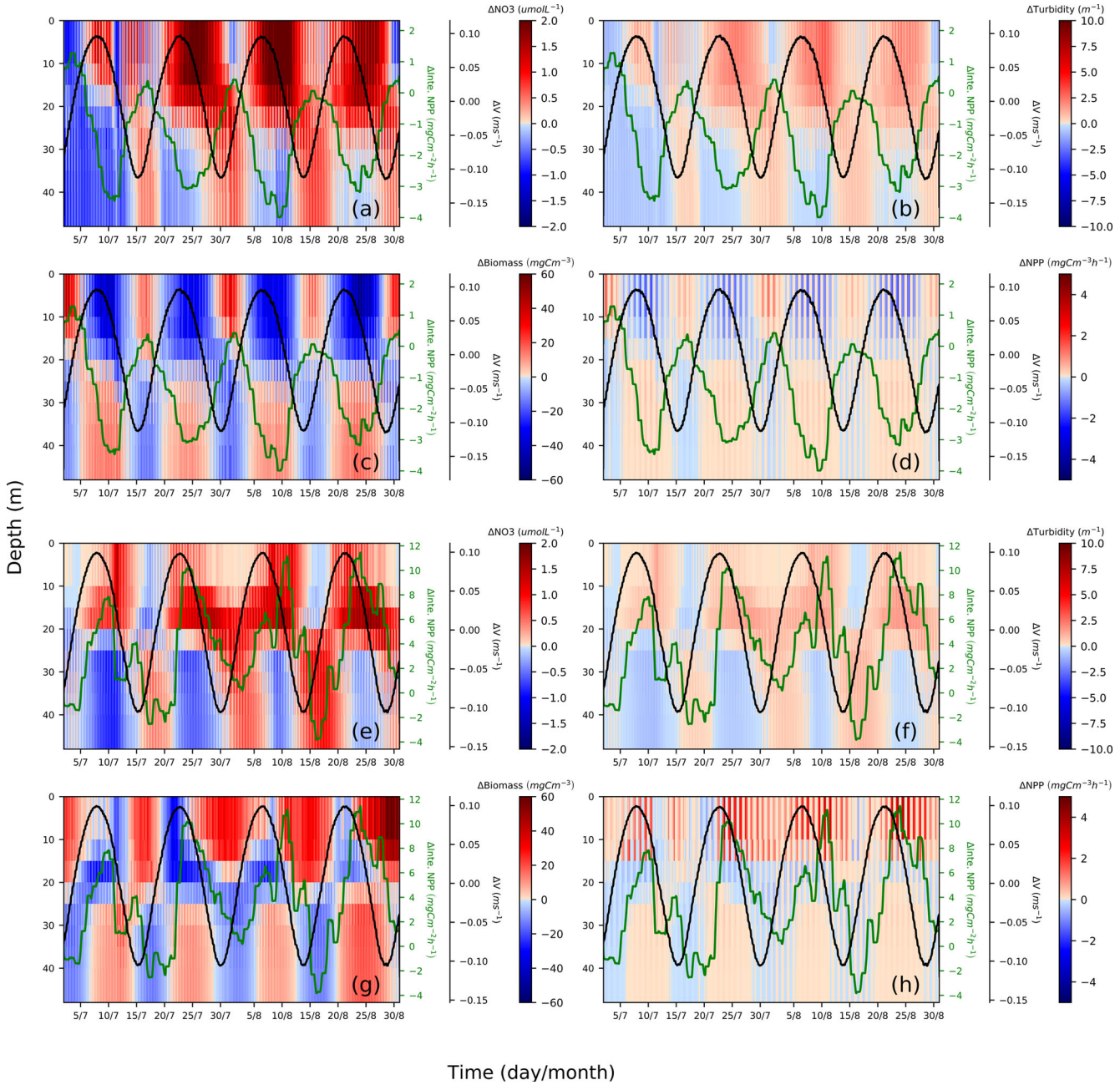

Figure 10. Spring–neap cycle impact on nitrate **(a, e)**, turbidity **(b, f)**, phytoplankton biomass **(c, g)** and primary production **(d, h)**. Differences between the two scenarios (tidal scenario $(M_2 + S_2) - M_2$ tidal scenario) are presented for two characteristic points, i.e., EH: **(a)–(d)**, WDB: **(e)–(h)**. To show the periodical fluctuation of currents and NPP and relate these fluctuations to changes in nitrate, turbidity, biomass and NPP, the differences in the depth-averaged velocity amplitude (black) and depth-integrated NPP (green) are presented in each subplot; both time series underwent smoothing with a 24 h running mean.

15 gC m^{-2}) we find this to be lower than Richardson's upscaling estimation (24–48 gC m^{-2} for the whole stratified season). The reason for this discrepancy is a oversimplified upscaling procedure used by Richardson et al. (2000), neglecting the sensitivity to seasonality. Conditions measured over a few days between July and August (Richardson et al., 2000) are not representative of the whole stratified season. In contrast to Richardson et al. (2000)'s conclusion that spring–neap cycle played the major role in fueling NPP, our study indicates further, that the semidiurnal tide plays the major role in pumping up nutrients and sustaining the NPP but not the spring–neap cycle as hypothesized by Richardson et al. (2000). Our estimate of, on average, 0.14 gC m^{-2} of NPP promoted by the spring–

neap tide during one tidal cycle (Fig. A5b) is considerably lower than that supported by the standard tidal forcing ($M_2 + S_2$) (5.99 gC m^{-2}) (Fig. A5a), and hence spring–neap tidal pumping contributes only little to the increase in NPP. Based on our simulation, tidal pumping sustaining subsurface NPP mainly occurs in July and August, with an average value of approximately 3 gC m^{-2} month^{-1} in frontal areas around Dogger Bank. This is close to the estimate of Richardsons et al. (2000). In other weakly stratified months, the value is no more than 1 gC m^{-2} month^{-1} or even negative (data not shown).

Sharples (2008) investigated a similar question for the Celtic Sea with model simulations. He found that the NPP varied up to 70 % with the spring–neap tidal cycle. We could not confirm such high tidal impacts on NPP for the North Sea; our estimates of the response of NPP to the spring–neap tidal cycle are only up to approximately 10 % of the tidal impact ($M_2 + S_2$) on NPP (Figs. 2 and 9). One explanation for this discrepancy is the higher spring–neap tidal current amplitude in the Celtic Sea compared to the North Sea, which may result in a stronger response of NPP to the spring–neap cycle. However, it is also possible that the simpler model setup used by Sharples, such as neglect of advection, a constant grazing rate and neglected impacts on resuspension and shading by DOM and detritus, resulted in higher NPP sensitivity to tidal forcing in their simulation.

As discussed in Sect. 3.2, tidal forcing not only impacts the magnitude of NPP but also spring bloom phenology. It is reasonable to assume that spring–neap tidal forcing also modulates the development of the spring bloom. To understand the impact of the spring–neap phase on the biomass build-up during the spring bloom, which typically occurs over one or several spring–neap cycles, we related the time periods with the maximum difference in NPP between the tidal scenario and the M_2 scenario to the spring–neap cycle phase (Fig. 11) at the SN (Spring–Neap) site (see Fig. 9). The SN site is located in the tidally energetic northwestern North Sea, where the development of the spring bloom often benefits from thermal stratification (Rodhe, 1998) but is sensitive to episodic "noise" added by wind forcing (Waniek, 2003). During the development of the spring bloom, in the difference between NPP time series (tidal scenario $- M_2$ scenario), an increase in NPP often occurs in neap phases, whereas NPP is often decreased in spring phases. This indicates that the development of the spring bloom benefits from the neap phase but is interrupted or dampened during the spring tide (Fig. 11). A similar phenomenon has been explored and confirmed by Sharples et al. (2006) at a site south of the SN site. As suggested by Sharples et al. (2006), the onset time of the spring bloom is shifted by the spring–neap tidal cycle because the onset or intensity of stratification is strengthened during neap tides when the vertical mixing is dampened.

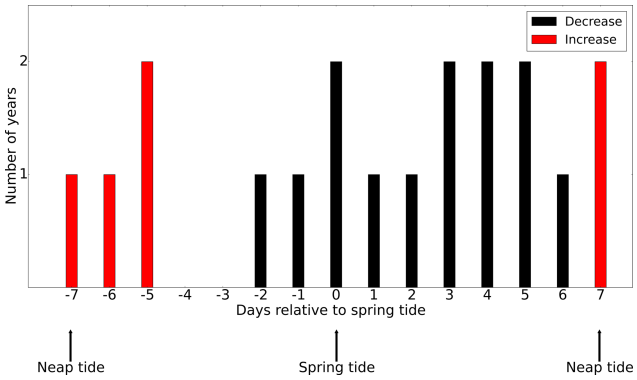

Figure 11. The occurrence of an increase (red) or decrease (black) in the NPP difference (tidal scenario $(M_2 + S_2) - M_2$ tidal scenario) relative to the nearest spring tide (spring and neap phase indicated). The development of the spring bloom period is defined as the time when NPP increases from 12.5 % to 87.5 % of the maximum NPP prior to the major peak of the spring bloom.

4 Summary and conclusions

A model-based sensitivity experiment with varied tidal forcing was performed to evaluate tidal impacts on NPP, considering the major bottom-up controlling processes, including the tidal mixing of nutrients, organic matter and plankton biomass and tidal resuspension of suspended matter. The responses to tides in the North Sea differ regionally and depend on the local hydrodynamic characteristics. In permanently mixed areas in the southern part of the North Sea, light availability is the major limiting factor. The enhanced tidal resuspension and mixing of suspended matter into the surface layers deteriorate light conditions in the upper layers for phytoplankton growth and thus hinder primary production. In contrast, in frontal areas and seasonally stratified areas in the SNS where stratification is susceptible to tidal mixing, nutrient replenishment due to tidal forcing sustains NPP in summer and thus contributes a significant increase in NPP in both the surface layer and within the pycnocline. In the NNS, which is characterized by relatively weak tidal forcing and deep bathymetry, the bottom and upper mixed layers are well separated, and the influence of tidal forcing on NPP is limited.

However, the quantitative estimates provided here are model and parameterization specific. Dominant biochemical processes are generally well represented in simplified NPZD-type models, and the ECOSMO model used here is applicable for resolving ecosystem dynamics at seasonal to decadal timescales when forced by realistic boundary conditions (Daewel and Schrum, 2017). However, parameterization and unconsidered processes, such as the role of macrobenthos in the system, internal waves at the shelf break and coastal light attenuation due to inorganic suspended matter, and simplified physiological processes could potentially modulate or change the model's sensitivity to tidal forcing.

Studies identifying the contribution of these processes to tidal impacts on primary production are needed; thus far, we can only speculate on potential impacts.

Macrobenthic grazing likely changes the biochemical cycling and turbidity in the water column, subsequently changing the sensitivity of NPP to tidal forcing. In shallower waters, high near-bottom concentrations of suspended organic matter are susceptible to mixing into the euphotic zone, and increasing light attenuation leads to decreasing production (see Fig. 7c; cf. Sect. 3.1). Macrobenthic biomass, specifically from filter feeders, might significantly reduce resuspension and near-bottom suspended matter concentrations, thereby increasing the proportion of organic matter that remains in the food web (Prins et al., 1996). From observations, we know that macrobenthos show a distinct spatial pattern following principle production patterns in the North Sea with higher biomass in the shallow SNS (Heip et al., 1992). Therefore, we can expect an increase in NPP sensitivity to tidal forcing due to macrobenthos activity.

Furthermore, we hypothesize that the positive response of NPP to tidal forcing in the NNS was underestimated by our simulation due to the implementation of identical boundary conditions for all scenarios. We neglected the influence of tidal-generated internal waves on nutrient conditions. Tidal-generated internal waves are initiated at the shelf edge and enhance turbulent mixing at the shelf break and on the shelf (Heathershaw et al., 1987; Loder et al., 1992; New and Da Silva, 2002; Sharples et al., 2001). As internal tides break at the shelf edge, energy dissipates mainly at the shelf break and other bathymetric features, which causes vertical mixing that drives vertical nutrient fluxes and sustains phytoplankton growth (Holligan et al., 1985; Pingree et al., 1981; Sharples et al., 2007). Therefore, internal tidal waves will likely lead to mixing and increase nutrient pulses onto the shelf, consequently supporting NPP. In our setup, the average impact of tidal-generated internal waves on nutrient concentrations was considered with the climatological boundary conditions (Conkright et al., 2002), and differences among the simulated scenarios were not considered.

Another source of uncertainty in our model stems from the neglecting feedbacks related to inorganic material, which influences underwater light conditions, especially in shallow areas. Seasonal differences in yellow substance concentrations coincide with freshwater input (Schaub and Gieskes, 1991; Warnock et al., 1999). There are two main sources of SPM plumes in the North Sea. One source lies at the southern British coast and originates from local discharges (Humber–Wash and Thames rivers), coastal erosion and influx from the English Channel (Eisma, 2009). The other major source of SPM originates from the large continental rivers and diffusive sources entering the North Sea from the European continental coast, particularly off the Belgian coast and the Wadden Sea (van Alphen, 1990; Postma, 1981). Waves and currents are the controlling factors of the dispersion, resuspension and deposition processes of SPM (Holt and James, 1999). In winter, the two SPM plumes expand further offshore due to intensified mixing and both SPM plume deposits in both the Skagerrak and Norwegian channels. We have evaluated the potential impacts of inorganic SPM on our findings (Appendix C) and found that the general results regarding the tidal impacts on NPP remain largely insensitive to consideration of inorganic SPM and its seasonality. The reason lies in the spatial and temporal distribution of the SPM in the North Sea. During summer, SPM concentrations are low (Fig. C1) especially in stratified conditions and upper water layers (Capuzzo et al., 2013; Dobrynin et al., 2010). Only in shallow areas with permanent mixing, SPM concentrations are high (Van Raaphorst et al., 1998). This is critical for our analysis since most differences in NPP actually occur in summer stratified conditions. A simulation study (Tian et al., 2009) in the German Bight found that implementing SPM is only critical at the onset of bloom, given reasonable parameterization, similar bloom amplitude was achieved in scenarios including or omitting SPM. Furthermore, measurements suggested that in the central North Sea, the water body itself triggers most of the attenuation (Jones et al., 1998). SPM is more relevant to attenuation in nearshore areas due to cliff erosion and river input (Eisma, 2009). The relevance to turbidity of fluvial SPM is confined to river mouths because SPM deposits quickly (Pleskachevsky et al., 2011; Siegel et al., 2009). Organic suspended matter (which is considered in the model) accounts for a high fraction of the total suspended matter (TSM) in most areas in the southern North Sea except for the very nearshore areas (Schartau et al., 2018). The areas where inorganic suspended matter dominates are in the negatively responding regions of our analysis (Fig. 2c). The distribution of inorganic suspended matter is influenced by many factors, such as transportation with residual currents, aggregation with organic matter, type of benthic sediments and so on. Clearly, interaction processes as mentioned above cannot be resolved by implementing a climatological SPM field. Thus, the numerical experiment presented here is considered to be a first step towards understanding the role of SPM for tidal impacts, and further studies specifically focusing on shallow coastal areas would require reasonable boundary conditions for inorganic matter from benthic sediments and river inputs as well as a more reasonable representation of biophysical interactions related to inorganic matter. However, this is beyond the scope of the current study and should be emphasized more thoroughly in future work.

The major tidal impacts on NPP are via vertical mixing. Given the small horizontal gradient of both nutrients and biomass and weak tidal residuals of no more than a few centimeters per second (Prandle, 1984), the impacts of horizontal advection are negligible. To investigate the influence of advection on the concentration of nutrients and phytoplankton biomass in our study, we estimated the net horizontal transport between grid cells. In most parts of the study domain, we found that the contribution of mean tidal advection does not exceed 5% (not shown here). Exceptions oc-

cur in the Skagerrak Channel, where relatively high residual currents drive water exchange between the North Sea and Baltic Sea (Brettschneider, 1967), and in the EC close to the model boundary, where relatively high current speeds caused by atmospheric forcing and topography emerge irregularly, mainly in spring and winter. However, this result is not true for smaller horizontal and temporal resolutions.

Since the North Sea can in general be considered as bottom-up controlled (Daewel et al., 2014; Heath, 2005), using a lower trophic level model for investigating tidal impacts on NPP is a valid approach. Although situations with clear top-down control on zooplankton have been observed (Munk and Nielsen, 1994), these events occurred highly restricted in time and space and assumed to be only of minor relevance for the general processes described in this paper. In previous studies, which addressed similar scientific questions, constant grazing rates (Sharples, 2008) or grazing loss proportional to phytoplankton biomass (Cloern, 1991) were prescribed in the simulations. In this study, we utilize a lower trophic level NPZD-type model, only considering lower trophic level dynamics up to zooplankton, which is simulated as a state variable considering feeding preference, growth, excretion and mortality. Fish predation is only implicitly considered as part of the zooplankton mortality rate. Simulations with ECOSMO E2E (an updated version of the ECOSMO model) including functional groups for fish and macrobenthos revealed that temporal and spatial variations in zooplankton mortality due to fish predation are determined by the specific hydrodynamics of the North Sea (Daewel et al., 2018). Repeating a similar study with an NPZD-Fish model would be interesting; however, it is beyond the scope of our study.

Given the importance of tidal forcing for NPP, especially in frontal areas, which are known to be biological hotspots (Belkin et al., 2009), tidal impacts on higher trophic levels than those studied here merit further consideration and investigation in the future. Regarding the growth of macrobenthos, tidal stirring influences the sinking and resuspension of organic matter and thus influences food quality and bioturbation (Foshtomi et al., 2015; Zhang and Wirtz, 2017). Tidal forcing in frontal areas not only provides enough prey for fish larvae due to nutrient enrichment and higher NPP but also influences convergence zones, which are typical places for fish spawning and nursing (Bakun, 2006). Further investigations based on a combination of observations and multiprocess coupled simulations could enable a better understanding of the impacts of tidal forcing on ecosystem processes and their variability. Long-term tidal variations, such as the 18.61-year nodal cycle or the 8.85-year lunar perigee cycle, merit particular consideration.

Data availability. Simulated data sets in this study are currently not publicly accessible but are available on request.

Appendix A

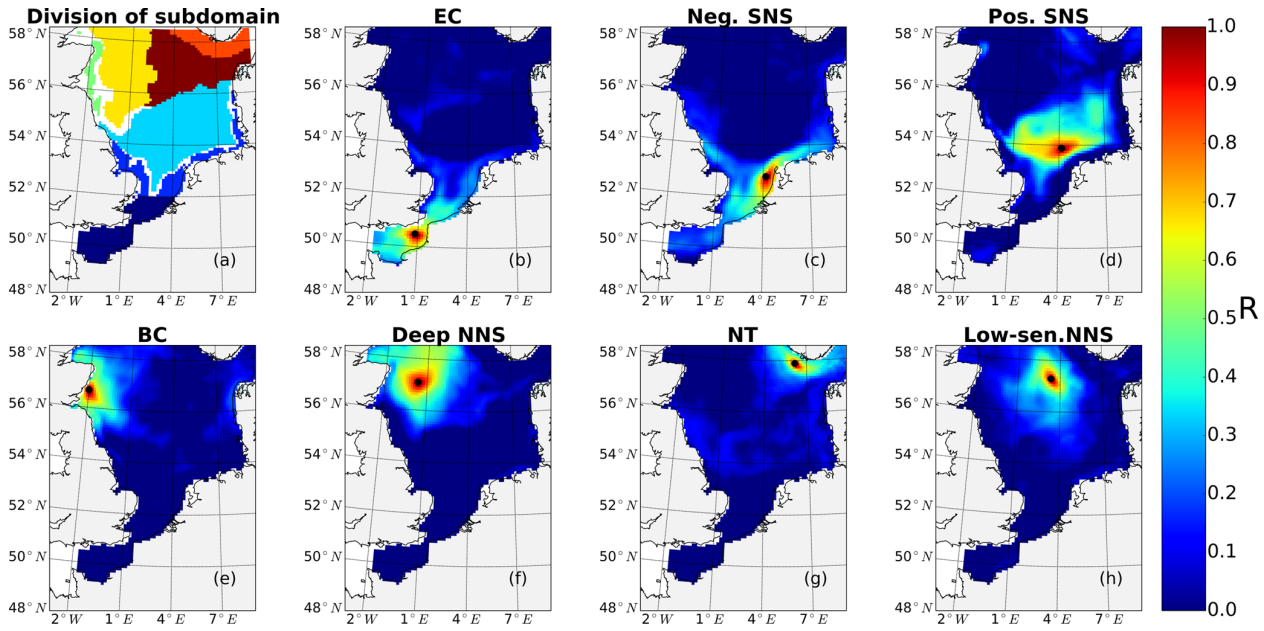

Figure A1. Subdomain divisions **(a)**, correlation coefficient of NPP variations at the most representative grid cell (black dot) and NPP variations in the surrounding grid cells for the English Channel **(b)**, negatively responding area in the southern North Sea **(c)**, positively responding area in the southern North Sea **(d)**, the eastern British coast **(e)**, the deeper part of northern North Sea **(f)**, the Norwegian Trench **(g)** and the low-sensitivity area in the northern North Sea **(h)**.

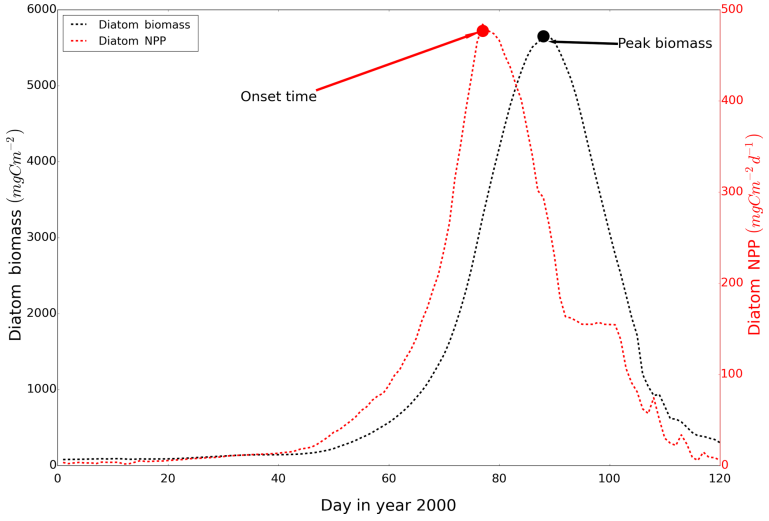

Figure A2. The definition of onset time of the spring bloom. The dashed black line is the time series of diatom biomass and the dashed red line is the time series of NPP. Both time series have undergone a 15 d running average. The black arrow depicts the time when the spring bloom reaches its maximum biomass. The red arrow depicts the time when the NPP reaches its maximum prior to biomass peak, which is defined as the onset time of the spring bloom. The time series is extracted from a grid cell (56° N, 4.2° E) from the ECOSMO simulation, for the year 2000.

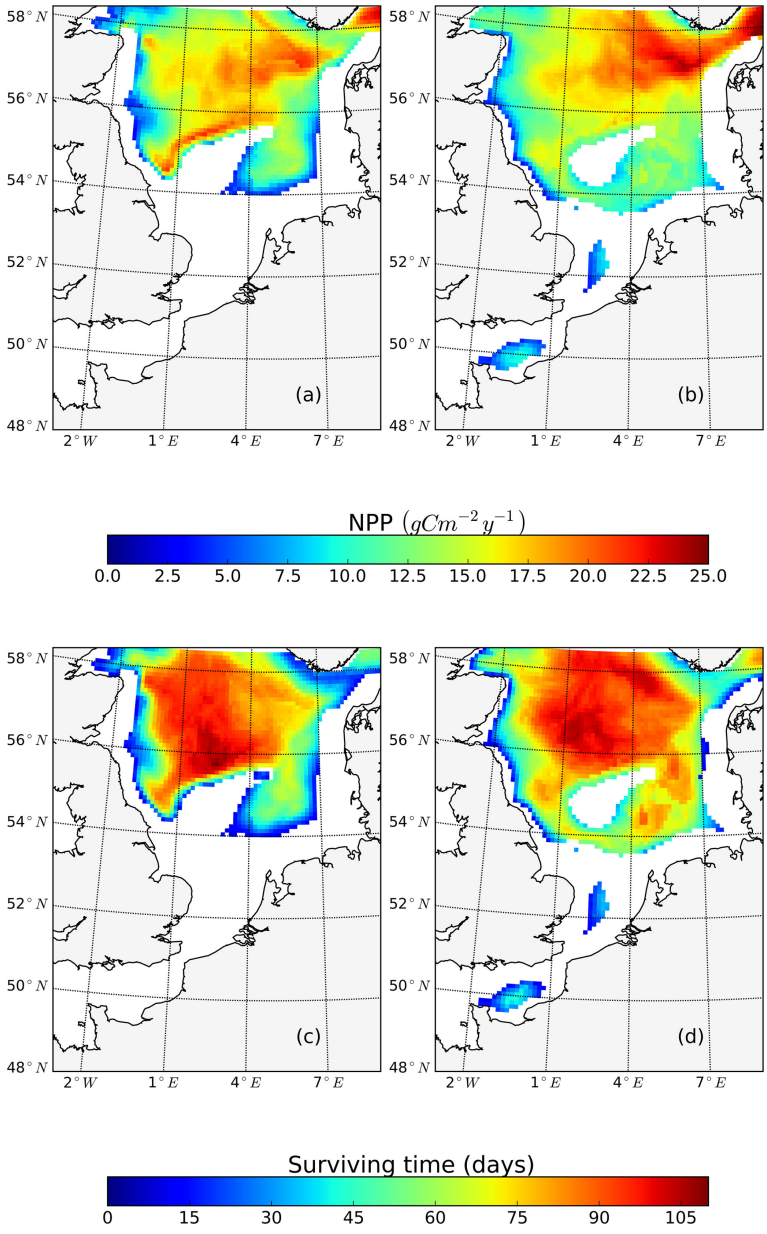

Figure A3. Annual mean NPP contributed by SBM in the tidal **(a)** and non-tidal scenarios **(b)**. Survival time of the SBM for the tidal **(c)** and non-tidal **(d)** scenarios.

Table A1. NPP contributed by tidal forcing in the transect where Richardson et al. conducted their observation (northern edge of DB) and in the transect where the most pronounced front is located in our simulation (frontal transect).

	Difference tide $(M_2 + S_2)$ − tide (M_2) (gC m^{-2} per spring–neap cycle)	Difference tide $(M_2 + S_2)$ − no tide (gC m^{-2} per spring–neap cycle)
Northern edge of DB	0.11	3.03
Frontal transect	0.14	5.99

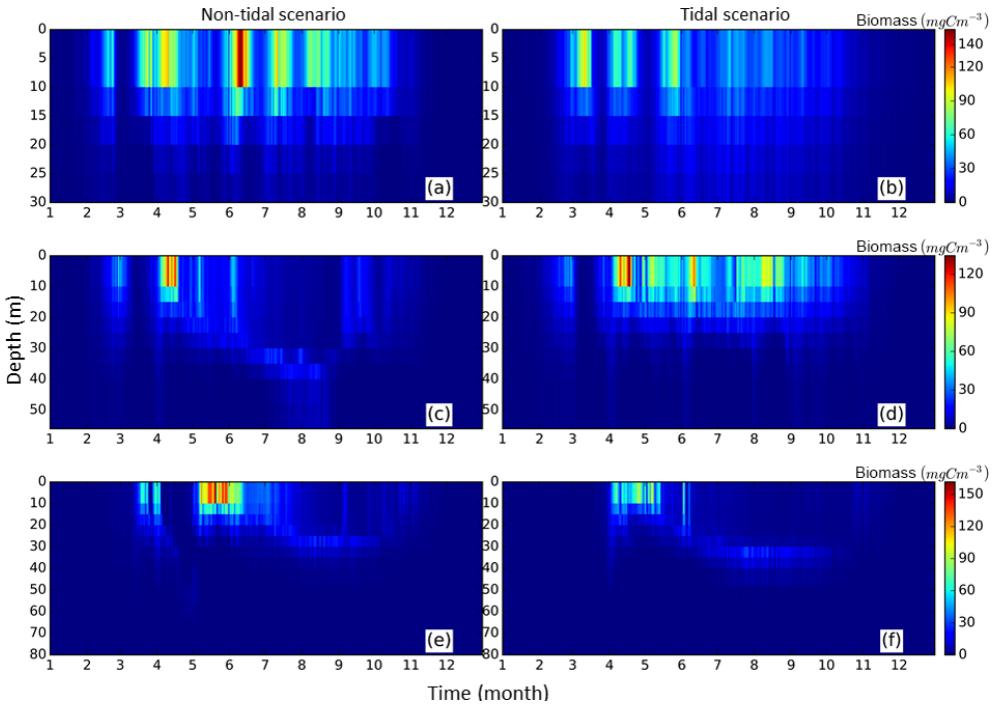

Figure A4. Annual mean (1990–2015) time series of vertical biomass profiles in the tidal **(b, d, f)** and non-tidal **(a, c, e)** scenarios at representative grid cells for the neg. SNS, the negatively responding southern North Sea **(a, b)**, pos. SNS, the positively responding southern North Sea **(c, d)** and for the deep NNS, the deeper northern North Sea **(e, f)**.

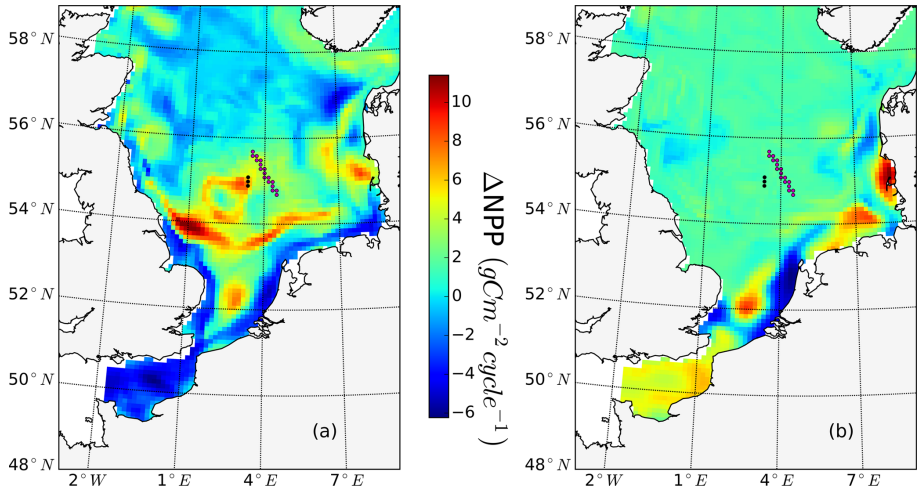

Figure A5. Vertically integrated NPP contributed by tide ($M_2 + S_2$) **(a)** and spring–neap tide **(b)** for one spring–neap cycle (26 July–8 August 1997) during the observational period studied by Richardson et al. (2000). Magenta dots depict the location of the transect which Richardson et al. (2000) has analyzed. Black dots depict the exact location of fronts in our simulation.

Appendix B

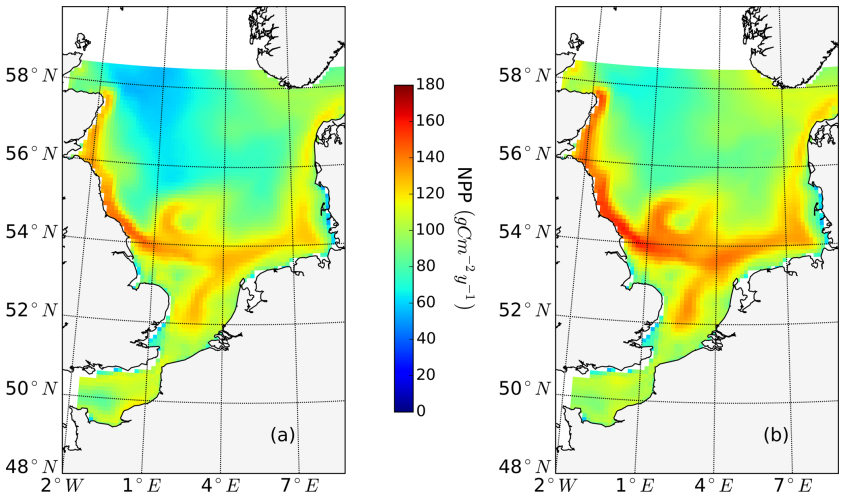

Figure B1. Mean annual net primary production for the analyzed period (1990–2015) simulated with the model configuration used by Daewel and Schrum (2013) **(a)** and the setup used in this study **(b)**.

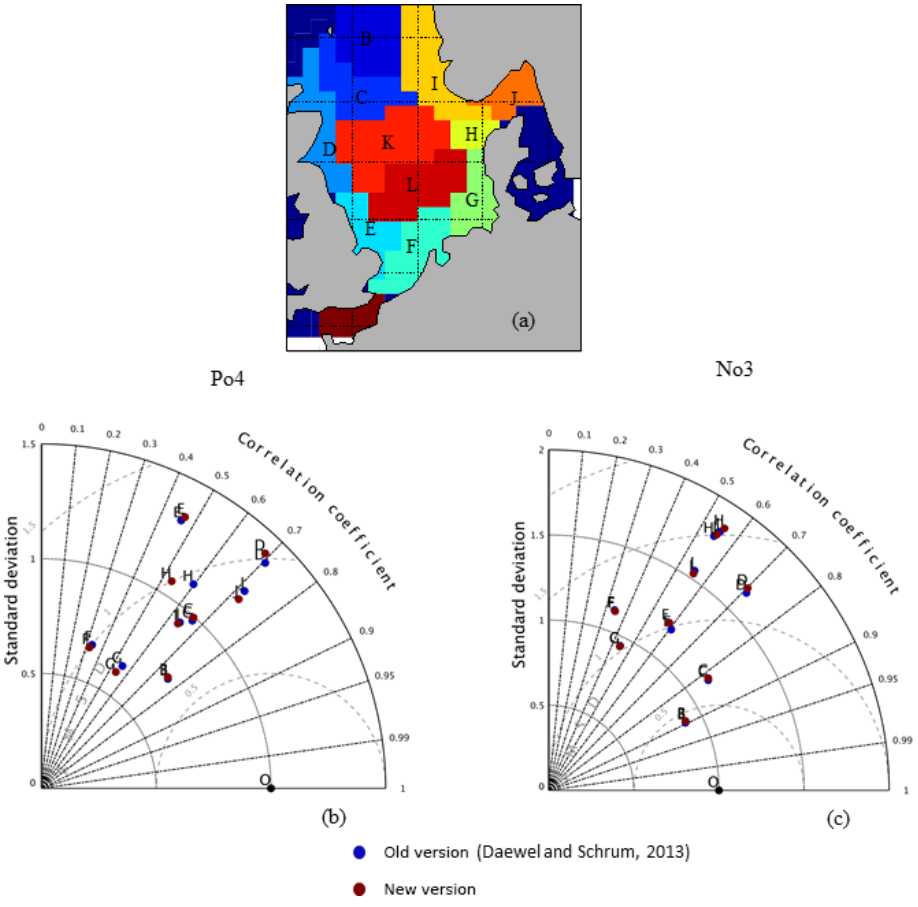

Figure B2. Taylor diagram for surface (above 20 m) nutrient validation (model vs. ICES data) in different areas of the North Sea for phosphate **(b)** and nitrogen **(c)**. Area separation is given in panel **(a)**.

Appendix C

To estimate the impact of SPM on the underwater light climate and primary production dynamics in the simulation, we implemented a climatological SPM field for the North Sea (available with daily resolution and 31 vertical layers) for our simulation. This SPM field was derived from a statistical regression model which considers tidal currents, salinity and water depth (Heath et al., 2002). The SPM field is able to resolve the spatial distribution pattern and seasonal cycling of SPM concentration in the North Sea (Fig. C1) and has been applied in many hydrodynamical–biogeochemical coupled models (Große et al., 2016; Kerimoglu et al., 2017).

Taking the parameterization scheme proposed by Tian et al. (2009), we parameterize shading effects due to SPM as

$$Kd_{\mathrm{spm}} = k_{\mathrm{spm}} \cdot \sqrt{\mathrm{SPM}}. \tag{C1}$$

The k_{spm} was set as $0.02\,\mathrm{m^2\,g^{-1}}$. We added the contribution of SPM to the light shading scheme as described in the paper (Eq. 1). We decreased the background attenuation coefficient k_{w1} (0.03) to $0.025\,\mathrm{m^{-1}}$ (k_{w2}) and use the following parameterization for light attenuation:

$$Kd_2 = k_{\mathrm{w2}} + k_{\mathrm{p}} \cdot P + k_{\mathrm{DOM}} \cdot \mathrm{DOM} + k_{\mathrm{Det}} \cdot \mathrm{Det} + k_{\mathrm{spm}} \cdot \sqrt{\mathrm{SPM}}. \tag{C2}$$

We implemented the new light shading scheme (Eq. C2) and evaluated the difference in NPP contributed by tide, by comparing the annual mean NPP in tidal and non-tidal scenarios using Eq. (C2) (Fig. C2). The general pattern remains largely insensitive to consideration of spatial and seasonal variations in SPM. The positive and negative responding areas hold the same distribution pattern, but the NPP's increasing amplitude with tidal forcing in frontal areas decreases slightly when SPM is explicitly considered. This is because the elevated NPP fueled by pumped-up nutrients is partly offset by increased shading effects due to SPM. However, the sensitivity to SPM is minor and does not affect the general results of our study.

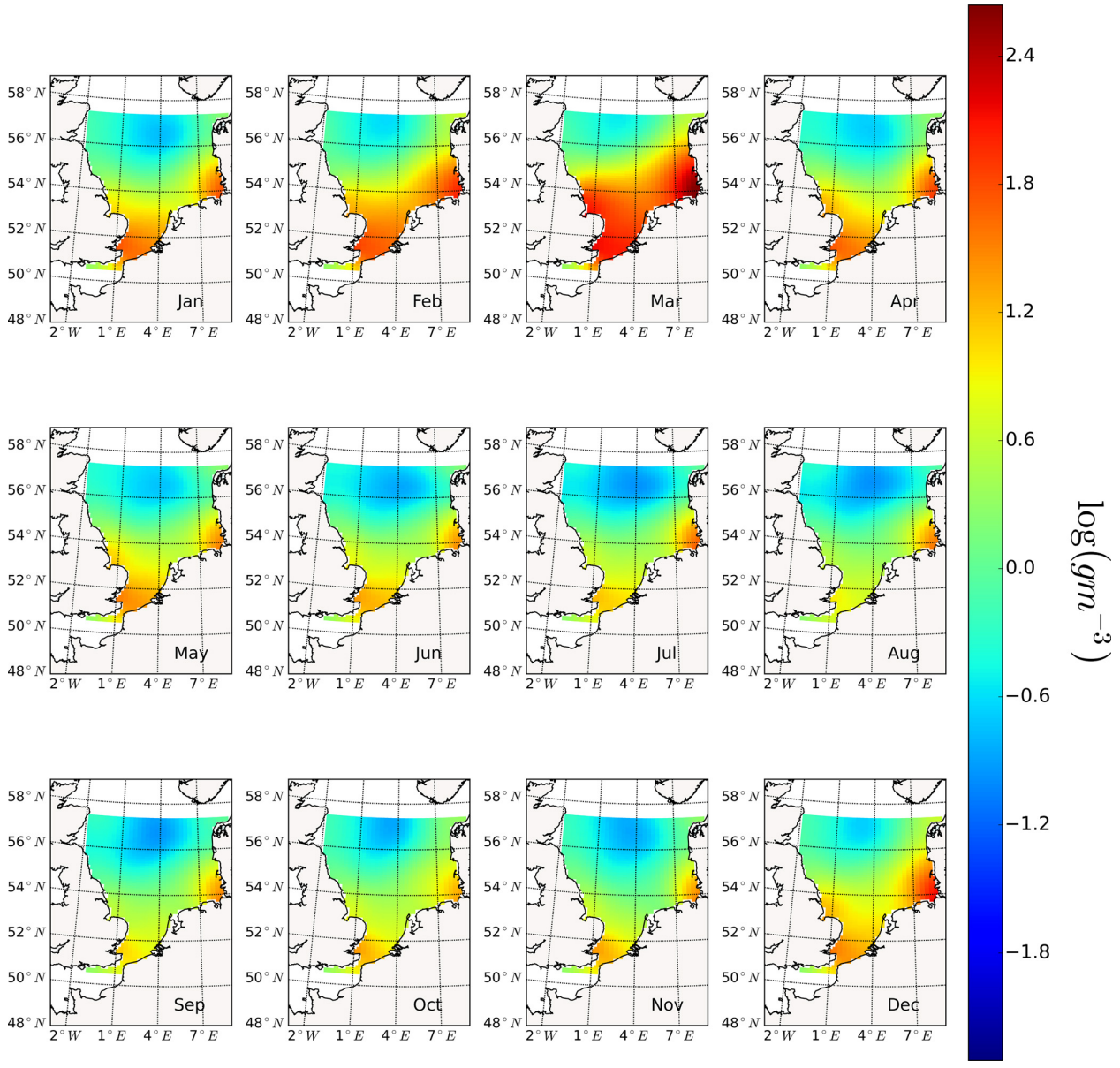

Figure C1. Monthly mean of inorganic SPM concentration in the first layer (upper 5 m).

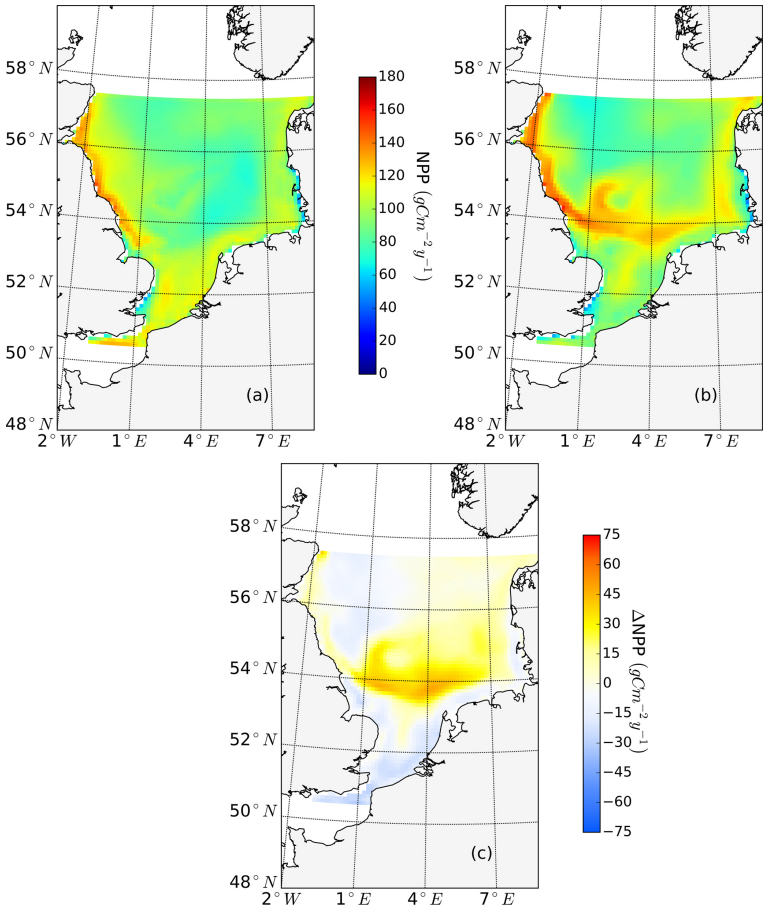

Figure C2. Mean annual net primary production for the analyzed period (1990–2015) of the non-tidal scenario **(a)** and tidal scenario **(b)**, both with SPM field implemented. The difference in the mean annual NPP of both scenarios is in panel **(c)**. The spatial coverage is smaller than original simulation domain since the SPM field data are available from 50.5 to 57.5° N.

Author contributions. ECOSMO code was maintained and provided by UD. New added parameterization for SPM field, scenario runs, data analysis and most graphical presentations were conducted by CZ under supervision of UD. Story building and text writing were conducted by CZ under supervision of UD and CS. Conception and overall supervision of the paper were done by CS.

Competing interests. The authors declare that they have no conflict of interest.

Acknowledgements. This work is funded by the Chinese Scholarship Council (no. 201406140121). We would like to thank Sonja M. van Leeuwen, Marie Maar and Johannes Pätsch for kindly sharing data with us. We appreciate the help provided by Richard Hofmeister related to technical issues in figure plotting. We would like to thank two reviewers, Thomas Pohlmann and Chuan-Yuan Hsu, for their valuable and constructive comments to improve the paper.

The article processing charges for this open-access publication were covered by a Research Centre of the Helmholtz Association.

Review statement. This paper was edited by Yun Liu and reviewed by Thomas Pohlmann and Chuan-Yuan Hsu.

References

Allen, J. I., Siddorn, J. R., Blackford, J. C., and Gilbert, F. J.: Turbulence as a control on the microbial loop in a temperate seasonally stratified marine systems model, J. Sea Res., 52, 1–20, https://doi.org/10.1016/j.seares.2003.09.004, 2004.

Arheimer, B., Dahné, J., Donnelly, C., Lindström, G., and Strömqvist, J.: Water and nutrient simulations using the HYPE model for Sweden vs. the Baltic Sea basin – Influence of input-data quality and scale, Hydrol. Res., 43, 315–329, https://doi.org/10.2166/nh.2012.010, 2012.

Backhaus, J. O.: A three-dimensional model for the simulation of shelf sea dynamics, Dtsch. Hydrogr. Zeitschrift, 38, 165–187, 1985.

Backhaus, J. O. and Hainbucher, D.: A finite difference general circulation model for shelf seas and its application to low frequency variability on the north european shelf, Elsev. Oceanogr. Serie., 45, 221–244, https://doi.org/10.1016/S0422-9894(08)70450-1, 1987.

Bagniewski, W., Fennel, K., Perry, M. J., and D'Asaro, E. A.: Optimizing models of the North Atlantic spring bloom using physical, chemical and bio-optical observations from a Lagrangian float, Biogeosciences, 8, 1291–1307, https://doi.org/10.5194/bg-8-1291-2011, 2011.

Bakun, A.: Fronts and eddies as key structures in the habitat of marine fish larvae: opportunity, adaptive response and competitive advantage, Sci. Mar., 70, 105–122, https://doi.org/10.3989/scimar.2006.70s2105, 2006.

Balch, W. M. K.: An apparent lunar tidal cycle of phytoplankton blooming and community succession in the Gulf of Maine, J. Exp. Mar. Biol. Ecol., 55, 65–77, https://doi.org/10.1016/0022-0981(81)90093-9, 1981.

Barthel, K., Daewel, U., Pushpadas, D., Schrum, C., Arthun, M., and Wehde, H.: Resolving frontal structures: On the payoff using a less diffusive but computationally more expensive advection scheme, Ocean Dynam., 62, 1457–1470, https://doi.org/10.1007/s10236-012-0578-9, 2012.

Belkin, I. M., Cornillon, P. C., and Sherman, K.: Fronts in Large Marine Ecosystems, Prog. Oceanogr., 81, 223–236, https://doi.org/10.1016/j.pocean.2009.04.015, 2009.

Benoit-Bird, K. J., Cowles, T. J., and Wingard, C. E.: Edge gradients provide evidence of ecological interactions in planktonic thin layers, Limnol. Oceanogr., 54, 1382–1392, https://doi.org/10.4319/lo.2009.54.4.1382, 2009.

Blauw, A. N., Benincà, E., Laane, R. W. P. M., Greenwood, N., and Huisman, J.: Dancing with the Tides: Fluctuations of Coastal Phytoplankton Orchestrated by Different Oscillatory Modes of the Tidal Cycle, PLoS One, 7, e49319, https://doi.org/10.1371/journal.pone.0049319, 2012.

Bowden, K. F. and Hamilton, P.: Some experiments with a numerical model of circulation and mixing in a tidal estuary, Estuar. Coast. Mar. Sci., 3, 281–301, https://doi.org/10.1016/0302-3524(75)90029-8, 1975.

Bowers, D. G., Boudjelas, S., and Harker, G. E. L.: The distribution of fine suspended sediments in the surface waters of the irish sea and its relation to tidal stirring, Int. J. Remote Sens., 19, 2789–2805, https://doi.org/10.1080/014311698214514, 1998.

Brettschneider, G.: Anwendung des hydrodynamisch-numerischen Verfahrens zur Ermittlung der M2-Mitschwingungsgezeit der Nordsee, Univ. Hamburg, Hamburg, 1967.

Capuzzo, E., Painting, S. J., Forster, R. M., Greenwood, N., Stephens, D. T., and Mikkelsen, O. A.: Variability in the sub-surface light climate at ecohydrodynamically distinct sites in the North Sea, Biogeochemistry, 113, 85–103, https://doi.org/10.1007/s10533-012-9772-6, 2013.

Cloern, J. E.: Tidal Stirring and Phytoplankton Bloom Dynamics in an Estuary, J. Mar. Res., 49, 203–221, https://doi.org/10.1357/002224091784968611, 1991.

Conkright, M. E., Locarnini, R. A., Garcia, H. E., O'Brien, T. D., Boyer, T. P., Stephens, C., and Antonov, J. I.: World Ocean Atlas 2001: Objective Analyses, Data Statistics, and Figures, CD-ROMDocumentation, National Oceanographic Data Center, Silver Spring, MD, 17 pp., 2002.

Cullen, J. J.: Subsurface chlorophyll maximum layers: enduring enigma or mystery solved?, Annu. Rev. Mar. Sci., 7, 207–39, https://doi.org/10.1146/annurev-marine-010213-135111, 2015.

Daewel, U. and Schrum, C.: Simulating long-term dynamics of the coupled North Sea and Baltic Sea ecosystem with ECOSMO II: Model description and validation, J. Marine Syst., 119–120, 30–49, https://doi.org/10.1016/j.jmarsys.2013.03.008, 2013.

Daewel, U. and Schrum, C.: Low-frequency variability in North Sea and Baltic Sea identified through simulations with the 3-D coupled physical–biogeochemical model ECOSMO, Earth Syst. Dynam., 8, 801–815, https://doi.org/10.5194/esd-8-801-2017, 2017.

Daewel, U., Hjøllo, S. S., Huret, M., Ji, R., Maar, M., Niiranen, S., Travers-Trolet, M., Peck, M. A., and Van De Wolfshaar, K. E.: Predation control of zooplankton dynamics: A review

of observations and models, ICES J. Mar. Sci., 71, 254–271, https://doi.org/10.1093/icesjms/fst125, 2014.

Daewel, U., Schrum, C., and Macdonald, J.: Towards End-2-End modelling in a consistent NPZD-F modelling framework (ECOSMOE2E_vs1.0): Application to the North Sea and Baltic Sea, Geosci. Model Dev. Discuss., https://doi.org/10.5194/gmd-2018-239, in review, 2018.

Daly, K. L. and Smith, W. O.: Physical-Biological Interactions Influencing Marine Plankton Production, Annu. Rev. Ecol. Syst., 24, 555–585, https://doi.org/10.1146/annurev.es.24.110193.003011, 1993.

Davies, A. M., Sauvel, J., and Evans, J.: Computing near coastal tidal dynamics from observations and a numerical model, Cont. Shelf Res., 4, 341–366, https://doi.org/10.1016/0278-4343(85)90047-0, 1985.

de Baar, H. J. W.: von Liebig's law of the minimum and plankton ecology (1899–1991), Prog. Oceanogr., 33, 347–386, https://doi.org/10.1016/0079-6611(94)90022-1, 1994.

Dekshenieks, M. M., Donaghay, P. L., Sullivan, J. M., Rines, J. E. B., Osborn, T. R., and Twardowski, M. S.: Temporal and spatial occurrence of thin phytoplankton layers in relation to physical processes, Mar. Ecol.-Prog. Ser., 223, 61–71, https://doi.org/10.3354/meps223061, 2001.

Deutsches Hydrographisches Institut: Tafeln der Astronomischen Argumente V0+v und der Korrektionen j,v, Deutsches Hydrographisches Insititut, Hamburg, 1967.

Dippner, J. W.: A frontal-resolving model for the German Bight, Cont. Shelf Res., 13, 49–66, https://doi.org/10.1016/0278-4343(93)90035-V, 1993.

Dobrynin, M., Gayer, G., Pleskachevsky, A., and Günther, H.: Effect of waves and currents on the dynamics and seasonal variations of suspended particulate matter in the North Sea, J. Marine Syst., 82, 1–20, https://doi.org/10.1016/j.jmarsys.2010.02.012, 2010.

Ebenhöh, W., Kohlmeier, C., Baretta, J. W., and Flöser, G.: Shallowness may be a major factor generating nutrient gradients in the Wadden Sea, Ecol. Model., 174, 241–252, https://doi.org/10.1016/j.ecolmodel.2003.07.011, 2004.

Eisma, D.: Supply and Deposition of Suspended Matter in the North Sea, in: Holocene Marine Sedimentation in the North Sea Basin, 415–428, 2009.

Eliasen, S. K., Hátún, H., Larsen, K. M. H., Hansen, B., and Rasmussen, T. A. S.: Phenologically distinct phytoplankton regions on the Faroe Shelf – identified by satellite data, in-situ observations and model, J. Marine Syst., 169, 99–110, https://doi.org/10.1016/j.jmarsys.2017.01.015, 2017.

Foshtomi, M. Y., Braeckman, U., Derycke, S., Sapp, M., Van Gansbeke, D., Sabbe, K., Willems, A., Vincx, M., and Vanaverbeke, J.: The link between microbial diversity and nitrogen cycling in marine sediments is modulated by macrofaunal bioturbation, PLoS One, 10, 1–20, https://doi.org/10.1371/journal.pone.0130116, 2015.

Franks, P. J. S. and Chen, C.: Plankton production in tidal fronts: A model of Georges Bank in summer, J. Mar. Res., 54, 631–651, https://doi.org/10.1357/0022240963213718, 1996.

George, J. A., Lonsdale, D. J., Merlo, L. R., and Gobler, C. J.: The interactive roles of temperature, nutrients, and zooplankton grazing in controlling the winter-spring phytoplankton bloom in a temperate, coastal ecosystem, Long Island Sound, Limnol. Oceanogr., 60, 110—126, https://doi.org/10.1002/lno.10020, 2015.

Geyer, W. R. and MacCready, P.: The Estuarine Circulation, Annu. Rev. Fluid Mech., 46, 175–197, https://doi.org/10.1146/annurev-fluid-010313-141302, 2014.

Gong, X., Shi, J., and Gao, H.: Modeling seasonal variations of subsurface chlorophyll maximum in South China Sea, J. Ocean Univ. China, 13, 561–571, https://doi.org/10.1007/s11802-014-2060-4, 2014.

Große, F., Greenwood, N., Kreus, M., Lenhart, H.-J., Machoczek, D., Pätsch, J., Salt, L., and Thomas, H.: Looking beyond stratification: a model-based analysis of the biological drivers of oxygen deficiency in the North Sea, Biogeosciences, 13, 2511–2535, https://doi.org/10.5194/bg-13-2511-2016, 2016.

Heath, M. R.: Changes in the structure and function of the North Sea fish foodweb, 1973–2000, and the impacts of fishing and climate, ICES J. Mar. Sci., https://doi.org/10.1016/j.icesjms.2005.01.023, 2005.

Heath, M. R., Edwards, A. C., Pätsch, J., and Turrell, W. R.: Modelling the behaviour of nutrient in the coastal waters of Scotland, Fisheries Research Services, Aberdeen, 2002.

Heathershaw, A. D., New, A. L., and Edwards, P. D.: Internal tides and sediment transport at the shelf break in the Celtic Sea, Cont. Shelf Res., 7, 485–517, https://doi.org/10.1016/0278-4343(87)90092-6, 1987.

Heip, C., Basford, D., Craeymeersch, J. A., Dewarumez, J. M., Dörjes, J., de Wilde, P., Duineveld, G., Eleftheriou, A., Herman, P. M. J., Niermann, U., Kingston, P., Künitzer, A., Rachor, E., Rumohr, H., Soetaert, K., and Soltwedel, T.: Trends in biomass, density and diversity of North Sea macrofauna, ICES Journal of Marine Science, 49, 13–22, https://doi.org/10.1093/icesjms/49.1.13, 1992.

Henriksen, H. J., Troldborg, L., Nyegaard, P., Sonnenborg, T. O., Refsgaard, J. C., and Madsen, B.: Methodology for construction, calibration and validation of a national hydrological model for Denmark, J. Hydrol., 280, 52–71, https://doi.org/10.1016/S0022-1694(03)00186-0, 2003.

Hofmeister, R., Flöser, G., and Schartau, M.: Estuary-type circulation as a factor sustaining horizontal nutrient gradients in freshwater-influenced coastal systems, Geo-Mar. Lett., 37, 179–192, https://doi.org/10.1007/s00367-016-0469-z, 2017.

Holligan, P. M., Pingree, R. D., and Mardell, G. T.: Oceanic solitons, nutrient pulses and phytoplankton growth, Nature, 314, 348–350, https://doi.org/10.1038/314348a0, 1985.

Holt, J., Butenschön, M., Wakelin, S. L., Artioli, Y., and Allen, J. I.: Oceanic controls on the primary production of the northwest European continental shelf: model experiments under recent past conditions and a potential future scenario, Biogeosciences, 9, 97–117, https://doi.org/10.5194/bg-9-97-2012, 2012.

Holt, J. T. and James, I. D.: A simulation of the southern North Sea in comparison with measurements from the North Sea Project Part 2 suspended particulate matter, Cont. Shelf Res., 19, 1617–1642, https://doi.org/10.1016/S0278-4343(99)00032-1, 1999.

Hu, S., Townsend, D. W., Chen, C., Cowles, G., Beardsley, R. C., Ji, R., and Houghton, R. W.: Tidal pumping and nutrient fluxes on Georges Bank: A process-oriented modeling study, J. Marine Syst., 74, 528–544, https://doi.org/10.1016/j.jmarsys.2008.04.007, 2008.

Jacobs, W.: Modelling the Rhine River Plume, TU Delft, 2004.

Jago, C. F., Jones, S. E., Latter, R. J., McCandliss, R. R., Hearn, M. R., and Howarth, M. J.: Resuspension of benthic fluff by tidal currents in deep stratified waters, northern North sea, J. Sea Res., 48, 259–269, https://doi.org/10.1016/S1385-1101(02)00181-8, 2002.

Janssen, F., Schrum, C., and Backhaus, J. O.: A climatological data set of temperature and salinity for the Baltic Sea and the North Sea, Dtsch. Hydrogr. Zeitschrift, 51, 5, https://doi.org/10.1007/BF02933676, 1999.

Janssen, F., Schrum, C., Hübner, U., and Backhaus, J. O.: Uncertainty analysis of a decadal simulation with a regional ocean model for the North Sea and Baltic Sea, Clim. Res., 18, 55–62, https://doi.org/10.3354/cr018055, 2001.

Joint, I. and Pomroy, A.: Phytoplankton biomass and production in the southern North Sea, Mar. Ecol. Ser., 99, 169–182, https://doi.org/10.3354/meps099169, 1993.

Joint, T. and Pomroy, A.: hytoplankton Biomass and Production in the North Sea. Results from the NERC North Sea Project August 1988–October 1989, Plymouth Marine Laboratory, Plymouth, 1992.

Jones, S. E., Jago, C. F., Bale, a J., Chapman, D., Howland, R. J. M., and Jackson, J.: Aggregation and resuspension of suspended particulate matter at a stratified site in the southern North Sea: physical and biological controls, Cont. Shelf Res., 18, 1283–1309, https://doi.org/10.1016/S0278-4343(98)00044-2, 1998.

Kalnay, E., Kanamitsu, M., Kistler, R., Collins, W., Deaven, D., Gandin, L., Iredell, M., Saha, S., White, G., Woollen, J., Zhu, Y., Chelliah, M., Ebisuzaki, W., Higgins, W., Janowiak, J., Mo, K. C., Ropelewski, C., Wang, J., Leetmaa, A., Reynolds, R., Jenne, R., and Joseph, D.: The NCEP/NCAR 40-year reanalysis project, B. Am. Meteorol. Soc., 77, 437–471, https://doi.org/10.1175/1520-0477(1996)077<0437:TNYRP>2.0.CO;2, 1996.

Karl, D. M. and Lukas, R.: The Hawaii Ocean Time-series (HOT) program: Background, rationale and field implementation, Deep-Sea Res. Pt. II, 43, 129–156, https://doi.org/10.1016/0967-0645(96)00005-7, 1996.

Kerimoglu, O., Hofmeister, R., Maerz, J., Riethmüller, R., and Wirtz, K. W.: The acclimative biogeochemical model of the southern North Sea, Biogeosciences, 14, 4499–4531, https://doi.org/10.5194/bg-14-4499-2017, 2017.

Lindström, G., Pers, C., Rosberg, J., Strömqvist, J., and Arheimer, B.: Development and testing of the HYPE (Hydrological Predictions for the Environment) water quality model for different spatial scales, Hydrol. Res., 43, 295–319, https://doi.org/10.2166/nh.2010.007, 2010.

Loder, J. W. and Greenberg, D. A.: Predicted positions of tidal fronts in the Gulf of Maine region, Cont. Shelf Res., 6, 397–414, https://doi.org/10.1016/0278-4343(86)90080-4, 1986.

Loder, J. W., Brickman, D., and Horne, E. P. W.: Detailed structure of currents and hydrography on the northern side of Georges Bank, J. Geophys. Res., 97, 14331–14351, https://doi.org/10.1029/92JC01342, 1992.

Longhurst, A. R.: Ecological Geography of the Sea, Academic Press, 2006.

Maar, M., Markager, S., Madsen, K. S., Windolf, J., Lyngsgaard, M. M., Andersen, H. E., and Møller, E. F.: The importance of local versus external nutrient loads for Chl a and primary production in the Western Baltic Sea, Ecol. Model., 320, 258–272, https://doi.org/10.1016/j.ecolmodel.2015.09.023, 2016.

Mahadevan, A., Tandon, A., and Ferrari, R.: Rapid changes in mixed layer stratification driven by submesoscale instabilities and winds, J. Geophys. Res.-Ocean., 115, 1–12, https://doi.org/10.1029/2008JC005203, 2010.

Martin, J. H.: Phytoplankton-Zooplankton Relationships in Narragansett Bay, Limnol. Oceanogr., 10, 185–191, 1965.

Matthias, V., Aulinger, A., and Quante, M.: Adapting CMAQ to investigate air pollution in North Sea coastal regions, Environ. Modell. Softw., 23, 356–368, https://doi.org/10.1016/j.envsoft.2007.04.010, 2008.

McCandliss, R. R., Jones, S. E., Hearn, M., Latter, R., and Jago, C. F.: Dynamics of suspended particles in coastal waters (southern North Sea) during a spring bloom, J. Sea Res., 47, 285–302, https://doi.org/10.1016/S1385-1101(02)00123-5, 2002.

McQuatters-Gollop, A., Raitsos, D. E., Edwards, M., and Attrill, M. J.: Spatial patterns of diatom and dinoflagellate seasonal cycles in the NE Atlantic Ocean, Mar. Ecol.-Prog. Ser., 339, 301–306, https://doi.org/10.3354/meps339301, 2007.

Monod, J.: Recherches sur la croissance des cultures bactèriennes, Hermann & cie, Paris, 1942.

Munk, P. and Nielsen, T. G.: Trophodynamics of the plankton community at Dogger Bank: Predatory impact by larval fish, J. Plankton Res., 16, 1225–1245, https://doi.org/10.1093/plankt/16.9.1225, 1994.

New, A. L. and Da Silva, J. C. B.: Remote-sensing evidence for the local generation of internal soliton packets in the central Bay of Biscay, Deep-Sea Res. Pt. I, 49, 915–934, https://doi.org/10.1016/S0967-0637(01)00082-6, 2002.

Nissen, C.: Physical-Biogeochemical Couplings in the Land-Ocean Transition Zone, The University of Bergen, available at: http://hdl.handle.net/1956/18682 (last access: 21 April 2019), 2014.

Otto, L., Adams, J. A., Adam, M. Y., Becker, G. A., Dahl, F. E., Davies, A. M., Dooley, H. D., Durance, J. A., Furness, G. K., Harding, F. D., Jefferies, D. J., Koltermann, K. P., Mork, M., Ronday, F. C., and Svansson, A.: Flushing times of the North Sea, International Council for the Exploration of the Sea, Copenhagen, 1983.

Otto, L., Zimmerman, J. T. F., Furnes, G. K., Mork, M., Saetre, R., and Becker, G.: Review of the physical oceanography of the North Sea, Neth. J. Sea Res., 26, 161–238, https://doi.org/10.1016/0077-7579(90)90091-T, 1990.

Pätsch, J. and Lenhart, H.-J.: Daily Loads of Nutrients, Total alkalinity, dissolved inorganic carbon and dissolved organic carbon of the European continental rivers for the years 1977–2002, in: Berichte aus dem Zentrum für Meeres- und Klimaforschung, Reihe B: Ozeanographie Nr. 48, p. 159, University of Hamburg, Germany, 2004.

Pedersen, F. B.: The Oceanographic and Biological Tidal Cycle Succession in Shallow Sea Fronts in the North Sea and the English Channel, Estuar. Coast. Shelf S., 38, 249–269, https://doi.org/10.1006/ecss.1994.1017, 1994.

Pietrzak, J. D., de Boer, G. J., and Eleveld, M. A.: Mechanisms controlling the intra-annual mesoscale variability of SST and SPM in the southern North Sea, Cont. Shelf Res., 31, 594–610, https://doi.org/10.1016/j.csr.2010.12.014, 2011.

Pingree, R. D. and Griffiths, D. K.: Tidal fronts on the shelf seas around the British Isles, J. Geophys. Res., 83, 4615, https://doi.org/10.1029/JC083iC09p04615, 1978.

Pingree, R. D., Mardell, G. T., and Cartwright, D. E.: Slope Turbulence, Internal Waves and Phytoplankton Growth at the Celtic Sea Shelf-Break [and Discussion], Philos. T. R. Soc. A, 302, 663–682, https://doi.org/10.1098/rsta.1981.0191, 1981.

Pleskachevsky, A., Dobrynin, M., Babanin, A. V., Günther, H., and Stanev, E.: Turbulent Mixing due to Surface Waves Indicated by Remote Sensing of Suspended Particulate Matter and Its Implementation into Coupled Modeling of Waves, Turbulence, and Circulation, J. Phys. Oceanogr., 41, 708–724, https://doi.org/10.1175/2010JPO4328.1, 2011.

Pohlmann, T.: Predicting the thermocline in a circulation model of the North Sea – Part I: Model description, calibration and verification, Cont. Shelf Res., 16, 131–146, https://doi.org/10.1016/0278-4343(95)90885-S, 1996.

Porter, E. T., Mason, R. P., and Sanford, L. P.: Effect of tidal resuspension on benthic-pelagic coupling in an experimental ecosystem study, Mar. Ecol.-Prog. Ser., 413, 33–53, https://doi.org/10.3354/meps08709, 2010.

Postma, H.: Exchange of materials between the North Sea and the Wadden Sea, Mar. Geol., 40, 199–213, https://doi.org/10.1016/0025-3227(81)90050-5, 1981.

Prandle, D.: A modelling study of the mixing of ^{137}Cs in the seas of the European Continental Shelf, Philos. T. R. Soc. A, 310, 408–435, https://doi.org/10.1098/rsta.1984.0002, 1984.

Prins, T. C., Smaal, A. C., Pouwer, A. J., and Dankers, N.: Filtration and resuspension of particulate matter and phytoplankton onan intertidal mussel bed in the Oosterschelde estuary (SW Netherlands), Mar. Ecol.-Prog. Ser., 142, 121–134, https://doi.org/10.3354/meps142121, 1996.

Richardson, A. J., Pfaff, M. C., Field, J. G., Silulwane, N. F., and Shillington, F. A.: Identifying characteristic chlorophyll a profiles in the coastal domain using an artificial neural network, J. Plankton Res., 24, 1289–1303, https://doi.org/10.1093/plankt/24.12.1289, 2002.

Richardson, K., Visser, A. W., and Bo Pedersen, F.: Subsurface phytoplankton blooms fuel pelagic production in the North Sea, J. Plankton Res., 22, 1663–1671, https://doi.org/10.1093/plankt/22.9.1663, 2000.

Rippeth, T. P., Wiles, P., Palmer, M. R., Sharples, J., and Tweddle, J.: The diapcynal nutrient flux and shear-induced diapcynal mixing in the seasonally stratified western Irish Sea, Cont. Shelf Res., 29, 1580–1587, https://doi.org/10.1016/j.csr.2009.04.009, 2009.

Rodhe, J.: The Baltic and Northern Seas: a process-orientated review of the physical oceanography, in: The sea, edited by: Robinson, A. R. and Brink, K. H., 699–732, Wildy, New York, 1998.

Rodhe, J., Tett, P., and Wulf, F.: Chapter 26. The Baltic and North Seas: a regional review of some important physical-checmial-biological interaction processes, Sea, 14, 1029–1072, 2004.

Ruddick, K. G., Deleersnijder, E., Luyten, P. J., and Ozer, J.: Haline stratification in the Rhine-Meuse freshwater plume: a three-dimensional model sensitivity analysis, Cont. Shelf Res., 15, 1597–1630, https://doi.org/10.1016/0278-4343(95)00034-X, 1995.

Sabine, C. L., Feely, R. A., Gruber, N., Key, R. M., Lee, K., Bullister, J. L., Wanninkhof, R., Wong, C. S., Wallace, D. W. R., Tilbrook, B., Millero, F. J., Peng, T. H., Kozyr, A., Ono, T., and Rios, A. F.: The oceanic sink for anthropogenic CO_2, Science, 305, 367–371, https://doi.org/10.1126/science.1097403, 2004.

Schartau, M., Riethmüller, R., Flöser, G., Beusekom, J. E. E. Van, Krasemann, H., Hofmeister, R., and Wirtz, K.: On the separation between inorganic and organic fractions of suspended matter in a marine coastal environment, Prog. Oceanogr., 171, 231–250, https://doi.org/10.1016/j.pocean.2018.12.011, 2018.

Schaub, B. E. M. and Gieskes, W. W. C.: Eutrophication of the North Sea: the relation between Rhine river discharge and chlorophyll-*a* concentration in Dutch coastal waters, Fredensborg, Estuaries and Coasts: Spatial and Temporal Intercomparisons, ECSA 19 Symposium, ECSA, 1991.

Schrum, C.: Thermohaline stratification and instabilities at tidal mixing fronts: Results of an eddy resolving model for the German Bight, Cont. Shelf Res., 17, 689–716, https://doi.org/10.1016/S0278-4343(96)00051-9, 1997.

Schrum, C. and Backhaus, J. O.: Sensivity of atmosphere-ocean heat exchange and heat content in the North Sea and the Baltic Sea, Tellus A, 51, 526–549, https://doi.org/10.1034/j.1600-0870.1992.00006.x, 1999.

Schrum, C., Siegismund, F., and John, M. S.: Decadal variations in the stratification and circulation patterns of the North Sea. Are the 1990s unusual?, ICES Mar. Sc., 219, 121–131, 2003.

Schrum, C., St. John, M., and Alekseeva, I.: ECOSMO, a coupled ecosystem model of the North Sea and Baltic Sea: Part II. Spatial-seasonal characteristics in the North Sea as revealed by EOF analysis, J. Marine Syst., 61, 100–113, https://doi.org/10.1016/j.jmarsys.2006.01.004, 2006.

Scott, B. E., Sharples, J., Ross, O. N., Wang, J., Pierce, G. J., and Camphuysen, C. J.: Sub-surface hotspots in shallow seas: Fine-scale limited locations of top predator foraging habitat indicated By tidal mixing and sub-surface chlorophyll, Mar. Ecol.-Prog. Ser., 408, 207–226, https://doi.org/10.3354/meps08552, 2010.

Sharples, J.: Potential impacts of the spring-neap tidal cycle on shelf sea primary production, J. Plankton Res., 30, 183–197, https://doi.org/10.1093/plankt/fbm088, 2008.

Sharples, J. and Simpson, J. H.: Periodic Frontogenesis in a Region of Freshwater Influence, Estuaries, 16, 74–82, https://doi.org/10.2307/1352765, 1993.

Sharples, J., Moore, M. C., Rippeth, T. P., Holligan, P. M., Hydes, D. J., Fisher, N. R., and Simpson, J. H.: Phytoplankton distribution and survival in the thermocline, Limnol. Oceanogr., 46, 486–496, https://doi.org/10.4319/lo.2001.46.3.0486, 2001.

Sharples, J., Ross, O. N., Scott, B. E., Greenstreet, S. P. R., and Fraser, H.: Inter-annual variability in the timing of stratification and the spring bloom in the North-western North Sea, Cont. Shelf Res., 26, 733–751, https://doi.org/10.1016/j.csr.2006.01.011, 2006.

Sharples, J., Tweddle, J. F., Green, J. A. M., Palmer, M. R., Kim, Y., Hickman, A. E., Holligan, P. M., Moore, C. M., Rippeth, T. P., Simpson, J. H., and Krivtsov, V.: Spring – neap modulation of internal tide mixing and vertical nitrate fluxes at a shelf edge in summer, Limnol. Oceanogr., 52, 1735–1747, 2007.

Siegel, H., Gerth, M., Heene, T., Ohde, T., Rüß, D., and Kraft, H.: Hydrography, currents and distribution of suspended matter during a dumping experiment in the western Baltic Sea at a site near Warnemünde, J. Marine Syst., 75, 397–408, https://doi.org/10.1016/j.jmarsys.2008.04.005, 2009.

Siegismund, F.: Long-term changes in the flushing times of the ICES-boxes, Senck. Marit., 31, 151–167, https://doi.org/10.1007/BF03043025, 2001.

Simpson, J. H. and Bowers, D.: Models of stratification and frontal movement in shelf seas, Deep-Sea Res. Pt. A, 28, 727–738, https://doi.org/10.1016/0198-0149(81)90132-1, 1981.

Simpson, J. H. and Hunter, J. R.: Fronts in the Irish Sea, Nature, 250, 404–406, https://doi.org/10.1038/250404a0, 1974.

Simpson, J. H. and Sharples, J.: Introduction to the Physical and Biological Oceanography of Shelf Seas, Cambridge University Press, 2012.

Simpson, J. H. and Souza, A. J.: Semidiurnal switching of stratification in the region of freshwater influence of the Rhine, J. Geophys. Res., 100, 7037–7044, https://doi.org/10.1029/95JC00067, 1995.

Smith, W. O. and Jones, R. M.: Vertical mixing, critical depths, and phytoplankton growth in the Ross Sea, ICES J. Mar. Sci., 72, 1952–1960, https://doi.org/10.1093/icesjms/fsu234, 2015.

Stedmon, C. A., Markager, S., and Kaas, H.: Optical Properties and Signatures of Chromophoric Dissolved Organic Matter (CDOM) in Danish Coastal Waters, Estuar. Coast. Shelf S., 51, 267–278, https://doi.org/10.1006/ecss.2000.0645, 2000.

Stoica, P., Moses, R. L., and Hall, P.: Introduction to Spectral Analysis, Technometrics, 47, 104–105, https://doi.org/10.1198/tech.2005.s841, 2005.

Tett, P. and Walne, A.: Observations and simulations of hydrography, nutrients and plankton in the southern north sea, Ophelia, 42, 371–416, https://doi.org/10.1080/00785326.1995.10431514, 1995.

Thomson, R. E. and Emery, W. J.: Chapter 5 – Time Series Analysis Methods, in: Data Analysis Methods in Physical Oceanography, 3rd Edn., 425–591, Elsevier, Boston, 2014.

Tian, T., Merico, A., Su, J., Staneva, J., Wiltshire, K., and Wirtz, K.: Importance of resuspended sediment dynamics for the phytoplankton spring bloom in a coastal marine ecosystem, J. Sea Res., 62, 214–228, https://doi.org/10.1016/j.seares.2009.04.001, 2009.

Urtizberea, A., Dupont, N., Rosland, R., and Aksnes, D. L.: Sensitivity of euphotic zone properties to CDOM variations in marine ecosystem models, Ecol. Model., 256, 16–22, https://doi.org/10.1016/j.ecolmodel.2013.02.010, 2013.

van Alphen, J. S. L. J.: A mud balance for Belgian-Dutch coastal waters between 1969 and 1986, Neth. J. Sea Res., 25, 19–30, https://doi.org/10.1016/0077-7579(90)90005-2, 1990.

Van Beusekom, J. and Diel-Christiansen, A.: Synthesis of phyto- and zooplankton dynamics in the North Sea environment, 148 pp., WWF – World Wide Fund For Nature, Godalming, 1994.

van der Woerd, H. J., Blauw, A., Peperzak, L., Pasterkamp, R., and Peters, S.: Analysis of the spatial evolution of the 2003 algal bloom in the Voordelta (North Sea), J. Sea Res., 65, 195–204, https://doi.org/10.1016/j.seares.2010.09.007, 2011.

van Leeuwen, S. M., van der Molen, J., Ruardij, P., Fernand, L., and Jickells, T.: Modelling the contribution of deep chlorophyll maxima to annual primary production in the North Sea, Biogeochemistry, 113, 137–152, https://doi.org/10.1007/s10533-012-9704-5, 2013.

Van Leeuwen, S., Tett, P., Mills, D., and Van Der Molen, J.: Stratified and nonstratified areas in the North Sea: Long-term variability and biological and policy implications, J. Geophys. Res.-Ocean., 120, 4670–4686, https://doi.org/10.1002/2014JC010485, 2015.

Van Raaphorst, W., Philippart, C. J. M., Smit, J. P. C., Dijkstra, F. J., and Malschaert, J. F. P.: Distribution of suspended particulate matter in the North Sea as inferred from NOAA/AVHRR reflectance images and in situ observations, J. Sea Res., 39, 197–215, https://doi.org/10.1016/S1385-1101(98)00006-9, 1998.

Wafar, M. V. M., Le Corre, P., and Birrien, J. L.: Nutrients and primary production in permanently well-mixed temperate coastal waters, Estuar. Coast. Shelf S., 17, 431–446, https://doi.org/10.1016/0272-7714(83)90128-2, 1983.

Waniek, J. J.: The role of physical forcing in initiation of spring blooms in the northeast Atlantic, J. Marine Syst., 39, 57–82, https://doi.org/10.1016/S0924-7963(02)00248-8, 2003.

Warnock, R. E., Gieskes, W. W. C., and Van Laar, S.: Regional and seasonal differences in light absorption by yellow substance in the Southern Bight of the North Sea, J. Sea Res., 42, 169–178, https://doi.org/10.1016/S1385-1101(99)00025-8, 1999.

Welch, P. D.: The use of fast Fourier transform for the estimation of power spectra: A method based on time averaging over short, modified periodograms, IEEE T. Audio Electroacoust., 15, 70–73, https://doi.org/10.1109/TAU.1967.1161901, 1967.

Windolf, J., Thodsen, H., Troldborg, L., Larsen, S. E., Bøgestrand, J., Ovesen, N. B., and Kronvang, B.: A distributed modelling system for simulation of monthly runoff and nitrogen sources, loads and sinks for ungauged catchments in Denmark, J. Environ. Monitor., 13, 2645–2658, https://doi.org/10.1039/c1em10139k, 2011.

Windolf, J., Blicher-Mathiesen, G., Carstensen, J., and Kronvang, B.: Changes in nitrogen loads to estuaries following implementation of governmental action plans in Denmark: A paired catchment and estuary approach for analysing regional responses, Environ. Sci. Policy, 24, 24–33, https://doi.org/10.1016/j.envsci.2012.08.009, 2012.

Yee, H. C., Warming, R. F., and Harten, A.: Implicit total variation diminishing (TVD) schemes for steady-state calculations, J. Comput. Phys., 57, 327–360, https://doi.org/10.1016/0021-9991(85)90183-4, 1985.

Zhang, W. and Wirtz, K.: Mutual Dependence Between Sedimentary Organic Carbon and Infaunal Macrobenthos Resolved by Mechanistic Modeling, J. Geophys. Res.-Biogeo., 122, 2509–2526, https://doi.org/10.1002/2017JG003909, 2017.

Zhao, C., Maerz, J., Hofmeister, R., Röttgers, R., Riethmüller, R., Wirtz, K., and Schrum, C.: Characterizing the vertical distribution of chlorophyll a in the German Bight, Cont. Shelf Res., 175, 127–146, https://doi.org/10.1016/j.csr.2019.01.012, 2019.

Chapter 5 (Manuscript 3).

Frontal dynamics and impacts on primary production in the North Sea

Changjin Zhao, Ute Daewel, Ingrid Angel Benavides,
Corinna Schrum

Frontal dynamics and impacts on primary production in the North Sea

Changjin Zhao, Ute Daewel, Ingrid Angel Benavides, Corinna Schrum

Helmholtz-Zentrum Geesthacht, Institute for Coastal Research, Geesthacht, Germany

Abstract

This study explores the variability of frontal systems in the North Sea and their implications for biological production on multiple spatial and temporal scales. Simulation results from the physical-biogeochemical coupled model ECOSMO, combined with remote sensing data of sea surface temperature (SST) and chlorophyll concentration (CHL), were used to reveal general physical-biological frontal dynamics. SST and squared buoyancy frequency (N2) (only available from simulations) were processed by histogram and gradient algorithms to map seasonal occurrence of fronts. Distribution pattern of high amplitude in biological fields relative to physical fronts were quantified statistically. The results revealed regional differences between frontal systems in the eastern part and the western part of the North Sea, due to local characteristics and stability of frontal systems. Higher biomass and net primary production (NPP) tends to appear in the mixed side of fronts in the western part of the North Sea, specifically at the nearshore side of the Scottish coastal front and north-western edge of Dogger Bank. In the eastern part, especially in the area east to Dogger Bank, higher biomass and NPP also tend to appear in the mixed side but with lower probability. In the nearshore area along the south-eastern coast, higher biomass and NPP tend to appear in the stratified side of fronts. To further explore biological response to frontal system in a process-oriented way, Hovmöller diagrams were built along representative transects crossing several characteristic frontal regions. Around the Dogger Bank, diffusive flux of NO3 supports the NPP and thus sustaining the ring-shaped productive area. In the south-eastern part, mixing-stratification status is susceptible to wind-mixing, river-runoff and tides, resulting in shifting fronts. High productive events were often triggered by moving fronts, due to pumping up nutrients in mixed events or improved light availability when stratification or reduced vertical turbulence occurs. The inter-annual variability of NPP associated with frontal systems was also investigated. A decrease in frontal production was detected from the 2000s onwards. Moreover, a substantial variability of fronts in the eastern part of North Sea was identified.

Key words: frontal probability, net primary production, North Sea, decadal variability

1. Introduction

Hydrographic fronts in shelf seas have been identified to play a key role in marine ecosystems and their importance in the modulation of biological processes is widely recognised (Mann and Lazier, 2013). Fronts were identified as hotspots for primary production and standing stocks (Le Fèvre, 1987; Iverson et al., 1979; Taylor and Ferrari, 2011). Literature on their influence on biological processes is exhaustive, with implications for trophic levels from autotrophs (e.g. Bracher et al., 1999; Laubscher et al., 1993), heterotrophs (Derisio et al., 2014; Russell et al., 1999), zooplankton (Russell,1999; Derisio, 2014), fish (Munk and Nielsen, 1994; Sabatés et al., 2007; Tiedemann and Brehmer, 2017) up to marine mammals (e.g. Bost et al., 2009; Woodson and Litvin, 2015).

Different physical dynamics in frontal systems, e.g. circulation pattern (Pedersen, 1994) and stability (O'Donnell, 1993) influence phytoplankton growth in a wide variety of ways, such as pumping up nutrients (Ryan et al., 2010a; Smayda, 2002), transport and aggregation (Carreto et al., 2008; Janowitz and Kamykowski, 2006), keeping biomass in euphotic zone (Pingree et al., 1975) and so on. The dominating mechanisms would differ among various frontal systems, which merit a clearer discrimination and detailed discussion (Ryan et al., 2010b).

Frontal systems are seldom steady, which hinders the observation and interpretation of frontal dynamics and the assessment of its importance for biochemical transformations. They often cover a wide range of spatial scales and display complicated geometries (Belkin et al., 2009). This challenges the quantitative description of hydrodynamical features of frontal system. Further implication on biological processes are superposed by temporal-spatial varying scales of biological organisms (Denman and Abbott, 1994; Miller and Christodoulou, 2014; Powell et al., 2006; Yoder et al., 2002). The detection of frontal structures and description conveying temporal and spatial variability for specific regions and their relation to biological productivity deemed necessary. Here we aim at assessing frontal structures and their relation to biological production for the North Sea system.

The North Sea is a highly productive regional shelf sea with different types of dynamic frontal systems (Daly and Smith, 1993; Otto et al., 1990) (Fig.1). Pure tidal mixing fronts and river plume fronts predominate in the shallow part of the sea (Krause et al., 1986) and shelf break fronts occur in the proximity of sharp topographic gradients in the Skagerrak and Norwegian Trench area (Otto et al., 1990). Tidal impacts to primary production were identified to be substantial in the North Sea, specifically large in the southern North Sea and tidal fronts were suggested to play a major role to promote NPP in the southern North Sea (Blauw et al., 2012;

Pietrzak et al., 2011; Simpson and Souza, 1995; Zhao et al., 2019) . Tidal mixing fronts are the result of local differences in the competition between buoyancy and vertical mixing, mainly due to tidal and wind mixing. In shallow waters of the North Sea, tidal stirring counteracts buoyancy forces from sea surface heat flux and inhibits the development of a seasonal thermocline in the shallower water (Schrum, 1997). Hence, tidal mixing fronts separate the vertically well mixed colder waters from seasonally stratified waters with higher surface temperatures. Early research in this area was carried out by Dietrich (1954), who developed a relationship between the buoyancy forcing, the maximum tidal velocities and the minimum water depth necessary for stratification. Later the widely used Simpson and Hunter parameter for estimating the position of a tidal mixing front was introduced and defined as a function of maximum tidal current speed and water depth (Simpson and Hunter, 1974). It succeed to describe the location of the tidal mixing fronts in the Celtic Sea and northestern European Shelf (Pingree et al., 1978).

Despite the usefulness of such parameters for a qualitative understanding of the system, the complex nature of time dependent systems require additional information about temporal variability with reasonable spatial coverage simultaneously (Miller, 2009). Frontal detection algorithms based on remote sensing of surface structures were early applied by Cayula and Cornillon (2002) and Canny (1986). These methods are generally based on detection of horizontal gradients or boundaries between water masses. They can provide general information about tidal fronts' occurrence, shifts in adjacent location and intensity. However, they would also add chaotic information (Ullman and Cornillon, 2000) since they cannot distinguish between frontal related SST difference and SST difference caused by other processes, such as changes in clouds and radiation, atmospheric forcing, higher SST due to shallow water depth. Additionally, they might also miss fronts which are not necessarily result in SST differences, for example, fronts induced by river run-off, which are not necessarily embodying SST gradients. These disadvantages would hinder the mechanical interpretation of frontal impacts on biological processes. From a mechanistic perspective, a 3D physical-biological coupled simulation is an expedient tool to study frontal dynamics and its relevance to biochemical fields. They employ the full equation of motion to simulate the hydrodynamics and coupling with ecosystem models which allow for resolving the biochemical processes. Therefore they are able to resolve the temporal and spatial variability of frontal systems and related biochemical responses. By combing remote sensing observation and 3D simulation, two different sources for information could be used to complement each other and synergies could be expected.

In this study, we lay out a quantitative description of frontal dynamics in the North Sea and explore the NPP's response to fronts on multiple temporal and spatial scales, indicating regional differences due to stability of fronts and local biogeochemical characteristics. Firstly, using a standard frontal detection algorithms, we lay out quantitative descriptions of frontal statistics such as the probability of occurrence on a basin scale. Secondly, we contrast biological-physical distribution patterns in various frontal systems. Thirdly, to provide process-oriented interpretations to statistical results, the mechanisms supporting production from event to seasonal scales were explored using Hovmöller diagrams, which were created from 3D simulation data along transects crossing different frontal systems. Finally, the decadal variability of NPP associated with frontsfrontal was quantified.

2. Data and methods

2.1 Remote sensing and model simulation

We employed the well-validated 3D-coupled physical-biochemical model ECOSMO (Daewel and Schrum, 2013) modified as described in Zhao et al., (2019). The hydrodynamic Ocean component of ECOSMO builds on the 3D baroclinic model HAMSOM (HAMburg Shelf Model) (Schrum and Backhaus, 1999). The capability to simulate the hydrodynamic dynamics of the marine ecosystem using a N(utrient)P(hytoplankton)Z(ooplankton)D(etritus) conceptual model framework. A detail description of ECOSMO can be found in Daewel and Schrum (2013). The model is able to simulate the nutrient cycling of silicate, phosphorus and nitrogen in the water column and in the sediments considering processes such as primary production, grazing and excretion by zooplankton, remineralization and sediment-water coupling. It resolves three functional groups for primary producers (diatoms, flagellates and cyanobacteria) and two groups of zooplankton were considered and differentiated based on feeding preferences. Underwater irradiance is reduced by phytoplankton self-shading, dissolved organic matter and detritus (Nissen, 2014; Zhao et al., 2019b) The model time step was 20 min and daily mean output was used compared to remote sensing data. ECOSMO is

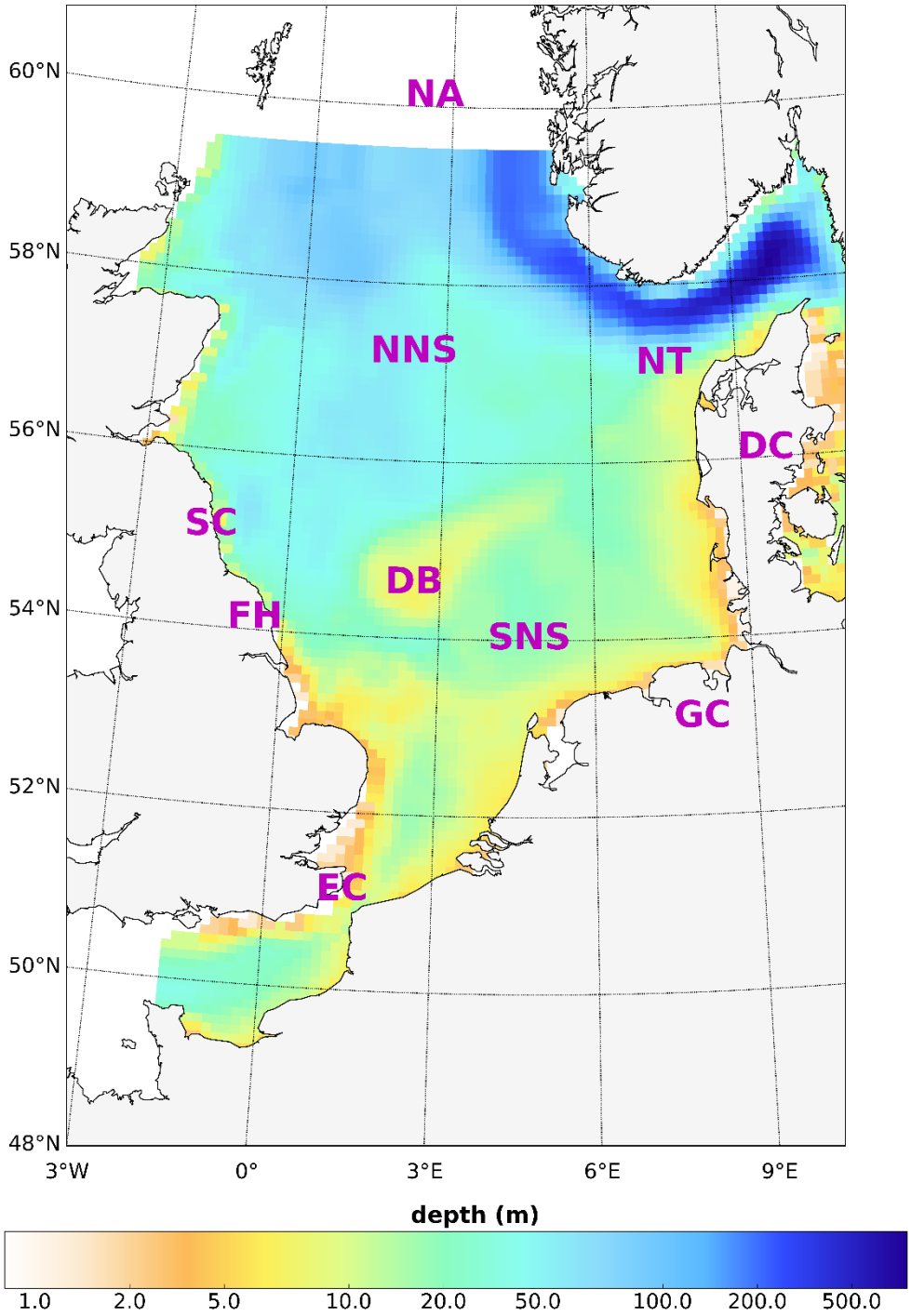

Figure 1. Bathymetry of North Sea. Abbreviations of geographic locations are also laid out: SNS and NNS are short for the southern and northern North Sea, respectively. NA is short for north Atlantic Ocean, NT for Norwegian Trench. Locations of Flamborough Head (FH), Scottish Coast (SC), Damark Coast (DC), German Coast (GC) were also marked out.

able to resolve evolution of physical fronts and biological response in frontal areas in a full dynamical way considering multiple time and spatial scales in the North Sea.

Daily SST and CHL data remotely sensed between 1997 and 2009 were used for the detection of biological-physical distribution patterns in the North Sea. This period corresponds to the overlapping years of the Pathfinder daytime SST (https://podaac.jpl.nasa.gov/dataset/AVHRR_PATHFINDER_L3_SST_DAILY_DAYTIME_V5) and the ESA Climate Change Initiative Ocean Colour (OC-CCI, version 3) CHL datasets. They are mapped onto a regular grid with uniform 4 km horizontal resolution and are subjected to strict quality assurance procedures. For SST, data assigned with quality flags lower than 7 (best quality flag possible) were discarded https://www.nodc.noaa.gov/sog/pathfinder4km/userguide.html The CHL data assigned with any warning flag, by atmospheric correction or bio-optical algorithms, are automatically excluded during the generation of Level 3 OC-CCI products (http://www.esa-oceancolour-cci.org/?q=webfm_send/684). The long temporal coverage of both datasets is achieved using data collected by different infrared and ocean color sensors. For our temporal subset, the Pathfinder dataset v.5 comprises Advanced Very High Resolution Radiometer (AVHRR) measurements (11-12 um) on board of the NOAA-9,-14,-16 and -18 satellites, while the OC-CCI dataset v.3.1 merges Sea-Viewing Wide Field-of-View Sensor (SeaWiFS), Moderate Resolution Imaging Spectroradiometer (Aqua-MODIS) and MEdium Resolution Imaging Spectrometer (MERIS) measurements (~ 400-1000 nm).

The SST (°C) data sets are based on multiple regression between in situ temperatures, measured by drifting and moored buoys, and the AVHRR radiances after atmospheric correction (https://www1.ncdc.noaa.gov/pub/data/sds/cdr/CDRs/Sea_Surface_Temperature_Pathfinder/AlgorithmDescription.pdf). The reported global accuracy of the Pathfider v5 dataset is of 0.02°C ± 0.5 (Kilpatrick et al., 2001). A comparison with the KLIWAS North Sea Climatology of Hydrographic Data v.1 (Bersch et al., 2016), shows that SST spatial patterns are appropriately represented by ECOSMO (Fig.A1). However, the satellite SST (Pathfinder daytime) are biased towards higher temperatures in the study region (Fig.A1), likely due to temperature difference between the skin layer and the water column. Since the frontal detection algorithm used here is mainly based on gradient magnitude fields instead of absolute value, the systematic bias of remote sensing does not affect its performance

The OC-CCI chlorophyll-a (CHL) is estimated from atmospherically corrected water leaving reflectance using an ocean color algorithm blending approach (Grant et al., 2017), 1. Usually, the level of optical complexity of the North Sea waters increases from medium (water classes 7 to 9) in the center of the basin, towards the higher complexity waters in the coast,

characterized by higher scattering due to increased particle concentration (Jackson et al., 2017). The highest complexity is found in the south and west coasts of the basin (water classes 12 to 14), and a medium-high complexity region is found in the shelf region at the east side of the basin (water classes 10 to 11) (Jackson et al., 2017). The general pattern of remote sensing CHL is also compared with simulated biomass in the upper 20 meters. Uncertainties of the CHL product are provided for the OC-CCI CHL products, in the form of bias and root-mean-squared differences (RMSD), derived from its validation with in situ observations. In the North Sea, CHL is underestimated in the central part but overestimated in the nearshore area in summer. The remote sensing based estimates of CHL are subject to large uncertainties which can be attributed to nonalgual water constituents, such as , dissolved organic matter and complicated hydrodynamic conditions (Babin, 2003; Barale and Gade, 2008; McKee et al., 2014; Zheng and DiGiacomo, 2017; Zhu et al., 2013). Further explanations are the systematic difference between a surface CHL pattern from remote sensing and vertically integrated biomass from the upper 20 meters as from ECOSMO. The fixed C:CHL ratio (Alvarez-Fernandez and Riegman, 2014) used for the conversion between biomass and chlorophyll further contributed to the discrepancy between satellite CHL and the results from ECOSMO.

For the validation of model results, we use gradients SST from remote sensing to be compared with SST gradients from model results. For the process-oriented analysis, we used the squared buoyancy frequency N^2 calculated from 3D model results instead of SST to better represent the stratification-mixing status and its impacts on biological fields.

2.2 Methods for frontal detection

To quantify spatial-temporal relationships between hydrodynamic fields and ecological factors, we first obtained frontal statistics. Secondly, we summarized statistical relationships, quantified as orientation of gradients between field gradients of hydrodynamic and ecological factors with coincident time range.

The detection of frontal systems was conducted using SST from ECOSMO simulations. The squared buoyancy frequency N^2 was used as calculated from ECOSMO model data to provide an account for frontal systems based on stratification. Frontal detection and frontal occurrence mapping was conducted in following steps.

Land data points were mask out from both datasets, as well as missing data due to cloud coverage in the remote sensing datasets. For AVHHR, data points with quality flag less than 7 (which is the best quality available) were also discarded.

2.2.1 Finding potential fronts (Edge detection algorithm)

To remove noise and prevent false front detection, data fields are spatially smoothed with a 2D Gaussian low-pass filter (Canny, 1986) before gradients calculation. The value of each element $(x_0,\ y_0)$ in the original data field I, is replaced by a weighted mean of the element itself and its neighbors. The weights are maximum at the central element $(x_0,\ y_0)$ and decrease away from it in a bell-shape, as determined by a 2D Gaussian function:

$$G = \frac{1}{2\pi\sigma^2} e^{\left(\frac{-(x^2+y^2)}{2\sigma^2}\right)} \quad (1)$$

where x and y are the data point indices, expressed as relative positions to the central element $(x = x_i - x_0,\ \ y = y_j - y_0)$, with $x_0 = 0\,, y_0 = 0$, and σ is the standard deviation that determines the width of the bell-shape distribution. The larger the σ, the higher weights of distant elements and therefore the larger the smoothing effects, and viceversa. Following Oram et al., (2008), the optimal value of σ was calculated as the ratio between the length scale of the interested structures and the horizontal resolution of input images (Eq.2)

$$\sigma = \frac{desired\ horizontal\ scale}{horizontal\ resolution\ in\ original\ image} \quad (2)$$

The larger the scales of interest, the stronger the smoothing is desired, aiming to discard smaller scale details, and vise versa. Here, we focus on horizontal structures with length scales larger than 10 km, a value comparable with resolution of the simulation results. Considering the resolution of satellite image (4km) and simulation (10km), the values of σ are chosen to be 3 for satellite and 1 for the simulation.

The first-derivatives are calculated in the longitudinal and latitudinal directions to obtain the directional gradients I_x and I_y, which are the components of the gradient vector. The magnitude of the gradient vector (I_m) is calculated as:

$$I_m = \sqrt{I_x^2 + I_y^2} \quad (3)$$

To find potential fronts (Edge detection algorithm), the calculated gradient filed I_m is first thinned to discard pixels where the local gradient is not a local maximum. Secondly, local maximum gradient amplitude is discarded if the amplitude is smaller than a given threshold. The threshold is determined by 70 percent of the histogram (I_{cri}) which considered all gradient values I_m (prior to thinning) in the whole data (Fig.A2).

2.2.2 Identifying front edges (statistical validation)

Even though frontal candidates detected here were based on high gradients, noises caused by other factors which resulted in high gradients were included in. To test whether detected frontal candidates separate two water masses which possess different characters (e.g. temperature, biological factors), pixels within a given distance (20 km) on different side of detected front candidates are sampled and go through variance test. If the two samples are verified statistically different at 95% confidence level, the frontal candidate was finally confirmed as a front edge (Cayula and Cornillon, 2002; Oram et al., 2008).

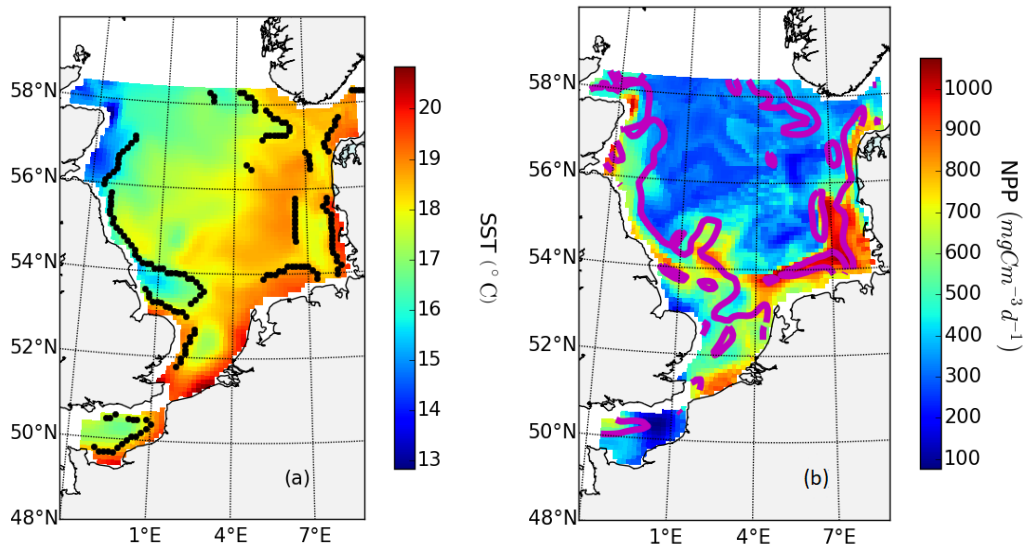

Figure 2. Examples of detected fronts on top of SST (a), detected frontal areas on top of NPP averaged within upper 40 meters (b). Fronts are depicted as black lines (a) and frontal areas are shown in magenta contours (b). Data shown here are simulation results of daily output on 02/08/1999.

2.3 Statistical analysis

2.3.1 Geographical mapping of probability of frontal edges and frontal areas

For a given pixel, the frontal occurrence (P_{front}) is defined by the ratio between numbers of times when a confirmed frontal edge (N_{front}) was detected and valid simulation/observed numbers (N_{valid}). For remote sensing data, missing data due to cloudiness and bad data quality were excluded from the denominator (N_{valid})

P_{front} gives the estimated probability that a grid cell is classified as a frontal grid cell.

$$P_{front} = \frac{N_{front}}{N_{valid}} \times 100\% \quad (4)$$

By mapping P_{front} for all pixels, we obtained the horizontal distribution of frontal occurrence for certain period of time.

Furthermore, frontal areas are identified. Considering that phytoplankton patches with higher biomass or higher NPP were observed closely related to frontal systems with varied spatial range (Franks, 1992b), we further consider a broader region neighbouring the frontal edges detected in SST and N2 fields, as a frontal area.

The frontal area is defined as pixels connected to a front edge with gradients in the physical field I_m higher than the critical value I_{cri} (Fig.A2). Practically, we use a 3×3 window to stepwise expand the frontal area connecting to the original frontal edge (Haralick et al., 1987), until gradients fall below the critical value I_{cri} or meet image boundaries (Fig.2b). For each grid cell, the probability of being included in frontal areas $P_{frontal\ area}$ is defined by the times a grid cell was determined within a frontal area ($N_{frontal\ area}$) divided by the number of times the grid cell has valid data (N_{valid}).

$$P_{frontal\ area} = \frac{N_{frontal\ area}}{N\ valid} \quad (5)$$

By mapping $P_{front\ area}$ for all pixels, we obtained the horizontal distribution of frontal area's occurrence for certain period of time.

2.3.2 Orientation of biological and physical fields

To further quantify the spatial relationship (i.e. higher biomass appear on mixed or stratified side of the front) between physical (SST, N^2) and biological fields (NPP, CHL, biomass) in frontal areas, for each pixel, we calculate the relative orientation angle (Shimada et al., 2005) between physical gradients and biological gradients

$$O = \arccos\left(\frac{\nabla T \cdot \nabla B}{|\nabla T||\nabla B|}\right) \quad (6)$$

The orientation angle (O) ranges from 0°- 180°. When O approaches 0°, the two gradient vectors are nearly parallel to each other and with the same direction. This indicates that the higher biological amplitude is on the same side of higher value in physical field (higher N^2 /SST). Lower biological productivity locates on the same side of front edge with lower values of N2/SST. Conversely, when O approaches 180°, the two gradients vectors are also parallel but with opposite directions (i.e. higher biological value lies on the physical side with lower value or vice versa). When O is around the value of 90°, the two gradients vectors are perpendicular to each other. Orientation angles were grouped into 8 categories for each 22.5°

interval. For each pixel, the probability of each orientation angle group P_{og}^{i}, is calculated by dividing counted number of each orientation angles $N_{og}^{i}$with counted frontal area numbers $N_{frontal\ area}$:

$$P_{OG}^{i} = \frac{N_{og}^{i}}{N_{frontal\ area}} \tag{7}$$

The probabilities of orientation groups 1 (P_{OG}^{1}) (0° to 22.5°) and 8 (P_{OG}^{8}) (157.5° and 180°), corresponding to higher NPP/CHL on the stratified and mixed side of the front, respectively, exhibit the highest amplitude and are therefore the focus of further analysis.

3. Results

We first analysed the map of frontal occurrence and summarized the general seasonality of frontal dynamics (section 3.1). Remote sensing data were used as reference to validate the simulation. We then analysed the orientation pattern focusing on summer when seasonal stratification persists in the southern North Sea (sections 3.2). In the following section 3.3, we explored potential mechanisms responsible for manifested regimes in section 3.2, mainly in seasonal and event time scales. Finally, making use our simulation results, we quantified decadal variability of frontal NPP (section 3.4).

3.1 Validation of fronts simulation in the North Sea

The ability of the ECOSMO model simulation results to resolve frontal structures was validated by comparing SST gradient estimated from ECOSMO simulation data and remote sensing data, in summer (Fig.3). High amplitudes of SST gradients occur both in simulation and satellite data. Higher gradients occurred from the eastern part of the North Sea to the western part of North Sea, mainly along the DC, FH and SC fronts (as named in Fig.1 1), which were identified from both datasets. Due to the sparseness of remote sensing SST data, the seasonality of SST fronts is poorly resolved and the occurrence of fronts is lower than that detected from ECOSMO. However, when we refer to the mean gradients of SST, we found that the general pattern manifested in ECOSMO simulation are confirmed by remote sensing data (Fig.3). Therefore, we conclude that the ECOSMO model is able to simulate the seasonal evolution of fronts in the North Sea.

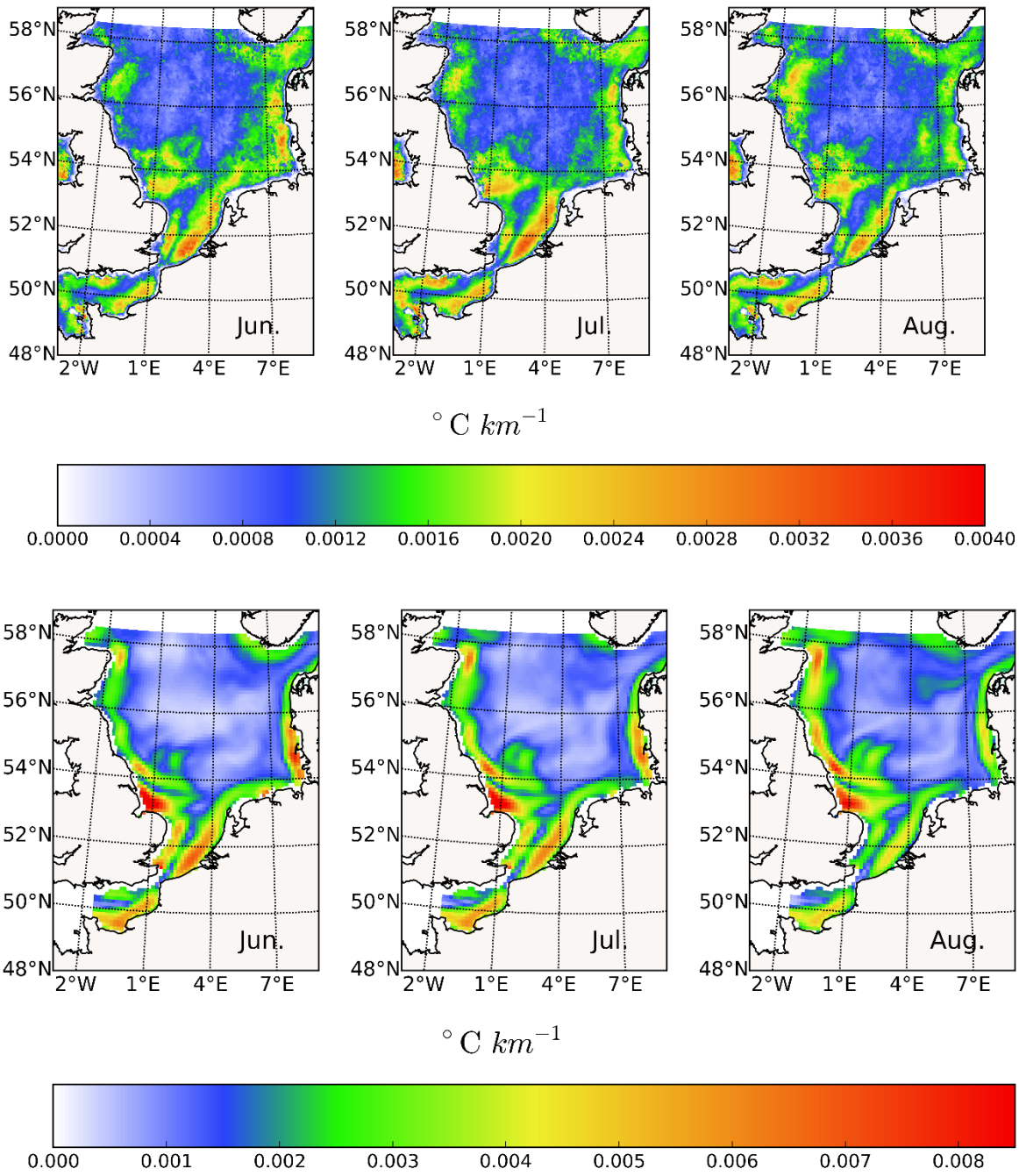

Figure 3. Averaged gradients of SST in summer from remote sensing (upper panel) (AVHRR, v5) and in ECOSMO (lower panel) for years from 1997 to 2009.

3.2 Seasonality of fronts in the North Sea

Fig.4 shows the seasonality of fronts as detected from the maximum N^2 in the water column. Fronts mentioned here were named according to Belkin et al., (2009) In winter, the frontal occurrence is confined in near shore area in the southern German Bight and the Norwegian Trench where haline stratification persists. In spring, after stratification developed fronts appear around the edge of the Dogger Bank (DB), along the German Bight (GBF) and the Danish coast (DF) in the east, along the Scottish coast (SCF) and offshore off Flamborough Head (FHF) in

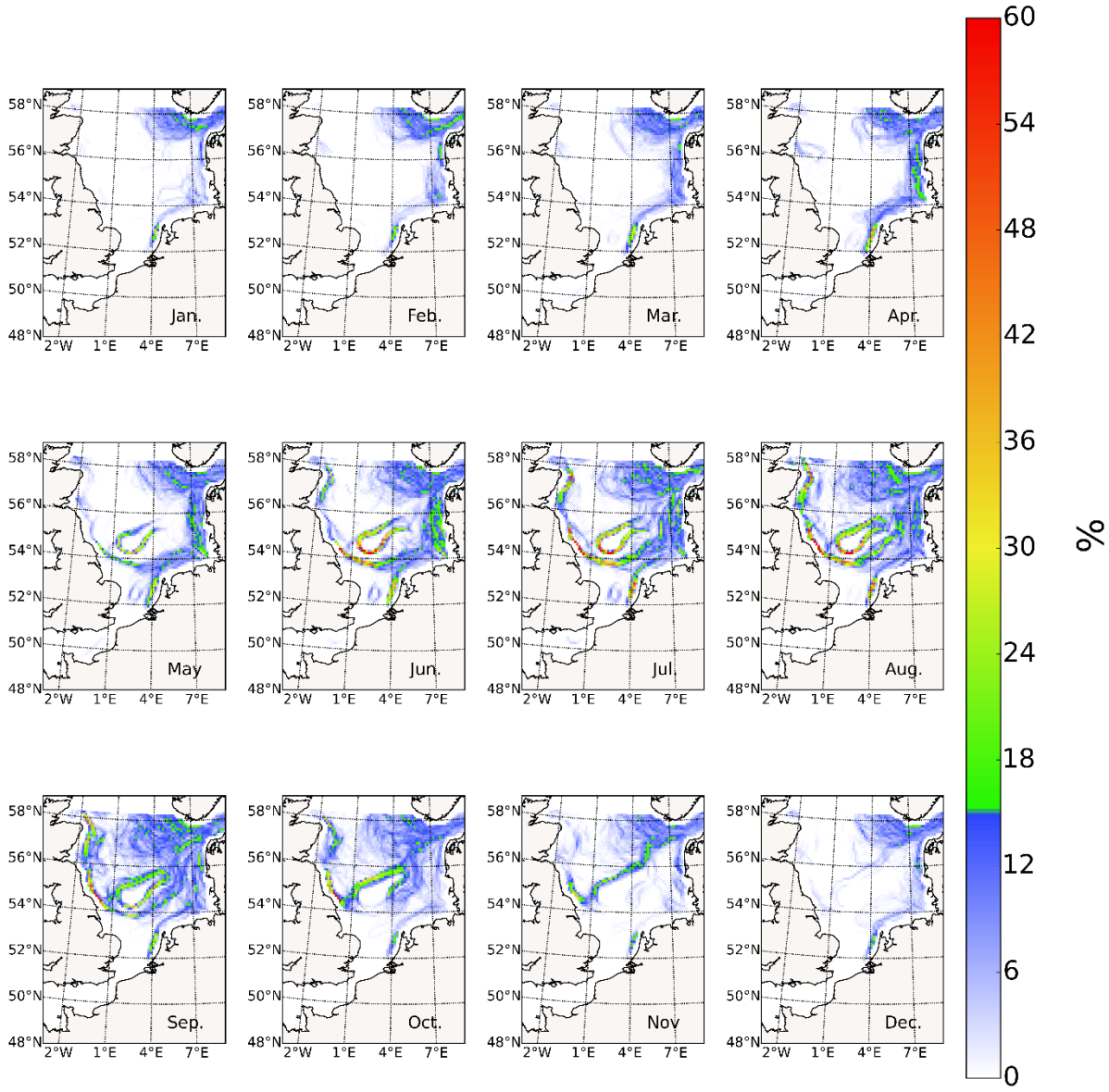

Figure4. Seasonality of detected fronts from squared buoyancy frequency N2 simulated in ECOSMO. Time period span is 1997-2009.

the west. In summer, due to the high stability of fronts, such as DB, SCF, FHF, the frontal occurrence centralized in a narrow ribbons, with some grid cells reaching values of more than 60% occurrence of fronts. However, in the eastern part of the southern North Sea, due to the instability and shifting of fronts, the occurrence disperse and the probability of frontal occurrence in a grid cell shows lower values, ranging from 6%-20%. When summer thermal stratification diminishes, the stratified area shrinks from the south to the north, centralizing along the 60 meter's isobaths in autumn (Oct., Nov.).

We also detected fronts from simulated SST (Fig.5). Here similar pattern reveal compared to those manifesting in frontal occurrence maps derived from N^2 (Fig.4). However, two SST frontal lines persist along the eastern and western side of the English Channel and one frontal

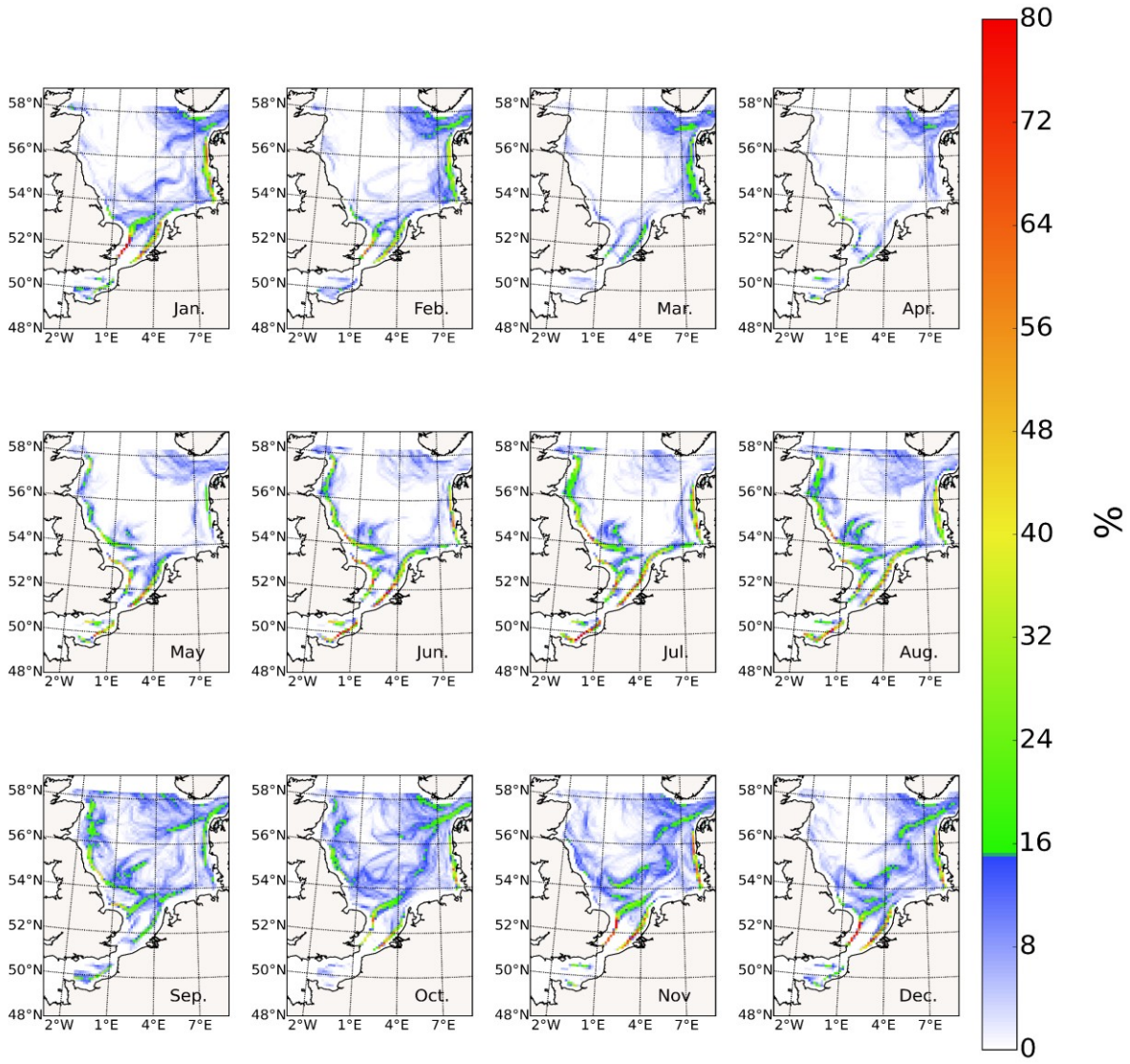

Figure 5. Seasonality of detected fronts from SST simulated by ECOSMO. Time period span is 1997-2009.

line persists along the southern boundary of Humber, which do not necessarily appear in frontal occurrence maps derived from N^2. These areas stay unstratified throughout the year and the N^2 in these two regions cannot meet the threshold I_{cri} for fronts. The SST fronts here may appear due to different heating of the mixed water column due to sharp changes of local water depth. Solar heating effects are larger in shallow water. Furthermore, the occurrence of SST fronts in DBF is much lower in the eastern boundary of compared to that detected from N^2. The steep

change of bathymetry results in the variation of stratification status (N^2) but the SST differences are not necessarily present.

The Frontal structures identified from the ECOSMO simulation (Fig.4,5) reveals great consistency with previous studies (Belkin et al., 2009). Therefore, we conclude that the ECOSMO is able to simulate the seasonal evolution of fronts in the North Sea.

3.3 frontal implications for primary production

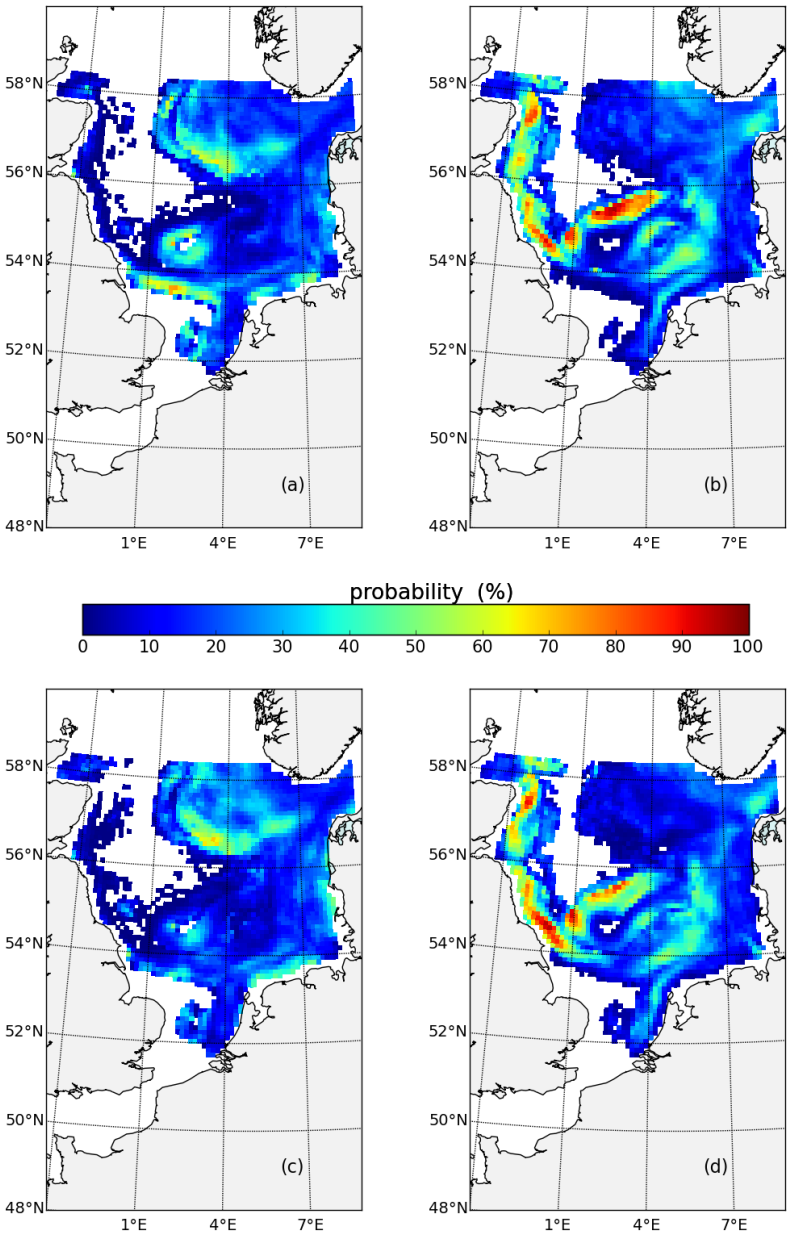

Figure 6. Orientation (P_{og}^{i}) of NPP and biomass in frontal areas in summer (1997-2009). The upper panel shows the probability of higher biomass locating on the stratified (a) or mixed side (b) of fronts. The lower panel shows the probability of higher NPP locating on the stratified (a) or mixed

side (b) of fronts. Grid cells which are not detected as frontal areas or probability equal to 0 were masked out.

The probability of orientation groups (P_{og}^{i}) is used to identify the relationship between the gradients of biological and physical fields in frontal areas. The results suggest that the difference in the orientation is related to the stability of the front: the more stable the front is, the more likely higher NPP appears on the mixed side of the front (Fig. 6b,d). This general pattern occurs predominantly at frontal systems in the north-western area were the probability can reach up to 90% (Fig. 6b,d). This includes SCF and north of DBF. This dominating pattern further expand to areas east to Dogger Bank, with decreased probability (around 50%, Fig.6b,d). In contrast, along the south-eastern coast of the North Sea, higher NPP and biomass appears more likely on the stratified side of the fronts, even though the probability is with around 50% lower than that for the pattern in the north-western North Sea (Fig.6a,c). Near the FHF, 50%-60% higher biomass appears on the stratified side of the fronts (P_{og}^{1}) (Fig.6a), whereas the probability for NPP at the stratified side decreases to 30% (Fig.6c).

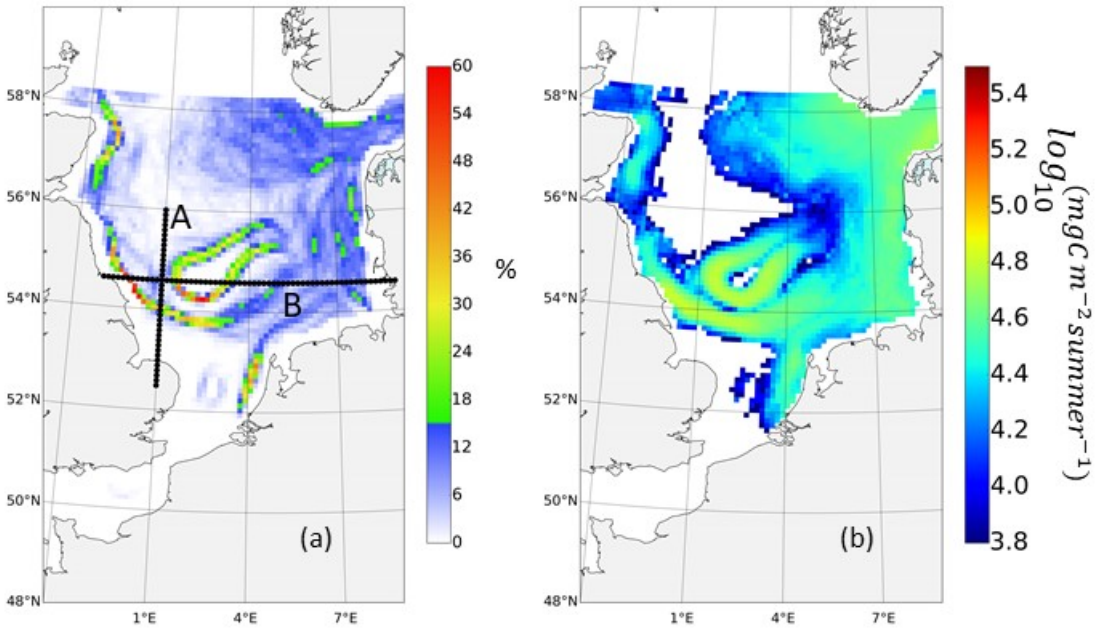

Figure 7. Transect plot (black) on top of frontal probability (a), and NPP in summer (June, July, August) in frontal areas (b).

To further investigate frontal evolution and corresponding biological responses, which might explain the orientation pattern revealed before, were investigated two transects across the typical frontal systems in the Southern North Sea more closely and analysed the temporal

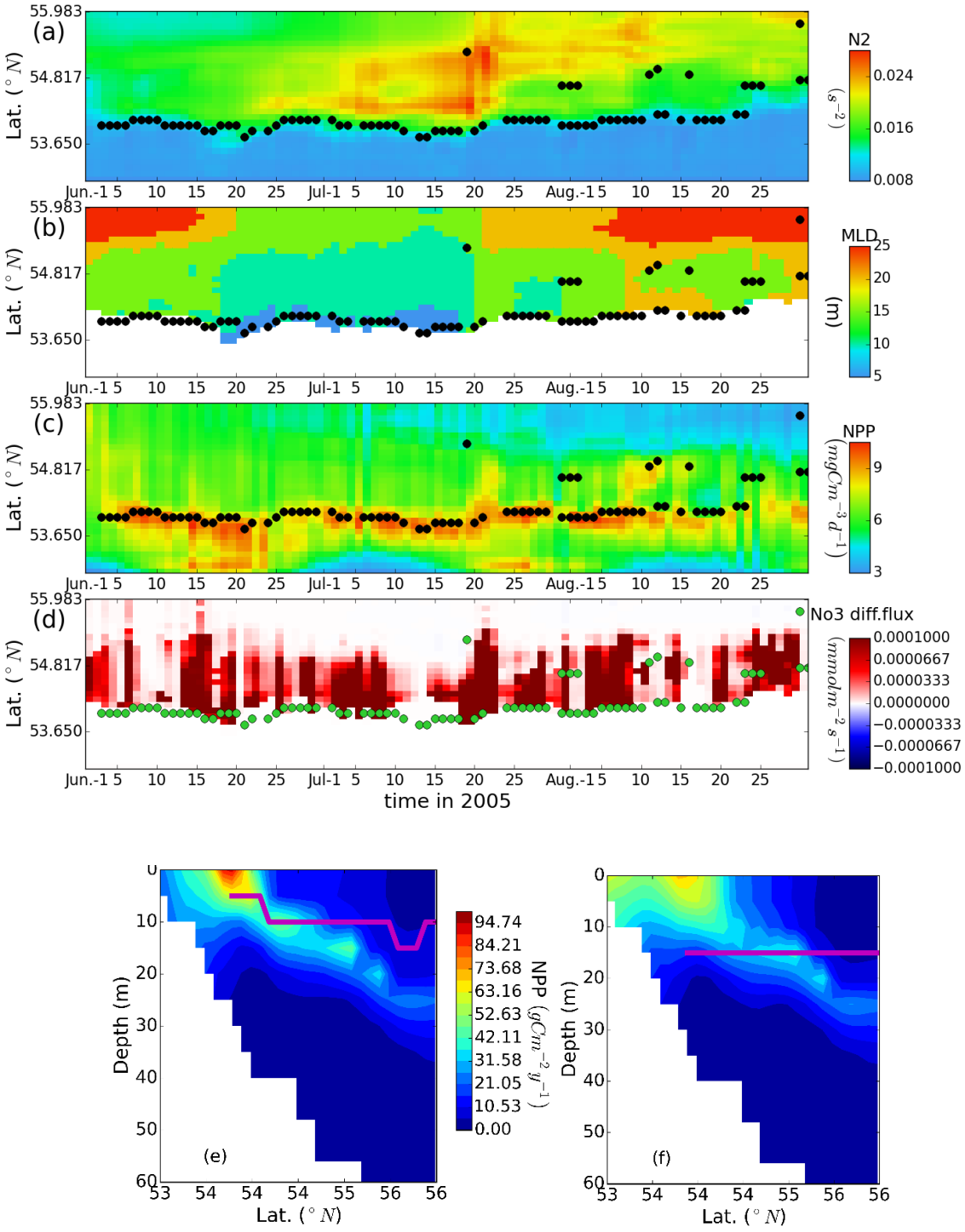

Figure 8. Hovmöller diagram for N^2 (a), mixed layer depth (b), NPP (c), NO3 vertical diffusive flux across pycnocline (d) in transect A in 2005. Threshold of 0.013 in N^2 was used to identify stratification and masked out areas where is unstratified in mixed layer depth (MLD) (b) and NO3 diffusive flux (d). Transect plot for NPP are under stable conditions (15/07/2005) (e) and mixing event (20/07/2005) (f) .Mixed layer depth was marked out by magenta lines in (e,f).

evolution using corresponding Hovmöller diagrams (Fig.7a). The transect A was built to cross the FHF, the most southern reach of the stratified water column in the western part of southern

North Sea, where frontal probability reaches around 50% in summer. Transect B was built to cross the SCF, the western and eastern part of the DBF, the DF and the unstable frontal regions between the Dogger Bank' eastern edge and DF.

For transect A, persisting patterns can be identified that sustain high NPP throughout the entire stratified season. The FHF (Fig.8e) shows the typical structure of a stable tidal front. Due to the shallowness of the water and enhanced mixing near shore, the pycnocline blend to surface and bottom (Fig.8e). In Fig.8a,b, we show exemplary the temporal evolution of physical characteristics, here N^2 and the mixed layer depth (MLD) at transect A for the year 2005 along with the variation in NPP and nitrate diffusive flux of NO_3 (Fig. 8d). Evidently both N^2 and MLD clearly identify the location of the front, which is changing only slightly during the whole stratified season. In addition, the physical indicators identify a time period of increased stratification between June 20th and July 20th. NPP mainly occurs inshore with highest NPP (around 9 $mgC\,m^{-3}d^{-1}$ averaged for the upper 40 m) around the front. However, phytoplankton biomass tends to accumulate at the stratified side (Fig.6a) of the fronts, mainly due to enhanced grazing in the mixed side (data not shown). NO3 shows highest concentration inshore and is used at the frontal edge due to high NPP (data not shown). Further offshore, stratification decouples the surface from nutrients in the deeper waters. Therefore, NPP is confined to the subsurface (Fig.8e), where it remains relatively low ($52mgC\,m^{-3}d^{-1}$) within the subsurface layer due to light limitation. In contrast maximum NPP at the frontal edge is much higher (94 $mgC\,m^{-3}d^{-1}$). The reason for the increased production in that area can be found in the high local diffusive nutrient fluxes in the vicinity of the front (Fig. 8d) as a consequence of the shallowness and instability of the MLD.

The transect Bes crosses several typical fronts in the southern North Sea from west to east such as SCF, DBF, DCF and unstable fronts in the south-eastern part. The shallow region along the British coast and at Dogger Bank are typically vertically mixed. However, there is a narrow band with high N^2 along the DCF, where fresh water contributes to the frontal system. We will discuss the results regarding the production pattern in the eastern and western part of the transect B, separately.

The SCF and the fronts west to the Dogger Bank have different NPP regimes, despite their regional vicinity. The SCF separates the well-mixed water column on its inshore side from the

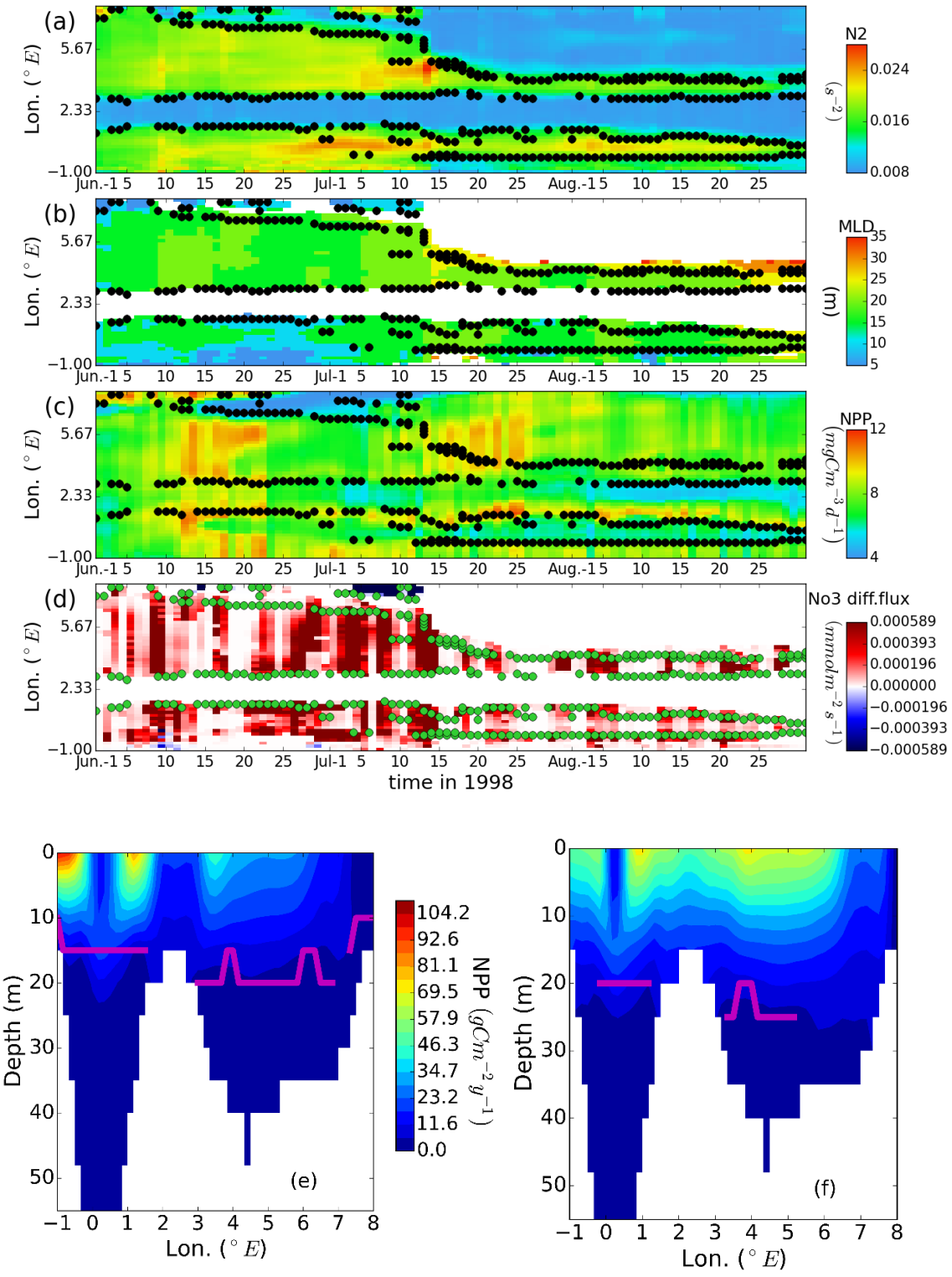

Figure 9. Hovmöller diagram for N^2 (a), mixed layer depth (b), NPP (c), NO3 vertical diffusive flux across pycnocline (d) in transect B in 1998. Threshold of 0.013 in N^2 was used to identify stratification and masked out areas where is unstratified in mixed layer depth (MLD) (b) and NO3 diffusive flux (d). Transect plot for NPP are under stable conditions (05/07/1998) (e) and mix event (15/07/1998) (f) .Mixed layer depth was marked out by magenta lines in (e,f).

stratified offshore side. From the British coast to the area west to SCF, bathymetry increases steeply to more than 60 meters and the water column on the deeper side stays stratified (Fig.9e). Above the Dogger Bank, due to the shallow depth, the water column stay well-mixed throughout the whole year. The frontal edge of DBF separates the stratified water column around the DB from the mixed water column above the top of the bank. Different from typical tidal fronts, such as FHF, the pycnocline in the western side of DB bend downwards to touch the bathymetry (Fig.9e). At the FHF high NPP persists and is confined to the mixed side of front (Fig.9c). Since nutrient fluxes were found to be non-regular during the year at the near shore mixed side of SCF (Fig.9d), nutrients from river loads were assumed to additionally contribute to the high NPP nearshore in the SCF frontal system. Additionally, baroclinic circulation was also suggested to transport nutrients along the pycnocline from the bottom to euphotic layer depth (Pedersen, 1994). Here a transient region between SCF and western branch of DBF is located, where NPP is generally lower than that in the coastal and frontal region (Fig. 9c). In the eastern and western edges of DBF, high productivity persists and forms the 'ring' shaped NPP along the frontal edges (Fig.7b, Fig.9c). Pumping up nutrient fluxes from the pycnocline persists throughout the entire stratified season, sustaining the high productivity at the front (Fig.9c & Fig.9d). The phenomenon mentioned above were supposed as the major mechanisms that responsible for the persisting high productive patterns in the western part of the southern North Sea. In summary, in the western part of the southern North Sea, fronts' location are mainly regulated by tidal mixing energy, bathymetry and solar heating. Benefiting from diffusive flux of nutrients from beneath pycnocline which is horizontally on the edge of the stratified area, the gradients of locally generated NPP has opposite direction compared to the horizontal gradient of N^2. Additionally, in the nearshore side of FHF, NPP flourishes due to the high nutrients concentration in the mixed inshore side. These are major mechanisms responsible for the dominating probability of P_{og}^{1} in the western part of the southern North Sea.

In the eastern part of the transect B, fronts show strong variability in location and in how long they persists (Fig.7a). The Danish Coast Front is strongly impacted by mixing, but also by changes in the freshwater plume along the Danish Coast. Substantial intra- and inter-annual variability in stratification status has been found between 2.4-5.5°E. The mixed area connected to the eastern coast, which was confined near shore in the beginning of June, either moved further offshore in July in some 'mixed years' (e.g. 2004, 2007, 2008, 2009), or was

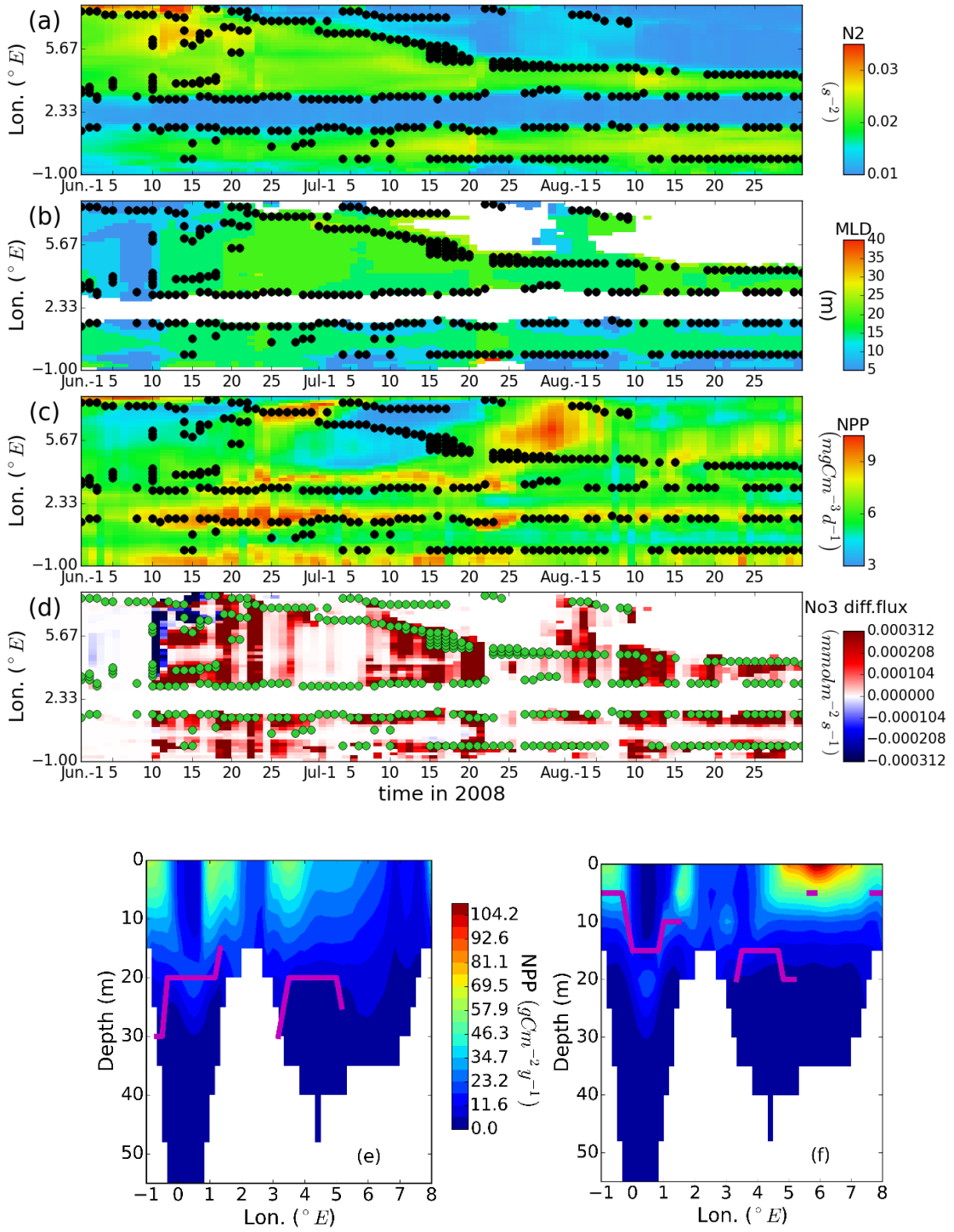

Figure 10. Hovmöller diagram for N^2 (a), mixed layer depth (b), NPP (c), NO3 vertical diffusive flux across pycnocline (d) in transect B in 2008. Threshold of 0.013 in N^2 was used to identify stratification and masked out areas where is unstratified in mixed layer depth (MLD) (b) and NO3 diffusive flux (d). Transect plot for NPP are under stable conditions (05/07/1998) (e) and mix event (28/07/2008) (f). Mixed layer depth was marked out by magenta lines in (e,f).

persistently confined nearshore until the end of stratified season in some 'stratified years' (e.g. 2005, 2006). In the mixed years, frontal location shifted as a consequence of MLD deepening,

causing high NPP. For example, on 15th of July, 1998 (Fig.9a), compared to 10 days before, the mixed layer depth (Fig.9b) has deepened from 20 m to 25 m (Fig.9f) and areas east to 6 °E became fully mixed afterwards. This event went along with an increase in NPP and the elevated NPP persisted during the rest of the stratified season in areas north to 2.5 °E, but was not anymore related to frontal areas. For frontal areas, the pumping up of nutrients intensified NPP during the whole 'shifting' events, with the duration time from 10th of July until 20th of July (Fig.9a & Fig.9c). While high NPP tends to appear at the stratified side of the front under stable frontal conditions, after the 'shifting' event, high NPP remained at the mixed side of the moving fronts. This indicates that the dominance of P_{og}^{i} is sensitive to the frontal movements.

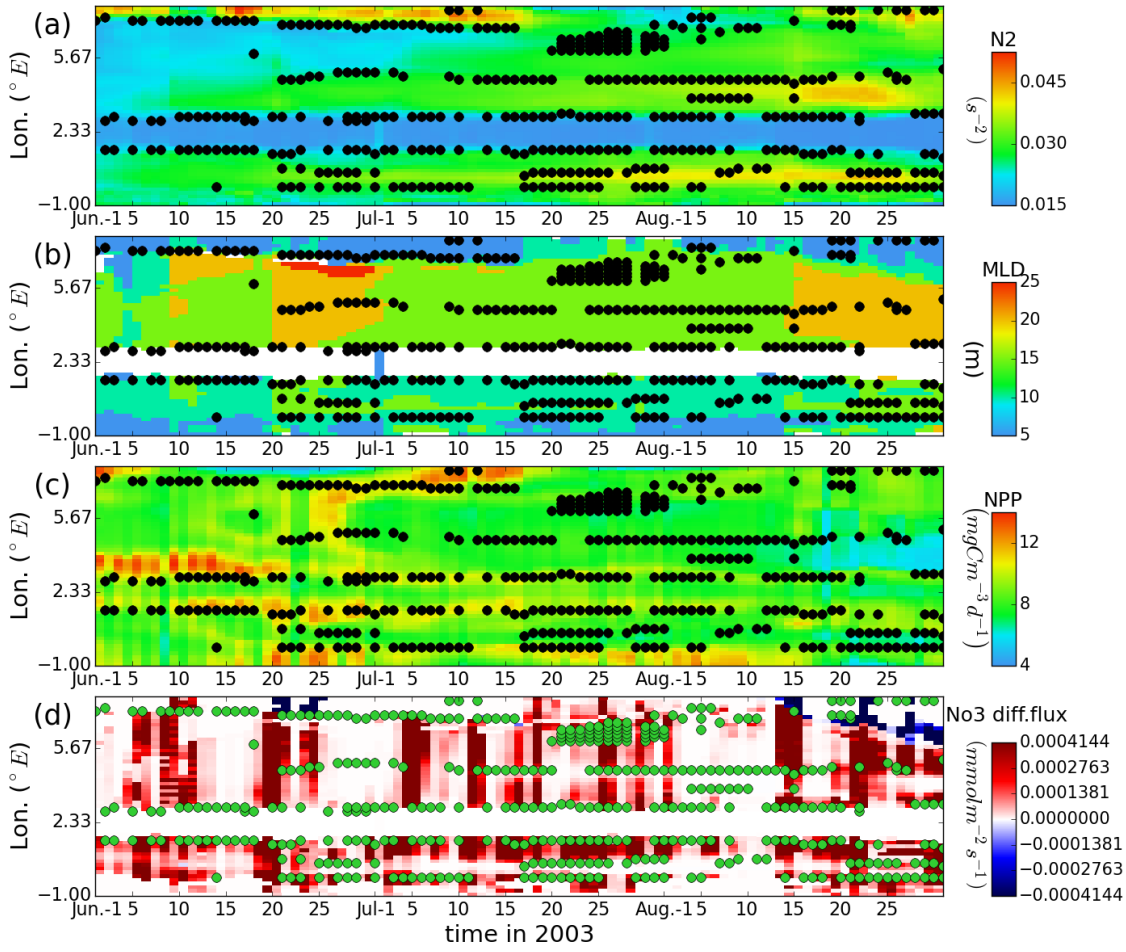

Figure 11. Hovmöller diagram for N² (a), mixed layer depth (b), NPP (c), NO3 vertical diffusive flux across pycnocline (d) in transect B in 2003. Threshold of 0.013 in N2 was used to identify stratification and masked out areas where is unstratified in mixed layer depth (MLD) (b) and NO3 diffusive flux (d).

In other more mixed years, after the expansion of mixed areas in July, in contrast to triggered blooms in previously stratified areas by mixing, higher NPP can also be initiated by stratification, particularly in further inshore areas (e.g. 2008) (Fig.10). In a similar situation for 1998, mixed areas move further offshore in the middle of July (Fig.9a). In the beginning of August, short-period stratification set the mixed layer depth to 5 m around 6 $°E$ (Fig.10b, Fig.10f). Without severe nutrient limitation, phytoplankton benefited from the shallowing of mixed layer depth and flourished on the stratified side of new fronts which locate at 8.8 $°N$.

As mentioned before, in some more stratified years, stratification persisted throughout the season between 2.4-5.5$°E$ (e.g. 2003, 2013, 2005, 2006). Even though the maximum N_2 remain high enough to sustain the stratification, the mixed layer depth also fluctuated, due to e.g. wind mixing, and generated irregular upward NO3 fluxes (Fig.11c, d). However, in some very 'calm' years (e.g. 2005, 2006, data not shown), upward NO3 flux was rare in the same area, probably because intensified stability and separation of upper and lower mixed layers. In near shore areas east of 8.8$°E$, where the water column stays well mixed due to the shallow depth (20m) and strong tidal mixing, high NPP can be triggered by stratification brought about by river run-off, as captured by observations (Czitrom et al., 1988). In our simulation, stratification established due to buoyancy force induced by substantial river runoff, with a pycnocline around 5m. Besides stratification, rivers provide additional nutrients, which sustain phytoplankton growth.

The NPP in stable fronts, such as FHF, also benefits from frontal shifting event. As revealed in Fig.8, the mixing events move the frontal edge further offshore and deepen the mixed layer depth during the shifting process (Fig.8b). High NPP was triggered by the upward pumping of nutrients, which mainly located on the mixed side of fronts (Fig.8c), as revealed by the statistical analysis (Fig.6b).

3.4 Decadal variability of NPP generated in frontal systems

To evaluate the inter-annual variability of frontal NPP, NPP produced within the frontal area as seen in daily model output (Fig.2b) was integrated for summer months (June, July, August) and converted to the unit of $gCm^{-2}summer^{-1}$ in Fig.12. The substantial decadal fluctuations, which were process based derived, coincided (p=0.62) with local productivity variability that supposed to be driven by wind variability (Daewel and Schrum, 2017). The time series of frontal NPP shows a similar decadal trend and fluctuations as local estimates based on observations data for recent decades (1988-2013) (Capuzzo et al., 2013). Generally, a significant decline has been captured. Both time series showed a moderate decrease in the beginning of 1990s and sustained in a higher level during the middle of 1990s. Since 2000 and

afterwards, the frontal NPP dropped down and kept lower than average levels (Fig.12). The lowest production period during late 2010s was identified in both time series. Suggested by Capuzzo et al. (2018), the eastern transitional area displayed most substantial decadal variability among all hydrodynamic subdomains. Compared to the eastern transitional area, the western transitional is more stable. Based on our results, this would be partly attributed to the difference stability of the eastern or western frontal systems, respectively. Moreover, the reduced NPP in the eastern frontal area, is proposed to be associated with increased warming and reduced riverine nutrients input (Capuzzo et al., 2013), which would be disentangled by sensitivity simulations.

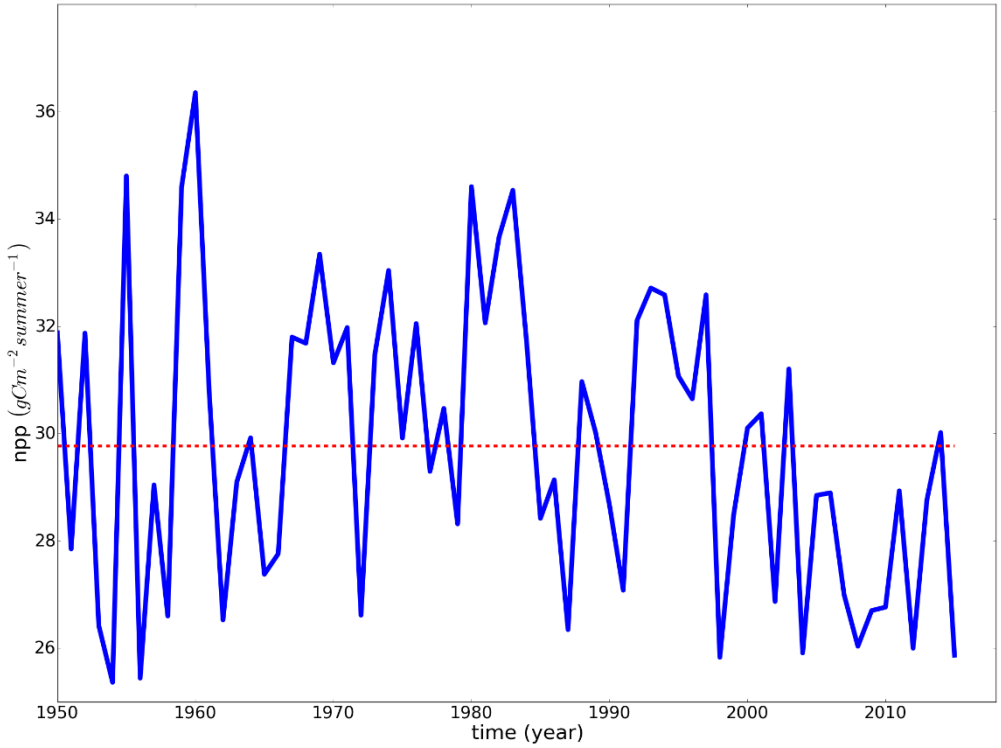

Figure.12 Time series of frontal NPP in summer (June, July, August) in the North Sea during 1950-2015. Dashed red line is the average value.

4. Conclusion and discussions

This study provides quantitative description of frontal dynamics in seasonal cycle. It highlights the stability of typical tidal fronts in the western part of North Sea and unstable fronts in the eastern part of the North Sea. In the latter, several different types of fronts completed the mechanism responsible for high productivity, particularly for short-time scale events, such as

river-run off and wind perturbations of frontal systems. In stable frontal systems in the western part, NPP tends to locate on the mixed side of fronts. NPP here benefits from enriched nutrients, which are confined nearshore or fuelled by the diffusive flux from the pycnocline below. In the eastern North Sea, higher NPP is associated more with events of frontal movement. Transient stratification in previously mixed areas, particularly driven by pronounced river run-off keeping phytoplankton cells within euphotic layers trigger blooms. Conversely, when mixed water body invades into the previously stratified side or mixed layer depth deepens, phytoplankton growth benefits from releasing nutrient limitation

Suggested by previous studies (Mann and Lazier, 2013), in coastal and shelf seas, replenishment of nutrients is potentially driven by the spring-neap tidal cycle, baroclinic eddies, residual currents and vertical transport (Lenhart and Pohlmann, 2004). Different mechanisms may be more relevant in specific time and spatial ranges, which needs further exploration using observed data or diagnose by simulation scenarios. For example, in the mixed side of fronts, especially in the inshore area along the coast such as the SCF and the FHF, riverine nutrient inputs, are transported baroclinic circulation or secondary circulation (van Aken et al., 1987), which merits investigation with higher resolutions. Adjustment of frontal location by the spring-neap tidal cycle renews water masses in frontal areas and nutrient enriched water gets exposed to well-lighted regions (Pedersen, 1994; Richardson et al., 2000). In the German Bight, even though water masses could also be renewed by upwelling driven by eastern winds, the amplitude of biological response also depends on the availability of nutrients conveyed by the water mass originally in lower water layers of the old Elbe Valley, where nutrient concentrations depend on advected ocean-source water trapped by topography and vertical current shear (Becker et al., 1983; Mathis et al., 2015). This likely contributes to the significant variability in the biological fields under similar physical forcing. In another frontal system on the Northwest European Shelf, the Ushant Front, vertical transport of nutrients is also a the dominating factor for sustaining high productivity (James, 1984; Loder and Platt, 1985) whereas in the Georges Bank, cross-frontal transport and residual currents play a more important role (Mann and Lazier, 2013). However, until today, the quantitative debate of relative importance between vertical and horizontal transport of nutrients and biomass, which potentially contribute to high NPP, is still going on due to limited measurements (Holigan 1984), parameterization of models (Hu et al., 2008), and unstable conditions of frontal systems (Loder and Platt, 1985).

In this study, we mainly discuss the shifting of fronts or mixing-stratification status based on counteracting processes between potential buoyancy (such as river runoff or solar heating) and stirring energy sources (e.g. wind and tide). Except for these mechanisms, baroclinic instability is also identified to be responsible for stratification, even in presence of winds or heat loss (Schrum, 1997; Taylor and Ferrari, 2011). Furthermore, the stratification process in specific time period may not only be influenced by simultaneous atmospheric condition or the tidal cycle, but pre-correlated with stratification conditions in earlier months of the respective year (Schrum et al., 2003). Inter-annual variability and intra-annual variability merits further investigation.

As revealed in our results (Fig.12), the frontal NPP underwent a decline since 2000. Suggested by Capuzzo et al.(2018), NPP in the eastern North Sea is particularly sensitive to environmental change. Besides the general decreasing trend of NPP, which has been quantified in this study, potential driving factors have to be further distinguished and diagnosed with the help of statistical methods and confirmation through numerical simulations (Weinert et al., 2016). For example, different wind directions in the German Bight result in different extension and pattern of fresh water thus generating different stratification processes. Rising temperatures would potentially extend the stratified season when fronts persists and intensify the frontal density gradient. Climate change's impacts on frontal systems has implications on ecosystem in multiple ecological levels. Variation in front's intensity and persisting time will alter the dispersal of passive drifting organisms, such as planktonic larvae (Suberg, 2015). Geographical distributions of benthic communities were observed to be influenced by tidal fronts, such as Flamborough Head Front (van Aken et al., 1987). Simulations with ECOSMO E2E, an extended version of the ECOSMO model including fish and macrobenthos groups (Daewel et al., 2018) will be able to investigate this open question.

Compared to other marine systems, most frontal systems in the North Sea are typically dominated by tidal mixing, which differ to those induced by upwelling, western boundary currents and topography. In contrast to stable fronts, which are stabilized by steep gradient of bathymetry, the shallow depth and high-latitude location of the North Sea results in substantial seasonal variability of the frontal system and makes it susceptible to mixing events (Belkin et al., 2009). However, for the mechanisms triggering high NPP, similar conclusion were achieved in different systems and can be applied more generally. The replenishment of nutrients is also able to trigger patchy blooms in oligotrophic subtropical waters (Lévy et al., 2003; McGillicuddy et al., 2007). Increasing mean light exposure of phytoplankton cells by reducing

vertical mixing is also beneficial to phytoplankton growth in areas such as subpolar systems where growth is more limited by light (Huisman et al., 1999). In many regions of the ocean, sub-mesoscale fronts on scales of 1-10km were found to influence the biological characteristics (Klein and Lapeyre, 2008). Simulation with higher resolution will better resolve frontal impacts (Mahadevan and Archer, 2000) at all relevant scales and give new insight into fronts' role for the regional (Pohlmann, 2006) or global carbon cycle (Stramska et al., 1995).

Appendix

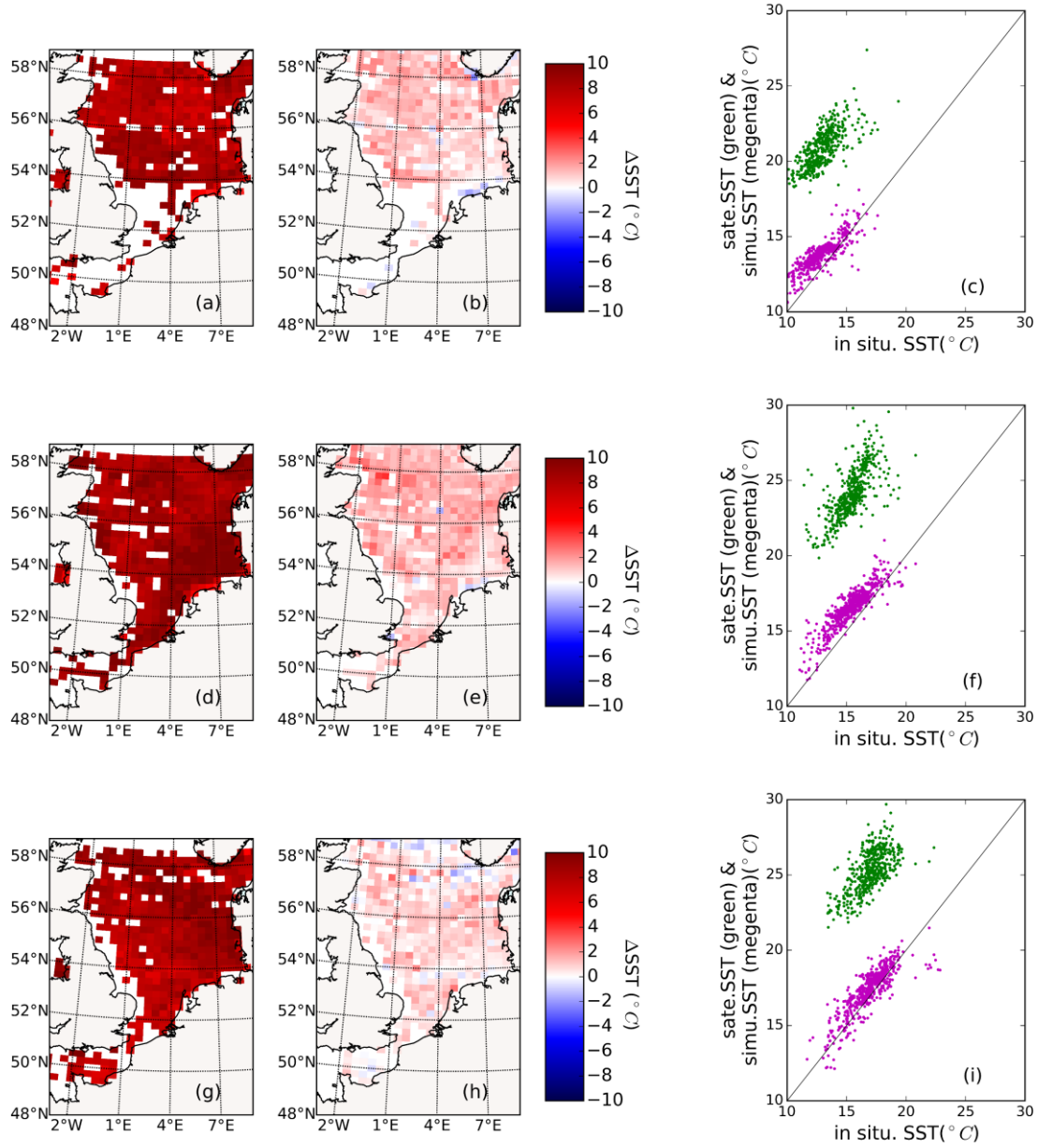

Figure A1. Comparison of the model and satellite SST monthly means with in situ. data from KLIWAS (average of depths 0m and 2m) for June (top panel), July (middle panel) and August (bottom panel). Maps of the satellite SST - in situ. SST difference (left panel, a,d,g), ECOSMO SST – in situ. SST (middle panel b,e,h) were laid out. Scatter plot of in situ. SST (x-axis) were plotted vs. satellite SST (green points) and ECOSMO SST (magenta points) (c,f,i). The ECOSMO and satellite SST maps were binned to match KLIWAS geographical grid (0.25°).

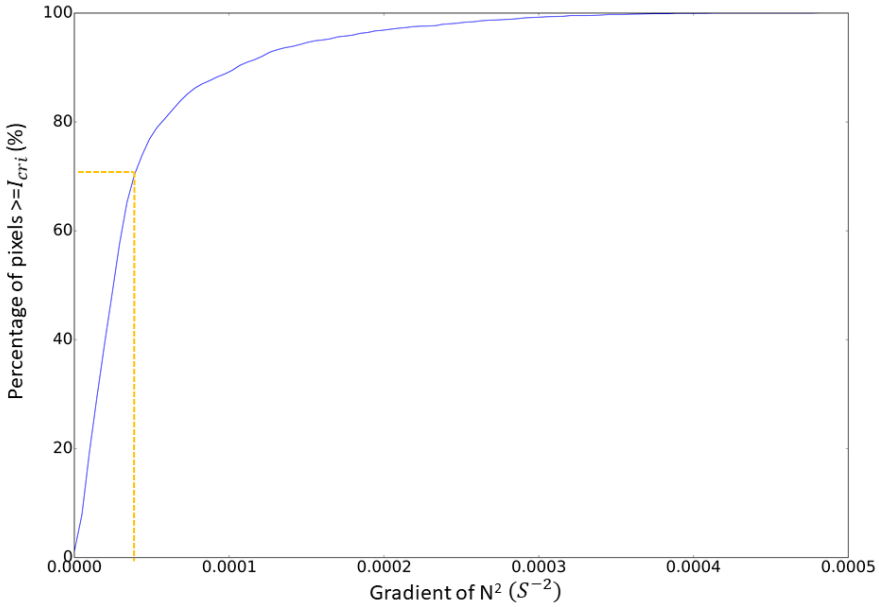

Figure A2. Histogram of gradient magnitudes of N^2 from ECOSMO simulation, covering period from 1997-2009, with daily output. The values of the critical threshold I_{cri} is determined by 70% (yellow dash line).

Reference

van Aken, H. M., van Heijst, G. J. F. and Maas, L. R. M.: Observations of fronts in the North Sea, J. Mar. Res., 45(3), 579–600, doi:10.1357/002224087788326830, 1987.

Alvarez-Fernandez, S. and Riegman, R.: Chlorophyll in North Sea coastal and offshore waters does not reflect long term trends of phytoplankton biomass, J. Sea Res., doi:10.1016/j.seares.2014.04.005, 2014.

Babin, M.: Variations in the light absorption coefficients of phytoplankton, nonalgal particles, and dissolved organic matter in coastal waters around Europe, J. Geophys. Res., doi:10.1029/2001jc000882, 2003.

Backhaus, J. o.: The North Sea and the climate, Dana, 8, 69–82, 1989.

Barale, V. and Gade, M.: Remote sensing of the European seas., 2008.

Barton, A. D., Ward, B. A., Williams, R. G. and Follows, M. J.: The impact of fine-scale turbulence on phytoplankton community structure, Limnol. Oceanogr. Fluids Environ., 4(1), 34–49, doi:10.1215/21573689-2651533, 2014.

Baschek, B., Schroeder, F., Brix, H., Riethmüller, R., Badewien, T. H., Breitbach, G., Brügge, B., Colijn, F., Doerffer, R., Eschenbach, C., Friedrich, J., Fischer, P., Garthe, S., Horstmann, J., Krasemann, H., Metfies, K., Merckelbach, L., Ohle, N., Petersen, W., Pröfrock, D., Röttgers, R., Schlüter, M., Schulz, J., Schulz-Stellenfleth, J., Stanev, E., Staneva, J., Winter, C., Wirtz, K., Wollschläger, J., Zielinski, O. and Ziemer, F.: The Coastal Observing System for Northern and Arctic Seas (COSYNA), Ocean Sci., doi:10.5194/os-13-379-2017, 2017.

Becker, G. A., Fiúza, A. F. G. and James, I. D.: Water mass analysis in the German Bight during Marsen, Phase I, J. Geophys. Res. Ocean., 88(C14), 9865–9870, doi:10.1029/jc088ic14p09865, 1983.

Belkin, I. M., Cornillon, P. C. and Sherman, K.: Fronts in Large Marine Ecosystems, Prog. Oceanogr., 81(1–4), 223–236, doi:10.1016/j.pocean.2009.04.015, 2009.

Berger,W. H., Smetacek, V. S. and Wefer, G.: Productivity of the Ocean. Present and Past, New yourk., 1989.

Bersch, M., Hinrichs, I., Gouretski, V. and Sadikni, R.: Hydrographic climatology of the North Sea and surrounding regions – version 2.0, Hamburg., 2016.

Van Beusekom, J., Diel-Christiansen, A.: Synthesis of phyto- and zooplankton dynamics in the North Sea environment 148 pp, Godalming., 1994.

Blauw, A. N., Benincà, E., Laane, R. W. P. M., Greenwood, N. and Huisman, J.: Dancing with the Tides: Fluctuations of Coastal Phytoplankton Orchestrated by Different Oscillatory Modes of the Tidal Cycle, PLoS One, 7(11), doi:10.1371/journal.pone.0049319, 2012.

Bost, C. A., Cotté, C., Bailleul, F., Cherel, Y., Charrassin, J. B., Guinet, C., Ainley, D. G. and Weimerskirch, H.: The importance of oceanographic fronts to marine birds and mammals of the southern oceans, J. Mar. Syst., doi:10.1016/j.jmarsys.2008.11.022, 2009.

Bracher, A. U., Kroon, B. M. A. and Lucas, M. I.: Primary production, physiological state and composition of phytoplankton in the Atlantic sector of the Southern Ocean, Mar. Ecol. Prog. Ser., doi:10.3354/meps190001, 1999.

Brickman, D. and Loder, J. W.: Energetics of the internal tide on northern Georges Bank, J. Phys. Oceanogr., doi:10.1175/1520-0485(1993)023<0409:EOTITO>2.0.CO;2, 1993.

Brockmann, U. H., Laane, R. W. P. M. and Postma, H.: Cycling of nutrient elements in the North Sea, Netherlands J. Sea Res., 26(2–4), 239–264, doi:https://doi.org/10.1016/0077-7579(90)90092-U, 1990a.

Brockmann, U. H., Laane, R. W. P. M. and Postma, J.: Cycling of nutrient elements in the North Sea, Netherlands J. Sea Res., doi:10.1016/0077-7579(90)90092-U, 1990b.

Brown, T.: Kelvin wave reflection at an oscillating boundary with applications to the North Sea, Cont. Shelf Res., 7(4), 351–365, doi:10.1016/0278-4343(87)90105-1, 1987.

Cadier, M., Gorgues, T., Sourisseau, M., Edwards, C. A., Aumont, O., Marié, L. and Memery, L.: Assessing spatial and temporal variability of phytoplankton communities' composition in the Iroise Sea ecosystem (Brittany, France): A 3D modeling approach. Part 1: Biophysical control over plankton functional types succession and distribution, J. Mar. Syst., 165, 47–68, doi:https://doi.org/10.1016/j.jmarsys.2016.09.009, 2017.

Canny, J.: A computational approach to edge detection., IEEE Trans. Pattern Anal. Mach. Intell., 8(6), 679–698, doi:10.1109/TPAMI.1986.4767851, 1986.

Capet, A., Beckers, J. M. and Grégoire, M.: Drivers, mechanisms and long-term variability of seasonal hypoxia on the Black Sea northwestern shelf - Is there any recovery after eutrophication?, Biogeosciences, doi:10.5194/bg-10-3943-2013, 2013.

Capuzzo, E., Painting, S. J., Forster, R. M., Greenwood, N., Stephens, D. T. and Mikkelsen, O. A.: Variability in the sub-surface light climate at ecohydrodynamically distinct sites in the North Sea, Biogeochemistry, 113(1–3), 85–103, doi:10.1007/s10533-012-9772-6, 2013.

Capuzzo, E., Lynam, C. P., Barry, J., Stephens, D., Forster, R. M., Greenwood, N., McQuatters-Gollop, A., Silva, T., van Leeuwen, S. M. and Engelhard, G. H.: A decline in primary production in the North Sea over 25 years, associated with reductions in zooplankton abundance and fish stock recruitment, Glob. Chang. Biol., 24(1), e352–e364, doi:10.1111/gcb.13916, 2018.

Carreto, J. I., Montoya, N., Akselman, R., Carignan, M. O., Silva, R. I. and Cucchi Colleoni, D. A.: Algal pigment patterns and phytoplankton assemblages in different water masses of the Río de la Plata

maritime front, Cont. Shelf Res., doi:10.1016/j.csr.2007.02.012, 2008.

Castelao, R. M., Barth, J. A. and Mavor, T. P.: Flow-topography interactions in the northern California Current System observed from geostationary satellite data, Geophys. Res. Lett., 32(24), 1–4, doi:10.1029/2005GL024401, 2005.

Cayula, J.-F. and Cornillon, P.: Edge Detection Algorithm for SST Images, J. Atmos. Ocean. Technol., doi:10.1175/1520-0426(1992)009<0067:edafsi>2.0.co;2, 2002.

Charnock, H., Dyer, K. R., Huthnance, J., LISS, P. and Simpson, B. H.: Understanding the North Sea System, 1st ed., Chapmann & Hall for the Royal Society, London., 1994.

Chen, C., Beardsley, R. C. and Limeburner, R.: A Numerical Study of Stratified Tidal Rectification over Finite-Amplitude Banks. Part II: Georges Bank, J. Phys. Oceanogr., 25(9), 2111–2128, doi:10.1175/1520-0485(1995)025<2111:ANSOST>2.0.CO;2, 1995.

Cinner, J. E., McClanahan, T. R., Graham, N. A. J., Daw, T. M., Maina, J., Stead, S. M., Wamukota, A., Brown, K. and Bodin, O.: Vulnerability of coastal communities to key impacts of climate change on coral reef fisheries, Glob. Environ. Chang., doi:10.1016/j.gloenvcha.2011.09.018, 2012.

Corten, A.: Long-term trends in pelagic fish stocks of the North Sea and adjacent waters and their possible connection to hydrographic changes, Netherlands J. Sea Res., doi:10.1016/0077-7579(90)90024-B, 1990.

Cullen, J. J.: Subsurface Chlorophyll Maximum Layers: Enduring Enigma or Mystery Solved?, Ann. Rev. Mar. Sci., doi:10.1146/annurev-marine-010213-135111, 2015.

Czitrom, S. P. R., Budéus, G. and Krause, G.: A tidal mixing front in an area influenced by land runoff, Cont. Shelf Res., 8(3), 225–237, doi:10.1016/0278-4343(88)90030-1, 1988.

Daewel, U. and Schrum, C.: Simulating long-term dynamics of the coupled North Sea and Baltic Sea ecosystem with ECOSMO II: Model description and validation, J. Mar. Syst., 119–120, 30–49, doi:10.1016/j.jmarsys.2013.03.008, 2013.

Daewel, U. and Schrum, C.: Low-frequency variability in North Sea and Baltic Sea identified through simulations with the 3-D coupled physical-biogeochemical model ECOSMO, Earth Syst. Dyn., 8(3), 801–815, doi:10.5194/esd-8-801-2017, 2017.

Daewel, U., Schrum, C. and Macdonald, J.: Towards End-2-End modelling in a consistent NPZD-F modelling framework (ECOSMOE2E_vs1.0): Application to the North Sea and Baltic Sea, Geosci. Model Dev. Discuss., (November), 1–40, doi:10.5194/gmd-2018-239, 2018.

Daly, K. L. and Smith, W. O.: Physical-Biological Interactions Influencing Marine Plankton Production, Annu. Rev. Ecol. Syst., doi:10.1146/annurev.es.24.110193.003011, 1993.

Dauwe, B., Herman, P. M. J. and Heip, C. H. R.: Community structure and bioturbation potential of macrofauna at four North Sea stations with contrasting food supply, Mar. Ecol. Prog. Ser., 173(1978),

67–83, doi:10.3354/meps173067, 1998.

Denman, K. R. and Abbott, M. R.: Time scales of pattern evolution form cross-spectrum analysis of Advanced Very High Resolution Radiometer and Coastal Zone Color Scanner imagery, J. Geophys. Res., 99(C4), 7433–7442, 1994.

Derisio, C., Alemany, D., Acha, E. M. and Mianzan, H.: Influence of a tidal front on zooplankton abundance, assemblages and life histories in Península Valdés, Argentina, J. Mar. Syst., doi:10.1016/j.jmarsys.2014.08.019, 2014.

Edwards, M., Beaugrand, G., Reid, P. C., Rowden, A. A. and Jones, M. B.: Ocean climate anomalies and the ecology of the North Sea, Mar. Ecol. Prog. Ser., 239(August), 1–10, doi:10.3354/meps239001, 2002.

Emeis, K. C., van Beusekom, J., Callies, U., Ebinghaus, R., Kannen, A., Kraus, G., Kröncke, I., Lenhart, H., Lorkowski, I., Matthias, V., Möllmann, C., Pätsch, J., Scharfe, M., Thomas, H., Weisse, R. and Zorita, E.: The North Sea - A shelf sea in the Anthropocene, J. Mar. Syst., doi:10.1016/j.jmarsys.2014.03.012, 2015.

Fernand, L., Weston, K., Morris, T., Greenwood, N., Brown, J. and Jickells, T.: The contribution of the deep chlorophyll maximum to primary production in a seasonally stratified shelf sea, the North Sea, Biogeochemistry, 113(1–3), 153–166, doi:10.1007/s10533-013-9831-7, 2013.

Le Fèvre, J.: Aspects of the Biology of Frontal Systems, Adv. Mar. Biol., doi:10.1016/S0065-2881(08)60109-1, 1987.

Fisher, J. A., Casini, M., Frank, K. T., Möllmann, C., Leggett, W. C. and Daskalov, G.: The importance of within-system spatial variation in drivers of Marine Ecosystem regime shifts, Philos. Trans. R. Soc. B Biol. Sci., doi:10.1098/rstb.2013.0271, 2015.

Floeter, J., van Beusekom, J. E. E., Auch, D., Callies, U., Carpenter, J., Dudeck, T., Eberle, S., Eckhardt, A., Gloe, D., Hänselmann, K., Hufnagl, M., Janßen, S., Lenhart, H., Möller, K. O., North, R. P., Pohlmann, T., Riethmüller, R., Schulz, S., Spreizenbarth, S., Temming, A., Walter, B., Zielinski, O. and Möllmann, C.: Pelagic effects of offshore wind farm foundations in the stratified North Sea, Prog. Oceanogr., doi:10.1016/j.pocean.2017.07.003, 2017.

Franks, P. J. S.: Phytoplankton blooms at fronts: patterns, scales, and physical forcing mechanisms, Rev. Aquat. Sci., 1992

Glibert, P. M., Icarus Allen, J., Artioli, Y., Beusen, A., Bouwman, L., Harle, J., Holmes, R. and Holt, J.: Vulnerability of coastal ecosystems to changes in harmful algal bloom distribution in response to climate change: Projections based on model analysis, Glob. Chang. Biol., doi:10.1111/gcb.12662, 2014.

Grant, M., Jackson, T., Chuprin, A., Sathyendranath, S., Zühlke, M., Dingle, J., Storm, T., Boettcher,

M. and Norman, F.: Product User Guide, Ocean Colour Climate Change Initiative (OC_CCI) – Phase Two., 2017.

Green, A. L., Fernandes, L., Almany, G., Abesamis, R., McLeod, E., Aliño, P. M., White, A. T., Salm, R., Tanzer, J. and Pressey, R. L.: Designing Marine Reserves for Fisheries Management, Biodiversity Conservation, and Climate Change Adaptation, Coast. Manag., doi:10.1080/08920753.2014.877763, 2014.

Gröger, M., Maier-Reimer, E., Mikolajewicz, U., Moll, A. and Sein, D.: NW European shelf under climate warming: Implications for open ocean - Shelf exchange, primary production, and carbon absorption, Biogeosciences, doi:10.5194/bg-10-3767-2013, 2013.

Haigh, I. D., Eliot, M. and Pattiaratchi, C.: Global influences of the 18.61 year nodal cycle and 8.85 year cycle of lunar perigee on high tidal levels, J. Geophys. Res. Ocean., doi:10.1029/2010JC006645, 2011.

Halpern, B. S., Selkoe, K. A., Micheli, F. and Kappel, C. V.: Evaluating and ranking the vulnerability of global marine ecosystems to anthropogenic threats, Conserv. Biol., doi:10.1111/j.1523-1739.2007.00752.x, 2007.

Haralick, R. M., Sternberg, S. R. and Zhuang, X.: Image Analysis Using Mathematical Morphology, IEEE Trans. Pattern Anal. Mach. Intell., doi:10.1109/TPAMI.1987.4767941, 1987.

Haren, H. Van and Howarth, M. J.: Enhanced stability during reduction of stratification in the North Sea, , 24, 805–819, doi:10.1016/j.csr.2004.01.008, 2004.

Hartman, S. E., Humphreys, M. P., Kivimäe, C., Woodward, E. M. S., Kitidis, V., McGrath, T., Hydes, D. J., Greenwood, N., Hull, T., Ostle, C., Pearce, D. J., Sivyer, D., Stewart, B. M., Walsham, P., Painter, S. C., McGovern, E., Harris, C., Griffiths, A., Smilenova, A., Clarke, J., Davis, C., Sanders, R. and Nightingale, P.: Seasonality and spatial heterogeneity of the surface ocean carbonate system in the northwest European continental shelf, Prog. Oceanogr., doi:10.1016/j.pocean.2018.02.005, 2018.

Hickel, W., Mangelsdorf, P. and Berg, J.: The human impact in the German Bight: Eutrophication during three decades (1962-1991), Helgoländer Meeresuntersuchungen, doi:10.1007/BF02367167, 1993.

Hicks, N., Ubbara, G. R., Silburn, B., Smith, H. E. K., Kröger, S., Parker, E. R., Sivyer, D., Kitidis, V., Hatton, A., Mayor, D. J. and Stahl, H.: Oxygen dynamics in shelf seas sediments incorporating seasonal variability, Biogeochemistry, doi:10.1007/s10533-017-0326-9, 2017.

Hofmeister, R., Flöser, G. and Schartau, M.: Estuary-type circulation as a factor sustaining horizontal nutrient gradients in freshwater-influenced coastal systems, Geo-Marine Lett., 37(2), 179–192, doi:10.1007/s00367-016-0469-z, 2017.

Holt, J. and Proctor, R.: The seasonal circulation and volume transport on the northwest European continental shelf: A fine-resolution model study, J. Geophys. Res. Ocean., 113(6), doi:10.1029/2006JC004034, 2008.

Holt, J., Harle, J., Proctor, R., Michel, S., Ashworth, M., Batstone, C., Allen, I., Holmes, R., Smyth, T., Haines, K., Bretherton, D. and Smith, G.: Modelling the global coastal ocean, Philos. Trans. R. Soc. A Math. Phys. Eng. Sci., doi:10.1098/rsta.2008.0210, 2009.

Holt, J., Wakelin, S., Lowe, J. and Tinker, J.: The potential impacts of climate change on the hydrography of the northwest European continental shelf, Prog. Oceanogr., doi:10.1016/j.pocean.2010.05.003, 2010.

Holt, J., Butenschön, M., Wakelin, S. L., Artioli, Y. and Allen, J. I.: Oceanic controls on the primary production of the northwest European continental shelf: Model experiments under recent past conditions and a potential future scenario, Biogeosciences, 9(1), 97–117, doi:10.5194/bg-9-97-2012, 2012.

Holt, J., Schrum, C., Cannaby, H., Daewel, U., Allen, I., Artioli, Y., Bopp, L., Butenschon, M., Fach, B. A., Harle, J., Pushpadas, D., Salihoglu, B. and Wakelin, S.: Physical processes mediating climate change impacts on regional sea ecosystems, Biogeosciences Discuss., 11, 1909–1975, doi:10.5194/bgd-11-1909-2014, 2014.

Holt, J., Schrum, C., Cannaby, H., Daewel, U., Allen, I., Artioli, Y., Bopp, L., Butenschon, M., Fach, B. A., Harle, J., Pushpadas, D., Salihoglu, B. and Wakelin, S.: Potential impacts of climate change on the primary production of regional seas: A comparative analysis of five European seas, Prog. Oceanogr., 140, 91–115, doi:10.1016/j.pocean.2015.11.004, 2016.

Holt, J., Hyder, P., Ashworth, M., Harle, J., Hewitt, H. T., Liu, H., New, A. L., Pickles, S., Porter, A., Popova, E., Icarus Allen, J., Siddorn, J. and Wood, R.: Prospects for improving the representation of coastal and shelf seas in global ocean models, Geosci. Model Dev., doi:10.5194/gmd-10-499-2017, 2017.

Hu, S., Townsend, D. W., Chen, C., Cowles, G., Beardsley, R. C., Ji, R. and Houghton, R. W.: Tidal pumping and nutrient fluxes on Georges Bank: A process-oriented modeling study, J. Mar. Syst., 74(1–2), 528–544, doi:10.1016/j.jmarsys.2008.04.007, 2008.

Hufnagl, M., Peck, M. A., Nash, R. D. M., Pohlmann, T. and Rijnsdorp, A. D.: Changes in potential North Sea spawning grounds of plaice (Pleuronectes platessa L.) based on early life stage connectivity to nursery habitats, J. Sea Res., doi:10.1016/j.seares.2012.10.007, 2013.

Hufnagl, M., Temming, A. and Pohlmann, T.: The missing link: Tidal-influenced activity a likely candidate to close the migration triangle in brown shrimp Crangon crangon (Crustacea, Decapoda), Fish. Oceanogr., 23(3), 242–257, doi:10.1111/fog.12059, 2014.

Huisman, J., Van Oostveen, P. and Weissing, F. J.: Critical depth and critical turbulence: Two

different mechanisms for the development of phytoplankton blooms, Limnol. Oceanogr., doi:10.4319/lo.1999.44.7.1781, 1999.

Huthnance, J., Weisse, R., Wahl, T., Thomas, H., Pietrzak, J., Souza, A. J., Heteren, S. Van, Schmelzer, N., Beusekom, J. Van, Colijn, F., Haigh, I., Hjøllo, S., Holfort, J., Kent, E. C., Kühn, W., Loewe, P., Lorkowski, I., Mork, K. A., Pätsch, J., Quante, M., Salt, L., Siddorn, J., Smyth, T., Sterl, A. and Woodworth, P.: North Sea Region Climate Change Assessment., 2016.

ICES: Flushing times of the North Sea. Co-operative Research Report, Copenhagen., 1983.

Iriarte, a, Daneri, G., Garcia, V. M. T., Purdie, D. a and Crawford, D. W.: Plankton community respiration and its relationship to chlorophyll a concentration in marine coastal waters, Oceanol. Acta, 14(4), 379–388, 1991.

Iverson, R. L., Whitledge, T. E. and Goering, J. J.: Chlorophyll and nitrate fine structure in the southeastern Bering Sea shelf break front [7], Nature, doi:10.1038/281664a0, 1979.

Jackson, T., Sathyendranath, S. and Mélin, F.: An improved optical classification scheme for the Ocean Colour Essential Climate Variable and its applications, Remote Sens. Environ., doi:10.1016/j.rse.2017.03.036, 2017.

Jacobs, W.: Modelling the Rhine River Plume, TU Delft., 2004.

Jago, C. F., Jones, S. E., Latter, R. J., McCandliss, R. R., Hearn, M. R. and Howarth, M. J.: Resuspension of benthic fluff by tidal currents in deep stratified waters, northern North sea, in Journal of Sea Research, vol. 48, pp. 259–269., 2002a.

Jago, C. F., Jones, S. E., Latter, R. J., McCandliss, R. R., Hearn, M. R. and Howarth, M. J.: Resuspension of benthic fluff by tidal currents in deep stratified waters, northern North sea, J. Sea Res., 48(4), 259–269, doi:10.1016/S1385-1101(02)00181-8, 2002b.

James, I. D.: A three-dimensional numerical shelf-sea front model with variable eddy viscosity and diffusivity, Cont. Shelf Res., doi:10.1016/0278-4343(84)90044-X, 1984.

Janowitz, G. S. and Kamykowski, D.: Modeled Karenia brevis accumulation in the vicinity of a coastal nutrient front, Mar. Ecol. Prog. Ser., doi:10.3354/meps314049, 2006.

Joint, I. and Pomroy, A.: Phytoplankton Biomass and Production in the Southern North-Sea, Mar. Ecol. Ser., 1993.

Jones, B. H. and Halpern, D.: Biological and physical aspects of a coastal upwelling event observed during March-April 1974 off northwest Africa, Deep Sea Res. Part A, Oceanogr. Res. Pap., doi:10.1016/0198-0149(81)90111-4, 1981.

Kautsky, H.: Investigations on the distribution of 137Cs, 134Cs and 9°Sr and the water mass transport times in the Nor- thern North Atlantic and the North Sea, Dtsch. hydrogr.Z., 40, 49–69, 1987.

Kerimoglu, O., Hofmeister, R., Maerz, J., Riethmüller, R. and Wirtz, K. W.: The acclimative

biogeochemical model of the southern North Sea, Biogeosciences, 14(19), 4499–4531, doi:10.5194/bg-14-4499-2017, 2017.

Klein, P. and Lapeyre, G.: The Oceanic Vertical Pump Induced by Mesoscale and Submesoscale Turbulence, Ann. Rev. Mar. Sci., 1(1), 351–375, doi:10.1146/annurev.marine.010908.163704, 2008.

Krause, G., Budeus, G., Gerdes, D., Schaumann, K. and Hesse, K.: Frontal systems in the german bight and their physical and biological effects, Elsevier Oceanogr. Ser., 42(C), 119–140, doi:10.1016/S0422-9894(08)71042-0, 1986.

Landeira, J. M., Ferron, B., Lunven, M., Morin, P., Marie, L. and Sourisseau, M.: Biophysical interactions control the size and abundance of large phytoplankton chains at the ushant tidal front, PLoS One, 9(2), doi:10.1371/journal.pone.0090507, 2014.

Laubscher, R. K., Perissinotto, R. and McQuaid, C. D.: Phytoplankton production and biomass at frontal zones in the Atlantic sector of the Southern Ocean, Polar Biol., doi:10.1007/BF00233138, 1993.

Laufkötter, C., Vogt, M. and Gruber, N.: Long-term trends in ocean plankton production and particle export between 1960-2006, Biogeosciences, doi:10.5194/bg-10-7373-2013, 2013.

Lavoie, D., Lambert, N. and Gilbert, D.: Projections of Future Trends in Biogeochemical Conditions in the Northwest Atlantic Using CMIP5 Earth System Models, Atmos. - Ocean, doi:10.1080/07055900.2017.1401973, 2017.

van Leeuwen, S. M., van der Molen, J., Ruardij, P., Fernand, L. and Jickells, T.: Modelling the contribution of deep chlorophyll maxima to annual primary production in the North Sea, Biogeochemistry, 113(1–3), 137–152, doi:10.1007/s10533-012-9704-5, 2013.

van Leeuwen, S., Tett, P., David, M. and van der Molen, J.: Stratified and nonstratified areas in the North Sea: Long-termvariability and biological and policy implications, J. Geophys. Res. Ocean., 120(7), 4670–4686, doi:10.1002/2014JC010485.Received, 2015.

Van Leeuwen, S., Tett, P., Mills, D. and Van Der Molen, J.: Stratified and nonstratified areas in the North Sea: Long-term variability and biological and policy implications, J. Geophys. Res. C Ocean., 120(7), 4670–4686, doi:10.1002/2014JC010485, 2015.

Lefèvre, D., Bentley, T. L., Robinson, C., Blight, S. P. and Williams, P. J. l. B.: The temperature response of gross and net community production and respiration in time-varying assemblages of temperate marine micro-plankton, J. Exp. Mar. Bio. Ecol., 184(2), 201–215, doi:10.1016/0022-0981(94)90005-1, 1994.

Lenhart, H. J. and Pohlmann, T.: North sea hydrodynamic modelling: A review, Senckenbergiana Maritima, doi:10.1007/BF03043229, 2004.

Lévy, M., Klein, P. and Treguier, A.-M.: Impact of sub-mesoscale physics on production and

subduction of phytoplankton in an oligotrophic regime, J. Mar. Res., doi:10.1357/002224001762842181, 2003.

Lewis, M. R., Horne, E. P. W., Cullen, J. J., Oakey, N. S. and Platt, T.: Turbulent motions may control phytoplankton photosynthesis in the upper ocean, Nature, doi:10.1038/311049a0, 1984.

Loder, J. W. and Platt, T.: Physical controls on phytoplankton production at tidal fronts, Proc. Ninet. Eur. Mar. Biol. Symp. Plymouth, Devon, U.K., 16 21 Sept. 1984.Gibbs, P.E.ed, (January 1985), 3–22, 1985.

Löder, M. G. J., Kraberg, A. C., Aberle, N., Peters, S. and Wiltshire, K. H.: Dinoflagellates and ciliates at Helgoland Roads, North Sea, Helgol. Mar. Res., 66(1), 11–23, doi:10.1007/s10152-010-0242-z, 2012.

Lough, R. G. and Aretxabaleta, A.: Transport and retention of vertically migrating adult mysid and decapod shrimp in the tidal front on Georges Bank, Mar. Ecol. Prog. Ser., 514(November 2014), 119–135, doi:10.3354/meps10977, 2014.

Mahadevan, A. and Archer, D.: Modeling the impact of fronts and mesoscale circulation on the nutrient supply and biogeochemistry of the upper ocean, J. Geophys. Res. Ocean., 105(C1), 1209–1225, doi:10.1029/1999jc900216, 2000.

Mann, K. H.: Physical influences on biological processes: How important are they?, South African J. Mar. Sci., 12(1), 107–121, doi:10.2989/02577619209504695, 1992.

Mann, K. H. and Lazier, J. R. N.: Dynamics of Marine Ecosystems: Biological-Physical Interactions in the Oceans: Third Edition., 2013.

Mathis, M.: Projected Forecast of Hydrodynamic Conditions in the North Sea for the 21st Century, University of Hamburg. [online] Available from: http://ediss.sub.uni-hamburg.de/volltexte/2013/6169/, 2013.

Mathis, M. and Pohlmann, T.: Projection of physical conditions in the north sea for the 21st century, Clim. Res., doi:10.3354/cr01232, 2014.

Mathis, M., Elizalde, A., Mikolajewicz, U. and Pohlmann, T.: Variability patterns of the general circulation and sea water temperature in the North Sea, Prog. Oceanogr., 135, 91–112, doi:10.1016/j.pocean.2015.04.009, 2015.

McCandliss, R. R., Jones, S. E., Hearn, M., Latter, R. and Jago, C. F.: Dynamics of suspended particles in coastal waters (southern North Sea) during a spring bloom, J. Sea Res., 47(3–4), 285–302, doi:10.1016/S1385-1101(02)00123-5, 2002.

McGillicuddy, D. J., Anderson, L. A., Bates, N. R., Bibby, T., Buesseler, K. O., Carlson, C. A., Davis, C. S., Ewart, C., Falkowski, P. G., Goldthwait, S. A., Hansell, D. A., Jenkins, W. J., Johnson, R., Kosnyrev, V. K., Ledwell, J. R., Li, Q. P., Siegel, D. A. and Steinberg, D. K.: Eddy/Wind interactions

stimulate extraordinary mid-ocean plankton blooms, Science (80-.)., doi:10.1126/science.1136256, 2007.

McKee, D., Röttgers, R., Neukermans, G., Calzado, V., Trees, C., Ampolo-Rella, M., Neil, C. and Cunningham, A.: Impact ofmeasurement uncertainties on determination of chlorophyll-specific absorption coefficient formarine phytoplankton David, , 119(12), 9013–9025, doi:10.1002/2014JC009909.Received, 2014.

McManus, M. A. and Woodson, C. B.: Plankton distribution and ocean dispersal, J. Exp. Biol., 215(6), 1008–1016, doi:10.1242/jeb.059014, 2012.

Mestres, M., Sierra, J. P. and Sánchez-Arcilla, A.: Modeled Dynamics of a Small-scale River Plume under Different Forcing Conditions, J. Coast. Res., doi:10.2112/1551-5036-47.sp1.84, 2007.

Meyer, E. M. I., Pohlmann, T. and Weisse, R.: Thermodynamic variability and change in the North Sea (1948-2007) derived from a multidecadal hindcast, J. Mar. Syst., doi:10.1016/j.jmarsys.2011.02.001, 2011.

Miller, P. I. and Christodoulou, S.: Frequent locations of oceanic fronts as an indicator of pelagic diversity: Application to marine protected areas and renewables, Mar. Policy, 45, 318–329, doi:10.1016/j.marpol.2013.09.009, 2014.

Mork, M.: Circulation Phenomena and Frontal Dynamics of the Norwegian Coastal Current, Philos. Trans. R. Soc. London. Ser. A, Math. Phys. Sci., doi:10.1098/rsta.1981.0188, 1981.

Munk, P. and Nielsen, T. G.: Trophodynamics of the plankton community at Dogger Bank: Predatory impact by larval fish, J. Plankton Res., doi:10.1093/plankt/16.9.1225, 1994.

Murphy, E. J., Watkins, J. L., Trathan, P. N., Reid, K., Meredith, M. P., Thorpe, S. E., Johnston, N. M., Clarke, A., Tarling, G. A., Collins, M. A., Forcada, J., Shreeve, R. S., Atkinson, A., Korb, R., Whitehouse, M. J., Ward, P., Rodhouse, P. G., Enderlein, P., Hirst, A. G., Martin, A. R., Hill, S. L., Staniland, I. J., Pond, D. W., Briggs, D. R., Cunningham, N. J. and Fleming, A. H.: Spatial and temporal operation of the Scotia Sea ecosystem: A review of large-scale links in a krill centred food web, Philos. Trans. R. Soc. B Biol. Sci., doi:10.1098/rstb.2006.1957, 2007.

Nelson, D. M. and Smith, W. 0.: Sverdrup revisited: Critical depths, maximum chlorophyll levels, and the control of Southern Ocean productivity by the irradiance-mixing regime, Limnol. Oceanogr., doi:10.4319/lo.1991.36.8.1650, 1991.

Nielsen, T. G., Lokkegaard, B., Richardson, K., Pedersen, F. B. and Hansen, L.: Structure of plankton communities in the Dogger Bank area (North Sea) during a stratified situation, Mar. Ecol. Prog. Ser., 95(1–2), 115–131, doi:10.3354/meps095115, 1993.

Nishihara, G. N. and Ackerman, J. D.: Diffusive boundary layers do not limit the photosynthesis of the aquatic macrophyte vallisneria americana at moderate flows and saturating light levels, Limnol.

Oceanogr., 54(6), 1874–1882, doi:10.4319/lo.2009.54.6.1874, 2009.

Nissen, C.: Physical-Biogeochemical Couplings in the Land-Ocean Transition Zone, The University of Bergen. [online] Available from: http://hdl.handle.net/1956/18682, 2014.

North, R. P., Riethmüller, R. and Baschek, B.: Estuarine , Coastal and Shelf Science Detecting small e scale horizontal gradients in the upper ocean using wavelet analysis, , 180, 221–229, doi:10.1016/j.ecss.2016.06.031, 2016.

O'Donnell, J.: Surface Fronts in Estuaries: A Review, Estuaries, 16(1), 12, doi:10.2307/1352761, 1993.

O'Donnell, J., Ackleson, S. G. and Levine, E. R.: On the spatial scales of a river plume, J. Geophys. Res. Ocean., 113(4), doi:10.1029/2007JC004440, 2008.

O'Driscoll, K., Mayer, B., Ilyina, T. and Pohlmann, T.: Modelling the cycling of persistent organic pollutants (POPs) in the North Sea system: Fluxes, loading, seasonality, trends, J. Mar. Syst., doi:10.1016/j.jmarsys.2012.09.011, 2013.

Oram, J. J., McWilliams, J. C. and Stolzenbach, K. D.: Gradient-based edge detection and feature classification of sea-surface images of the Southern California Bight, Remote Sens. Environ., 112(5), 2397–2415, doi:10.1016/j.rse.2007.11.010, 2008.

Ottersen, G., Planque, B., Belgrano, A., Post, E., Reid, P. C. and Stenseth, N. C.: Ecological effects of the North Atlantic Oscillation, Oecologia, doi:10.1007/s004420100655, 2001.

Otto, L., Zimmerman, J. T. F., Furnes, G. K., Mork, M., Saetre, R. and Becker, G.: Review of the physical oceanography of the North Sea, Netherlands J. Sea Res., 26(2–4), 161–238, doi:10.1016/0077-7579(90)90091-T, 1990.

Oziel, L., Sirven, J. and Gascard, J. C.: The Barents Sea frontal zones and water masses variability (1980-2011), Ocean Sci., 12(1), 169–184, doi:10.5194/os-12-169-2016, 2016.

Palmer, M. R., Polton, J. A., Inall, M. E., Rippeth, T. P., Green, J. A. M., Sharples, J. and Simpson, J. H.: Variable behavior in pycnocline mixing over shelf seas, Geophys. Res. Lett., 40(1), 161–166, doi:10.1029/2012GL054638, 2013.

Pätsch, J., Burchard, H., Dieterich, C., Gräwe, U., Gröger, M., Mathis, M., Kapitza, H., Bersch, M., Moll, A., Pohlmann, T., Su, J., Ho-Hagemann, H. T. M., Schulz, A., Elizalde, A. and Eden, C.: An evaluation of the North Sea circulation in global and regional models relevant for ecosystem simulations, Ocean Model., 116, 70–95, doi:10.1016/j.ocemod.2017.06.005, 2017.

Pedersen, F. B.: The Oceanographic and Biological Tidal Cycle Succession in Shallow Sea Fronts in the North Sea and the English Channel, Estuar. Coast. Shelf Sci., 38(3), 249–269, doi:10.1006/ecss.1994.1017, 1994.

Peng, D., Hill, E. M., Meltzner, A. J. and Switzer, A. D.: Tide Gauge Records Show That the 18.61-

Year Nodal Tidal Cycle Can Change High Water Levels by up to 30 cm, J. Geophys. Res. Ocean., doi:10.1029/2018JC014695, 2019.

Pietrzak, J. D., de Boer, G. J. and Eleveld, M. A.: Mechanisms controlling the intra-annual mesoscale variability of SST and SPM in the southern North Sea, Cont. Shelf Res., 31(6), 594–610, doi:10.1016/j.csr.2010.12.014, 2011.

Pingree, R. D., Pugh, P. R., Holligan, P. M. and Forster: Summer phytoplankton blooms and red tides along tidal fronts in the approaches to the English Channel, Nature, 258(5537), 672–677, doi:10.1038/258672a0, 1975.

Pingree, R. D., Holligan, P. M. and Mardell, G. T.: The effects of vertical stability on phytoplankton distributions in the summer on the northwest European Shelf, Deep. Res., 25(11), doi:10.1016/0146-6291(78)90584-2, 1978.

Pohlmann, T.: Calculating the development of the thermal vertical stratification in the North Sea with a three-dimensional baroclinic circulation model, Cont. Shelf Res., doi:10.1016/0278-4343(95)00018-V, 1996a.

Pohlmann, T.: Predicting the thermocline in a circulation model of the North Sea - Part I: Model description, calibration and verification, Cont. Shelf Res., 16(2), 131–146, doi:DOI: 10.1016/0278-4343(95)90885-S, 1996b.

Pohlmann, T.: A meso-scale model of the central and southern North Sea: Consequences of an improved resolution, Cont. Shelf Res., doi:10.1016/j.csr.2006.06.011, 2006.

Powell, T. M., Lewis, C. V. W., Curchitser, E. N., Haidvogel, D. B., Hermann, A. J. and Dobbins, E. L.: Results from a three-dimensional, nested biological-physical model of the California Current System and comparisons with statistics from satellite imagery, J. Geophys. Res. Ocean., 111(7), 1–14, doi:10.1029/2004JC002506, 2006.

Prairie, J. C., Sutherland, K. R., Nickols, K. J. and Kaltenberg, A. M.: Biophysical interactions in the plankton: A cross-scale review, Limnol. Oceanogr. Fluids Environ., 2(1), 121–145, doi:10.1215/21573689-1964713, 2012.

Richardson, K. and Pedersen, F. B.: Estimation of new production in the North Sea : consequences for temporal and spatial variability of phytoplankton, , 574–580, 1998.

Richardson, K., Visser, A. W. and Bo Pedersen, F.: Subsurface phytoplankton blooms fuel pelagic production in the North Sea, J. Plankton Res., 22(9), 1663–1671, doi:10.1093/plankt/22.9.1663, 2000.

Rokkan Iversen, K., Primicerio, R., Larsen, A., Egge, J. K., Peters, F., Guadayol, Ó., Jacobsen, A., Havskum, H. and Marrasé, C.: Effects of small-scale turbulence on lower trophic levels under different nutrient conditions, J. Plankton Res., doi:10.1093/plankt/fbp113, 2010.

Ross, O. N. and Sharples, J.: Phytoplankton motility and the competition for nutrients in the

thermocline, Mar. Ecol. Prog. Ser., doi:10.3354/meps06999, 2007.

Ruddick, K. G., Deleersnijder, E., Luyten, P. J. and Ozer, J.: Haline stratification in the Rhine-Meuse freshwater plume: a three-dimensional model sensitivity analysis, Cont. Shelf Res., doi:10.1016/0278-4343(95)00034-X, 1995.

Russell, R. W., Harrisone, N. M. and Jr, G. L. H.: avian planktivory in the northern Bering Sea, Mar. Ecol. Prog. Ser., 182, 77–93, doi:10.3354/meps182077, 1999.

Ryan, J. P., McManus, M. A. and Sullivan, J. M.: Interacting physical, chemical and biological forcing of phytoplankton thin-layer variability in Monterey Bay, California, Cont. Shelf Res., doi:10.1016/j.csr.2009.10.017, 2010a.

Ryan, J. P., Fischer, A. M., Kudela, R. M., McManus, M. A., Myers, J. S., Paduan, J. D., Ruhsam, C. M., Woodson, C. B. and Zhang, Y.: Recurrent frontal slicks of a coastal ocean upwelling shadow, J. Geophys. Res. Ocean., doi:10.1029/2010JC006398, 2010b.

Sabatés, A., Olivar, M. P., Salat, J., Palomera, I. and Alemany, F.: Physical and biological processes controlling the distribution of fish larvae in the NW Mediterranean, Prog. Oceanogr., doi:10.1016/j.pocean.2007.04.017, 2007.

Sager, G.: Gezeiten und Schiffahrt, Fachbuchverlag, Leipzig, 173 pp., 1959.

Sammartino, M., Marullo, S., Santoleri, R. and Scardi, M.: Modelling the Vertical Distribution of Phytoplankton Biomass in the Mediterranean Sea from Satellite Data: A Neural Network Approach, Remote Sens., 10(10), doi:10.3390/rs10101666, 2018.

Sauzède, R., Claustre, H., Jamet, C., Uitz, J., Ras, J., Mignot, A. and D'Ortenzio, F.: Retrieving the vertical distribution of chlorophyll a concentration and phytoplankton community composition from in situ fluorescence profiles: A method based on a neural network with potential for global-scale applications, J. Geophys. Res. Ocean., doi:10.1002/2014JC010355, 2015a.

Sauzède, R., Lavigne, H., Claustre, H., Uitz, J., Schmechtig, C., D'Ortenzio, F., Guinet, C. and Pesant, S.: Vertical distribution of chlorophyll a concentration and phytoplankton community composition from in situ fluorescence profiles: A first database for the global ocean, Earth Syst. Sci. Data, doi:10.5194/essd-7-261-2015, 2015b.

Schrum, C.: Thermohaline stratification and instabilities at tidal mixing fronts: Results of an eddy resolving model for the German Bight, Cont. Shelf Res., 17(6), 689–716, doi:10.1016/S0278-4343(96)00051-9, 1997.

Schrum, C. and Backhaus, J. O.: Sensivity of atmosphere-ocean heat exchange and heat content in the North Sea and the Baltic Sea, Tellus, 51A, 526–549, doi:10.1034/j.1600-0870.1992.00006.x, 1999.

Schrum, C., Siegismund, F. and John, M. S.: Decadal variations in the stratification and circulation patterns of the North Sea. Are the 1990s unusual?, ICES Mar. Sci. Symp., 219, 121–131, 2003.

Schrum, C., Alekseeva, I. and St. John, M.: Development of a coupled physical-biological ecosystem model ECOSMO. Part I: Model description and validation for the North Sea, J. Mar. Syst., doi:10.1016/j.jmarsys.2006.01.005, 2006a.

Schrum, C., St. John, M. and Alekseeva, I.: ECOSMO, a coupled ecosystem model of the North Sea and Baltic Sea: Part II. Spatial-seasonal characteristics in the North Sea as revealed by EOF analysis, J. Mar. Syst., 61(1–2), 100–113, doi:10.1016/j.jmarsys.2006.01.004, 2006b.

Schrum, C., Lowe, J., Meier, M., Grabeman, I., Holt, J., Mathis, M., Pohlmann, T., Skogen, M., Sterl, A. and Wakelin, S.: Projected Change - North Sea and interface regions, in North Climate Change Assessment, Springer., 2016.

Shimada, T., Sakaida, F., Kawamura, H. and Okumura, T.: Application of an edge detection method to satellite images for distinguishing sea surface temperature fronts near the Japanese coast, Remote Sens. Environ., 98(1), 21–34, doi:10.1016/j.rse.2005.05.018, 2005.

Siegismund, F.: Long-term changes in the flushing times of the ICES-boxes, Senckenbergiana maritima, 31(2), 151–167, doi:10.1007/BF03043025, 2001.

Simpson, J. H. and Hunter, J. R.: Fronts in the Irish Sea, Nature, 250(5465), 404–406, doi:10.1038/250404a0, 1974.

Simpson, J. H. and Rippeth, T. P.: The Clyde Sea: a Model of the Seasonal Cycle of Stratification and Mixing, Estuar. Coast. Shelf Sci., doi:http://dx.doi.org/10.1006/ecss.1993.1047, 1993.

Simpson, J. H. and Souza, A. J.: Semidiurnal switching of stratification in the region of freshwater influence of the Rhine, J. Geophys. Res., doi:10.1029/95JC00067, 1995.

Simpson, J. H. J. and Sharples, J.: Introduction to the Physical and Biological Oceanography of Shelf Seas, Cambridge University Press., 2012.

Skogen, M. D., Svendsen, E., Berntsen, J., Aksnes, D. and Ulvestad, K. B.: Modelling the primary production in the North Sea using a coupled three-dimensional physical-chemical-biological ocean model, Estuar. Coast. Shelf Sci., doi:10.1016/0272-7714(95)90026-8, 1995.

Skogen, M. D., Drinkwater, K., Hjøllo, S. S. and Schrum, C.: North Sea sensitivity to atmospheric forcing, J. Mar. Syst., 85(3–4), 106–114, doi:10.1016/j.jmarsys.2010.12.008, 2011.

Smayda, T. J.: Turbulence, watermass stratification and harmful algal blooms: An alternative view and frontal zones as “pelagic seed banks,” Harmful Algae, doi:10.1016/S1568-9883(02)00010-0, 2002.

Stanev, E. V., Badewien, T., Freund, H., Grayek, S., Hahner, F., Meyerjürgens, J., Ricker, M., Schöneich-Argent, R. I., Wolff, J. O. and Zielinski, O.: Extreme westward surface drift in the North Sea: Public reports of stranded drifters and Lagrangian tracking, Cont. Shelf Res., doi:10.1016/j.csr.2019.03.003, 2019.

Stramska, M., Dickey, T. D., Plueddemann, A., Weller, R., Langdon, C. and Marra, J.: Bio-optical

variability associated with phytoplankton dynamics in the North Atlantic Ocean during spring and summer of 1991, J. Geophys. Res., doi:10.1029/94JC01447, 1995.

Suberg, L. A.: Investigations of the varibility of tidal mixing fronts and their importance for shelf-sea ecosystems across multiple trophic levels, University of Southampton., 2015.

Sukhanova, I. N., Flint, M. V., Pautova, L. A., Stockwell, D. A., Grebmeier, J. M. and Sergeeva, V. M.: Phytoplankton of the western Arctic in the spring and summer of 2002: Structure and seasonal changes, Deep. Res. Part II Top. Stud. Oceanogr., doi:10.1016/j.dsr2.2008.12.030, 2009.

Sullivan, J. M., Donaghay, P. L. and Rines, J. E. B.: Coastal thin layer dynamics: Consequences to biology and optics, Cont. Shelf Res., doi:10.1016/j.csr.2009.07.009, 2010.

Sündermann, J.: The changing North Sea: Knowledge, speculation and new challenges, Oceanologia, 2003.

Sündermann, J. and Pohlmann, T.: A brief analysis of North Sea physics, Oceanologia, 53(3), 663–689, doi:10.5697/oc.53-3.663, 2011.

Svendsen, E., Słtre, R. and Mork, M.: Features of the northern North Sea circulation, Cont. Shelf Res., 11(5), 493–508, doi:10.1016/0278-4343(91)90055-B, 1991.

Sverdrup, H. U.: On Conditions for the Vernal Blooming of Phytoplankton, ICES J. Mar. Sci., doi:10.1093/icesjms/18.3.287, 1953.

Taylor, G. I.: Tidal oscillations in gulfs and rectangular basins, Proc. London Math. Soc., s2-20(1), 148–181, doi:10.1112/plms/s2-20.1.148, 1922.

Taylor, J. R. and Ferrari, R.: Ocean fronts trigger high latitude phytoplankton blooms, Geophys. Res. Lett., 38(23), 1–5, doi:10.1029/2011GL049312, 2011.

Tett, P. and Walne, A.: Observations and simulations of hydrography, nutrients and plankton in the southern north sea, Ophelia, 42(1), 371–416, doi:10.1080/00785326.1995.10431514, 1995.

Tett P, W. A.: Observations and simulations of hydrography, nutrients and plankton in the southern north sea, Ophelia, 42(issue 1), 371–416 [online] Available from: http://dx.doi.org/10.1080/00785326.1995.10431514, 1995.

Thessen, A.: Adoption of Machine Learning Techniques in Ecology and Earth Science, One Ecosyst., doi:10.3897/oneeco.1.e8621, 2016.

Tiedemann, M. and Brehmer, P.: Larval fish assemblages across an upwelling front: Indication for active and passive retention, Estuar. Coast. Shelf Sci., doi:10.1016/j.ecss.2016.12.015, 2017.

Tilstone, G. H., Miller, P. I., Brewin, R. J. W. and Priede, I. G.: Enhancement of primary production in the North Atlantic outside of the spring bloom, identified by remote sensing of ocean colour and temperature, Remote Sens. Environ., doi:10.1016/j.rse.2013.04.021, 2014.

Turner, B. L., Matson, P. A., McCarthy, J. J., Corell, R. W., Christensen, L., Eckley, N., Hovelsrud-Broda, G. K., Kasperson, J. X., Kasperson, R. E., Luers, A., Martello, M. L., Mathiesen, S., Naylor, R., Polsky, C., Pulsipher, A., Schiller, A., Selin, H. and Tyler, N.: Illustrating the coupled human–environment system for vulnerability analysis: Three case studies, Proc. Natl. Acad. Sci., doi:10.1073/pnas.1231334100, 2003.

Turrell, W. R., Henderson, E. W., Slesser, G., Payne, R. and Adams, R. D.: Seasonal changes in the circulation of the northern North Sea, Cont. Shelf Res., doi:10.1016/0278-4343(92)90032-F, 1992.

Uitz, J., Claustre, H., Morel, A. and Hooker, S. B.: Vertical distribution of phytoplankton communities in open ocean: An assessment based on surface chlorophyll, J. Geophys. Res. Ocean., doi:10.1029/2005JC003207, 2006.

Ullman, D. S. and Cornillon, P. C.: Evaluation of Front Detection Methods for Satellite-Derived SST Data Using In Situ Observations, J. Atmos. Ocean. Technol., 17(12), 1667–1675, doi:10.1175/1520-0426(2000)017<1667:EOFDMF>2.0.CO;2, 2000.

Vermaat, J. E., McQuatters-Gollop, A., Eleveld, M. A. and Gilbert, A. J.: Past, present and future nutrient loads of the North Sea: Causes and consequences, Estuar. Coast. Shelf Sci., doi:10.1016/j.ecss.2008.07.005, 2008.

Weinert, M., Mathis, M., Kröncke, I., Neumann, H., Pohlmann, T. and Reiss, H.: Modelling climate change effects on benthos: Distributional shifts in the North Sea from 2001 to 2099, Estuar. Coast. Shelf Sci., doi:10.1016/j.ecss.2016.03.024, 2016.

Weston, K., Fernand, L., Mills, D. K., Delahunty, R. and Brown, J.: Primary production in the deep chlorophyll maximum of the central North Sea, J. Plankt. Res., 2005.

Wiltshire, K. H. and Manly, B. F. J.: The warming trend at Helgoland Roads, North Sea: Phytoplankton response, Helgol. Mar. Res., 58(4), 269–273, doi:10.1007/s10152-004-0196-0, 2004.

Woodson, C. B. and Litvin, S. Y.: Ocean fronts drive marine fishery production and biogeochemical cycling, Proc. Natl. Acad. Sci., doi:10.1073/pnas.1417143112, 2015.

Yoder, J. A., Schollaert, S. E. and O'Reilly, J. E.: Climatological phytoplankton chlorophyll and sea surface temperature patterns in continental shelf and slope waters off the northeast U.S. coast, Limnol. Oceanogr., doi:10.4319/lo.2002.47.3.0672, 2002.

Zhao, C., Maerz, J., Hofmeister, R., Röttgers, R., Riethmüller, R., Wirtz, K. and Schrum, C.: Characterizing the vertical distribution of chlorophyll a in the German Bight, Cont. Shelf Res., 175, 127–146, doi:10.1016/j.csr.2019.01.012, 2019a.

Zhao, C., Daewel, U. and Schrum, C.: Tidal impacts on primary production in the North Sea, Earth Syst. Dyn., 10(2), 287–317, doi:10.5194/esd-2018-74, 2019b.

Zheng, G. and DiGiacomo, P. M.: Uncertainties and applications of satellite-derived coastal water

quality products, Prog. Oceanogr., 159(September), 45–72, doi:10.1016/j.pocean.2017.08.007, 2017.

Zhu, W., Yu, Q. and Tian, Y. Q.: Uncertainty analysis of remote sensing of colored dissolved organic matter: Evaluations and comparisons for three rivers in North America, ISPRS J. Photogramm. Remote Sens., 84, 12–22, doi:10.1016/j.isprsjprs.2013.07.005, 2013.

Chapter 6. Conclusion and perspectives

6.1 Major conclusion

Variations in primary production of the North Sea are dominantly structured by the hydrodynamics. Particularly, in the North Sea, hydrodynamic factors regulating the phytoplankton environment by control the distribution of phytoplankton growth factors, such as nutrient supply, under-water light availability and the distribution of standing stocks of plankton cells.

The goal of this study was to understand and quantify the role of the dominant hydrodynamic features in the area, namely seasonal stratification, mixing by tides and optimal growth conditions provided by frontal systems, mainly for vertical variation in primary production on different temporal scales. 3D physical-biogeochemical numerical simulation, ship-based *in situ* sampling of vertical transects and remote sensing datasets were combined for this study.

The study consists of 3 main subtopics: i) the study of the vertical distribution of Chlorophyll a (CHL) in the German Bight, ii) the quantification of the impacts of tides on primary production on basin scales in the North Sea, iii) the study of frontal dynamics in the North Sea and related NPP (net primary production) structures in frontal areas. In the following paragraphs, the major results from these studies are discussed in the overall context of the thesis and conclusions were drawn, followed by an outlook.

Based on variability of duration times of mixing-stratification patterns, Van Leeuwen et al. (2015), provided a delineation of the general North Sea regimes, such as permanently stratified regime (Norwegian Trench), permanently mixed area and intermittently stratified area (mainly in the English Channel and along coasts in the southern North Sea), ROFI (region of fresh water influence, mainly along the Dutch and Danish coastal line) The most central part of the northern North Sea was classified into the seasonal stratified regions, where regular and stable stratification in summer provides hydrodynamic environments for recurrent and persistent subsurface CHL maximum layers (SCML) (Nielsen et al., 1993; Richardson and Pedersen, 1998). Apart from this regular occurrence, the SCML was suggested to contribute significantly to the primary production in summer (Fernand et al., 2013), particularly if the SCMLs are adjacent to frontal areas (e.g. Dogger Bank) where injection of nutrients elevated the NPP.

Unlike the northern North Sea, large portion of the southern North Sea could not be classified into specific regions (Van Leeuwen et al., 2015), due to substantial inter-annual variability. These ‘un-classified’ areas mainly locate in the German Bight, and in addition the eastern edge of the Dogger Bank, the boundary of the

Norwegian Trench and a narrow belt along the Scottish coast. All of these areas contain frontal systems in the North Sea, which were further investigated in **manuscript 3**. For the German Bight, seasonal stratification has already been confirmed by numerical simulation (Pohlmann, 1996a) and observations (Haren and Howarth, 2004), with substantial variability in duration and extension of the stratified season. However, while the horizontal distribution of primary productivity has already been addressed in several studies (e.g. Daewel and Schrum, 2017; Kerimoglu et al., 2017), the vertical distribution of CHL has seldom been addressed given water depths are less than 40 m, and tidal & wind-driven mixing were thought to homogenize the vertical CHL distribution. Most available samplings in this area are confined to the surface (e.g. Hickel et al., 1993). Making use of vertical transects sampled in the German Bight (Baschek et al., 2017), **manuscript 1** aimed at filling the knowledge gap and provided first quantitative description on CHL vertical distribution in the GB. The statistical results resolved the seasonality of CHL vertical distribution, which can be associated with seasonal variations of potential driving mechanisms, such as stratification-mixing status, biogeochemical cycling and resuspension.

Even though in such a shallow and energetic system as the German Bight, heterogeneous vertical distribution of CHL is smoothed to a large extent (68.7%), during the stratified season, the CHL does not distribute evenly in the water column. With 3.2% occurrence of SCML and 16.6% of profiles with highest CHL in the lower part of the water column (HCL). Apart from the three CHL distribution patterns mentioned above, 11.5% of all profiles show that high CHL locates in the upper water column. This occurs mainly during early spring and late autumn, when the nutrient limitation is not severe due to weak stratification and phytoplankton cells have a better accessibility to sufficient light irradiance in the upper layer. This result questioned the representativeness of surface sampling (such as Hegoland Time series, Hickel et al., 1993), particularly when stratification sets on or under low vertical turbulent conditions.

The SCML was found to develop under strong stratified conditions (squared buoyance frequency N_2 higher than 0.02 s^{-2}). The location of SCMLs' vertical center coincides with oxygen saturation maxima and the pycnocline but stays within the euphotic layer, which suggested that the biomass in the SCML or even HCL were photosynthetically active by itself. Indicated by the observation datasets in **manuscript 1**, the SCML is short-lived in the GB since the stratification is susceptible to mixing events driven by wind and tide. The unstable characteristics and limited observation data further hinder the exploration of duration time, spatial extension and contribution of the SCML to NPP. To further generalize the SCML phenomenon, evaluate its contribution to NPP, and make comparison between basin scales, utilizing numerical simulation is indispensable, which actually was done in **manuscript 2**. Based on simulation results in

manuscript 2, in the area southeast of Dogger Bank, the averaged survival time of subsurface biomass maximum (SBM) (CHL was not simulated in ECOSMO) is on average no more than 60 days annually, which is substantially shorter than SBMs located in the northern North Sea. That is also why the SBM in the northern North Sea is confirmed as a seasonally re-occurring phenomenon (Fernand et al., 2013) whereas the SBM in the southern North Sea has been rarely addressed. The amount of NPP, which was contributed by SBM to the overall NPP in the deeper part to of GB is about $15 gCm^{-2}y^{-1}$, which accounts for one sixth of the overall NPP and thus contributes a substantial part to the total NPP for one year and thus merits further attention.
The resuspension signal, which further complicates the CHL vertical distribution, is closely correlated with tidal signal as identified in **manuscript 1** and other studies (e.g. Jago et al., 2002). Furthermore, by analyzing vertical transects observed prior to and after a wind event (07/2010), the stability of stratification (also SCML structure surviving within the pycnocline) is in line with results deducted from the Simpson Hunter parameter (Simpson and Hunter, 1974), which considers the counteracting stratifying and mixing processes such as solar heating and tidal stirring. Considering the dominating role played by the tides in regulating the stability of stratification and distribution of ecological components in this system, tidal impacts on primary production were explored in **manuscript 2** by comparing NPP in different scenarios with varied tidal constituents.

In the whole North Sea domain, the average annual NPP was elevated by tides by 3 % compared to the scenario without tidal forcing. Even though this does not seem a lot, the local impacts are much larger. The results emphasize a significant spatial variability caused by different hydrodynamic processes, with major NPP increase in frontal areas (90%) and substantial decrease in the English channel of about 30%. In the English Channel and the coastal areas of the southern North Sea, where vertical mixing persists throughout the whole year, light availability is the major limiting factor. The enhanced tidal resuspension and mixing of suspended matter into the surface layers deteriorates light conditions in the upper layers for phytoplankton growth and thus hinders NPP. In contrast, in frontal areas and seasonally stratified areas in the SNS where stratification is susceptible to tidal mixing, nutrient replenishment due to tidal forcing sustains NPP in summer and thus generates a significant increase in NPP. In the NNS, which is characterized by relatively weak tidal forcing and deep bathymetry, the bottom and upper mixed layers are well separated, and the influence of tidal forcing on NPP is comparably small. The underling mechanisms for elevated NPP in frontal areas were then further explored in **manuscript 3**.

In **manuscript 2**, we also have done subdomain division mainly based on NPP's response to tidal forcing. Most of the 'un-classified' areas in van Leeuwen et al.'s study (2015) were identified within the positively responding areas in the southern

North Sea. Furthermore, the positively responding areas also include Dogger Bank, areas south to the Flamborough Head, which were identified as mixed or intermittently stratified areas in Van Leeuwen et al.'s study (2015). Areas along the coastal line which were mainly recognized as permanently mixed, ROFI and intermittently stratified area in Van Leeuwen et al.'s study (2015), were recognized as negatively responding area with respect to tidal forcing in **manuscript 2**. The distinct characteristics among those adjacent areas initiated an exploration of relevant processes in **manuscript 3**, which further emphasize the spatial variability and the strong linkage between physical and biogeochemical properties. The frontal area is the narrow belt which separates water mass with distinct characteristics. Areas with substantially elevated NPP coincide with 'un-classified' area in van Leeuwen et al.'s study (2015).

In **manuscript 3**, Hovmöller diagrams were built along representative transects across several characteristic frontal regions. At the Scottish coast fronts and areas around the Dogger Bank, diffusive flux of NO3 supports the NPP and thus sustaining the highly productive area. In the south-eastern part, mixing-stratification status is susceptible to shifting due to wind driven advection and mixing, river-runoff and tides. High productive events were often triggered by moving fronts. It is either because of pumping up nutrients in previously stratified areas or increase of biomass in previously mixed areas when stratification or reduced vertical turbulence occurs, which expose the biomass to more favorable light conditions. The regionally systematic difference is not only because of varied dominating limiting factor as revealed in **manuscript 2** (nutrients liming vs. light limiting), but also associated with stability of fronts.

Stability, indicated by the local occurrence of fronts in each grid cells, were derived statistically based on frontal detection for each daily output in **manuscript 3.** Furthermore, NPP within frontal areas was also quantified, which made investigations on the frontal NPP's temporal evolution possible. The area occupied by easy-shifting fronts coincides with the wide extension band of the 'un-classified' area in the in van Leeuwen et al.'s study (2015), particularly in the eastern part of the North Sea. For the inter-annual variability, the frontal NPP also showed similar fluctuations and decreasing trends since 2000, which was confirmed by estimation from observed data (Capuzzo et al., 2018). Apparently, the eastern part of the North Sea, where variability was highlighted, was suggested sharing large proportion of the decline of NPP in recent decades (Capuzzo et al., 2018).

6.2 Perspectives

Our analysis of **manuscript 1** provided the first quantitative description on heterogeneity and homogeneity of vertical CHL distribution in the GB. The results in **manuscript 1** question the representativeness of remote sensing and surface sampling for the overall productivity of the system. Even when sampled in the areas around Helgoland Road, subsurface CHL maximum layers have been observed under strongly stratified conditions. In this case, our study points towards the need to develop new approaches to conclude on systematic productivity by combining several observational datasets and modeling approaches. SCM in those regions may provide a reasonable source of error for remote sensing based estimates; for the application of ship-based vertical fluorescence profile, the disadvantage is lower spatial-temporal coverage and lack of simultaneous HPLC (high-performance liquid chromatography) data for validation, which all together hinder the complete description and understanding of CHL variability on a larger scale (Sauzède et al., 2015b). This study can serve as a first step to quantify the general pattern of fluorescence vertical profiles and associate these patterns with physical-biological processes. Providing better understanding and categorizing of CHL vertical profiles, attempts of cross estimation among different observed data source (i.e. different indexes of phytoplankton characteristics , such as vertical fluorescence, surface CHL value from remote sensing, vertical distribution of phytoplankton biomass in $mgC\ m^{-3}$, information of species composition) using neural networks or machine-learning technics are ongoing (Sammartino et al., 2018; Sauzède et al., 2015a; Thessen, 2016; Uitz et al., 2006). The categories of CHL profiles in this study might serve as one of those co-predictors for CHL concentration in remote sensing and column-integrated production in the future.

As suggested in **manuscript 1**, simultaneous collection of physical and biogeochemical data is necessary to give further interpretation of CHL vertical distributions. The quantification of CHL vertical distribution in our study could be combined with horizontal alignability between temperature and CHL (North et al., 2016). Given that more observation data are available covering different weather conditions instead of calm weather conditions only, it is possible to extrapolate our conclusion to the full range of weather conditions and give conclusions that are more representative in the GB. Pursuing further implementation of CHL vertical distributions biologically requires species differentiating sampling, instead of speculations on the basis of fluorometer measurements (Sauzède et al., 2015a, 2015b). With more information about organic matter and phytoplankton species, better answers can be obtained to questions regarding the quantification of sinking remains of phytoplankton cells in the SCM (Sukhanova et al., 2009), active photosynthesis and new production within the SCM (Palmer et al., 2013).

Summarized phenomena from observations point to some structural limitations and development of new approaches in modeling tools. In case more observed data and robust modelling tools are become available in the GB, the highlighted phenomena in this study, such as SCM and HCL, will be more sufficiently discussed. However, the prerequisite is that the related mechanisms are well–represented. As highlighted in our analysis, the phenomenon with high CHL in the lower layer is frequently observed in late spring. The mechanism responsible for this phenomenon is still poorly understood. When water masses with high CHL (probably with floating *phaeosystis*) below the pycnoline were overlaid by a water masses with low CHL above the pycnocline, the HCL could be detected. It has been observed at the Netherland's coast (McCandliss et al., 2002) and in areas near the Rhine plume (personal communication with Rüdiger Röttgers, Helmholtz-Zentrum Geesthacht, Germany), and is mainly supposed to be associated with plume circulation. However, we have observed HCL in the most western branch of the sampling transects, which locates at the Oyster Grounds and beyond the influence of river runoff. The 3D biogeochemical-physical model used here is not able to resolve HCL phenomenon properly, even if sinking of diatoms and resuspension have already been considered (Fernand, 2013; Kerimoglu, 2017). The underlying reason may be some miss-representativeness of benthic-pelagic coupling and physiological adaptation, as pointed out in **manuscript 1**.

In **manuscript 2**, the two major tidal constituents (M_2, S_2) were considered. Similar experiments should be conducted by considering other tidal constituents, such as nodal cycle of 18.61 years' period (Peng et al., 2019) and lunar cycle of 8.85 years' period (Haigh et al., 2011). Using models with higher trophic levels, contributions of tide on migration behaviors can be further evaluated (Hufnagl et al., 2014).

Suggested by **manuscript 3**, substantial decadal variability of frontal NPP merits further investigations. Increase of sea surface temperature and particularly changes of the inflow from the North Atlantic (Gröger et al., 2013) are suggested to be major drivers of variability in hydrodynamics and ecosystem in the North Sea in the coming decades (Huthnance et al., 2016).

As a semi-enclosed system, the North Sea is susceptible to changes in the inflow driven by large scale atmospheric variability (Edwards et al., 2002; Ottersen et al., 2001; Tilstone et al., 2014). There has been documented inflow anomalous events in late 1980s and early 1990s (Turrell et al., 1992), which affected all trophic levels from phytoplankton to fish (Corten, 1990). For the future, stronger northern inflow and decreasing inflow through Dover Strait in summer were predicted (Mathis, 2013; Mathis and Pohlmann, 2014), which will modify the water mass characteristics and vary the frontal NPP in **manuscript 3**. Even though

the contributions from temperature increase leading to increases and decreases in NPP tend to cancel out when the NPP was averaged over the entire North Sea (Skogen et al., 2011), distinct response patterns are expected because different dominating processes underlying.

Increased temperature (Meyer et al., 2011) results in earlier onset and later breakdown of stratification (Holt et al., 2010), which is particularly important for the Northwest European Shelf and near the shelf break (Holt et al., 2012, 2014). In the northern North Sea, where NPP is more sensitive to the oceanic input, the reduced cross-pycnocline nutrient flux will lead to decrease of NPP but to some extend offset by pro-longed stratification time and elevated growth rate due to higher temperature (Holt et al., 2012). In the southern North Sea, changes in stratification is not consequential and the increase of NPP mainly results from increased growth rate, faster remineralization and related changes in the benthic-pelagic coupling (Skogen et al., 2011). When considering complete climate scenarios, NPP's change in the southern North Sea is more related to changes in wind and thermal forcing (Holt et al., 2014). At the nearshore coast, the trophic levels' response is also sensitive to increased temperature. Warmer water body lead to a longer persistence of grazing in autumn and early winter and depressed the over-winter phytoplankton biomass, resulting in a delay of the spring bloom (Wiltshire and Manly, 2004).

Considering the importance of oceanic flux's variations on future scenarios (Sündermann, 2003), it is necessary to have reasonable coverage of regional models if climate change's impacts on ecosystem is the North Sea is planned to be addressed. With proper parametrization of benthic systems, it is possible to resolve the propagation of increased temperature in the benthic-pelagic systems, covering several trophic levels, which is more important in shallower areas (Holt et al., 2012). Improvements in these two aspects will reduce the uncertainty in addressing frontal NPP's response to future climate change.

Overall, the study highlights the importance of biogeochemical-physical coupling processes in the North Sea, particularly in the southern part. Aiming at better understanding of this system, sufficient integration of simulation and observed datasets is indispensable, especially for areas with significant temporal variability, such as the German Bight. As pointed out by this study, tidal forcing and frontal systems play pivotally important role in ecosystems. Thoroughly representativeness of characteristics of frontal system is necessary in future development of models.

Reference of the thesis

Here are references which do not belong to individual chapters. In another words, references mentioned in chapter 1,2,6 are listed out below.

Backhaus, J. o.: The North Sea and the climate, Dana, 8, 69–82, 1989.

Barton, A. D., Ward, B. A., Williams, R. G. and Follows, M. J.: The impact of fine-scale turbulence on phytoplankton community structure, Limnol. Oceanogr. Fluids Environ., 4(1), 34–49, doi:10.1215/21573689-2651533, 2014.

Baschek, B., Schroeder, F., Brix, H., Riethmüller, R., Badewien, T. H., Breitbach, G., Brügge, B., Colijn, F., Doerffer, R., Eschenbach, C., Friedrich, J., Fischer, P., Garthe, S., Horstmann, J., Krasemann, H., Metfies, K., Merckelbach, L., Ohle, N., Petersen, W., Pröfrock, D., Röttgers, R., Schlüter, M., Schulz, J., Schulz-Stellenfleth, J., Stanev, E., Staneva, J., Winter, C., Wirtz, K., Wollschläger, J., Zielinski, O. and Ziemer, F.: The Coastal Observing System for Northern and Arctic Seas (COSYNA), Ocean Sci., doi:10.5194/os-13-379-2017, 2017.

Belkin, I. M., Cornillon, P. C. and Sherman, K.: Fronts in Large Marine Ecosystems, Prog. Oceanogr., 81(1–4), 223–236, doi:10.1016/j.pocean.2009.04.015, 2009.

Berger,W. H., Smetacek, V. S. and Wefer, G.: Productivity of the Ocean. Present and Past, New yourk., 1989.

Van Beusekom, J., Diel-Christiansen, A.: Synthesis of phyto- and zooplankton dynamics in the North Sea environment 148 pp, Godalming., 1994.

Brickman, D. and Loder, J. W.: Energetics of the internal tide on northern Georges Bank, J. Phys. Oceanogr., doi:10.1175/1520-0485(1993)023<0409:EOTITO>2.0.CO;2, 1993.

Brockmann, U. H., Laane, R. W. P. M. and Postma, H.: Cycling of nutrient elements in the North Sea, Netherlands J. Sea Res., 26(2–4), 239–264, doi:https://doi.org/10.1016/0077-7579(90)90092-U, 1990.

Brown, T.: Kelvin wave reflection at an oscillating boundary with applications to the North Sea, Cont. Shelf Res., 7(4), 351–365, doi:10.1016/0278-4343(87)90105-1, 1987.

Cadier, M., Gorgues, T., Sourisseau, M., Edwards, C. A., Aumont, O., Marié, L. and Memery, L.: Assessing spatial and temporal variability of phytoplankton communities' composition in the Iroise Sea ecosystem (Brittany, France): A 3D modeling approach. Part 1: Biophysical control over plankton functional types succession and distribution, J. Mar. Syst., 165, 47–68, doi:https://doi.org/10.1016/j.jmarsys.2016.09.009, 2017.

Capet, A., Beckers, J. M. and Grégoire, M.: Drivers, mechanisms and long-term variability of seasonal hypoxia on the Black Sea northwestern shelf - Is there any recovery after eutrophication?, Biogeosciences, doi:10.5194/bg-10-3943-2013, 2013.

Capuzzo, E., Lynam, C. P., Barry, J., Stephens, D., Forster, R. M., Greenwood, N., McQuatters-Gollop, A., Silva, T., van Leeuwen, S. M. and Engelhard, G. H.: A decline in primary production in the North Sea over 25 years, associated with reductions in zooplankton abundance and fish stock recruitment, Glob. Chang. Biol., 24(1), e352–e364, doi:10.1111/gcb.13916, 2018.

Castelao, R. M., Barth, J. A. and Mavor, T. P.: Flow-topography interactions in the northern California Current System observed from geostationary satellite data, Geophys. Res. Lett., 32(24), 1–4, doi:10.1029/2005GL024401, 2005.

Charnock, H., Dyer, K. R., Huthnance, J., LISS, P. and Simpson, B. H.: Understanding the North Sea System, 1st ed., Chapmann & Hall for the Royal Society, London., 1994.

Chen, C., Beardsley, R. C. and Limeburner, R.: A Numerical Study of Stratified Tidal Rectification over Finite-Amplitude Banks. Part II: Georges Bank, J. Phys. Oceanogr., 25(9), 2111–2128,

doi:10.1175/1520-0485(1995)025<2111:ANSOST>2.0.CO;2, 1995.

Cinner, J. E., McClanahan, T. R., Graham, N. A. J., Daw, T. M., Maina, J., Stead, S. M., Wamukota, A., Brown, K. and Bodin, O.: Vulnerability of coastal communities to key impacts of climate change on coral reef fisheries, Glob. Environ. Chang., doi:10.1016/j.gloenvcha.2011.09.018, 2012.

Corten, A.: Long-term trends in pelagic fish stocks of the North Sea and adjacent waters and their possible connection to hydrographic changes, Netherlands J. Sea Res., doi:10.1016/0077-7579(90)90024-B, 1990.

Cullen, J. J.: Subsurface Chlorophyll Maximum Layers: Enduring Enigma or Mystery Solved?, Ann. Rev. Mar. Sci., doi:10.1146/annurev-marine-010213-135111, 2015.

Daewel, U. and Schrum, C.: Low-frequency variability in North Sea and Baltic Sea identified through simulations with the 3-D coupled physical-biogeochemical model ECOSMO, Earth Syst. Dyn., 8(3), 801–815, doi:10.5194/esd-8-801-2017, 2017.

Dauwe, B., Herman, P. M. J. and Heip, C. H. R.: Community structure and bioturbation potential of macrofauna at four North Sea stations with contrasting food supply, Mar. Ecol. Prog. Ser., 173(1978), 67–83, doi:10.3354/meps173067, 1998.

Edwards, M., Beaugrand, G., Reid, P. C., Rowden, A. A. and Jones, M. B.: Ocean climate anomalies and the ecology of the North Sea, Mar. Ecol. Prog. Ser., 239(August), 1–10, doi:10.3354/meps239001, 2002.

Emeis, K. C., van Beusekom, J., Callies, U., Ebinghaus, R., Kannen, A., Kraus, G., Kröncke, I., Lenhart, H., Lorkowski, I., Matthias, V., Möllmann, C., Pätsch, J., Scharfe, M., Thomas, H., Weisse, R. and Zorita, E.: The North Sea - A shelf sea in the Anthropocene, J. Mar. Syst., doi:10.1016/j.jmarsys.2014.03.012, 2015.

Fernand, L., Weston, K., Morris, T., Greenwood, N., Brown, J. and Jickells, T.: The contribution of the deep chlorophyll maximum to primary production in a seasonally stratified shelf sea, the North Sea, Biogeochemistry, 113(1–3), 153–166, doi:10.1007/s10533-013-9831-7, 2013.

Le Fèvre, J.: Aspects of the Biology of Frontal Systems, Adv. Mar. Biol., doi:10.1016/S0065-2881(08)60109-1, 1987.

Fisher, J. A., Casini, M., Frank, K. T., Möllmann, C., Leggett, W. C. and Daskalov, G.: The importance of within-system spatial variation in drivers of Marine Ecosystem regime shifts, Philos. Trans. R. Soc. B Biol. Sci., doi:10.1098/rstb.2013.0271, 2015.

Floeter, J., van Beusekom, J. E. E., Auch, D., Callies, U., Carpenter, J., Dudeck, T., Eberle, S., Eckhardt, A., Gloe, D., Hänselmann, K., Hufnagl, M., Janßen, S., Lenhart, H., Möller, K. O., North, R. P., Pohlmann, T., Riethmüller, R., Schulz, S., Spreizenbarth, S., Temming, A., Walter, B., Zielinski, O. and Möllmann, C.: Pelagic effects of offshore wind farm foundations in the stratified North Sea, Prog. Oceanogr., doi:10.1016/j.pocean.2017.07.003, 2017.

Franks, P. J. S.: Phytoplankton blooms at fronts: patterns, scales, and physical forcing mechanisms, Rev. Aquat. Sci., 1992.

Glibert, P. M., Icarus Allen, J., Artioli, Y., Beusen, A., Bouwman, L., Harle, J., Holmes, R. and Holt, J.: Vulnerability of coastal ecosystems to changes in harmful algal bloom distribution in response to climate change: Projections based on model analysis, Glob. Chang. Biol., doi:10.1111/gcb.12662, 2014.

Green, A. L., Fernandes, L., Almany, G., Abesamis, R., McLeod, E., Aliño, P. M., White, A. T., Salm, R., Tanzer, J. and Pressey, R. L.: Designing Marine Reserves for Fisheries Management, Biodiversity Conservation, and Climate Change Adaptation, Coast. Manag., doi:10.1080/08920753.2014.877763, 2014.

Gröger, M., Maier-Reimer, E., Mikolajewicz, U., Moll, A. and Sein, D.: NW European shelf under climate warming: Implications for open ocean - Shelf exchange, primary production, and carbon absorption, Biogeosciences, doi:10.5194/bg-10-3767-2013, 2013.

Haigh, I. D., Eliot, M. and Pattiaratchi, C.: Global influences of the 18.61 year nodal cycle and 8.85

year cycle of lunar perigee on high tidal levels, J. Geophys. Res. Ocean., doi:10.1029/2010JC006645, 2011.

Halpern, B. S., Selkoe, K. A., Micheli, F. and Kappel, C. V.: Evaluating and ranking the vulnerability of global marine ecosystems to anthropogenic threats, Conserv. Biol., doi:10.1111/j.1523-1739.2007.00752.x, 2007.

Haren, H. Van and Howarth, M. J.: Enhanced stability during reduction of stratification in the North Sea, , 24, 805–819, doi:10.1016/j.csr.2004.01.008, 2004.

Hartman, S. E., Humphreys, M. P., Kivimäe, C., Woodward, E. M. S., Kitidis, V., McGrath, T., Hydes, D. J., Greenwood, N., Hull, T., Ostle, C., Pearce, D. J., Sivyer, D., Stewart, B. M., Walsham, P., Painter, S. C., McGovern, E., Harris, C., Griffiths, A., Smilenova, A., Clarke, J., Davis, C., Sanders, R. and Nightingale, P.: Seasonality and spatial heterogeneity of the surface ocean carbonate system in the northwest European continental shelf, Prog. Oceanogr., doi:10.1016/j.pocean.2018.02.005, 2018.

Hickel, W., Mangelsdorf, P. and Berg, J.: The human impact in the German Bight: Eutrophication during three decades (1962-1991), Helgoländer Meeresuntersuchungen, doi:10.1007/BF02367167, 1993.

Hicks, N., Ubbara, G. R., Silburn, B., Smith, H. E. K., Kröger, S., Parker, E. R., Sivyer, D., Kitidis, V., Hatton, A., Mayor, D. J. and Stahl, H.: Oxygen dynamics in shelf seas sediments incorporating seasonal variability, Biogeochemistry, doi:10.1007/s10533-017-0326-9, 2017.

Hofmeister, R., Flöser, G. and Schartau, M.: Estuary-type circulation as a factor sustaining horizontal nutrient gradients in freshwater-influenced coastal systems, Geo-Marine Lett., 37(2), 179–192, doi:10.1007/s00367-016-0469-z, 2017.

Holt, J. and Proctor, R.: The seasonal circulation and volume transport on the northwest European continental shelf: A fine-resolution model study, J. Geophys. Res. Ocean., 113(6), doi:10.1029/2006JC004034, 2008.

Holt, J., Harle, J., Proctor, R., Michel, S., Ashworth, M., Batstone, C., Allen, I., Holmes, R., Smyth, T., Haines, K., Bretherton, D. and Smith, G.: Modelling the global coastal ocean, Philos. Trans. R. Soc. A Math. Phys. Eng. Sci., doi:10.1098/rsta.2008.0210, 2009.

Holt, J., Wakelin, S., Lowe, J. and Tinker, J.: The potential impacts of climate change on the hydrography of the northwest European continental shelf, Prog. Oceanogr., doi:10.1016/j.pocean.2010.05.003, 2010.

Holt, J., Butenschön, M., Wakelin, S. L., Artioli, Y. and Allen, J. I.: Oceanic controls on the primary production of the northwest European continental shelf: Model experiments under recent past conditions and a potential future scenario, Biogeosciences, 9(1), 97–117, doi:10.5194/bg-9-97-2012, 2012.

Holt, J., Schrum, C., Cannaby, H., Daewel, U., Allen, I., Artioli, Y., Bopp, L., Butenschon, M., Fach, B. A., Harle, J., Pushpadas, D., Salihoglu, B. and Wakelin, S.: Physical processes mediating climate change impacts on regional sea ecosystems, Biogeosciences Discuss., 11, 1909–1975, doi:10.5194/bgd-11-1909-2014, 2014.

Holt, J., Schrum, C., Cannaby, H., Daewel, U., Allen, I., Artioli, Y., Bopp, L., Butenschon, M., Fach, B. A., Harle, J., Pushpadas, D., Salihoglu, B. and Wakelin, S.: Potential impacts of climate change on the primary production of regional seas: A comparative analysis of five European seas, Prog. Oceanogr., 140, 91–115, doi:10.1016/j.pocean.2015.11.004, 2016.

Holt, J., Hyder, P., Ashworth, M., Harle, J., Hewitt, H. T., Liu, H., New, A. L., Pickles, S., Porter, A., Popova, E., Icarus Allen, J., Siddorn, J. and Wood, R.: Prospects for improving the representation of coastal and shelf seas in global ocean models, Geosci. Model Dev., doi:10.5194/gmd-10-499-2017, 2017.

Hufnagl, M., Peck, M. A., Nash, R. D. M., Pohlmann, T. and Rijnsdorp, A. D.: Changes in potential North Sea spawning grounds of plaice (Pleuronectes platessa L.) based on early life stage connectivity to nursery habitats, J. Sea Res., doi:10.1016/j.seares.2012.10.007, 2013.

Hufnagl, M., Temming, A. and Pohlmann, T.: The missing link: Tidal-influenced activity a likely candidate to close the migration triangle in brown shrimp Crangon crangon (Crustacea, Decapoda), Fish. Oceanogr., 23(3), 242–257, doi:10.1111/fog.12059, 2014.

Huthnance, J., Weisse, R., Wahl, T., Thomas, H., Pietrzak, J., Souza, A. J., Heteren, S. Van, Schmelzer, N., Beusekom, J. Van, Colijn, F., Haigh, I., Hjøllo, S., Holfort, J., Kent, E. C., Kühn, W., Loewe, P., Lorkowski, I., Mork, K. A., Pätsch, J., Quante, M., Salt, L., Siddorn, J., Smyth, T., Sterl, A. and Woodworth, P.: North Sea Region Climate Change Assessment., 2016.

ICES: Flushing times of the North Sea. Co-operative Research Report, Copenhagen., 1983.

Iriarte, a, Daneri, G., Garcia, V. M. T., Purdie, D. a and Crawford, D. W.: Plankton community respiration and its relationship to chlorophyll a concentration in marine coastal waters, Oceanol. Acta, 14(4), 379–388, 1991.

Jacobs, W.: Modelling the Rhine River Plume, TU Delft., 2004.

Jago, C. F., Jones, S. E., Latter, R. J., McCandliss, R. R., Hearn, M. R. and Howarth, M. J.: Resuspension of benthic fluff by tidal currents in deep stratified waters, northern North sea, in Journal of Sea Research, vol. 48, pp. 259–269., 2002a.

Jago, C. F., Jones, S. E., Latter, R. J., McCandliss, R. R., Hearn, M. R. and Howarth, M. J.: Resuspension of benthic fluff by tidal currents in deep stratified waters, northern North sea, J. Sea Res., 48(4), 259–269, doi:10.1016/S1385-1101(02)00181-8, 2002b.

Joint, I. and Pomroy, A.: Phytoplankton Biomass and Production in the Southern North-Sea, Mar. Ecol. Ser., 1993.

Jones, B. H. and Halpern, D.: Biological and physical aspects of a coastal upwelling event observed during March-April 1974 off northwest Africa, Deep Sea Res. Part A, Oceanogr. Res. Pap., doi:10.1016/0198-0149(81)90111-4, 1981.

Kautsky, H.: Investigations on the distribution of 137Cs, 134Cs and 9°Sr and the water mass transport times in the Nor- thern North Atlantic and the North Sea, Dtsch. hydrogr.Z., 40, 49–69, 1987.

Kerimoglu, O., Hofmeister, R., Maerz, J., Riethmüller, R. and Wirtz, K. W.: The acclimative biogeochemical model of the southern North Sea, Biogeosciences, 14(19), 4499–4531, doi:10.5194/bg-14-4499-2017, 2017.

Krause, G., Budeus, G., Gerdes, D., Schaumann, K. and Hesse, K.: Frontal systems in the german bight and their physical and biological effects, Elsevier Oceanogr. Ser., 42(C), 119–140, doi:10.1016/S0422-9894(08)71042-0, 1986.

Landeira, J. M., Ferron, B., Lunven, M., Morin, P., Marie, L. and Sourisseau, M.: Biophysical interactions control the size and abundance of large phytoplankton chains at the ushant tidal front, PLoS One, 9(2), doi:10.1371/journal.pone.0090507, 2014.

Laufkötter, C., Vogt, M. and Gruber, N.: Long-term trends in ocean plankton production and particle export between 1960-2006, Biogeosciences, doi:10.5194/bg-10-7373-2013, 2013.

Lavoie, D., Lambert, N. and Gilbert, D.: Projections of Future Trends in Biogeochemical Conditions in the Northwest Atlantic Using CMIP5 Earth System Models, Atmos. - Ocean, doi:10.1080/07055900.2017.1401973, 2017.

van Leeuwen, S. M., van der Molen, J., Ruardij, P., Fernand, L. and Jickells, T.: Modelling the contribution of deep chlorophyll maxima to annual primary production in the North Sea, Biogeochemistry, 113(1–3), 137–152, doi:10.1007/s10533-012-9704-5, 2013.

van Leeuwen, S., Tett, P., David, M. and van der Molen, J.: Stratified and nonstratified areas in the North Sea: Long-termvariability and biological and policy implications, J. Geophys. Res. Ocean., 120(7), 4670–4686, doi:10.1002/2014JC010485.Received, 2015.

Van Leeuwen, S., Tett, P., Mills, D. and Van Der Molen, J.: Stratified and nonstratified areas in the North Sea: Long-term variability and biological and policy implications, J. Geophys. Res. C Ocean., 120(7), 4670–4686, doi:10.1002/2014JC010485, 2015.

Lefèvre, D., Bentley, T. L., Robinson, C., Blight, S. P. and Williams, P. J. l. B.: The temperature response of gross and net community production and respiration in time-varying assemblages of temperate marine micro-plankton, J. Exp. Mar. Bio. Ecol., 184(2), 201–215, doi:10.1016/0022-0981(94)90005-1, 1994.

Lewis, M. R., Horne, E. P. W., Cullen, J. J., Oakey, N. S. and Platt, T.: Turbulent motions may control phytoplankton photosynthesis in the upper ocean, Nature, doi:10.1038/311049a0, 1984.

Löder, M. G. J., Kraberg, A. C., Aberle, N., Peters, S. and Wiltshire, K. H.: Dinoflagellates and ciliates at Helgoland Roads, North Sea, Helgol. Mar. Res., 66(1), 11–23, doi:10.1007/s10152-010-0242-z, 2012.

Lough, R. G. and Aretxabaleta, A.: Transport and retention of vertically migrating adult mysid and decapod shrimp in the tidal front on Georges Bank, Mar. Ecol. Prog. Ser., 514(November 2014), 119–135, doi:10.3354/meps10977, 2014.

Mann, K. H.: Physical influences on biological processes: How important are they?, South African J. Mar. Sci., 12(1), 107–121, doi:10.2989/02577619209504695, 1992.

Mathis, M.: Projected Forecast of Hydrodynamic Conditions in the North Sea for the 21st Century, University of Hamburg. [online] Available from: http://ediss.sub.uni-hamburg.de/volltexte/2013/6169/, 2013.

Mathis, M. and Pohlmann, T.: Projection of physical conditions in the north sea for the 21st century, Clim. Res., doi:10.3354/cr01232, 2014.

Mathis, M., Elizalde, A., Mikolajewicz, U. and Pohlmann, T.: Variability patterns of the general circulation and sea water temperature in the North Sea, Prog. Oceanogr., 135, 91–112, doi:10.1016/j.pocean.2015.04.009, 2015.

McCandliss, R. R., Jones, S. E., Hearn, M., Latter, R. and Jago, C. F.: Dynamics of suspended particles in coastal waters (southern North Sea) during a spring bloom, J. Sea Res., 47(3–4), 285–302, doi:10.1016/S1385-1101(02)00123-5, 2002.

McManus, M. A. and Woodson, C. B.: Plankton distribution and ocean dispersal, J. Exp. Biol., 215(6), 1008–1016, doi:10.1242/jeb.059014, 2012.

Mestres, M., Sierra, J. P. and Sánchez-Arcilla, A.: Modeled Dynamics of a Small-scale River Plume under Different Forcing Conditions, J. Coast. Res., doi:10.2112/1551-5036-47.sp1.84, 2007.

Meyer, E. M. I., Pohlmann, T. and Weisse, R.: Thermodynamic variability and change in the North Sea (1948-2007) derived from a multidecadal hindcast, J. Mar. Syst., doi:10.1016/j.jmarsys.2011.02.001, 2011.

Mork, M.: Circulation Phenomena and Frontal Dynamics of the Norwegian Coastal Current, Philos. Trans. R. Soc. London. Ser. A, Math. Phys. Sci., doi:10.1098/rsta.1981.0188, 1981.

Murphy, E. J., Watkins, J. L., Trathan, P. N., Reid, K., Meredith, M. P., Thorpe, S. E., Johnston, N. M., Clarke, A., Tarling, G. A., Collins, M. A., Forcada, J., Shreeve, R. S., Atkinson, A., Korb, R., Whitehouse, M. J., Ward, P., Rodhouse, P. G., Enderlein, P., Hirst, A. G., Martin, A. R., Hill, S. L., Staniland, I. J., Pond, D. W., Briggs, D. R., Cunningham, N. J. and Fleming, A. H.: Spatial and temporal operation of the Scotia Sea ecosystem: A review of large-scale links in a krill centred food web, Philos. Trans. R. Soc. B Biol. Sci., doi:10.1098/rstb.2006.1957, 2007.

Nelson, D. M. and Smith, W. 0.: Sverdrup revisited: Critical depths, maximum chlorophyll levels, and the control of Southern Ocean productivity by the irradiance-mixing regime, Limnol. Oceanogr., doi:10.4319/lo.1991.36.8.1650, 1991.

Nielsen, T. G., Lokkegaard, B., Richardson, K., Pedersen, F. B. and Hansen, L.: Structure of plankton communities in the Dogger Bank area (North Sea) during a stratified situation, Mar. Ecol. Prog. Ser., 95(1–2), 115–131, doi:10.3354/meps095115, 1993.

Nishihara, G. N. and Ackerman, J. D.: Diffusive boundary layers do not limit the photosynthesis of the aquatic macrophyte vallisneria americana at moderate flows and saturating light levels, Limnol. Oceanogr., 54(6), 1874–1882, doi:10.4319/lo.2009.54.6.1874, 2009.

North, R. P., Riethmüller, R. and Baschek, B.: Estuarine , Coastal and Shelf Science Detecting small e scale horizontal gradients in the upper ocean using wavelet analysis, , 180, 221–229, doi:10.1016/j.ecss.2016.06.031, 2016.

O'Donnell, J., Ackleson, S. G. and Levine, E. R.: On the spatial scales of a river plume, J. Geophys. Res. Ocean., 113(4), doi:10.1029/2007JC004440, 2008.

O'Driscoll, K., Mayer, B., Ilyina, T. and Pohlmann, T.: Modelling the cycling of persistent organic pollutants (POPs) in the North Sea system: Fluxes, loading, seasonality, trends, J. Mar. Syst., doi:10.1016/j.jmarsys.2012.09.011, 2013.

Ottersen, G., Planque, B., Belgrano, A., Post, E., Reid, P. C. and Stenseth, N. C.: Ecological effects of the North Atlantic Oscillation, Oecologia, doi:10.1007/s004420100655, 2001.

Otto, L., Zimmerman, J. T. F., Furnes, G. K., Mork, M., Saetre, R. and Becker, G.: Review of the physical oceanography of the North Sea, Netherlands J. Sea Res., 26(2–4), 161–238, doi:10.1016/0077-7579(90)90091-T, 1990.

Oziel, L., Sirven, J. and Gascard, J. C.: The Barents Sea frontal zones and water masses variability (1980-2011), Ocean Sci., 12(1), 169–184, doi:10.5194/os-12-169-2016, 2016.

Palmer, M. R., Polton, J. A., Inall, M. E., Rippeth, T. P., Green, J. A. M., Sharples, J. and Simpson, J. H.: Variable behavior in pycnocline mixing over shelf seas, Geophys. Res. Lett., 40(1), 161–166, doi:10.1029/2012GL054638, 2013.

Pätsch, J., Burchard, H., Dieterich, C., Gräwe, U., Gröger, M., Mathis, M., Kapitza, H., Bersch, M., Moll, A., Pohlmann, T., Su, J., Ho-Hagemann, H. T. M., Schulz, A., Elizalde, A. and Eden, C.: An evaluation of the North Sea circulation in global and regional models relevant for ecosystem simulations, Ocean Model., 116, 70–95, doi:10.1016/j.ocemod.2017.06.005, 2017.

Peng, D., Hill, E. M., Meltzner, A. J. and Switzer, A. D.: Tide Gauge Records Show That the 18.61-Year Nodal Tidal Cycle Can Change High Water Levels by up to 30 cm, J. Geophys. Res. Ocean., doi:10.1029/2018JC014695, 2019.

Pingree, R. D., Pugh, P. R., Holligan, P. M. and Forster: Summer phytoplankton blooms and red tides along tidal fronts in the approaches to the English Channel, Nature, 258(5537), 672–677, doi:10.1038/258672a0, 1975.

Pohlmann, T.: Calculating the development of the thermal vertical stratification in the North Sea with a three-dimensional baroclinic circulation model, Cont. Shelf Res., doi:10.1016/0278-4343(95)00018-V, 1996a.

Pohlmann, T.: Predicting the thermocline in a circulation model of the North Sea - Part I: Model description, calibration and verification, Cont. Shelf Res., 16(2), 131–146, doi:DOI: 10.1016/0278-4343(95)90885-S, 1996b.

Prairie, J. C., Sutherland, K. R., Nickols, K. J. and Kaltenberg, A. M.: Biophysical interactions in the plankton: A cross-scale review, Limnol. Oceanogr. Fluids Environ., 2(1), 121–145, doi:10.1215/21573689-1964713, 2012.

Richardson, K. and Pedersen, F. B.: Estimation of new production in the North Sea : consequences for temporal and spatial variability of phytoplankton, , 574–580, 1998.

Rokkan Iversen, K., Primicerio, R., Larsen, A., Egge, J. K., Peters, F., Guadayol, Ó., Jacobsen, A., Havskum, H. and Marrasé, C.: Effects of small-scale turbulence on lower trophic levels under different nutrient conditions, J. Plankton Res., doi:10.1093/plankt/fbp113, 2010.

Ross, O. N. and Sharples, J.: Phytoplankton motility and the competition for nutrients in the thermocline, Mar. Ecol. Prog. Ser., doi:10.3354/meps06999, 2007.

Ruddick, K. G., Deleersnijder, E., Luyten, P. J. and Ozer, J.: Haline stratification in the Rhine-Meuse freshwater plume: a three-dimensional model sensitivity analysis, Cont. Shelf Res., doi:10.1016/0278-4343(95)00034-X, 1995.

Sager, G.: Gezeiten und Schiffahrt, Fachbuchverlag, Leipzig, 173 pp., 1959.

Sammartino, M., Marullo, S., Santoleri, R. and Scardi, M.: Modelling the Vertical Distribution of Phytoplankton Biomass in the Mediterranean Sea from Satellite Data: A Neural Network Approach, Remote Sens., 10(10), doi:10.3390/rs10101666, 2018.

Sauzède, R., Claustre, H., Jamet, C., Uitz, J., Ras, J., Mignot, A. and D'Ortenzio, F.: Retrieving the vertical distribution of chlorophyll a concentration and phytoplankton community composition from in situ fluorescence profiles: A method based on a neural network with potential for global-scale applications, J. Geophys. Res. Ocean., doi:10.1002/2014JC010355, 2015a.

Sauzède, R., Lavigne, H., Claustre, H., Uitz, J., Schmechtig, C., D'Ortenzio, F., Guinet, C. and Pesant, S.: Vertical distribution of chlorophyll a concentration and phytoplankton community composition from in situ fluorescence profiles: A first database for the global ocean, Earth Syst. Sci. Data, doi:10.5194/essd-7-261-2015, 2015b.

Schrum, C.: Thermohaline stratification and instabilities at tidal mixing fronts: Results of an eddy resolving model for the German Bight, Cont. Shelf Res., 17(6), 689–716, doi:10.1016/S0278-4343(96)00051-9, 1997.

Schrum, C., Siegismund, F. and John, M. S.: Decadal variations in the stratification and circulation patterns of the North Sea. Are the 1990s unusual?, ICES Mar. Sci. Symp., 219, 121–131, 2003.

Schrum, C., Alekseeva, I. and St. John, M.: Development of a coupled physical-biological ecosystem model ECOSMO. Part I: Model description and validation for the North Sea, J. Mar. Syst., doi:10.1016/j.jmarsys.2006.01.005, 2006a.

Schrum, C., St. John, M. and Alekseeva, I.: ECOSMO, a coupled ecosystem model of the North Sea and Baltic Sea: Part II. Spatial-seasonal characteristics in the North Sea as revealed by EOF analysis, J. Mar. Syst., 61(1–2), 100–113, doi:10.1016/j.jmarsys.2006.01.004, 2006b.

Schrum, C., Lowe, J., Meier, M., Grabeman, I., Holt, J., Mathis, M., Pohlmann, T., Skogen, M., Sterl, A. and Wakelin, S.: Projected Change - North Sea and interface regions, in North Climate Change Assessment, Springer., 2016.

Siegismund, F.: Long-term changes in the flushing times of the ICES-boxes, Senckenbergiana maritima, 31(2), 151–167, doi:10.1007/BF03043025, 2001.

Simpson, J. H. and Hunter, J. R.: Fronts in the Irish Sea, Nature, 250(5465), 404–406, doi:10.1038/250404a0, 1974.

Simpson, J. H. and Rippeth, T. P.: The Clyde Sea: a Model of the Seasonal Cycle of Stratification and Mixing, Estuar. Coast. Shelf Sci., doi:http://dx.doi.org/10.1006/ecss.1993.1047, 1993.

Simpson, J. H. J. and Sharples, J.: Introduction to the Physical and Biological Oceanography of Shelf Seas, Cambridge University Press., 2012.

Skogen, M. D., Svendsen, E., Berntsen, J., Aksnes, D. and Ulvestad, K. B.: Modelling the primary production in the North Sea using a coupled three-dimensional physical-chemical-biological ocean model, Estuar. Coast. Shelf Sci., doi:10.1016/0272-7714(95)90026-8, 1995.

Skogen, M. D., Drinkwater, K., Hjøllo, S. S. and Schrum, C.: North Sea sensitivity to atmospheric forcing, J. Mar. Syst., 85(3–4), 106–114, doi:10.1016/j.jmarsys.2010.12.008, 2011.

Stanev, E. V., Badewien, T., Freund, H., Grayek, S., Hahner, F., Meyerjürgens, J., Ricker, M., Schöneich-Argent, R. I., Wolff, J. O. and Zielinski, O.: Extreme westward surface drift in the North Sea: Public reports of stranded drifters and Lagrangian tracking, Cont. Shelf Res., doi:10.1016/j.csr.2019.03.003, 2019.

Sukhanova, I. N., Flint, M. V., Pautova, L. A., Stockwell, D. A., Grebmeier, J. M. and Sergeeva, V. M.: Phytoplankton of the western Arctic in the spring and summer of 2002: Structure and seasonal changes, Deep. Res. Part II Top. Stud. Oceanogr., doi:10.1016/j.dsr2.2008.12.030, 2009.

Sullivan, J. M., Donaghay, P. L. and Rines, J. E. B.: Coastal thin layer dynamics: Consequences to biology and optics, Cont. Shelf Res., doi:10.1016/j.csr.2009.07.009, 2010.

Sündermann, J.: The changing North Sea: Knowledge, speculation and new challenges, Oceanologia, 2003.

Sündermann, J. and Pohlmann, T.: A brief analysis of North Sea physics, Oceanologia, 53(3), 663–689, doi:10.5697/oc.53-3.663, 2011.

Svendsen, E., Słtre, R. and Mork, M.: Features of the northern North Sea circulation, Cont. Shelf Res., 11(5), 493–508, doi:10.1016/0278-4343(91)90055-B, 1991.

Sverdrup, H. U.: On Conditions for the Vernal Blooming of Phytoplankton, ICES J. Mar. Sci., doi:10.1093/icesjms/18.3.287, 1953.

Taylor, G. I.: Tidal oscillations in gulfs and rectangular basins, Proc. London Math. Soc., s2-20(1), 148–181, doi:10.1112/plms/s2-20.1.148, 1922.

Tett, P. and Walne, A.: Observations and simulations of hydrography, nutrients and plankton in the southern north sea, Ophelia, 42(1), 371–416, doi:10.1080/00785326.1995.10431514, 1995.

Thessen, A.: Adoption of Machine Learning Techniques in Ecology and Earth Science, One Ecosyst., doi:10.3897/oneeco.1.e8621, 2016.

Tilstone, G. H., Miller, P. I., Brewin, R. J. W. and Priede, I. G.: Enhancement of primary production in the North Atlantic outside of the spring bloom, identified by remote sensing of ocean colour and temperature, Remote Sens. Environ., doi:10.1016/j.rse.2013.04.021, 2014.

Turner, B. L., Matson, P. A., McCarthy, J. J., Corell, R. W., Christensen, L., Eckley, N., Hovelsrud-Broda, G. K., Kasperson, J. X., Kasperson, R. E., Luers, A., Martello, M. L., Mathiesen, S., Naylor, R., Polsky, C., Pulsipher, A., Schiller, A., Selin, H. and Tyler, N.: Illustrating the coupled human–environment system for vulnerability analysis: Three case studies, Proc. Natl. Acad. Sci., doi:10.1073/pnas.1231334100, 2003.

Turrell, W. R., Henderson, E. W., Slesser, G., Payne, R. and Adams, R. D.: Seasonal changes in the circulation of the northern North Sea, Cont. Shelf Res., doi:10.1016/0278-4343(92)90032-F, 1992.

Uitz, J., Claustre, H., Morel, A. and Hooker, S. B.: Vertical distribution of phytoplankton communities in open ocean: An assessment based on surface chlorophyll, J. Geophys. Res. Ocean., doi:10.1029/2005JC003207, 2006.

Vermaat, J. E., McQuatters-Gollop, A., Eleveld, M. A. and Gilbert, A. J.: Past, present and future nutrient loads of the North Sea: Causes and consequences, Estuar. Coast. Shelf Sci., doi:10.1016/j.ecss.2008.07.005, 2008.

Weston, K., Fernand, L., Mills, D. K., Delahunty, R. and Brown, J.: Primary production in the deep chlorophyll maximum of the central North Sea, J. Plankt. Res., 2005.

Wiltshire, K. H. and Manly, B. F. J.: The warming trend at Helgoland Roads, North Sea: Phytoplankton response, Helgol. Mar. Res., 58(4), 269–273, doi:10.1007/s10152-004-0196-0, 2004.

Zhao, C., Maerz, J., Hofmeister, R., Röttgers, R., Riethmüller, R., Wirtz, K. and Schrum, C.: Characterizing the vertical distribution of chlorophyll a in the German Bight, Cont. Shelf Res., 175, 127–146, doi:10.1016/j.csr.2019.01.012, 2019a.

Zhao, C., Daewel, U. and Schrum, C.: Tidal impacts on primary production in the North Sea, Earth Syst. Dyn., 10(2), 287–317, doi:10.5194/esd-2018-74, 2019b.

Description of the individually scientific contributions to the multi-author manuscripts

Manuscript 1

"Characterizing the vertical distribution of chlorophyll a in the German Bight"

For the data preprocessing, Changjin Zhao has contribute evaluations of signal-lag of oxygen sensors, sensitivity analysis of criterions, calibration of fluorescence signal and evaluation of related uncertainties. Changjin Zhao wrote scripts for data processing, result analysis and graphical presentation. Defining ideas of this manuscript, storying building and most part of text writing were mainly conducted by Changjin Zhao.

Dr. Rolf Riethmüller has undertaken most part of data pre-processing and supervised Changjin Zhao for part of data pre-processing. Dr. Rüdiger Röttgers has supervised Changjin Zhao to conduct calibration of fluorescence signal and evaluation of related uncertainties. Interpolation of hydrodynamic parameters from GETM simulation was conducted by Dr. Richard Hofmeister. Dr. Joeran Maerz and Dr. Richard Hofmeister has actively cooperate with Changjin Zhao in writing scripts for data processing, result analysis and graphical presentation. Classification of CHL vertical profiles was initially suggested by Prof. Dr. Kai Wirtz. Text writing was contributed by all co-authors. Overall supervision of the paper was done by Prof. Dr. Corinna Schrum.

Manuscript 2

"Tidal impacts on primary production in the North Sea"

Changjin Zhao has undertaken adding parameterization for SPM field, scenario runs, result analysis, graphical presentation (except for Fig.B2), storying building and most part of text writing.

ECOSMO code was maintained and provided by Dr. Ute Daewel. Dr. Ute Daewel has supervised Changjin Zhao for updating of new parameterization of SPM field, result analysis, graphical presentation and text writing. The comparison with prior ECOSMO version was mainly conducted by Dr. Ute Daewel. Conception and overall supervision of the paper was provided by Prof. Dr. Corinna Schrum.

Manuscript 3

"Frontal dynamics and impacts on primary production in the North Sea"

Changjin Zhao has undertaken simulation runs, collecting of remote sensing data, updating and applying frontal detecting methods to simulation and remote sensing dataset, geographical presentation and result analysis. Storying building and text writing were mainly conducted by Changjin Zhao.

Ingrid Angel Benavides has programed the original version of algorithms for frontal detecting and supported Changjin Zhao for scripts' updating and validation of simulation results with remote sensing data. Ingrid Angel Benavides actively cooperated with Changjin Zhao for collecting of remote sensing data, applying frontal detecting methods, writing text particularly for the method part. ECOSMO code was maintained and provided by Dr. Ute Daewel. Dr. Ute Daewel has supervised Changjin Zhao for result analysis, storying building and text writing.Conception and overall supervision of the manuscript was provided by Prof. Dr. Corinna Schrum.

List of publications

Zhao, C., Maerz, J., Hofmeister, R., Röttgers, R., Riethmüller, R., Wirtz, K. and Schrum, C.: Characterizing the vertical distribution of chlorophyll a in the German Bight, Cont. Shelf Res., 175, 127–146, doi:10.1016/j.csr.2019.01.012, 2019. (manuscript 1)

Zhao, C., Daewel, U. and Schrum, C.: Tidal impacts on primary production in the North Sea, Earth Syst. Dyn., 10(2), 287–317, doi:10.5194/esd-2018-74, 2019. (manuscript 2)

Zhao,C., Daewel,U., Benavides, I. A., Schrum, C.: Frontal dynamics and impacts on primary production in the North Sea. In preparation. (manuscript 3)

Versicherung an Eides statt (*Affirmation on oath*)

Hiermit versichere ich an Eides statt, dass ich die vorliegende Dissertation mit dem Titel: „Phytoplanktondynamik in der Nordsee: Einfluss von Fronten und Gezeiten auf die Phytoplanktonproduktion“ selbstständig verfasst und keine anderen als die angegebenen Hilfsmittel – insbesondere keine im Quellenverzeichnis nicht benannten Internet-Quellen – benutzt habe. Alle Stellen, die wörtlich oder sinngemäß aus Veröffentlichungen entnommen wurden, sind als solche kenntlich gemacht. Ich versichere weiterhin, dass ich die Dissertation oder Teile davon vorher weder im In- noch im Ausland in einem anderen Prüfungsverfahren eingereicht habe und die eingereichte schriftliche Fassung der auf dem elektronischen Speichermedium entspricht.

I hereby declare on oath that I have written this dissertation on my own with the title:"Phytoplankton dynamics in the North Sea: influence of fronts and tidal stirring on phytoplankton production " and that I have not used any resources other than those specified - in particular not Internet sources not mentioned in the bibliography I further declare that I have not previously submitted the dissertation or parts of it in another examination procedure either at home or abroad and that the submitted written version corresponds to that on the electronic storage medium.

Date : 29/04/2019

Place: Geesthacht

Acknowlegements

My sincerest gratitude is dedicated to Doctormutter, Prof. Dr. Corinna Schrum, for her constant encouragement, support, patience, tolerance and excellent scientific supervision. She is always very willing to share her experience about life and science. Her scientific enthusiasm and creativity inspire me and her constructive suggestions guided me throughout the whole Ph.D thesis. With such a kind friend in life and such a strict supervisor in science, no matter which kind of obstacles I had encountered during my Ph.D, her encouragement kept me calm, confident, and shoulder responsibilities unswervingly. I am so fortunate to be under her umbrella.

Great appreciation is dedicated to my co-supervisor Dr. Ute Daewel, who is always beside me whenever I need help. Her door is always open, for discussions about basic scientific questions, solutions to technical problems of numerical modelling, algorithms to dig out scientific mysteries, ideas to build scientific stories and strategies for scientific writing. As the most impressive team member, she let me find the clue to unite a team, to work together efficiently and happily. Whenever I was stressed out, she comforted me emotionally and encouraged me to be positive, to relax a little bit and do not forget to cherish daily life. I am willing to share what would happen in the future with her, at least whenever we change the first number of our age together.

Thanks to my panel chair Prof. Dr. Myron Peck, of whom curiosities to science inspired me a lot. Every panel meeting was long, interesting and impressive. My presentations were always interrupted by his questions which provided new insights from a biologist's standpoint and also stimulated my thinking.

I enjoyed the atmosphere in our group KST. I appreciate the happy experience as working here every day with every member of this team. I own my scientific obtains to their cooperation, patient listening and kind suggestions for my raw results in almost every discussion meeting. Richard Hofmeister is the first colleague I got to know when I first arrived. During the past 5 years, Richard helped me handled many daily troubles as a foreign student could encountered in Germany. He is unstintingly generous with his rich experience in Python program language. I am impressed by Johannes Bieser who bears enthusiasm for science and exploring nice food around the whole world. Chartings in our office 330 is unforgettable for me, with amazing officemate Deborah Benkort and Onur

Kerimoglu. We not only help and encourage each other on the way pursuing science, but also exchange ideas about the whole world. There are so many interesting topics we have chatted about, such as regulations of data sharing in science, gender equality, cherishing family life, how to utilize science and technology to create better life for human being's future, work-life balance and so on. They also have helped me for my moving or shelter me during my final phase of Ph.D. I appreciate nice experience sharing from Dr. Wenyan Zhang, regarding scientific research and future career plan. Feifei Liu, my elder academical sister, stayed beside me, listened to me and offered shoulder for my crying face when I felt down. I appreciate the special care offered by my academical younger brother and sisters, Lucas Porz, Elena Mikheeva, Phillippa Schindler, who keep calling me to lunch during my final stage when I suffered from stress and depression. Sometimes I also knocked their door which is next to my office and called them 'young and cute guys!' Special gratitude to Peter Arlinghaus, who offered help to translate the abstract to German.

I thank many friendly colleagues in HZG. I learned a lot from scientific chatting with them, namely Hajo Krasemann, Rolf Riethmüller, Götz Flöser, Wilhelm Petersen, Ulrich Callies, Ryan North, Jeff Carpenter, Susanne Reinke, Insa Meinke, Lucas Merckelbach and my former roommate Matthias Zahn and Niousha Taherzadeh. Particularly, I enjoyed scientific discussion with Rüdiger Röttgers who offered me great support during the publication of my first manuscript. It is fascinating that he is able to guide a layman of ocean color remote sensing, such as myself, to grasp basic disciplines and develop a strategy to tackling scientific problems very efficiently. Rich in knowledge as he is, he is also open to different opinions and methods. Special gratitude to Carsten Lemmen, Maria Moreno de Castro, Joeran Maerz, who welcomed me warmly when I first arrived. Thank Kai Wirtz for guiding me into basic concepts in ecosystem modelling. Ingrid Angle's persistent support makes the completion of my third manuscript possible. Many thanks to the administration staff at HZG, Sabine Hartmann, Sabine Billerbeck and Hendrik Weidemann, without whom the careless Changjin would not survive. Great appreciation is dedicated to Anne Hartlich, Peter Kummerow and Uwe Benn, for facilitating my life in Germany. My thanks also own to Chinses fellows at HZG and particularly my friends, Jiangfeng Song, Jianlong Feng, Delei Li, Yijuan Wu, Wenying Mi, Zhiyong Xie, Jin Lu, Meng Zhang, Wei Chen, Shengquan Tang, Weidan Wang, Feifei Deng, Zhenzhen Zhang and Jing Li.

I cherish the short stay at Biologische Anstalt Helgoland, Alfred Wegener Institute for Polar and Marine Research. I enjoyed the patient chatting and help from Mirco Scharfe and Prof. Dr. Karen Wiltshire. Special thanks to Yangyang Liu, from AWI in Bremen, for her persisting encouragement and kind help in Science. I am very grateful to Prof. Dr. Inga Hense and Dr. Thomas Pohlmann from Hamburg University, for their thoughtful suggestions for my scientific study and improvements for my manuscripts.

Staying more than 10000 kilometers away, I am still motivated by SKLEC (State Key Lab for Estuary and Coastal Research in East China Normal University) in Shanghai. I was encouraged by fellows and alumni there.

My sincere gratitude is dedicated to my soulmate, Hongwei Yu, with whom I feel free share every corner of my inner mind. I am so fortunate to have a friend since primary school, Yi Liu. We can encourage each other to complete Ph.D studies.

Last but not least, I expressed my deepest gratitude to my parents and other family members, who provide unconditional trust and unrestricted support for me for past 30 years.